PROPERTIES OF TWO ENZYMES INVOLVED IN PHOSPHOINOSITIDE CYCLE

PROPERTIES OF TWO ENZYMES INVOLVED IN THE PHOSPHOINOSITIDE CYCLE – DIACYLGLYCEROL KINASE AND PHOSPHATIDYLINOSITOL 4-PHOSPHATE 5-KINASE

By

YULIA V. SHULGA, B.Sc., M.Sc.

A Thesis

Submitted to the School of Graduate Studies

in Partial Fulfilment of the requirements

for the Degree

Doctor of Philosophy

McMaster University

DOCTOR OF PHILOSOPHY (2012) McMaster University

(Department of Biochemistry and Biomedical Sciences) Hamilton, Ontario

TITLE: Properties of two enzymes involved in the phosphoinositide cycle – diacylglycerol kinase and phosphatidylinositol 4-phosphate 5-kinase

AUTHOR: Yulia V. Shulga, B.Sc., M.Sc. (Novosibirsk State University)

SUPERVISOR: Professor Richard M. Epand

NUMBER OF PAGES: xiii, 211

ABSTRACT

The two lipid kinases, diacylglycerol kinase (DGK) and phosphatidylinositol 4-phosphate 5-kinase (PIP5K), are vital players of the phosphatidylinositol cycle. DGK regulates the intracellular balance between two important lipid signaling molecules, diacylglycerol and phosphatidic acid. PIP5K produces another key signal messenger, phosphatidylinositol 4,5-bisphosphate. We studied several fundamental aspects of DGK and PIP5K properties. We investigated the topology of the hydrophobic segment of FLAG-tagged DGK epsilon, and showed that a single amino acid mutation P32A caused the hydrophobic segment to favor a transmembrane orientation. We demonstrated that DGKε is localized in both the plasma membrane and endoplasmic reticulum. Our work helped to better elucidate the substrate specificity of DGKε and PIP5K isoforms, and it lead us to discover the motif that is common for several enzymes that exhibit specificity for substrates containing polyunsaturated fatty acids. We studied the organ distribution of murine DGK isoforms, and also expanded our knowledge of DGK expression in diabetic animals, showing that the expression profiles of several DGK isoforms are altered in adipocytes isolated from diabetic mice. Moreover, DGK expression profiles change dramatically during adipocyte differentiation. Taken together, our findings contribute to the growing knowledge about two enzymes, DGK and PIP5K, by providing the fundamental information about the structural and functional properties of these lipid kinases. Both PIP5K and DGK enzymes have a strong potential for use as drug targets. Although at present their clinical importance has not been completely assessed, we believe that their significance as drug targets will be recognized in the nearest future.

ACKNOWLEDGEMENTS

Foremost, I would like to thank my supervisor, Dr. Richard Epand for all his help, support and patience. I am grateful to Dr. Epand for the opportunity to work in his laboratory. His kindness and liberal approach made working in his lab a pleasure, and his guidance and assistance during my graduate studies were exceptional.

Also I would like to thank my supervisory committee members, Dr. Daniel Yang, Dr. Tony Collins and Dr. Gregory Steinberg, as well as our collaborator Dr. Matthew Topham, for their constructive comments and guidance.

I am grateful to all members of Dr. Epand's lab and my friends from McMaster University, especially Iva and Satoko, for their friendship, discussions and support.

Special thanks to my family – my husband Kirill, my parents and Sherlock, for their caring support, love and encouragement. I can never thank them enough for enriching my life in so many ways.

TABLE OF CONTENTS

LIST OF FIGURES

CHAPTER ONE

CHAPTER TWO

CHAPTER THREE

CHAPTER FOUR

CHAPTER FIVE

LIST OF TABLES

CHAPTER TWO

CHAPTER THREE

CHAPTER FOUR

CHAPTER FIVE

CHAPTER SIX

LIST OF ABBREVIATIONS USED IN CHAPTERS 1 AND 8

ARF	ADP-ribosylation factor
C1	Cys-rich domains
CDP-DAG	cytidine-diphosphate-DAG
DAG	diacylglycerol
DGK	diacylglycerol kinase
ER	endoplasmic reticulum
EST	expressed sequence tag
FLAG	an N-terminal FLAG epitope tag
GAP	GTPase activating protein
GPCR	G-protein coupled receptor
KO	knockout
LOX	lipoxygenase
M1R	M1 muscarinic receptor
MARCKS	myristoylated alanine rich C kinase substrate
MEF	mouse embryonic fibroblasts
p235PIKfyve	phosphatidylinositol 3-phosphate 5-kinase
PAK1	Serine/threonine-protein kinase 1
PAP	phosphatidic acid phosphohydrolase
PC	phosphatidylcholine
PH	pleckstrin homology domain
PI3K	phosphatidylinositol 3-kinase
PI4K	phosphatidylinositol 4-kinase
PIP4K	phosphatidylinositol 5-phosphate 4-kinase
PIP5K	phosphatidylinositol 4-phosphate 5-kinase
PKC	protein kinase C
PLC	protein lipase C
PLD	protein lipase D
PPIn	polyphosphoinositides
PTEN	phosphatase and tensin homolog
PtdOH	phosphatidic acid
PtdIns	phosphatidylinositol
PtdIns4*P*	phosphatidylinositol-4-phosphate
PtdIns(4,5)P_2	phosphatidylinositol-4,5-bisphosphate
PUFA	polyunsaturated fatty acid
RasGEF	Ras- guanidine-nucleotide-exchange factor
RasGRP	Ras-guanyl-nucleotide-releasing protein
RhoA	Ras homolog gene family, member A
SAM	sterile alpha motif
SHIP	SH2 domain-containing inositol-5’-phosphatase
Sos	Son of Sevenless
TPA	12-O-tetradecanoylphorbol-13-acetate
WT	wild-type

CHAPTER ONE

INTRODUCTION

1. Phosphoinositide cycle in the cell

Phosphoinositides are a minor component in the cytosolic side of eukaryotic cell membranes. They are grouped into a family of phosphoglycerides containing *myo*-inositol as their headgroup. Seven different molecules of polyphosphoinositides (PPIn) can be produced by phosphorylation of single or multiple hydroxyl groups on the inositol ring of the parent lipid, phosphatidylinositol (PtdIns) (Fig. 1.1). Typically, the three, four and five hydroxyl groups, which are exposed to the cytosol, are phosphorylated, while the two and six hydroxyl groups are not phosphorylated due to steric hindrance.

Eukaryotic cells contain less than 10% of phosphoinositides as total phospholipids, with PtdIns comprising a major fraction of 6 – 8 %, while the most prevalent polyphosphoinositides, phosphatidylinositol 4-phosphate (PtdIns4*P*) and phosphatidylinositol (4,5)-bisphosphate (PtdIns(4,5)P_2), constitute about 1% and 0.25-0.5% respectively.[1, 2] But despite their low abundance, phosphoinositides play a crucial role in the regulation of cellular physiology due to their high rate of interconversion by multiple lipases, phosphatases and kinases. This conversion and recycling of phosphoinositides was first demonstrated in 1960-70s,[3-5] and it is now referred to as "canonical PtdIns cycle". Since then many new players involved in this pathway were discovered.

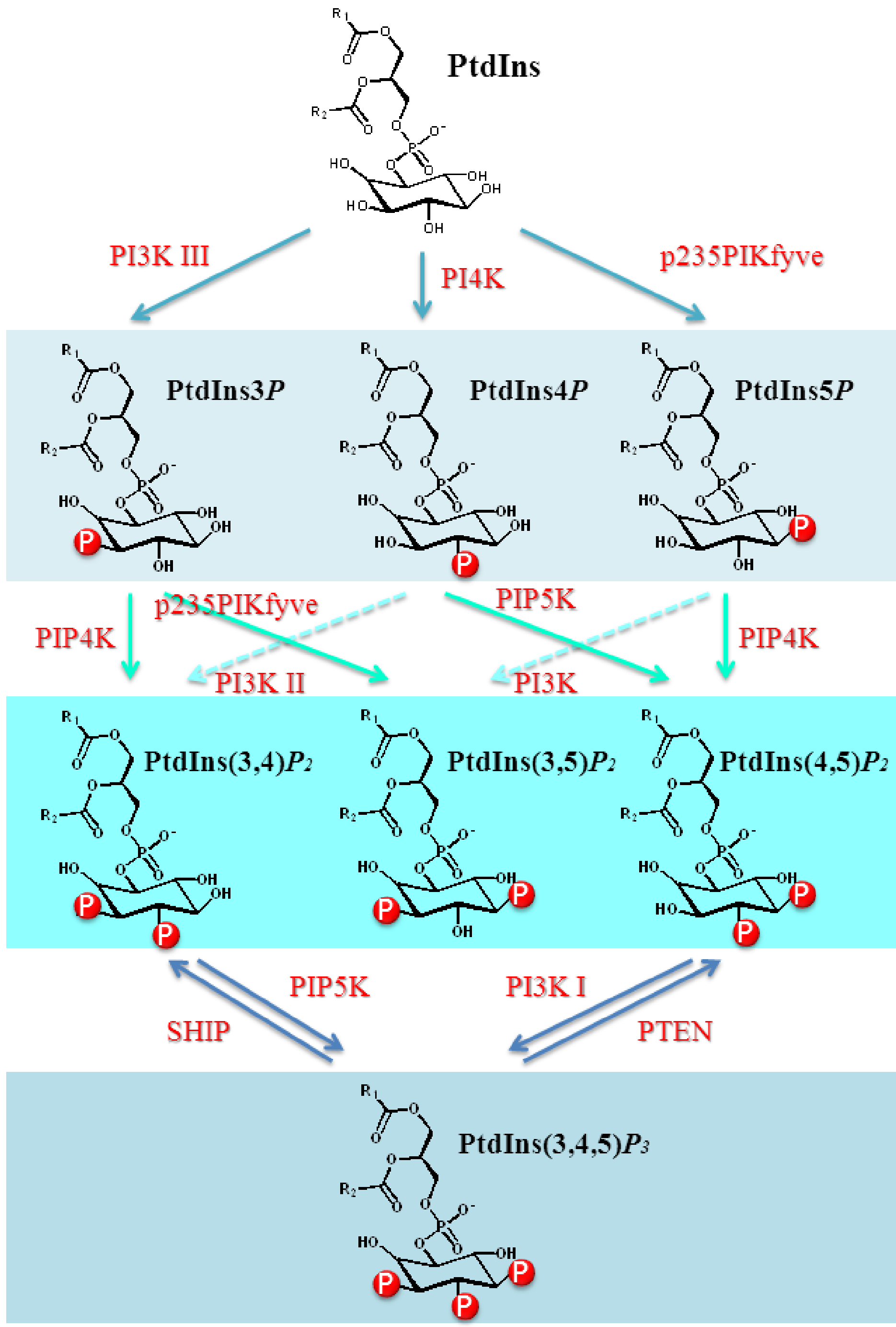

Figure 1.1. The generation and interconversion of phosphoinositides. Red circles represent a newly added phosphate group. p235PIKfyve, phosphatidylinositol 3-phosphate 5-kinase; PTEN, phosphatase and tensin homolog; SHIP, SH2 domain-containing inositol-5'-phosphatase.

In the PtdIns cycle, PtdIns is converted to PtdIns4*P* by phosphatidylinositol 4-kinase (PI4K), which is next phosphorylated to PtdIns(4,5)P_2 by phosphatidylinositol 4-phosphate 5-kinase (PIP5K) (Fig. 1.2). In resting cells the level of PtdIns(4,5)P_2 seems to be relatively high for a signal lipid and does not change dramatically upon stimulation of the whole cells. Therefore, it is proposed that there are two types of PtdIns(4,5)P_2 – dynamic and static, and that the local concentration of membrane PtdIns(4,5)P_2 in the restricted areas, such as lipid rafts, is critical for cellular signaling. One possibility for regulation would involve the existence of mechanisms to locally concentrate and mask PtdIns(4,5)P_2 at the inner leaflet of the cell membrane, where its accessibility to actin regulatory proteins would be linked to extracellular signals.[6]

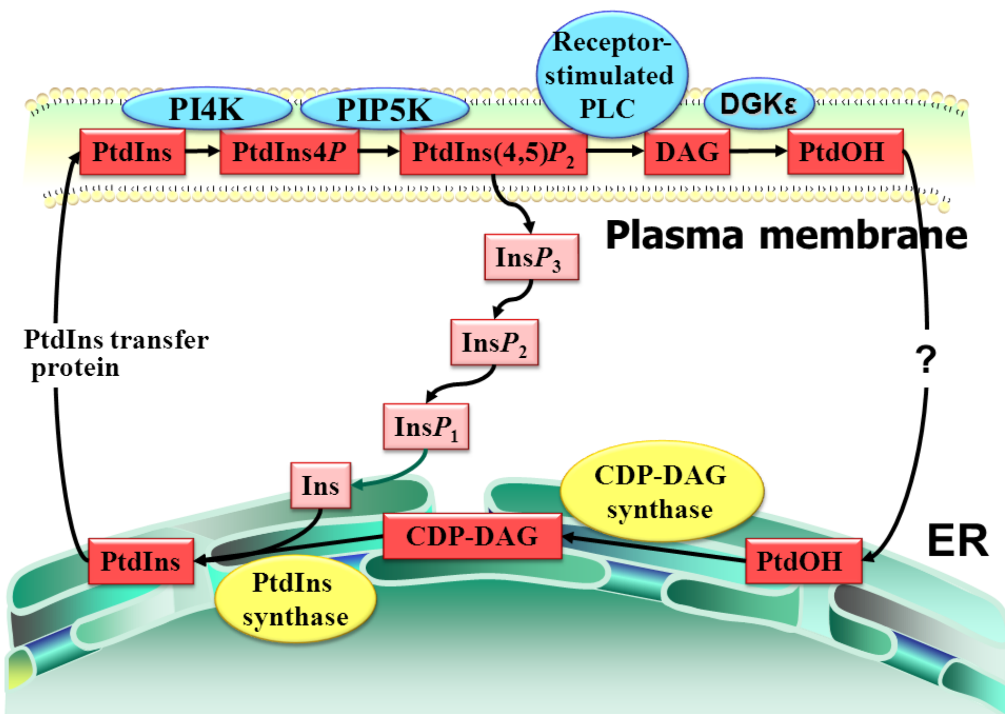

Figure 1.2. Phosphatidylinositol cycle in the cell.

PtdIns(4,5)P_2 can also be synthesized from PtdIns5P by phosphatidylinositol 5-phosphate 4-kinase (PIP4K) family that includes three isoforms, α, β and γ (Fig. 1.1).[7-9] PtdIns5P is produced by a phosphatidylinositol 3-phosphate 5-kinase (p235PIKfyve) which utilizes both PtdIns and PtdIns3P substrates.[10, 11]

PtdIns(4,5)P_2 is a substrate for phospholipase C (PLC), which cleaves the phosphodiester bond between *myo*-inositol and the diacylglycerol (DAG) backbone, producing inositol (1,4,5)-trisphosphate (Ins(1,4,5)P_3) and DAG, both of which function as second messengers. DAG remains on the cell membrane and initiates the signal cascade by activating protein kinase C (PKC) and other C1-domain-containing proteins, such MUNC-13.[10, 12] PKC in turn activates other cytosolic proteins through phosphorylation. Ins(1,4,5)P_3 enters the cytoplasm and activates Ins(1,4,5)P_3 receptors on the smooth endoplasmic reticulum (ER). This causes calcium channels on the smooth ER to open, allowing mobilization of Ca^{2+} into the cytosol and therefore producing complex Ca^{2+} concentration signals including propagating waves and temporal oscillations. These signals activate a number of other proteins and initiate a strong cellular response.

As the next step in the PtdIns cycle, DAG is phosphorylated to phosphatidic acid (PtdOH) by diacylglycerol kinases (DGKs). Further PtdOH can be transferred to ER, where it is converted to cytidine-diphosphate-DAG (CDP-DAG) by CDP-DAG synthase. CDP-DAG, together with inositol, is used to regenerate PtdIns, which is then transferred back to plasma membrane, completing the PtdIns cycle (Fig. 1.2).

In addition to PPIn, phosphorylated at 4 and 5 hydroxyl groups of inositol ring, the group of PPIn, phosphorylated at D3 position, was discovered in late 1980s.[13, 14]

Phosphoinositide 3-kinase (PI3K) family of enzymes, catalyzing this reaction, includes nine members in mammalian cells, which are grouped into three classes according to their preferred substrates.[15, 16] PI3K can generate four different products, PtdIns3*P*, PtdIns(3,4)P_2, PtdIns(3,5)P_2 and PtdIns(3,4,5)P_3. PtdIns(3,4,5)P_3 plays an important role as second messenger,[17] which is below detectable levels in resting cells but is generated immediately upon cell stimulation. Thus, PI3K signaling pathway is involved in several fundamental cellular processes, including cell proliferation and survival, by means of regulation of the activities of a wide range of downstream molecular effectors.[18] Several reports demonstrate that PI3K activity is essential in the inflammatory response,[19, 20] as we as in the immune recognition of tumor cells.[21, 22] On the other hand, PI3K pathway, in conjunction with v-akt murine thymoma viral oncogene homologue (AKT) and mitogen-activated protein kinase (MAPK), was shown to be essential for glucose homeostasis. Deregulation of PI3K/AKT/MAPK pathway often results in obesity and diabetes.[23] For example, an R409Q amino acid substitution in p85α subunit of PI3K was shown to compromise insulin-stimulated PI3K activity in humans.[24, 25] Further, transgenic mice lacking either p85α or all three isoforms of *Pik3r1* (gene encoding p85α, p55α and p50α subunits of PI3K) were shown to be hypoglycaemic and displayed increased glucose tolerance.[26]

Phosphoinositides contain mainly polyunsaturated fatty acids, with the 1-stearoyl-2-arachidonyl species comprising 30–80% (depending on the cell type).[27-30] One particular isoform of DGK, DGKε, was shown to contribute to the enrichment of phosphoinositides with 1-stearoyl-2-arachidonyl moiety,[31] acting selectively on DAGs containing arachidonoyl chains.[32, 33] In Chapter 3 we further explored the involvement of this enzyme in the PtdIns cycle by comparing the phospholipid compositions of plasma membrane and ER isolated from embryonic fibroblasts obtained from DGKε knockout (KO) and wild-type (WT) mice. The PtdIns cycle occurs between two membranes – the plasma membrane and ER. Using mass spectrometry, we determined the distribution of PtdOH and phosphoinositides and their acyl chain compositions in these two subcellular membranes. We found that the PtdIns cycle is slowed in the plasma membrane of DGKε KO cells, but there is less of an effect of DGKε depletion in the ER, likely due to *de novo* synthesis of PtdOH in this organelle.

2. Diacylglycerol kinases (DGKs)

Preface:

The material presented in Section 2 "Diacylglycerol kinases (DGKs)" includes excerpts from the work that was published previously in *Chemical Reviews*, volume 111(10), pages 6186-6208, in 2011.

Adapted with permission from "Shulga Y.V., Topham M.K., Epand R.M. (2011) Regulation and functions of diacylglycerol kinases. *Chem Rev.* 111(10):6186-208".

2.1. Overview of DGKs

DGKs play a major role in cellular signaling by converting DAG to PtdOH, regulating the balance between these two important lipid signaling molecules. Further modulation of this balance can be achieved by formation of DGK complexes with proteins that regulate DAG production or act as downstream effectors of DAG, or with proteins that act downstream of PtdOH to efficiently couple with the PtdOH dependent signaling.[34-36]

The majority of signaling DAG is generated by hydrolysis of PtdIns(4,5)P_2 by PLC, but DAG can also be generated when phosphatidic acid phosphatases remove the phosphate head group from PtdOH (Fig. 1.3). DAG is well known to regulate different cellular processes, mostly through binding to C1 domains that are found in many proteins including protein kinase C (PKC).[37, 38] In addition to modulating classical and novel DAG-sensitive PKC isoforms by removing DAG, DGKs have also been found to negatively regulate several other signaling proteins, such as RasGRP1,[39] RasGRP3,[40] UNC-13,[41, 42] β_2-chimaerin,[43] and protein kinase D.[44] Also it was found that DAG activates some transient receptor potential channels that do not have C1 domains.[45]

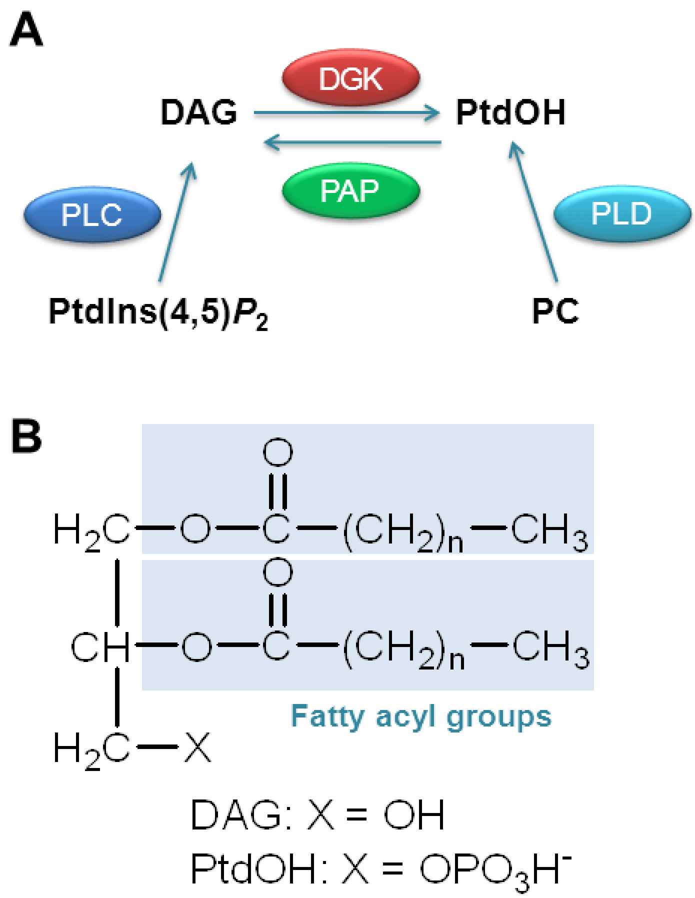

Figure 1.3. Adapted with permission from "Shulga Y.V., Topham M.K., Epand R.M. (2011) Regulation and functions of diacylglycerol kinases. Chem Rev. 111(10):6186-208". Copyright (2011) American Chemical Society.

A. Different enzymatic pathways can produce diacylglycerol (DAG) and phosphatidic acid (PtdOH). PLC enzymes generate DAG that can be phosphorylated by DGKs to produce PtdOH. In another pathway, phospholipase D (PLD) hydrolyzes phosphatidylcholine (PC) – or phosphatidylethanolamine – making PtdOH that can be further hydrolyzed by PAPs to generate DAG. To date, there is little definitive evidence to suggest that the DGK and PAP reactions are coupled. Both DAG and PtdOH can act as signaling lipids and are also intermediates in lipid biosynthetic pathways. **B.** DAG and PtdOH have the same general structure but contain different functional groups attached to the third (*sn*-3) carbon. Depending on their molecular structure, the fatty acyl groups confer different signaling properties to the DAG or PtdOH.

The product of the reaction catalyzed by DGK, PtdOH, has also been shown to regulate a wide variety of cellular events, including cytoskeletal rearrangement, proliferation, and cell survival.[46] It is also required for vesicle trafficking, stimulation of DNA synthesis and is potentially mitogenic. These effects are likely due to the ability of PtdOH to regulate a number of signaling proteins, such as Sos, a Ras GEF (guanidine-nucleotide-exchange factor), Ras-GAP, phosphatidylinositol 5-kinases, Raf-1, PAK1 and PKCζ.

It is believed that each PtdOH species, saturated and unsaturated, can differentially activate proteins. PtdOH produced by DGKs is enriched in polyunsaturated fatty acids, particularly arachidonate. It was shown that the PtdOH produced by DGKα was necessary for stimulated T lymphocytes to progress to S phase of the cell cycle[47] and that PtdOH produced by DGKζ activates PAK1 that then caused actin rearrangements.[48]

Because of their importance, it is crucial that the intracellular levels of DAG and PtdOH should be tightly regulated, which is accomplished by the diacylglycerol kinases and phosphatidic acid phosphatases. As such, these enzymes have numerous important functional roles.

2.2. Mammalian isoforms of DGK

Unlike bacteria and yeast, multicellular organisms express more than one, and often several, DGK isoforms that can be grouped by common structural elements into five subfamilies (Fig. 1.4). The DGKs expressed in mammals are the best characterized, and ten of them have been identified.[35, 49, 50] Like DGKs in other multicellular organisms, all of the mammalian DGKs have two common structural features: at least two cysteine-rich, C1 domains and a catalytic domain. The C1 domains are homologous to the DAG-binding C1A and C1B motifs of PKCs,[51] but the C1 domain closest to the catalytic domain has an extended region of fifteen amino acids not present in C1 domains from other proteins or in the other C1 domains of DGKs. Mutations within this extended region significantly reduced kinase activity, indicating that this extension appears to contribute to DGK activity.[52] In theory, DGK C1 domains bind DAG, perhaps localizing them to where DAG accumulates. However, it is still controversial whether all DGK C1 domains can bind DAG or if only some of them are capable of binding this lipid. Of several that were tested, only the C1 domains of DGKs β and γ could bind DAG analogues (phorbol esters), while the C1 domains of DGKs δ, η, and θ did not bind.[53-55] These results were in agreement with sequence alignments performed by Hurley and colleagues,[51] who predicted that only the C1 domains from DGKs β and γ could bind DAG while other DGK C1 domains were sufficiently different from those in PKCs that they might not bind DAG. Supporting the possibility that DGK C1 domains might serve alternative functions, the C1 domains of some DGKs, like those in other proteins, can act as protein-protein interaction sites. Indeed, the C1 domains of DGKζ associate with β-arrestins,[56] and they bind directly to Rac1.[57] It will be enlightening to test the phorbol ester binding capacity of all DGK C1 domains and to solve their crystal structures so that we can understand the differences between the C1 domains of DGKs and other proteins that contain them.

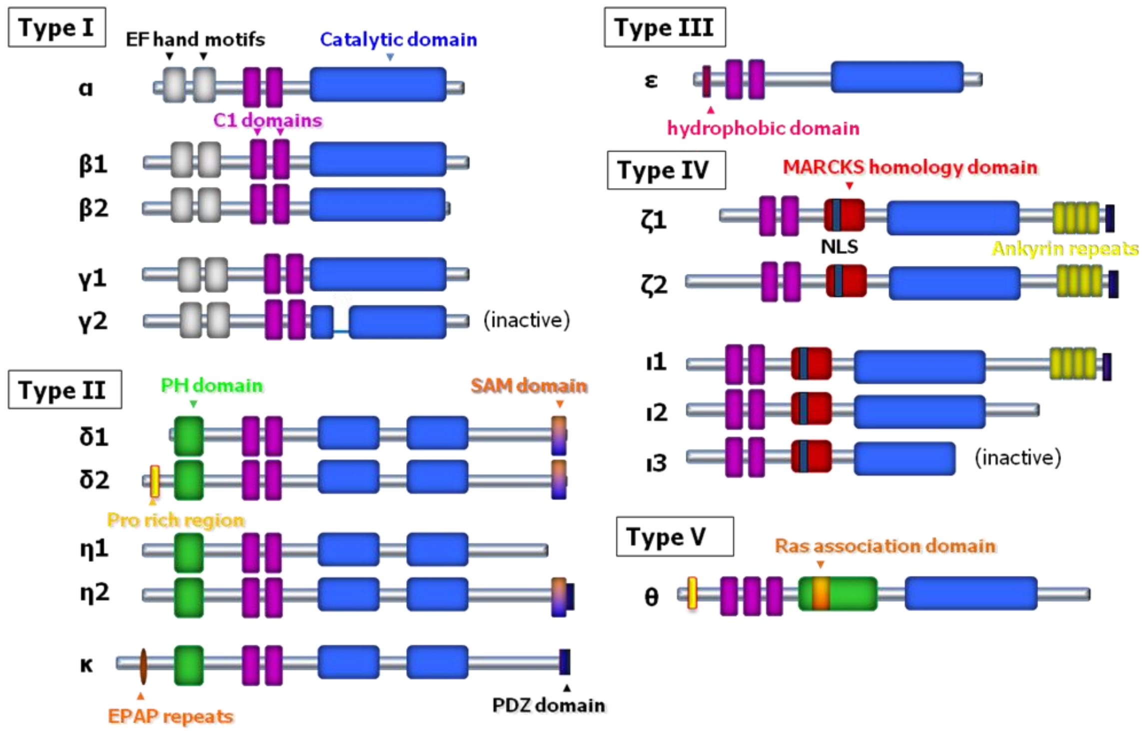

Figure 1.4. The mammalian DGK family. Based on structural motifs, the ten mammalian DGKs are divided into five subtypes. Alternative splicing of some DGK isotypes generates even more structural diversity. Alternative splicing variants are designated by a number following the Greek letter. Many of the DGKs contain other unique structural domains that are not shown. Reprinted with permission from "Shulga Y.V., Topham M.K., Epand R.M. (2011) Regulation and functions of diacylglycerol kinases. *Chem Rev.* 111(10):6186-208". Copyright (2011) American Chemical Society.

The catalytic domains in DGKs are composed of accessory and catalytic subunits. In most cases, these subunits are joined to create an uninterrupted catalytic domain. However, in the type II DGKs δ, η and κ [49, 58, 59] these domains are separated by a long peptide sequence that does not have any apparent functional motif. Each catalytic subunit has an ATP binding site where mutation of a glycine in this motif to an aspartate or alanine renders the DGK kinase dead.[60-62] Evidence suggests that some DGK catalytic domains may also require other motifs for maximal activity because catalytic domains from DGKs ε, ζ, and θ have very little DGK activity when expressed as isolated subunits (M.K.T. and R.M.E unpublished observations and[52]), although the isolated catalytic domain of DGKα retained about 1/3 the activity of a fully active DGKα N-terminal truncation mutant.[55] Thus, it appears that unlike bacterial DGK, several mammalian DGK catalytic domains require other motifs for maximal activity. It is possible that these other motifs somehow function in coordination with the catalytic domain.

In addition to the C1 and catalytic domains, DGKs contain other structural domains that form the basis of the five subtypes. In general, these other domains help regulate the level of kinase activity and/or the localization of the enzyme. For example, type I DGKs, α, β, and γ, have calcium-binding EF hand motifs that make these enzymes more active in the presence of calcium. Evidence from mutational studies indicates that when the EF hand motifs of DGKα bind calcium, a conformational change occurs that allows membrane association and activation of the enzyme.[63] Type II DGKs, δ, η, and κ, have pleckstrin homology (PH) domains near their amino termini. This domain in DGKδ has been shown to bind weakly and non-selectively to phosphatidylinositols,[64, 65] but binding these lipids did not significantly affect its activity.[64] DGKs δ and η also have a sterile alpha motif (SAM) at their carboxy termini. A recent study shows that SAM domains of DGKδ bind zinc at multiple sites and might allow DGKδ to form oligomers.[66] Mutant of DGKδ, containing a SAM domain refractory to zinc binding, exhibits partially impaired localization to the cytoplasmic puncta and enhanced localization to the plasma membrane in response to TPA stimulation, thus suggesting that zinc may play an important role in the assembly and physiology of DGKδ.[66] There is also further evidence that SAM domain interactions sequester DGKδ away from membranes to limit its access to diacylglycerol.[67]

The only type III DGK, ε, does not have identifiable structural motifs outside of its C1 and catalytic domains. It is also the only mammalian DGK isoform with a hydrophobic segment that comprises approximately residues 20-40 and promotes attachment of the protein to membranes.[68] In the work presented in Chapter 2, we showed that the hydrophobic segment of FLAG-DGKε has a U-bent conformation that determines the deep insertion of this protein into the cell membranes. Thus, we concluded that FLAG-DGKε is a monotopic enzyme with both the C and N-terminus of the protein oriented on the cytoplasmic side of the membrane. The single residue mutation P32A in the middle of the hydrophobic segment of FLAG-DGKε changes the topology of this segment, causing it to protrude through the membrane. Further studies using *in vitro* translation in the presence of dog pancreas rough microsomes showed that the topology of this N-terminal hydrophobic segment in DGKε depends on the presence of FLAG-tag, and that the native DGKε without FLAG-tag attains a bitopic rather than a monotopic structure in this experimental system.[69]

Type IV DGKs, ζ and ι, have a motif enriched in lysines and arginines that acts as a nuclear localization signal and is a substrate for conventional PKCs. This motif is homologous to the phosphorylation site domain of the myristoylated alanine rich C kinase substrate (MARCKS) protein and phosphorylation of this domain limits nuclear localization of these DGKs. The ζ and ι DGK isoforms also have four ankyrin repeats and a PDZ binding motif at their carboxy termini that may be sites of protein-protein interactions. The only type V DGK, θ, is distinguished by three C1 domains, a PH domain, and a Ras-association domain within the PH domain. To date, no binding partners for the PH and Ras-association domains have been identified.

2.3. Organ distribution

Most tissues express several different DGK isoforms, and even within the same cell type, more than one DGK isoform can exist. For example, all known DGK isoforms were detected in mouse brain extracts,[70] and at least six DGK isoforms are expressed in mouse embryo fibroblasts (unpublished observations). In general, when several DGKs are expressed in tissues or cells, they are from different subfamilies, suggesting that each subfamily carries out a distinct biological function. But because no one has assayed the relative expression levels of the DGK family in a systematic way it is difficult to directly compare the expression levels of DGK isoforms in each tissue. However, one way to compare the levels of DGKs in tissues is to examine the frequency at which cDNA clones – called expressed sequence tags (ESTs) – of each DGK are identified in cDNA libraries prepared from different tissues. This information is available at the National Center for Biotechnology Information (NCBI, www.ncbi.nlm.nih.gov), which collects EST profile data. It should be noted that these data only approximate the levels of DGK mRNA in a given tissue and are not meant to be definitive. Given that caveat, this database suggests that most tissues express at least one member of each DGK subfamily, with brain and hematopoeitic organs particularly enriched in DGKs. The EST data also suggests that DGKs α and ζ are the most commonly expressed isoforms, with both of them being expressed in almost every tissue examined. Conversely, DGKs β, κ, and ι are expressed at much lower levels and in fewer tissues compared to other DGK isoforms. DGKβ, for example, is expressed predominantly in nerves and brain, indicating an important role for this isoform in neural tissue. Because of the fairly ubiquitous expression patterns of most DGK isoforms, it is perhaps more interesting to consider outliers in this dataset such as tissues that express a single DGK isoform or only a few DGKs. The limited DGK expression profile in these tissues probably suggests that the DGKs that are expressed have particularly important functions. For example, according to EST profile data, DGKε is the only DGK isoform that has been identified in adipose tissue, DGKγ is the only isoform isolated from pituitary tissue, only DGKs α and θ have been identified in bone marrow, and DGKs α, δ, and ζ are the most abundant isoforms in lymphocyte-rich tissues such as lymph nodes, spleen, and thymus. Alternatively, no DGK ESTs have been isolated from parathyroid tissue, suggesting that DGK activity might be dispensable in parathyroid glands. In Chapter 7 we discuss our study of DGK expression in murine adipose tissue and 3T3-L1 cultured adipocytes. In contrast to EST data, we found that DGKε is not the only isoform expressed in adipocytes, but rather seven isoforms are present in this type of cells. We also showed that DGK expression levels change dramatically during adipocyte differentiation. Further, there was a significant difference in the expression levels of several DGK isoform in adipocytes isolated from diabetic mice in comparison with control mice, implicating a possible role for this enzyme in type 2 diabetes melitus.

2.4. Subcellular distribution

DGKs have been identified in a number of cell compartments, including the nucleus (Fig. 1.5). Their localization within the nucleus is not surprising because it has a phosphatidylinositol cycle that is regulated separately from plasma membrane phosphatidylinositol signaling.[71] DGKs α, ζ, and ι shuttle into and out of the nucleus,[47, 62, 72, 73] while a significant fraction of DGKθ localizes there constitutively.[74] These nuclear DGKs appear to be confined to separate, distinct regions of the nucleus: DGKs θ, ζ and ι have been identified in discrete, unidentified regions within the body of the nucleus,[62, 72, 74, 75] while DGKα appeared to predominantly localize around its periphery.[47]

In addition to localizing within the nucleus, DGKs are also found throughout other parts of the cell (Fig. 1.5). Most of them are at least partly localized at the plasma membrane either constitutively – in the case of DGKκ[49] – or following stimulation with specific agonists. For example, DGKα translocates to the plasma membrane following engagement of the T cell receptor,[76] DGKδ1 translocates there upon exposure to phorbol esters,[77] and DGKs ζ and θ are found at the plasma membrane following activation of some G protein-coupled receptors.[78, 79] Presumably, their function at the plasma membrane is to attenuate DAG signaling initiated by specific receptors.

In addition to the plasma membrane, DGK activity has been detected in cell fractions containing cytoskeleton components along with other proteins involved in cytoskeleton dynamics.[80] Consistent with this, DGKθ was found to associate with RhoA,[81] DGKβ co-localized with actin filaments,[82] and DGKζ interacted with several proteins involved in actin dynamics.[35] In most cases, the physiological significance of their interactions with cytoskeleton components is not entirely clear, but there are data demonstrating that DGKs can modulate cytoskeleton remodeling. For example, DGK inhibitors augmented platelet secretion and aggregation,[83] and DGKζ is involved in actin dynamics.[48] DGKs have also been found to co-localize with organelles. DGKγ, for example, co-localizes with the Golgi,[82] DGKδ appear to reside in the endoplasmic reticulum,[61] and DGKs δ and η have been found to be localized on endosomes.[84] In Chapter 2 we studied the subcellular distribution of DGKε isoform and showed that it is localized in both ER and plasma membrane in COS-7 cells.

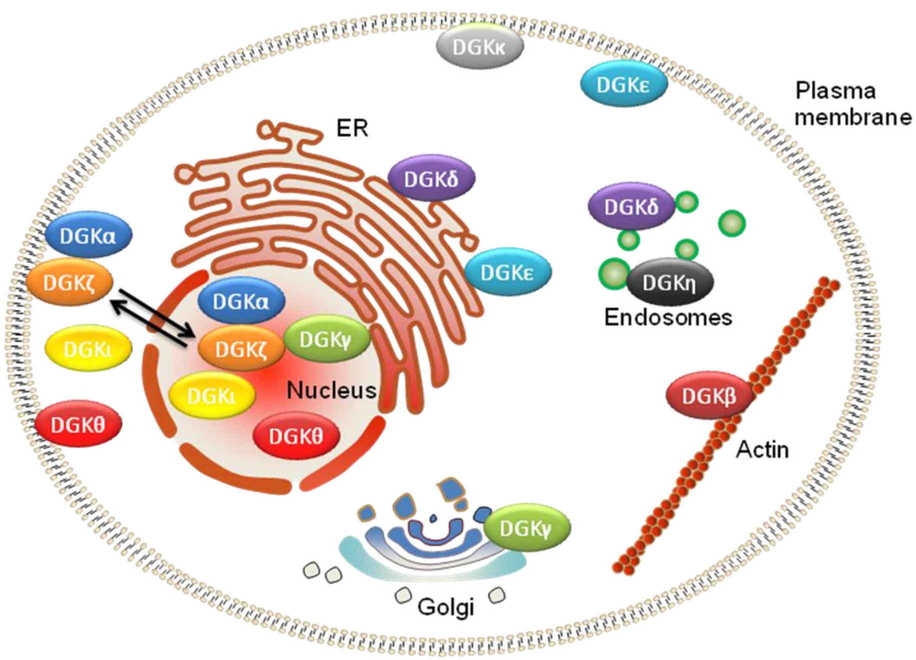

Figure 1.5. Cell distribution of mammalian DGKs. Reprinted with permission from "Shulga Y.V., Topham M.K., Epand R.M. (2011) Regulation and functions of diacylglycerol kinases. *Chem Rev.* 111(10):6186-208". Copyright (2011) American Chemical Society.

2.5. DGK epsilon and its role in the PtdIns cycle

DGK epsilon isoform is the smallest known mammalian DGK (64 kDa) and it is unique in several aspects among other DGKs. Despite its lack of identifiable regulatory domains, DGKε is the only DGK that displays specificity toward acyl chains of DAG. Previously it was shown that DGKε dramatically prefers DAGs with an arachidonoyl group at the *sn*-2 (middle) position of the glycerol backbone.[33, 85] In Chapter 5 we tested the acyl chain specificity of DGKε in more details, particularly for the *sn*-1 position of DAG. We showed that DGKε exhibits a similar activity with 1,2-diarachidonoyl-DAG (20:4/20:4-DAG) in comparison with 1-stearoyl-2-arachidonoyl-DAG (18:0/20:4-DAG). Surprisingly, we found that DGKε exhibits higher activity with 18:2/18:2-DAG than with 18:0/18:2-DAG *in vitro*, although it was a common believe that DGKε has a preference for 18:0 acyl chain at the *sn*-1 position.

It is intriguing, that there is no identified distinct domain responsible for the substrate recognition and specificity of DGKε. Nevertheless, in Chapter 4 we discuss the region, located in the accessory domain of DGKε, that we demonstrated to be important for DGKε specificity for arachidonoyl-DAGs. We identified a motif L-$X_{(3-4)}$-R-$X_{(2)}$-L-$X_{(4)}$-G, in which -$X_{(n)}$- represents n residues of any amino acids, that is very similar to that in lipoxygenases, an enzyme family that catalyze the formation of fatty acid hydroperoxides from polyunsaturated fatty acids.[86, 87] We found that mutations of the essential residues in this motif result in the loss of arachidonoyl specificity. Furthermore, when DGKα was mutated so that it gained the identified motif, the enzyme also gained some specificity for arachidonoyl-DAG.

DGKε preference for arachidonoyl-DAG suggests that it may be a component of the biosynthetic pathway that accounts for the enrichment of PtdIns(4,5)P_2 with arachidonic acid.[88] All of the lipid intermediates in the PtdIns-cycle are enriched in arachidonoyl groups in the *sn*-2 position. Both the substrate and product of the reaction catalyzed by DGK – DAG and PtdOH – are intermediates in the PtdIns -cycle (Fig. 1.2). Hence the DGK-catalyzed step is a fundamental step in the PtdIns-cycle. Recently lipidomics analysis has been carried out to compare the acyl chain composition of the major phospholipids in normally proliferating mouse embryonic fibroblasts (MEFs) derived from wild type versus DGKε or DGKα knockout mice.[31] Dramatic differences between wild-type and DGKε knock out cells in arachidonate-containing lipids were observed for multiple classes of glycerophospholipids and poly-phospoinositides. The peaks from mass spec are identified by their mass/charge ratio and presented in the form X:Y where X is the total number of carbon atoms and Y the total number of double bonds in both acyl chains of the phospholipid. The lipidomics data demonstrated that the 38:4 species of phosphoinositides decreased from 33% of the total cellular phosphoinositides in the wild type cells to 24% in the DGKε knock out cells, a significant decrease of 27%.[31] Further, 18:0 (stearoyl)-containing phosphoinositides decreased by 29% in DGKε knock out cells compared with the wild type samples ($p<0.01$).[89] This is in contrast to the observation that despite the similarity between 16:0 and 18:0 acyl chains, deletion of DGKε results in a larger decrease in 18:0 compared with 16:0 phosphoinositides, supporting DGKε's selectivity for an *sn*-1 stearoyl acyl chain of DAG[89] in addition to the arachidonoyl specificity for the *sn*-2 position. These results provide *in vivo* evidence of

DGKε's selectivity for DAG with a 1-stearoyl-2-arachidonoyl acyl chain composition results in the enrichment of phosphoinositides with this acyl chain composition. Hence, DGKε can affect phosphoinositides that are neither substrates nor products of the DGK reaction but are influenced by DGKε through the PtdIns-cycle.

In contrast to the observations with DGKε, no differences in the acyl chain composition of any phospholipid class or DAG were observed between wild-type and DGKα knock out cells. There was also no significant difference in the concentrations of any of the DAG species between the wild-type and DGKε knock out MEFs. However, the cells from the DGKα knock out mice had a higher concentration of DAG, consistent with the lack of down regulation of the major fraction of DAG because of the absence of DGKα. This is in contrast with DGKε that is primarily responsible for enrichment of only a fraction of PPIn, i.e. species with arachidonoyl acyl chains.

One of the proposed roles of DGK in regulating metabolism has been suggested to be the removal of the signaling lipid DAG. The results with the DGKα knockout MEFs are in accord with this explanation, since removal of this isoform results in a slower loss of DAG and hence an increase in its concentration. We anticipate that this effect is typical of most, if not all, mammalian isoforms of DGK, apart from DGKε, because these isoforms phosphorylate all forms of DAG with equal rates. This is not the case, however, for DGKε that has specificity for catalyzing the phosphorylation of arachidonoyl-DAG.

Another observation, that goes counter to the hypothesis that the sole function of DGK is to down-regulate the DAG signal, comes from observations that electrical stimulation of the brains of mice leads to a transient increase in arachidonoyl-containing

DAG.[85] Interestingly, this increase is greater in wild type mice compared with DGKε-knockout mice. Again this observation is contrary to the concept of DGK lowering the level of DAG. However, the observation would be consistent with the idea that removing DGKε slows the PtdIns-cycle and hence results in the lowering of all the intermediates in the cycle. In Chapter 3 we discuss the involvement of DGKε in PtdIns-cycle in more details.

We can thus conclude that whatever the details of the regulation of lipid intermediates of the PtdIns-cycle, it is clear that DGKε, but not other isoforms of DGK, is the predominant enzyme that catalyzes the step of the PtdIns-cycle in which 1-stearoyl-2-arachidonoyl-DAG is phosphorylated to 1-stearoyl-2-arachidonoyl-PtdOH.

2.6. Role of PtdOH derived from DGK activity

PtdOH itself has a broad array of signaling properties that are very distinct from those of DAG. For example, PtdOH can bind and regulate numerous proteins including phosphatidylinositol-4-phosphate 5-kinase,[90] RasGAP,[91] Raf-1 kinase,[92] p21-activated kinase 1,[93] mammalian target of rapamycin (mTOR),[94] atypical PKCs,[95] p47phox,[96] sphingosine kinase,[97] the transcriptional repressor Opi1p,[98] and the catalytic subunit of protein phosphatase-1.[99] As such, their ability to generate PtdOH suggests that DGKs might also influence biological events not only by metabolizing DAG but also by producing PtdOH. This would not be surprising based on what is known about PtdOH signaling in plants. Seven DGK genes (AtDGK1-7) have been identified in *Arabidopsis thaliana,*[100] and in rice there are eight putative DGK isoforms.[101] In plants, numerous PtdOH targets have been identified[102] and they vastly outnumber DAG targets, so it has been hypothesized that the primary role of DGKs in plants is to generate PtdOH rather than to consume DAG.[103] PtdOH in plants is usually produced in response to stress, suggesting that DGKs might influence the stress response. Supporting this possibility, expression of plant DGKs is induced in response to stresses such as wounding, chemicals, and fungal infection,[100, 101] and over-expression of a rice DGK in tobacco plants enhanced the resistance of those plants to disease.[101] Although it is not clear exactly how plant DGKs are protective in conditions of stress, they are probably critical effectors in the stress response.

Given their potential role in PtdOH signaling in plants, it was not surprising that mammalian DGKs appear to modulate proteins by producing PtdOH. One example of this mechanism is the ability of DGKζ to modulate the activity of phosphatidylinositol-4-phosphate 5-kinase (PIP5K) α. The PIP5K enzymes are potently activated by PtdOH[104] and DGK activity was found to co-immunoprecipitate with a complex that included a PIP5K.[80] Together, these observations suggested that DGKs might modulate PIP5K activity by generating PtdOH. Indeed, DGKζ co-localized and co-immunoprecipitated with PIP5Kα, and its expression dramatically promoted the generation of PtdIns(4,5)P_2 in cells.[35] A kinase dead DGKζ also co-immunoprecipitated with the PIP5K, but failed to enhance its activity. Collectively, these data indicate that localized PtdOH generation, rather than a conformational change mediated by association of the PI4P5K with DGKζ, augmented PIP5K activity.

In a separate study, DGKζ was shown to mediate DAG signaling downstream of the M1 muscarinic receptor (M1R), a seven-transmembrane receptor (GPCR).[56, 78] Its translocation to M1R required binding to β-arrestins – which are scaffolding proteins that bind GPCRs. It was subsequently shown that PIP5Kα also translocated to GPCRs by binding to β-arrestins, and its function at the GPCR was to promote internalization of the receptor.[79] Since DGKζ also binds β-arrestins, this collection of observations raises the possibility that DGKζ might function in this complex not only to metabolize DAG, but also to promote PIP5K activity by generating PtdOH. This would provide a two-step mechanism to shut down the M1R receptor, where DGKζ first metabolizes DAG to reduce this signaling lipid, and then the PtdOH that it produces activates the PIP5K enzyme in order to promote receptor internalization. This hypothetical model has not been specifically tested, but it agrees with data showing that transgenic over-expression of DGKζ in mouse myocardium protects the mice against cardiac hypertrophy initiated by excessive activation of a GPCR.[105]

The serine/threonine kinase mammalian target of rapamycin (mTOR) is an important intermediate in several pathways that manage cellular responses to environmental stress. Its activity is regulated, in part, by PtdOH, which appears to compete with rapamycin for a binding site on mTOR. There is strong evidence indicating the phospholipase D (PLD) isoforms are largely responsible for providing the pool of PtdOH that activates mTOR.[106] But there is evidence that DGKζ might also activate mTOR under some circumstances. For example, overexpression of DGKζ, but not DGKα, led to enhanced, serum-induced phosphorylation of p70 S6 kinase (p70S6K) – a major downstream target of mTOR – and rendered the cells resistant to the effects of rapamycin.[36] PtdOH appeared to be important in this mechanism to activate mTOR, because DGKζ could not promote activation of a mutant mTOR that had reduced ability to bind PtdOH. The target of PtdOH produced by DGKζ, however, is not clear because another report showed in the same cell line that inhibiting PLD almost completely abolished serum-induced S6 kinase activity, indicating that PLD is largely responsible for activating mTOR.[94] It is possible then that instead of directly activating mTOR, DGKζ instead activates PIP5Ks, which could provide PtdIns(4,5)P_2, an important activator of PLD enzymes.[107] Regardless of the mechanism, these data suggest that DGKζ can potentially activate mTOR and that it does so by producing PtdOH.

Finally, there is evidence that DGKs might regulate additional cell responses through their ability to modulate the levels of PtdOH. But the targets of PtdOH in these cases are not as well defined. For example, compound mutant mice lacking both DGKζ and DGKα have defects in T cell development that can be partially rescued by exogenous PtdOH.[108] And defective Toll-like receptor (TLR) signaling in macrophages from DGKζ deficient mice was rescued by addition of exogenous PtdOH.[109] The role of PtdOH is not clear, but it might be necessary to inhibit PI3Ks, which were excessively active in the DGKζ deficient cells. Finally, a recent report suggested that PtdOH derived from DGKα influenced neutrophil responses to anti-neutrophil cytoplasmic antibodies.[110] Collectively, these observations indicate that DGKs α and ζ regulate immune cell function not only by influencing DAG levels, but also by producing PtdOH.

3. Phosphatidylinositol-4-phosphate 5-kinases (PIP5K)

Phosphatidylinositol-4-phosphate 5-kinase (PIP5K) supposedly accounts for more than 95% of the total synthesis of PtdIns(4,5)P_2 from PtdIns4*P*. Up to date, three isoforms of PIP5Ks, α, β and γ, are identified. In 1996, mouse and human PIP5K isoforms were cloned independently by two laboratories,[111, 112] which led to the confusion in the nomenclature of the human and mouse PIP5K isozymes, with human α corresponding to mouse β, and human β corresponding to mouse α. Recently this discrepancy was corrected in the National Center for Biotechnology Information (NCBI) database, where the nomenclature corresponding to the human enzyme was accepted. Therefore, in this work I follow the NCBI guidelines and hereafter refer to human PIP5Kα/mouse PIP5Kβ as PIP5Kα, and human PIP5Kβ/mouse PIP5Kα as PIP5Kβ.

Each PIP5K isoform produces multiple splicing variants.[7, 111-113] The catalytic domain of PIP5K was identified in the center of the protein, with about 80% identity of its amino acid sequence between three isoforms.[113, 114] The N- and C-terminal domains outside of the catalytic domain are less conserved among the PIP5K isoforms. For example, the splicing variants of PIP5Kγ contain a different number of additional amino acids at the C-terminus. Therefore, the difference in N- and C-terminal regions of the PIP5Ks is likely to be responsible for generating functions that are specific for each splicing variant. One example of such function is selective binding of talin and AP-2 by the C-terminal domain of PIP5Kγ661, which are required for the regulation of focal adhesion assembly and the clathrin-dependent endocytosis.[115, 116]

3.1. Cell and tissue distribution of PIP5Ks

While PIP5K isoforms are shown to co-express in most tissues, each isoform also exhibits an individual tissue distribution. Thus, PIP5Kα is abundant in skeletal muscles, PIP5Kβ – in the heart, and PIP5Kγ is highly expressed in the brain. Therefore, it was suggested that PIP5Ks have not only overlapping biological roles, but isoform specific functions as well, when isoforms cannot compensate for each other.[117, 118] For example, isoform α of PIP5K is involved in cytoskeleton rearrangements and actin dynamics.[119, 120] PIP5Kβ is implicated in the formation of clathrin-coated pits during receptor endocytosis.[121] PIP5Kγ is shown to play a critical role for the assembly of focal contacts and cell–cell contacts.[115, 122, 123]

This idea is also supported by the fact that each PIP5K isoform localizes to distinct subcellular compartments. PIP5Kα localizes to the Golgi complex and, upon stimulation, to the plasma membrane. It is also concentrated at sites of membrane ruffling formed in response to the Rho GTPase Rac. PIP5Kα has also been detected in the nuclear speckles.[124] PIP5Kβ localizes to the plasma membrane and to punctate structures in the perinuclear region.[120] Different splicing variants of PIP5Kγ have been shown to have distinct cellular localizations. Thus, PIP5Kγ661 localizes to focal adhesions[115, 125] and to adherens junctions in epithelial cells.[126] Exogenously expressed PIP5Kγ635 has been observed in the cytosol. PIP5Kγ700 have been shown to localize to the nucleus, and PIP5Kγ707 – to punctate structures in the cytosol.[127]

3.2. Regulation of PIP5K activity by other proteins

Regulation of PIP5Ks by the small GTPases of the Rho family is important for actin cytoskeleton rearrangements, since PtdIns(4,5)P_2 regulates cytoskeletal dynamics through interactions with actin-capping proteins, talin, vinculin, and α-actinin. PIP5K is suggested to be a downstream effector of Rho activation in mammalian cells.[128] The activation of PIP5K likely occurs not through a direct interaction between PIP5K and Rho, but rather through Rho kinase (ROCK), which has been implicated in the PIP5K activation.[129]

In contrast, Rac was shown to regulate PIP5K localization and activity through a direct interaction with all PIP5K isoforms in a GTP-independent manner.[130] Furthermore, it seems that there is a feedback regulation of Rac by the product of PIP5K, PtdIns(4,5)P_2, that can affect the localisation and activity of Rac.

PIP5K activity is also regulated by ADP-ribosylation factors (ARFs), a family of small GTPases that control membrane trafficking and actin cytoskeletal dynamics.[131] The mammalian Arf family comprises six gene products, Arf1–Arf6, and based on the sequence homology they are divided into three classes.[132] PIP5K is shown to be stimulated by different Arf isoforms depending on the types of cells. Thus, ARF1 and ARF6 activate PIP5K in the presence of PtdOH in HeLa cells and HL60 cells respectively.[133, 134]

Several observations suggest that PIP5K is phosphorylated during the cell resting state, and dephosphorylated or further phosphorylated upon cell stimulation, a process that is controlled by agonists and cell stresses.[114] All three PIP5K isoforms are capable of autophosphorylation, which was shown to be enhanced by PtdIns, leading to inhibition of PIP5K lipid kinase activity.[135] The phosphorylation/dephosphorylation process also regulates the binding of talin to PIP5Kγ661,[136] since talin can interact with the dephosphorylated form, but not the phosphorylated form of PIP5Kγ661. Talin affects cell signaling and adhesion through binding to integrin and altering the affinity of integrin for its ligand. Therefore, the phosphorylation/dephosphorylation of PIP5Kγ661 by multiple kinases and phosphatases regulates the focal adhesion assembly and disassembly events.

3.3. Regulation of PIP5K activity by phosphatidic acid

Enzymatic activity of all three PIP5Ks was shown to be activated by PtdOH, produced either through PLD or several isoforms of DGK.[104, 113, 137] Furthermore, PLD2 and DGKζ were demonstrated to colocalize substantially with PIP5K in the cell.[35, 138] Feed-forward loop model was proposed to describe the interaction of these enzymes, where ARF6 activates PLD to generate PtdOH, and PIP5K to generate PtdIns(4,5)P_2 (Fig. 1.6). Resulting increased synthesis of PtdOH further activates PIP5K, leading to increased synthesis of PtdIns(4,5)P_2, which further activates PLD. This PLD-PIP5K loop may play an important role in driving clathrin- and non-clathrin-mediated endocytosis by changing the local concentrations of PtdIns(4,5)P_2 and PtdOH at the membrane.[139, 140]

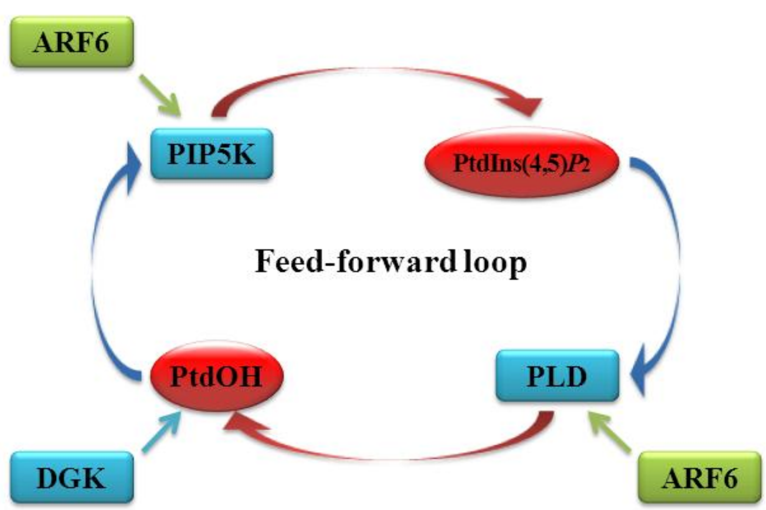

Figure 1.6. A proposed model for a feed-forward loop regulating production of PtdOH and PtdIns(4,5)P_2. Lipid enzymes are shown in blue and lipid products in red. Red arrows indicate conversion to a lipid product, while blue arrows indicate activation of a downstream protein. ARF6, activating enzymes PLD and PIP5K, is shown in green.

Multiple domains of PIP5K were demonstrated to bind PtdOH directly through both ionic and hydrophobic interactions.[141] Further, comparison of several PtdOH with shorter saturated acyl chains and one di-unsaturated PtdOH showed the preference of murine PIP5Kα for the latest.[141] Nevertheless, in all previous reports the importance of choice of the substrate PtdIns4*P* for the extent of PIP5K activation by PtdOH was ignored, leading to varying results. In Chapter 6 we showed that all three isoforms of PIP5Ks discriminate between the acyl chains of the substrate, although with a different degree, and that the activation by PtdOH is dependent on the used substrate. We also studied in more details the PIP5K sensitivity for the acyl chain composition of PtdOH and demonstrated that PIP5K has preference for the PtdOH with two unsaturated fatty acids. Therefore, it seems possible that the acyl chain preference of PIP5Ks for the activator PtdOH and the substrate PtdIns4*P* may regulate the production of PtdIns(4,5)P_2 species, required for proper downstream cascades. This may be an important factor, determining the involvement of different PtdIns(4,5)P_2 species in cellular events.

References

1. Chuang, D. M. Neurotransmitter Receptors and Phosphoinositide Turnover. *Annu. Rev. Pharmacol. Toxicol.* **29**, 71-110 (1989).

2. Hilgemann, D. Local PIP_2 signals: when, where, and how? *Pflugers Arch.* **455**, 55-67 (2007).

3. Robert H., M. Inositol phospholipids and cell surface receptor function. *Biochim. Biophys. Acta* **415**, 81-147 (1975).

4. Thompson, W., Strickland, K. P. & Rossiter, R. J. Biosynthesis of phosphatidylinositol in rat brain. *Biochem. J.* **87**, 136-142 (1963).

5. Hokin, L. E. & Hokin, M. R. The incorporation of 32P from triphosphate into polyphosphoinositides [γ-32P]adenosine and phosphatidic acid in erythrocyte membranes. *Biochim. Biophys. Acta* **84**, 563-575 (1964).

6. Laux, T. *et al*. GAP43, MARCKS, and CAP23 Modulate PI(4,5)P2 at Plasmalemmal Rafts, and Regulate Cell Cortex Actin Dynamics through a Common Mechanism. *J. Cell Biol.* **149(7)**, 1455-1472 (2000).

7. Itoh, T., Ijuin, T. & Takenawa, T. A Novel Phosphatidylinositol-5-phosphate 4-Kinase (Phosphatidylinositol-phosphate Kinase IIgamma) Is Phosphorylated in the Endoplasmic Reticulum in Response to Mitogenic Signals. *J. Biol. Chem.* **273**, 20292-20299 (1998).

8. Boronenkov, I. V. & Anderson, R. A. The Sequence of Phosphatidylinositol-4-phosphate 5-Kinase Defines a Novel Family of Lipid Kinases. *J. Biol. Chem.* **270**, 2881-2884 (1995).

9. Castellino, A. M., Parker, G. J., Boronenkov, I. V., Anderson, R. A. & Chao, M. V. A Novel Interaction between the Juxtamembrane Region of the p55 Tumor Necrosis Factor Receptor and Phosphatidylinositol-4-phosphate 5-Kinase. *J. Biol. Chem.* **272**, 5861-5870 (1997).

10. Brose, N. & Rosenmund, C. Move over protein kinase C, you've got company: alternative cellular effectors of diacylglycerol and phorbol esters. *J. Cell. Sci.* **115**, 4399-4411 (2002).

11. Sbrissa, D., Ikonomov, O. C. & Shisheva, A. PIKfyve, a Mammalian Ortholog of Yeast Fab1p Lipid Kinase, Synthesizes 5-Phosphoinositides. *J. Biol. Chem.* **274**, 21589-21597 (1999).

12. Irvine, R. F. 20 years of Ins(1,4,5)P3, and 40 years before. *Nat. Rev. Mol. Cell Biol.* **4**, 580-585 (2003).

13. Auger, K. R., Serunian, L. A., Soltoff, S. P., Libby, P. & Cantley, L. C. PDGF-dependent tyrosine phosphorylation stimulates production of novel polyphosphoinositides in intact cells. *Cell* **57**, 167-175 (1989).

14. Whitman, M., Downes, C. P., Keeler, M., Keller, T. & Cantley, L. Type I phosphatidylinositol kinase makes a novel inositol phospholipid, phosphatidylinositol-3-phosphate. *Nature* **332**, 644-646 (1988).

15. Fruman, D. A., Meyers, R. E. & Cantley, L. C. Phosphoinositide kinases. *Annu. Rev. Biochem.* **67**, 481-507 (1998).

16. Wymann, M. P. & Pirola, L. Structure and function of phosphoinositide 3-kinases. *Biochim. Biophys. Acta* **1436**, 127-150 (1998).

17. Vanhaesebroeck, B. *et al*. Synthesis and function of 3-phosphorylated inositol lipids. *Annu. Rev. Biochem.* **70**, 535-602 (2001).

18. Dituri, F., Mazzocca, A., Giannelli, G. & Antonaci, S. PI3K Functions in Cancer Progression, Anticancer Immunity and Immune Evasion by Tumors. *Clin. Dev. Immunol.* **2011** (2011).

19. Fortin, C. F. *et al*. A class IA PI3K controls inflammatory cytokine production in human neutrophils. *Eur. J. Immunol.* **41**, 1709-1719 (2011).

20. Martin, A. L., Schwartz, M. D., Jameson, S. C. & Shimizu, Y. Selective Regulation of CD8 Effector T Cell Migration by the p110gamma Isoform of Phosphatidylinositol 3-Kinase. *The Journal of Immunology* **180**, 2081-2088 (2008).

21. Upshaw, J. L. & Leibson, P. J. NKG2D-mediated activation of cytotoxic lymphocytes: Unique signaling pathways and distinct functional outcomes. *Semin. Immunol.* **18**, 167-175 (2006).

22. Lanier, L. L. Up on the tightrope: natural killer cell activation and inhibition. *Nat. Immunol.* **9**, 495-502 (2008).

23. Schultze, S. M., Hemmings, B. A., Niessen, M. & Tschopp, O. PI3K/AKT, MAPK and AMPK signalling: protein kinases in glucose homeostasis. *Expert Reviews in Molecular Medicine* **14** (2012).

24. Kossila, M. *et al*. Gene encoding the catalytic subunit p110beta of human phosphatidylinositol 3-kinase: cloning, genomic structure, and screening for variants in patients with type 2 diabetes. *Diabetes* **49**, 1740-1743 (2000).

25. Baynes, K. C. *et al*. Natural variants of human p85 alpha phosphoinositide 3-kinase in severe insulin resistance: a novel variant with impaired insulin-stimulated lipid kinase activity. *Diabetologia* **43(3)**, 321-331 (2000).

26. Fruman, D. A. *et al*. Hypoglycaemia, liver necrosis and perinatal death in mice lacking all isoforms of phosphoinositide 3-kinase p85alpha. *Nat. Genet.* **26**, 379-382 (2000).

27. Pessin, M. S. & Raben, D. M. Molecular species analysis of 1,2-diglycerides stimulated by alpha-thrombin in cultured fibroblasts. *J. Biol. Chem.* **264**, 8729-8738 (1989).

28. Pettitt, T. R. & Wakelam, M. J. Bombesin stimulates distinct time-dependent changes in the sn-1,2-diradylglycerol molecular species profile from Swiss 3T3 fibroblasts as analysed by 3,5-dinitrobenzoyl derivatization and h.p.l.c. separation. *Biochem. J.* **289 (2)**, 487-495 (1993).

29. Holbrook, P. G., Pannell, L. K., Murata, Y. & Daly, J. W. Molecular species analysis of a product of phospholipase D activation. Phosphatidylethanol is formed from phosphatidylcholine in phorbol ester- and bradykinin-stimulated PC12 cells. *J. Biol. Chem.* **267**, 16834-16840 (1992).

30. Lee, C., Fisher, S. K., Agranoff, B. W. & Hajra, A. K. Quantitative analysis of molecular species of diacylglycerol and phosphatidate formed upon muscarinic receptor activation of human SK-N-SH neuroblastoma cells. *J. Biol. Chem.* **266**, 22837-22846 (1991).

31. Milne, S. B. *et al*. Dramatic differences in the roles in lipid metabolism of two isoforms of diacylglycerol kinase. *Biochemistry* **47(36)**, 9372-9379 (2008).

32. Tang W., Bunting M., Zimmerman G. A., McIntyre T. M. & Prescott S. M. Molecular cloning of a novel human diacylglycerol kinase highly selective for arachidonate-containing substrates. *J. Biol. Chem.* **271**, 10237-10241 (1996).

33. Walsh, J. P., Suen, R., Lemaitre, R. N. & Glomset, J. A. Arachidonoyl-diacylglycerol kinase from bovine testis. Purification and properties. *J. Biol. Chem.* **269**, 21155-21164 (1994).

34. Cai, J., Abramovici, H., Gee, S. H. & Topham, M. K. Diacylglycerol kinases as sources of phosphatidic acid. *Biochim. Biophys. Acta* **1791**, 942-948 (2009).

35. Luo, B., Prescott, S. M. & Topham, M. K. Diacylglycerol kinase zeta regulates phosphatidylinositol 4-phosphate 5-kinase Ialpha by a novel mechanism. *Cell Signal.* **16(8)**, 891-897 (2004).

36. Avila-Flores, A., Santos, T., Rincón, E. & Mérida, I. Modulation of the mammalian target of rapamycin pathway by diacylglycerol kinase-produced phosphatidic acid. *J. Biol. Chem.* **280(11)**, 10091-10099 (2005).

37. Sakane, F., Imai, S., Kai, M., Yasuda, S. & Kanoh, H. Diacylglycerol kinases: Why so many of them? *Biochim. Biophys. Acta* **1771**, 793-806 (2007).

38. Nishizuka, Y. Intracellular signaling by hydrolysis of phospholipids and activation of protein kinase C. *Science* **258(5082)**, 607-614 (1992).

39. Topham, M. K. & Prescott, S. M. Diacylglycerol kinase zeta regulates Ras activation by a novel mechanism. *J Cell Biol.* **152(6)**, 191135-43 (2001).

40. Regier, D. S. *et al*. Diacylglycerol kinase iota regulates Ras guanyl-releasing protein 3 and inhibits Rap1 signaling. *Proc. Natl. Acad. Sci. U. S. A.* **102(21)**, 7595-7600 (2005).

41. Chase, D. L., Pepper, J. S. & Koelle, M. R. Mechanism of extrasynaptic dopamine signaling in Caenorhabditis elegans. *Nat. Neurosci.* **7(10)**, 1096-1103 (2004).

42. Nurrish, S., Ségalat, L. & Kaplan, J. M. Serotonin inhibition of synaptic transmission: Galpha(0) decreases the abundance of UNC-13 at release sites. *Neuron.* **24(1)**, 231-242 (1999).

43. Yasuda, S., Kai, M., Imai, S., Kanoh, H. & Sakane, F. Diacylglycerol kinase gamma interacts with and activates beta2-chimaerin, a Rac-specific GAP, in response to epidermal growth factor. *FEBS Lett.* **581(3)**, 551-557 (2007).

44. Rozengurt, E., Sinnett-Smith, J. & Zugaza, J. L. Protein kinase D: a novel target for diacylglycerol and phorbol esters. *Biochem. Soc. Trans.* **25(2)**, 565-571 (1997).

45. Lucas, P., Ukhanov, K., Leinders-Zufall, T. & Zufall, F. A diacylglycerol-gated cation channel in vomeronasal neuron dendrites is impared in TRPC2 mutant mice. *Neuron* **40**, 551-561 (2003).

46. Cazzolli, R., Shemon, A. N., Fang, M. Q. & Hughes, W. E. Phospholipid signalling through phospholipase D and phosphatidic acid. *IUBMB Life* **58(8)**, 457-461 (2006).

47. Flores, I., Casaseca, T., Martinez-A, C., Kanoh, H. & Merida, I. Phosphatidic acid generation through interleukin 2 (IL-2)-induced alpha-diacylglycerol kinase activation is an essential step in IL-2-mediated lymphocyte proliferation. *J. Biol. Chem.* **271(17)**, 10334-10340 (1996).

48. Abramovici, H. *et al*. Diacylglycerol kinase zeta regulates actin cytoskeleton reorganization through dissociation of Rac1 from RhoGDI. *Mol. Biol. Cell.* **20(7)**, 2049-2059 (2009).

49. Imai, S., Kai, M., Yasuda, S., Kanoh, H. & Sakane, F. Identification and characterization of a novel human type II diacylglycerol kinase, DGK kappa. *J. Biol. Chem.* **280**, 39870-39881 (2005).

50. Topham, M. K. & Prescott, S. M. Diacylglycerol kinases: regulation and signaling roles. *Thromb. Haemost.* **88**, 912-918 (2002).

51. Hurley, J. H., Newton, A. C., Parker, P. J., Blumberg, P. M. & Nishizuka, Y. Taxonomy and function of C1 protein kinase C homology domains. *Protein Science* **6**, 477-480 (1997).

52. Los, A. P., van Baal, J., de Widt, J., Divecha, N. & van Blitterswijk, W. J. Structure-activity relationship of diacylglycerol kinase theta. *Biochim. Biophys. Acta* **1636**, 169-174 (2004).

53. Shindo, M., Irie, K., Ohigashi, H., Kuriyama, M. & Saito, N. Diacylglycerol kinase gamma is one of the specific receptors of tumor-promoting phorbol esters. *Biochem. Biophys. Res. Commun.* **289**, 451-456 (2001).

54. Shindo, M. *et al*. Synthesis and Phorbol Ester Binding of the Cysteine-rich Domains of Diacylglycerol Kinase (DGK) Isozymes. *J. Biol. Chem.* **278**, 18448-18454 (2003).

55. Sakane, F., Kai, M., Wada, I., Imai, S. & Kanoh, H. The C-terminal part of diacylglycerol kinase alpha lacking zinc fingers serves as a catalytic domain. *Biochem. J.* **318 (Pt 2)**, 583-590 (1996).

56. Nelson, C. D. *et al*. Targeting of diacylglycerol degradation to M1 muscarinic receptors by -arrestins. *Science* **315**, 663-666 (2007).

57. Yakubchyk, Y. *et al*. Regulation of neurite outgrowth in N1E-115 cells through PDZ-mediated recruitment of diacylglycerol kinase zeta. *Mol. Cell. Biol.* **25(16)**, 7289-7302 (2005).

58. Sakane, F., Imai, S. I., Kai, M., Wada, I. & Kanoh, H. Molecular cloning of a novel diacylglycerol kinase isozyme with a pleckstrin homology domain and a C-terminal tail similar to those of the EPH family of protein tyrosine kinases. *J. Biol. Chem.* **271TY - INPR**, 8394-8401 (1996).

59. Klauck, T. M., Xu, X., Mousseau, B. & Jaken, S. Cloning and characterization of a glucocorticoid-induced diacylglycerol kinase. *J. Biol. Chem.* **271**, 19781-19788 (1996).

60. Sanjuan, M. A., Jones, D. R., Izquierdo, M. & Merida, I. Role of diacylglycerol kinase alpha in the attenuation of receptor signaling. *J. Cell Biol.* **153**, 207-220 (2001).

61. Nagaya, H., Wada, I., Jia, Y. -. & Kanoh, H. Diacylglycerol Kinase deta Suppresses ER-to-Golgi Traffic via Its SAM and PH Domains. *Mol. Biol. Cell* **13**, 302-316 (2002).

62. Topham, M. K. *et al*. Protein kinase C regulates the nuclear localization of diacylglycerol kinase-zeta. *Nature* **394**, 697-700 (1998).

63. Merino, E., Sanjuan, M. A., Moraga, I., Cipres, A. & Merida, I. Role of the diacylglycerol kinase alpha-conserved domains in membrane targeting in intact T cells. *J. Biol. Chem.* **282**, 35396-35404 (2007).

64. Takeuchi, H. *et al*. Distinct specificity in the binding of inositol phosphates by pleckstrin homology domains of pleckstrin, RAC-protein kinase, diacylglycerol kinase and a new 130 kDa protein. *Biochim. Biophys. Acta* **1359**, 275-285 (1997).

65. Park, W. S. *et al*. Comprehensive identification of PIP3-regulated PH domains from C. elegans to H. sapiens by model prediction and live imaging. *Mol. Cell* **30**, 381-392 (2008).

66. Knight, M. J. *et al*. Zinc Binding Drives Sheet Formation by the SAM Domain of Diacylglycerol Kinase delta. *Biochemistry* **49**, 9667-9676 (2010).

67. Harada, B. T. *et al*. Regulation of enzyme localization by polymerization: polymer formation by the SAM domain of diacylglycerol kinase delta1. *Structure* **16**, 380-387 (2008).

68. Dicu, A. O., Topham, M. K., Ottaway, L. & Epand, R. M. Role of the Hydrophobic Segment of Diacylglycerol Kinase epsilon. *Biochemistry* **46**, 6109-6117 (2007).

69. Norholm, M. H. H., Shulga, Y. V., Aoki, S., Epand, R. M. & von Heijne, G. Flanking Residues Help Determine Whether a Hydrophobic Segment Adopts a Monotopic or Bitopic Topology in the Endoplasmic Reticulum Membrane. *J. Biol. Chem.* **286**, 25284-25290 (2011).

70. Crotty, T. *et al*. Diacylglycerol kinase d regulates protein kinase C and epidermal growth factor receptor signaling. *Proc.Natl.Acad.Sci (USA)* **103**, 15485-15490 (2006).

71. Irvine, R. Nuclear Lipid Signaling. *Sci. STKE* **2000**, re1 (2000).

72. Ding, L., Traer, E., McIntyre, T. M., Zimmerman, G. A. & Prescott, S. M. The cloning and characterization of a novel human diacylglycerol kinase, DGKiota. *J. Biol. Chem.* **273**, 32746-32752 (1998).

73. Wada, I., Kai, M., Imai, S., Sakane, F. & Kanoh, H. Translocation of diacylglycerol kinase a to the nuclear matrix of rat thymocytes and peripheral T-lymphocytes. *FEBS Lett.* **393**, 48-52 (1996).

74. van Blitterswijk, W. J. & Houssa, B. Properties and functions of diacylglycerol kinases. *Cell. Signal.* **12**, 595-605 (2000).

75. Tabellini, G. *et al*. Diacylglycerol kinase-theta is localized in the speckle domains of the nucleus. *Exp. Cell. Res.* **287**, 143-154 (2003).

76. Sanjuan, M. A. *et al*. T Cell Activation In Vivo Targets Diacylglycerol Kinase alpha to the Membrane: A Novel Mechanism for Ras Attenuation. *J. Immunol.* **170**, 2877-2883 (2003).

77. Sakane, F. *et al*. Alternative Splicing of the Human Diacylglycerol Kinase delta Gene Generates Two Isoforms Differing in Their Expression Patterns and in Regulatory Functions. *J. Biol. Chem.* **277**, 43519-43526 (2002).

78. Santos, T., Carrasco, S., Jones, D. R., Merida, I. & Eguinoa, A. Dynamics of diacylglycerol kinase zeta translocation in living T-cells. Study of the structural domain requirements for translocation and activity. *J. Biol. Chem.* **277**, 30300-30309 (2002).

79. van Baal, J., de Widt, J., Divecha, N. & van Blitterswijk, W. J. Translocation of diacylglycerol kinase theta from cytosol to plasma membrane in response to activation of G protein-coupled receptors and protein kinase C. *J. Biol. Chem.* **280**, 9870-9878 (2005).

80. Tolias, K. F., Couvillon, A. D., Cantley, L. C. & Carpenter, C. L. Characterization of a Rac1- and RhoGDI-associated lipid kinase signaling complex. *Mol. Cell. Biol.* **18**, 762-770 (1998).

81. Houssa, B., de Widt, J., Kranenburg, O., Moolenaar, W. H. & van Blitterswijk, W. J. Diacylglycerol Kinase q binds to and is negatively regulated by active RhoA. *J. Biol. Chem.* **274**, 6820-6822 (1999).

82. Kobayashi, N. *et al*. Differential subcellular targeting and activity-dependent subcellular localization of diacylglycerol kinase isozymes in transfected cells. *Eur. J. Cell Biol.* **86**, 433-444 (2007).

83. Nunn, D. L. & Watson, S. P. A diacylglycerol kinase inhibitor, R59022, potentiates secretion by and aggregation of thrombin-stimulated platelets. *Biochem. J.* **243**, 809-813 (1987).

84. Murakami, T., Sakane, F., Imai, S., Houkin, K. & Kanoh, H. Identification and characterization of two splice variants of human diacylglycerol kinase eta. *J. Biol. Chem.* **278**, 34364-34372 (2003).

85. Rodriguez de Turco, E. B. *et al*. Diacylglycerol kinase epsilon regulates seizure susceptibility and long-term potentiation through arachidonoylinositol lipid signaling. *Proc. Natl. Acad. Sci. U. S. A.* **98**, 4740-4745 (2001).

86. Brash, A. R. Lipoxygenases: Occurrence, Functions, Catalysis, and Acquisition of Substrate. *J. Biol. Chem.* **274**, 23679-23682 (1999).

87. Neau, D. B. *et al*. The 1.85 A structure of an 8R-lipoxygenase suggests a general model for lipoxygenase product specificity. *Biochemistry* **48(33)**, 7906-7915 (2009).

88. Prescott, S. M. & Majerus, P. W. The fatty acid composition of phosphatidylinositol from thrombin-stimulated human platelets. *J. Biol. Chem.* **256TY - JOUR**, 579-582 (1981).

89. Lung, M. *et al*. Diacylglycerol kinase epsilon is selective for both acyl chains of phosphatidic acid or diacylglycerol. *J. Biol. Chem.* **284**, 31062-31073 (2009).

90. Jenkins, G. H., Fisette, P. L. & Anderson, R. A. Type I phosphatidylinositol 4-phosphate 5-kinase isoforms are specifically stimulated by phosphatidic acid. *J. Biol. Chem.* **269**, 11547-11554 (1994).

91. Tsai, M. H., Yu, C. L. & Stacey, D. W. A cytoplasmic protein inhibits the GTPase activity of H-Ras in a phospholipid-dependent manner. *Science* **250**, 982-985 (1990).

92. Ghosh, S., Strum, J. C., Sciorra, V. A., Daniel, L. & Bell, R. M. Raf-1 kinase possesses distinct binding domains for phosphatidylserine and phosphatidic acid. *J. Biol. Chem.* **271**, 8472-8480 (1996).

93. Bokoch, G. M. *et al*. A GTPase-independent mechanism of p21-activated kinase activation. *Jrnl Biol Chem* **273**, 8137-8144 (1998).

94. Fang, Y., Vilella-Bach, M., Bachmann, R., Flanigan, A. & Chen, J. Phosphatidic acid-mediated mitogenic activation of mTOR signaling. *Science* **294**, 1942-1945 (2001).

95. Limatola, C., Schaap, D., Moolenaar, D. & van Blitterswijk, W. J. Phosphatidic acid activation of protein kinase C zeta overexpressed in COS cells:

comparison with other protein kinase C isotypes and other acidic phospholipids. *Biochem. J.* **304**, 1001-1008 (1994).

96. Karathanassis, D. *et al*. Binding of the PX domain of p47(phox) to phosphatidylinositol 3,4-bisphosphate and phosphatidic acid is masked by an intramolecular interaction. *EMBO J.* **21**, 5057-5068 (2002).

97. Delon, C. *et al*. Sphingosine kinase 1 is an intracellular effector of phosphatidic acid. *J. Biol. Chem.* **279**, 44763-44774 (2004).

98. Loewen, C. J. *et al*. Phospholipid metabolism regulated by a transcription factor sensing phosphatidic acid. *Science* **304**, 1644-1647 (2004).

99. Jones, J. A. & Hannun, Y. A. Tight binding and inhibition of protein phosphatase-1 by phosphatidic acid. *J. Biol. Chem.* **277**, 15530-15538 (2002).

100. Gomez-Merino, F. C. *et al*. Arabidopsis AtDGK7, the smallest member of plant diacylglycerol kinases (DGKs), displays unique biochemical features and saturates at low substrate concentration: the DGK inhibitor R59022 differentially affects AtDGK2 and AtDGK7 activity in vitro and alters plant growth and development. *J. Biol. Chem.* **280**, 34888-34899 (2005).

101. Zhang, W., Chen, J., Zhang, H. & Song, F. Overexpression of a rice diacylglycerol kinase gene OsBIDK1 enhances disease resistance in transgenic tobacco. *Mol. Cells* **26**, 258-264 (2008).

102. Testerink, C. *et al*. Isolation and identification of phosphatidic acid targets from plants. *Plant J.* **39**, 527-536 (2004).

103. Meijer, H. J. & Munnik, T. Phospholipid-based signaling in plants. *Annu Rev Plant Biol.* **54**, 265-306 (2003).

104. Moritz, A., De Graan, P. N., Gispen, W. H. & Wirtz, K. W. Phosphatidic acid is a specific activator of phosphatidylinositol-4-phosphate kinase. *J. Biol. Chem.* **267**, 7207-7210 (1992).

105. Arimoto, T. *et al*. Cardiac-specific overexpression of diacylglycerol kinase zeta prevents Gq protein-coupled receptor agonist-induced cardiac hypertrophy in transgenic mice. *Circulation* **113**, 60-66 (2006).

106. Foster, D. A. Regulation of mTOR by phosphatidic acid? *Cancer Res.* **67**, 1-4 (2007).

107. Powner, D. J. & Wakelam, M. J. The regulation of phospholipase D by inositol phospholipids and small GTPases. *FEBS Lett.* **531**, 62-64 (2002).

108. Guo, R. *et al*. Synergistic control of T cell development and tumor suppression by diacylglycerol kinase alpha and zeta. *Proc. Natl. Acad. Sci. U. S. A.* **105**, 11909-11914 (2008).

109. Liu, C. H. *et al*. Diacylglycerol kinase zeta regulates microbial recognition and host resistance to Toxoplasma gondii. *J. Exp. Med.* **204**, 781-792 (2007).

110. Williams, J. M. *et al*. Antineutrophil cytoplasm antibody-stimulated neutrophil adhesion depends on diacylglycerol kinase-catalyzed phosphatidic acid formation. *J. Am. Soc. Nephrol.* **18**, 1112-1120 (2007).

111. Ishihara, H. *et al*. Cloning of cDNAs Encoding Two Isoforms of 68-kDa Type I Phosphatidylinositol4-phosphate 5-Kinase. *J. Biol. Chem.* **271**, 23611-23614 (1996).

112. Loijens, J. C. & Anderson, R. A. Type I Phosphatidylinositol-4-phosphate 5-Kinases Are Distinct Members of This Novel Lipid Kinase Family. *J. Biol. Chem.* **271**, 32937-32943 (1996).

113. Ishihara, H. *et al*. Type I phosphatidylinositol-4-phosphate 5-kinases. Cloning of the third isoform and deletion/substitution analysis of members of his novel lipid kinase family. *J. Biol. Chem.* **273**, 8741-8748 (1998).

114. Funakoshi, Y., Hasegawa, H. & Kanaho, Y. Regulation of PIP5K activity by Arf6 and its physiological significance. *J. Cell. Physiol.* **226**, 888-895 (2011).

115. Ling, K., Doughman, R. L., Firestone, A. J., Bunce, M. W. & Anderson, R. A. Type Igamma phosphatidylinositol phosphate kinase targets and regulates focal adhesions. *Nature* **420**, 89-93 (2002).

116. Nakano-Kobayashi, A. *et al*. Role of activation of PIP5K[gamma]661 by AP-2 complex in synaptic vesicle endocytosis. *EMBO J.* **26**, 1105-1116 (2007).

117. Tolias, K. F. *et al*. Type Ialpha phosphatidylinositol-4-phosphate 5-kinase mediates Rac-dependent actin assembly. *Current Biology* **10**, 153-156 (2000).

118. Kwiatkowska, K. One lipid, multiple functions: how various pools of $PI(4,5)P_2$ are created in the plasma membrane. *Cellular and Molecular Life Sciences* **67**, 3927-3946 (2010).

119. Coppolino, M. G. *et al*. Inhibition of phosphatidylinositol-4-phosphate 5-kinase Ialpha impairs localized actin remodeling and suppresses phagocytosis. *J. Biol. Chem.* **277**, 43849-43857 (2002).

120. Doughman, R. L., Firestone, A. J., Wojtasiak, M. L., Bunce, M. W. & Anderson, R. A. Membrane Ruffling Requires Coordination between Type Ialpha Phosphatidylinositol Phosphate Kinase and Rac Signaling. *J. Biol. Chem.* **278**, 23036-23045 (2003).

121. Padron, D., Wang, Y. J., Yamamoto, M., Yin, H. & Roth, M. G. Phosphatidylinositol phosphate 5-kinase Ibeta recruits AP-2 to the plasma membrane and regulates rates of constitutive endocytosis. *J. Cell Biol.* **162(4)**, 693-701 (2003).

122. Ling, K. *et al*. Tyrosine phosphorylation of type gamma phosphatidylinositol phosphate kinase by Src regulates an integrin-talin switch. *J. Cell Biol.* **163**, 1339-1349 (2003).

123. Powner, D. J. *et al*. Phospholipase D2 stimulates integrin-mediated adhesion via phosphatidylinositol 4-phosphate 5-kinase Igamma. *J. Cell. Sci.* **118**, 2975-2986 (2005).

124. Mellman, D. L. *et al*. A PtdIns4,5P2-regulated nuclear poly(A) polymerase controls expression of select mRNAs. *Nature* **451**, 1013-1017 (2008).

125. Di Paolo, G. *et al*. Recruitment and regulation of phosphatidylinositol phosphate kinase type 1[gamma] by the FERM domain of talin. *Nature* **420**, 85-89 (2002).

126. Ling, K. *et al*. Type Igamma phosphatidylinositol phosphate kinase modulates adherens junction and E-cadherin trafficking via a direct interaction with a1B adaptin. *J. Cell Biol.* **176**, 343-353 (2007).

127. Schill, N. J. & Anderson, R. A. Two novel phosphatidylinositol-4-phosphate 5-kinase type Igamma splice variants expressed in human cells display distinctive cellular targeting. *Biochem. J.* **422**, 473-482 (2009).

128. Shibasaki, Y. *et al*. Massive Actin Polymerization Induced by Phosphatidylinositol-4-phosphate 5-Kinase in Vivo. *J. Biol. Chem.* **272**, 7578-7581 (1997).

129. Weernink, P. A. O. *et al*. Stimulation of Phosphatidylinositol-4-phosphate 5-Kinase by Rho-Kinase. *J. Biol. Chem.* **275**, 10168-10174 (2000).

130. Oude Weernink, P. A., Schmidt, M. & Jakobs, K. H. Regulation and cellular roles of phosphoinositide 5-kinases. *Eur. J. Pharmacol.* **500**, 87-99 (2004).

131. Aikawa, Y. & Martin, T. F. ADP-ribosylation factor 6 regulation of phosphatidylinositol-4,5-bisphosphate synthesis, endocytosis, and exocytosis. *Methods Enzymol.* **404**, 422-431 (2005).

132. D'Souza-Schorey, C. & Chavrier, P. ARF proteins: roles in membrane traffic and beyond. *Nat. Rev. Mol. Cell Biol.* **7**, 347-358 (2006).

133. Martin, A. *et al*. Activation of Phospholipase D and Phosphatidylinositol 4-Phosphate 5-Kinase in HL60 Membranes Is Mediated by Endogenous Arf but Not Rho. *J. Biol. Chem.* **271**, 17397-17403 (1996).

134. Honda, A. *et al*. Phosphatidylinositol 4-Phosphate 5-Kinase Alpha Is a Downstream Effector of the Small G Protein ARF6 in Membrane Ruffle Formation. *Cell* **99**, 521-532 (1999).

135. Itoh, T., Ishihara, H., Shibasaki, Y., Oka, Y. & Takenawa, T. Autophosphorylation of Type I Phosphatidylinositol Phosphate Kinase Regulates Its Lipid Kinase Activity. *J. Biol. Chem.* **275**, 19389-19394 (2000).

136. Lee, S. Y. *et al*. Regulation of the interaction between PIPKIgamma and talin by proline-directed protein kinases. *J. Cell Biol.* **168**, 789-799 (2005).

137. Pettitt, T. R. *et al*. Diacylglycerol and phosphatidate generated by phospholipases C and D, respectively, have distinct fatty acid compositions and functions. Phospholipase D-derived diacylglycerol does not activate protein kinase C in porcine aortic endothelial cells. *J. Biol. Chem.* **272**, 17354-17359 (1997).

138. Divecha, N. *et al*. Interaction of the Type Ia PIPkinase with Phospholipase D: a role for the local generation of phosphatidylinositol 4,5-bisphosphate in the regulation of PLD2 activity. *EMBO J.* **19**, 5440-5449 (2000).

139. Arneson, L. S., Kunz, J., Anderson, R. A. & Traub, L. M. Coupled Inositide Phosphorylation and Phospholipase D Activation Initiates Clathrin-coat Assembly on Lysosomes. *J. Biol. Chem.* **274**, 17794-17805 (1999).

140. Brown, F. D., Rozelle, A. L., Yin, H. L., Balla, T. & Donaldson, J. G. Phosphatidylinositol 4,5-bisphosphate and Arf6-regulated membrane traffic. *J. Cell Biol.* **154**, 1007-1018 (2001).

141. Jarquin-Pardo, M., Fitzpatrick, A., Galiano, F. J., First, E. A. & Davis, J. N. Phosphatidic acid regulates the affinity of the murine phosphatidylinositol 4-phosphate 5-kinase-Ibeta for phosphatidylinositol-4-phosphate. *J Cell Biochem.* **100(1)**, 112-128 (2007).

CHAPTER TWO

DETERMINATION OF THE TOPOLOGY OF THE HYDROPHOBIC SEGMENT OF MAMMALIAN DIACYLGLYCEROL KINASE EPSILON IN A CELL MEMBRANE AND ITS RELATIONSHIP TO PREDICTIONS FROM MODELING

CHAPTER TWO PREFACE

The work presented in this chapter was published previously in *Journal of Molecular Biology*, volume 383(4), pages 797-809, in 2008.

Shulga Y.V. conducted all the experiments described in this chapter. Decaffmeyer M. conducted computer modeling.

Research objective: to determine the topology of the hydrophobic segment of diacylglycerol kinase epsilon.

Research highlights:

- Although simple predictive algorithms suggest that the hydrophobic segment of DGKε will form a TM helix, calculations using PepLook demonstrate that two different stable conformations are possible for this segment;
- Experimental studies of FLAG-DGKε expressed in COS-7 cells indicate that a U-bent conformation predominates;
- The conformational state of the protein can be shifted toward the transmembrane arrangement of the helix by a single amino acid mutation, changing the Pro32 residue to Ala;
- FLAG-DGKε is localized in both plasma membrane and endoplasmic reticulum of COS-7 cells.

Determination of the Topology of the Hydrophobic Segment of Mammalian Diacylglycerol Kinase Epsilon in a Cell Membrane and Its Relationship to Predictions from Modeling

Marc Decaffmeyer[1, †], Yulia V. Shulga[2, †], Armela O. Dicu[2], Annick Thomas[1], Ray Truant[2], Matthew K. Topham[3], Robert Brasseur[1], Richard M. Epand[2*]

[†]M.D. and Y.V.S. contributed equally to this work.

[1] Faculté Universitaire des Sciences Agronomiques de Gembloux, Centre de Biophysique Moléculaire Numérique, Passage des Déportés, 2, 5030 Gembloux, Belgium

[2] Department of Biochemistry and Biomedical Sciences, McMaster University Health Science Center, Hamilton, Ontario, Canada L8N 3Z5

[3] Huntsman Cancer Institute, University of Utah, Salt Lake City, UT 84112, USA

[*]Corresponding author.

ABSTRACT

The epsilon isoform of diacylglycerol kinase (DGKε) is unique among mammalian DGKs in having a segment of hydrophobic amino acids comprising approximately residues 20 to 41. Several algorithms predict this segment to be a transmembrane (TM) helix. Using PepLook, we have performed an *in silico* analysis of the conformational preference of the segment in a hydrophobic environment comprising residues 18 to 42 of DGKε. We find that there are two distinct groups of stable conformations, one corresponding to a straight helix that would traverse the membrane

and the second corresponding to a bent helix that would enter and leave the same side of the membrane. Furthermore, the calculations predict that substituting the Pro32 residue in the hydrophobic segment with an Ala will cause the hydrophobic segment to favor a TM orientation. We have expressed the P32A mutant of DGKε, with a FLAG tag (an N-terminal 3×FLAG epitope tag) at the amino terminus, in COS-7 cells. We find that this mutation causes a large reduction in both k_{cat} and K_m while maintaining k_{cat}/K_m constant. Specificity of the P32A mutant for substrates with polyunsaturated acyl chains is retained. The P32A mutant also has higher affinity for membranes since it is more difficult to extract from the membrane with high salt concentration or high pH compared with the wild-type DGKε. We also evaluated the topology of the proteins with confocal immunofluorescence microscopy using NIH 3T3 cells. We find that the FLAG tag at the amino terminus of the wild-type enzyme is not reactive with antibodies unless the cell membrane is permeabilized with detergent. We also demonstrate that at least a fraction of the wild-type DGKε is present in the plasma membrane and that comparable amounts of the wild-type and P32A mutant proteins are in the plasma membrane fraction. This indicates that in these cells the hydrophobic segment of the wild-type DGKε is not TM but takes up a bent conformation. In contrast, the FLAG tag at the amino terminus of the P32A mutant is exposed to antibody both before and after membrane permeabilization. This modeling approach thus provides an explanation, not provided by simple predictive algorithms, for the observed topology of this protein in cell membranes. The work also demonstrates that the wild-type DGKε is a monotopic protein.

Abbreviations used

DGK, diacylglycerol kinase; DGKε, epsilon isoform of DGK; TM, transmembrane; PLC, phospholipase C; FLAG, an N-terminal 3×FLAG epitope tag; EDTA, ethylenediaminetetraacetic acid; OG, octylglucoside; PtdIns(4,5)P2, phosphatidylinositol (4,5)-bisphosphate; DAG, diacylglycerol; SAG, 1-stearoyl-2-oleoylglycerol; DMEM, Dulbecco's modified Eagle's medium; PBS, phosphate-buffered saline; gRMSD, global RMSD; GFP, green fluorescent protein; RFP, red fluorescent protein; PNS, post-nuclear supernatant; PMF, post-mitochondrial fraction; PM, plasma membrane; ER, endoplasmic reticulum; GRP 94, a chaperone glucose-regulated protein.

Keywords

diacylglycerol kinase; hydrophobic segment; transmembrane helix; monotopic protein

INTRODUCTION

Diacylglycerol kinase (DGK) is a family of enzymes that appears unique to multicellular organisms. Bacteria also have DGK, but its structure and substrate specificity are very different from that of the mammalian isoforms. The bacterial enzyme is an integral membrane protein with several transmembrane (TM) segments with specificity for ceramide as well as diacylglycerol (DAG). A unique species of DGK has recently been reported in yeast that uses cytidine triphosphate as the phosphate donor.[1] It has been suggested that the mammalian forms of DGK control functions unique to multicellular organisms, such as the immune response or nerve signal conduction. The only mammalian DGK isoform with a putative TM domain is DGKε. This putative TM comprises approximately residues 20–40 and is found in all forms of mammalian DGKε as well as in *Drosophila* and in DGK2 from *Arabidopsis thaliana*. Predictive algorithms that identify this segment as a TM helix include IMPALA,[2] TM Finder[3] and DAS.[4]

The epsilon isoform is the smallest known mammalian DGK, a 64-kDa protein having only two Cys-rich regions (C1 domains) and a catalytic domain that are homologous to segments found in all other mammalian DGK isoforms. DGKε is unique in not having any domain involved in regulation of the enzyme activity. DGKε is also unique in having specificity for DAG substrates with an arachidonate moiety [5, 6]. This may also account for the enrichment of phosphatidylinositides with arachidonate, since one path for its synthesis involves phosphorylation of DAG as the first step.[7] It appears that the physiologically relevant DAGs are those containing a polyunsaturated acyl chain in the *sn*-2 position. This DAG is formed as a result of phosphatidylinositol (4,5)-bisphosphate [PtdIns(4,5)P2]-specific phospholipase C (PLC)-catalyzed hydrolysis of PtdIns(4,5)P2 that itself is highly enriched in arachidonic acid. Thus, DGKε may be responsible for down-regulating the DAG signaling resulting from inositol cycling.[8] The importance of DGKε in neuronal function has been demonstrated in studies with knockout mice.[9, 10, 11] It has been suggested that cell localization is a major factor determining the specific biological roles of the various DGK isoforms.[12] Since DGKε is unique in having a putative TM domain, it is important to understand the role of this hydrophobic segment in membrane interactions since they are likely to contribute to the unique functional properties of this isoform.

Although the segment from residues 20 to 40 in DGKε is predicted to be a TM helix, several observations do not coincide with this prediction. A model peptide corresponding to this region of DGKε is only partially helical when embedded in a phospholipid bilayer.[13] In addition, although the hydrophobic segment of DGKε contributes to its membrane partitioning,[14] the intact enzyme can be partially extracted from a membrane with 2 M KCl, indicating that the protein cannot be classified as an integral membrane protein. There are other protein segments that are predicted to be TM helices that form reentrant loops.[15] To test whether DGKε truly has a TM topology, we expressed an N-terminal Flag-tag-labeled form of DGKε in cells to determine if the epitope is exposed to the cell exterior, as would occur if the hydrophobic segment were a TM helix. These studies were supplemented with *in silico* calculations that are in accord with several of the experimental findings and provide a thermodynamic basis for the experimental observations.

RESULTS

Experimental studies

Kinetic analysis of 1-stearoyl-2-oleoylglycerol as substrate

We compared the kinetic properties of FLAG- DGKε [DGKε with an N-terminal 3×FLAG epitope tag (FLAG)] with that of its P32A mutant (Table 2.1). The proteins were obtained from transfected COS-7 cells and were assayed in a 1-stearoyl-2-oleoylglycerol (SAG)–detergent–phospholipid mixed micellar system using a high concentration of ATP (0.5 mM). The concentration of SAG is expressed as its mole fraction in the lipid–detergent mixture, since the binding of the lipid substrate to the catalytic site is determined not by its bulk concentration but by its concentration within the water-insoluble phase of micelles.[16] The initial rate of the enzyme-catalyzed reaction was determined as a function of the concentration of SAG in the micellar phase to obtain the kinetic constants k_{cat} and K_m. Similar analysis was carried out for 1,2-dioleoylglycerol but the rate of reaction was about fourfold lower than for SAG. The activity with 1,2-dioleoylglycerol was too low for us to obtain an accurate analysis of the kinetic constants k_{cat} and K_m. However, the results clearly show the retention of enzymatic specificity for arachidonoyl-containing substrates for this mutant.

Table 2.1. Apparent Michaelis-Menten constants of DGKε constructs using SAG as substrate.

Isoform	Km, mol%	Vmax, nmolPA/min/ng	k_{cat}, sec^{-1}	K_{cat}/Km, sec^{-1} $mol\%^{-1}$
FLAG-DGKε	0.59 ± 0.19	0.0022 ± 0.0005	2.35 ± 0.36	3.9
FLAG-DGKε-P32A	0.13 ± 0.05	0.00054 ± 0.00006	0.53 ± 0.05	4.1

Solubilization of the enzymes from the cell membranes

An integral membrane protein is defined as one that cannot be extracted from a membrane without disruption of the membrane structure. An integral membrane protein should thus not be extracted by use of high salt concentrations or extremes of pH. It would be expected that a protein with a TM helix would behave as an integral membrane protein and not be extracted even by harsh aqueous conditions. Only 14% of the FLAG-DGKε and 6% of the FLAG-P32A-DGKε activity are extracted with 2 M KCl (Fig. 2.1). When buffers at physiological pH and salt concentration are used, negligible amounts of FLAG-DGKε or the P32A mutant (4% or 2%, respectively) are extracted from the membrane, compared with extraction by Na_2CO_3 at high pH that solubilizes 11% and 4%

of the native and P32A proteins, respectively (Fig. 2.2). Thus, the P32A mutant is more strongly anchored to the membrane than the native enzyme under a variety of conditions.

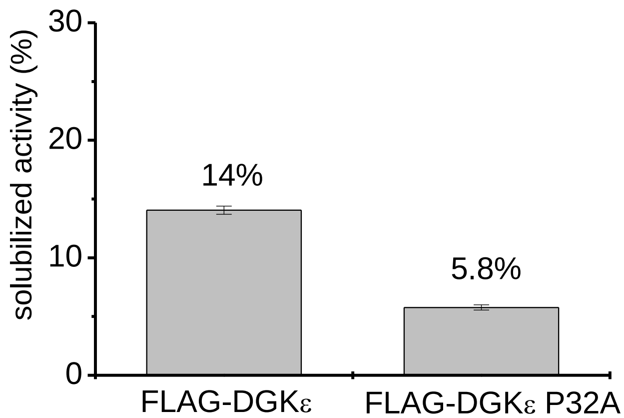

Figure 2.1. Percent activity found in the salt-extracted lysate from transfected COS-7 cells. Total cell lysates of FLAG- DGKε and FLAG- DGKε P32A were extracted with 2 M KCl by centrifugation at 73,000 rpm at 20 °C. Activity assay was done in OG mixed micellar system as described in Materials and Methods. Activity was measured for the extracted lysates and compared to the activity of the starting cell pellet.

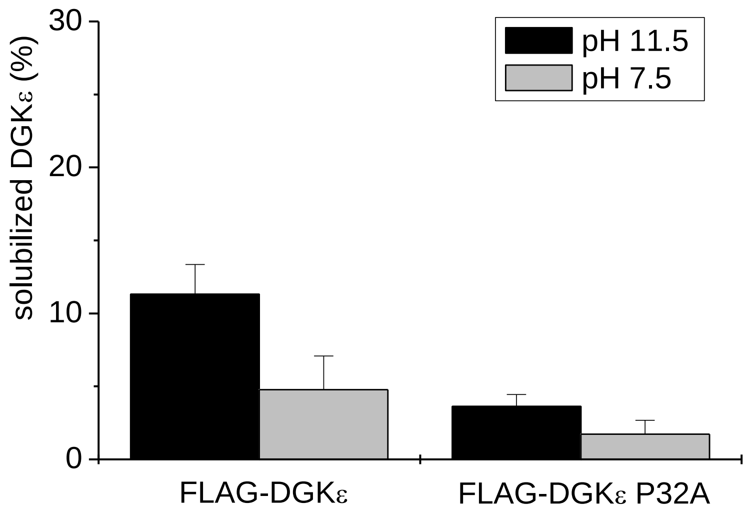

Figure 2.2. Percent of FLAG- DGKε extracted from a lysate of transfected COS-7 cells at pH 11.5 and 7.5. Total cell lysates of FLAG- DGKε and FLAG- DGKε P32A were extracted with either 0.2 M Na_2CO_3 (pH 11.5) or with physiological buffer (pH 7.5)

by centrifugation at 80,000 rpm at 4 °C. The amount of FLAG-tag protein in the aqueous extract was measured by Western blotting and compared to the total amount in the starting cell pellet. The average of two experiments is shown.

Fluorescence microscopy immunodetection of the FLAG epitope of FLAG-DGKε and of the P32A mutant

The present study allowed detection of the topology of the N-terminus FLAG-tag proteins by comparing the exposure of the FLAG tag to antibody before and after detergent permeabilization. The results show that for the wild-type FLAG- DGKε, much more of the N-terminus FLAG tag is detected upon cell permeabilization (Fig. 2.3a and b). There is some variability in the extent of staining of the non-permeabilized cells that we ascribe to some membrane damage as a result of the fixing procedure. We show a representative result. Empty vector control cells (not shown) exhibit only background fluorescence, similar to the non-permeabilized cells expressing wild-type FLAG-DGKε. In contrast, with the P32A mutant, the fluorescent signals from the permeabilized and non-permeabilized cells (Fig. 2.3c and d) are very similar, indicating that the amino terminus of the P32A-DGKε is exposed to the cell exterior as a result of it forming a TM helix.

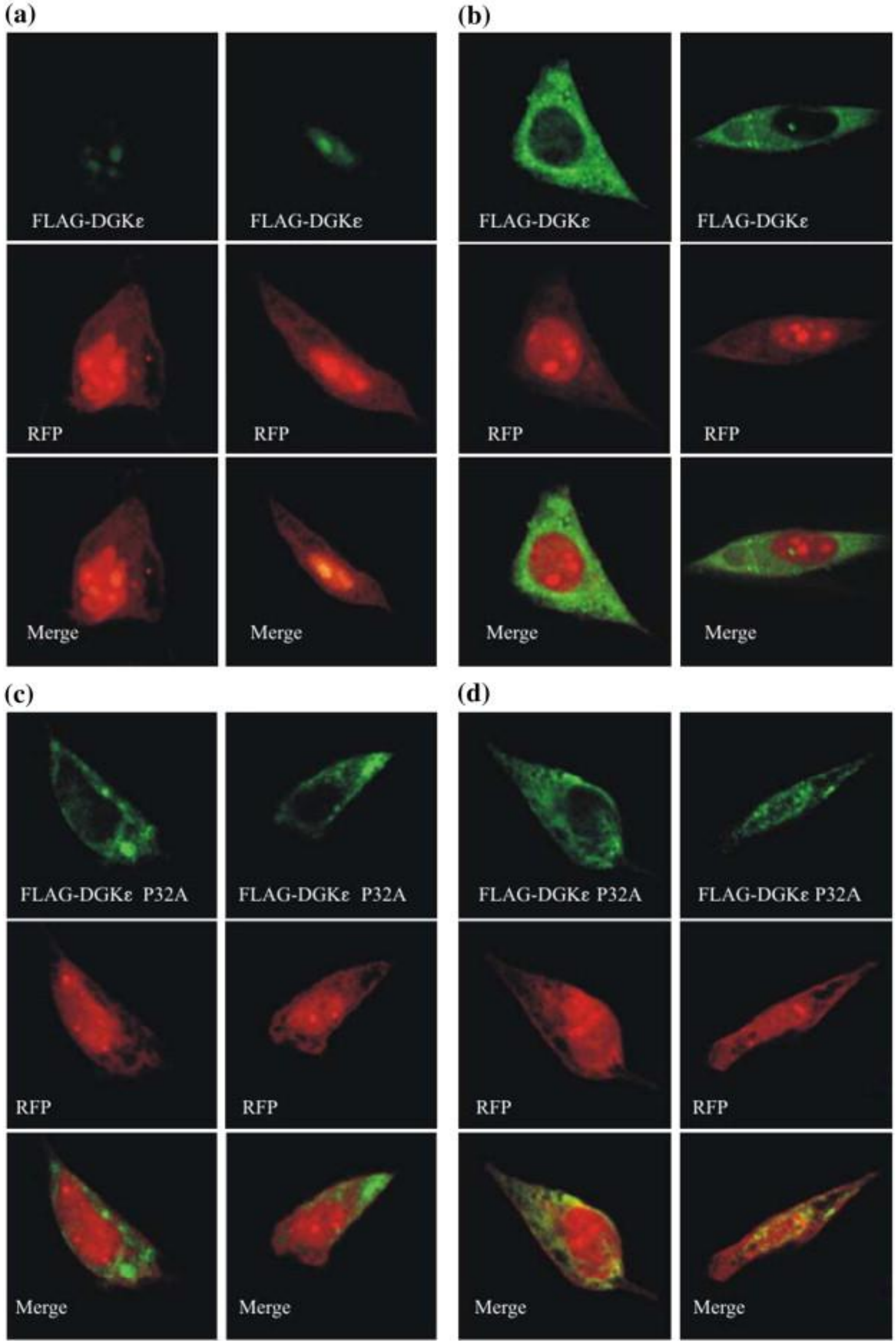
(a)
(b)
FLAG-DGKε
FLAG-DGKε
FLAG-DGKε
FLAG-DGKε
RFP
RFP
RFP
RFP
Merge
Merge
Merge
Merge
(c)
(d)
FLAG-DGKε P32A
FLAG-DGKε P32A
FLAG-DGKε P32A
FLAG-DGKε P32A
RFP
RFP
RFP
RFP
Merge
Merge
Merge
Merge

Figure 2.3. Confocal fluorescence microscopy of NIH 3T3 cells cotransfected with the pmRFP-C1 vector and the p3×FLAG- DGKε vector (a and b) or with the p3×FLAG-P32A- DGKε vector (c and d). (a and c) Non-permeabilized cells. The cells were fixed with paraformaldehyde and left non-permeabilized prior to indirect immunofluorescence using an antibody directed against the FLAG tag and an Alexa Fluor 488 secondary antibody. (b and d) Permeabilized cells. The cells were fixed with paraformaldehyde and permeabilized with Triton X-100 prior to indirect immunofluorescence using an antibody directed against the FLAG tag and an Alexa Fluor 488 secondary antibody. Columns show examples of different cells. The top rows show the 3×FLAG signal from DGK. Middle rows show the pmRFP-C1 signal. Bottom rows show the merged images. The intensity level of images from cells before and after permeabilization were kept identical. This resulted in the intensity of the Alexa Fluor 488 signal (green) from the non-permeabilized cells transfected with FLAG- DGKε (a) to be very weak.

Detection of FLAG- DGKε in an affinity-purified plasma membrane fraction

Although the results from fluorescence microscopy indicate that some of the DGKε is present in the plasma membrane (PM), we wished to confirm this with the use of an affinity-purified PM fraction that was free of intracellular membranes. Using a method that combines cell surface biotinylation with affinity enrichment by streptavidin beads, we prepared the affinity-purified PM fraction from NIH 3T3 cells transiently transfected with FLAG-DGKε.[17] The results of Western blot analysis showed the presence of FLAG-DGKε in the purified PM fraction (Fig. 2.4). We confirmed the absence of membranes from the endoplasmic reticulum (ER), which is the major contaminant in PM preparations, using antibodies against a chaperone glucose-regulated protein (GRP) 94, a marker protein for the ER. No detectable contamination was found (Fig. 2.4).

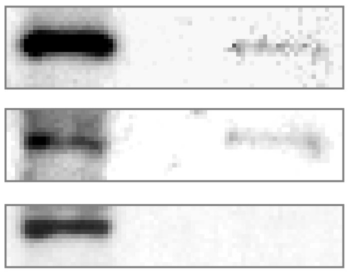

Figure 2.4. Detection of FLAG- DGKε and organelle-specific proteins in an affinity-purified PM fraction by Western blotting analysis. Proteins were separated in a 7.5% SDS-PAGE and transferred to a polyvinylidene fluoride membrane. The blot was probed with antibodies against FLAG-tag and organelle-specific proteins: anti-Na/K ATPase α for PM and anti-GRP 94 for endoplasmic reticulum (ER). PMF, post mitochondrial fraction; PM, affinity-purified membrane fraction.

Subcellular fractionation of cells overexpressing either FLAG-DGKε or the P32A mutant

Although the results presented in Fig. 2.4 unequivocally demonstrate that FLAG-DGKε is expressed in a PM fraction that is not contaminated with ER, we wished to better compare the relative amounts of FLAG-DGKε in the PM *versus* the ER. This question is of particular importance because there is evidence that some DGKε is present in the ER.[18] We therefore separated the membranes of transfected cells by using an OptiPrep gradient. We used antibodies to the proteins GRP-94 and Na/K ATPase α as markers for the ER and the PM, respectively. The ER is exclusively in the higher density fractions, but the PM has a broader distribution, with the major portion being in the lighter density fractions. Both FLAG-DGKε and the P32A mutant are detectable in all of the fractions (Fig. 2.5). The density of the bands was quantified by densitometry (Fig. 6). ER membranes are absent in fractions 3–5, but Na/K ATPase α is present in these fractions. The findings that FLAG-DGKε and the P32A mutant are present in these fractions and in comparable amounts indicate that these proteins are present in the PM, and the fact that FLAG- DGKε could not be detected by immunofluorescence in intact cells is not a result of the protein being sequestered on intracellular membranes. However, FLAG-DGKε and the P32A mutant are also present in fractions ~ 10–15. Since there is some contamination of these fractions with the PM marker, it is not possible to unequivocally state what fraction of the DGKε proteins is in the ER. The amounts of FLAG-DGKε and the P32A mutant in these higher density fractions are comparable; however, the fractionation pattern of the FLAG-DGKε in this region of the gradient is different from that of the P32A mutant. How this relates to the role and location of these proteins on intracellular membranes is currently under investigation.

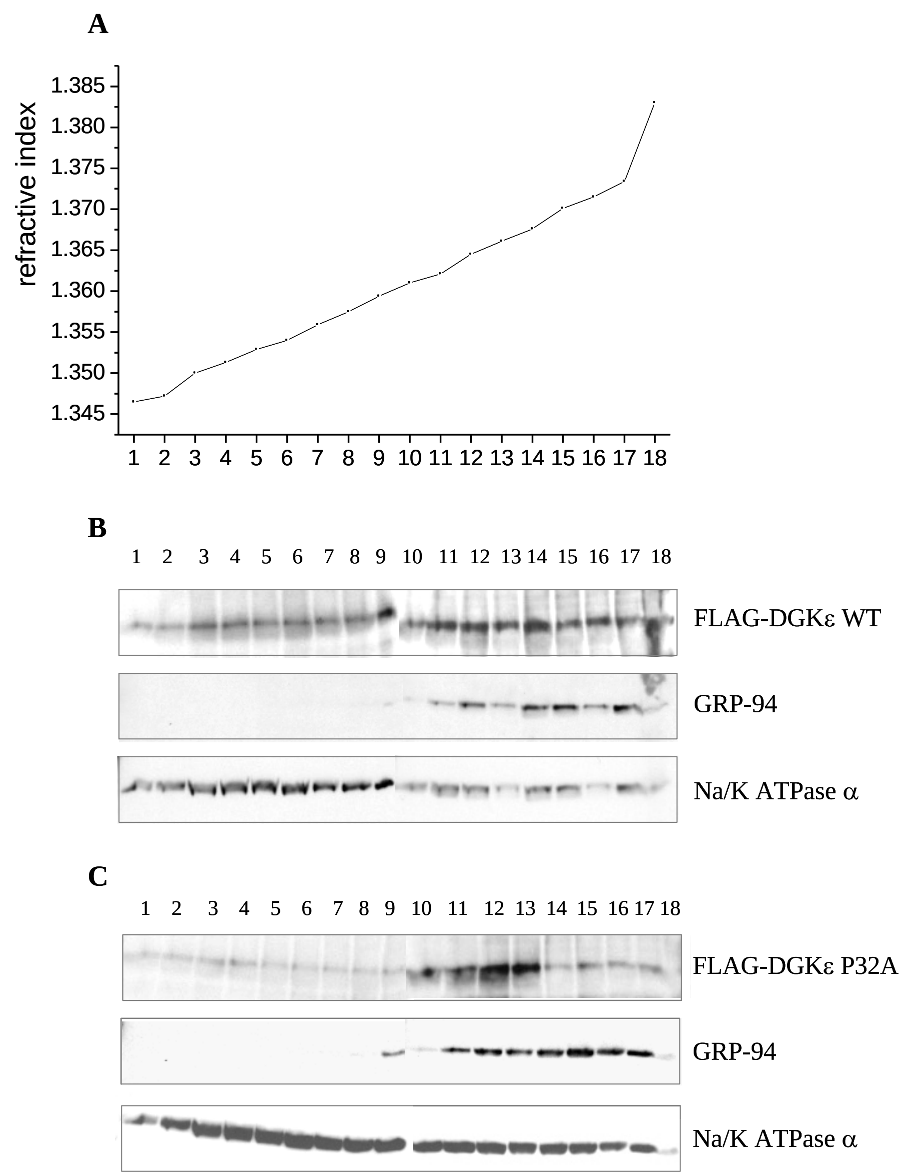

Figure 2.5. Subcellular fractionation of COS-7 cells transiently transfected with FLAG- DGKε WT and P32A mutant. Fractionation was performed using an OptiPrep gradient, and fractions were analyzed by immunoblotting with antibodies against the indicated protein. (a) Density profile of 3–25% iodixanol gradient used for subcellular fractionation. (b and c) The detection of marker proteins for PM (anti-Na–K ATPase), ER (GRP-94) and FLAG-DGKε WT (b) and P32A mutant (c) proteins.

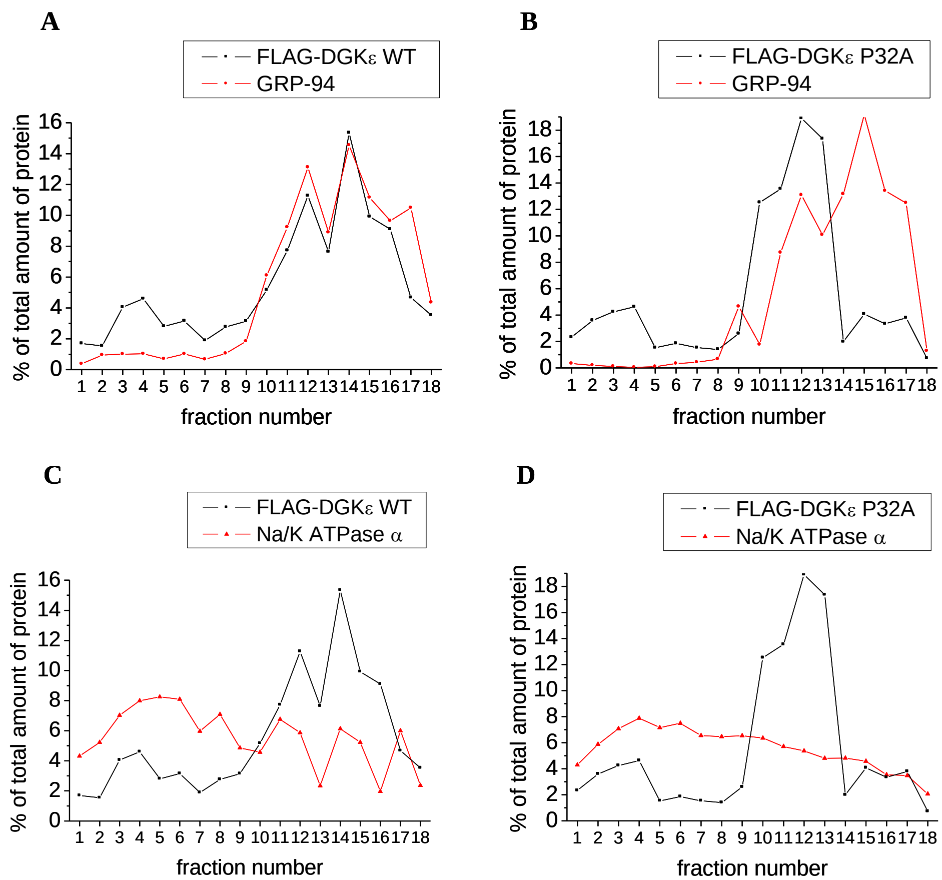

Figure 2.6. Quantification of immunoblots by densitometry. Results are presented normalized for the total amount of each protein. Shown for comparison are the distribution of ER (GRP-94) (a and b), PM (anti-Na–K ATPase) (c and d) markers, and FLAG-DGKε WT (a and c) and P32A mutant (b and d) proteins.

Modeling

Structural prediction of the D18–Q42 peptide: PepLook

Analysis of the native TM fragment structure and polymorphism

Using PepLook, we generated 2.5×10^6 different conformations of D18–Q42 and selected the 99 best energy models. Calculations assumed a hydrophobic medium to simulate the membrane environment. The 99 best models for D18–Q42 have a large (mean, 74%) helical contribution; the balance is mainly due to random coiled (21%) and beta-extended (5%) conformations (Supplementary Fig. 1). The 99 models cluster into two different groups that are equally represented by subpopulations of structures (close to 50% each). Each subpopulation was analyzed as a variation around its best structure, i.e., the lowest-energy structure. For the first subpopulation, the best structure is the Prime, i.e., the conformation of lower energy (Fig. 2.7); for the second subpopulation, the best structure is the second model, i.e., the conformation next to the Prime in energy (Fig. 2.7). In the first subpopulation, all models diverge from the Prime with a global RMSD (gRMSD) within 3.5 Å and a small variation of secondary structure as demonstrated by the fact that the RMSD on a sliding window of nine residues (RMSD [9])[19] (Fig. 2.7) is not higher than 1.5 Å all through the sequence. The Prime conformation is 88% helical and the corresponding subpopulation is mainly a straight helix. The models of the other subpopulations of D18–Q42 have a gRMSD of 4 to 10 with respect to the Prime, supporting a different 3D structure. They have a low RMSD [9] with respect to the Prime at both ends of the sequence, but diverge in the middle with an RMSD [9] increasing up to 3 Å between C27 and I35. The second population and its best model (model 2) are partly helical and have a random coil and extended conformation at the fragment center (L31V33) (Fig. 2.7 and Supplementary Fig. 1, left), which enables the peptide to adopt a bent conformation. Values of secondary structures of this population better match the CD data of peptide L22W39, which indicate a partly (~ 30%) helical conformation when in phospholipid bilayers containing anionic lipid.[13] All together, this indicates that secondary structures of the N- and C-terminal residues are similar for both subpopulations but vary in the middle of the peptide (Fig. 2.7). Both populations are individually homogeneous, correspond to similar energy and account for a similar percentage of the 99 most stable models. The Prime is a helix, while model 2 is a U-bent conformation of two short helical fragments (Fig. 2.7).

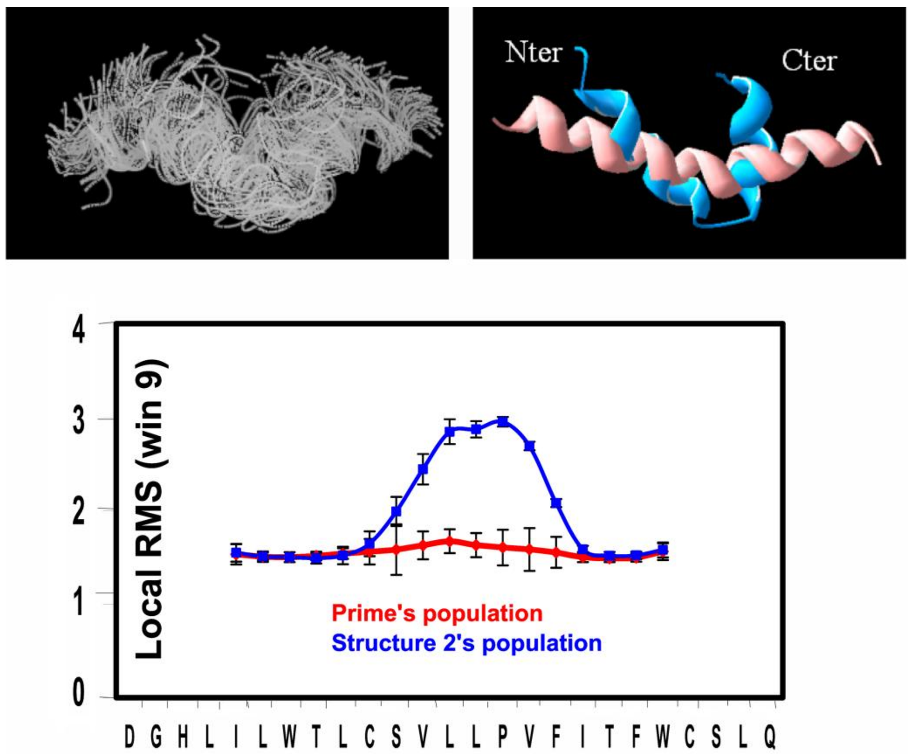

Figure 2.7. D18–Q42 models of the native DGKε calculated by PepLook. Top: Snapshot of the 99 best structures provided by PepLook (left). View of the best model of each population (Prime's structure in pink and model 2 in blue) (right). Bottom: Local RMS (window of nine residues) along the sequence. The reference structure is the Prime. The red plot represents the mean values of all models of the Prime's subpopulation, the blue one represents the mean value for all models of the second subpopulation. The standard deviations clearly indicate that the two populations are homogenous.

Analysis of stability

As previously described by Thomas *et al.*,[20] the stability of residues was scored as the ratio (in percent) of their mean force potential values in the calculated models to their reference mean force potential values in a large series of stably folded proteins.[21] Structures with a mean stability score of 100 are considered as stable as in proteins. Because they are shorter than proteins, peptides with a mean stability score over 60 are likely to be stable conformations. Residues under 50–60% are considered as unstable and are priority candidates for external partner binding.

Analysis of the stability score supports the conclusion that most residues are ready for external partnership: the mean stability score of model 2 is 51%; the mean stability score of the Prime is 47% (Fig. 2.8). In addition, the N-terminal (D18–W24) and the C-terminal (V33–Q42) moieties of the Prime show a lower stability score (42%) than the center of the peptide (56%). In the bent form (i.e., model 2), some of the Prime's unstable residues, notably L21, T25, V29, L31, F34, W38 and L41, are stabilized thanks to intramolecular interactions, but two hydrophobic residues, L30 and V33, have low stability scores.

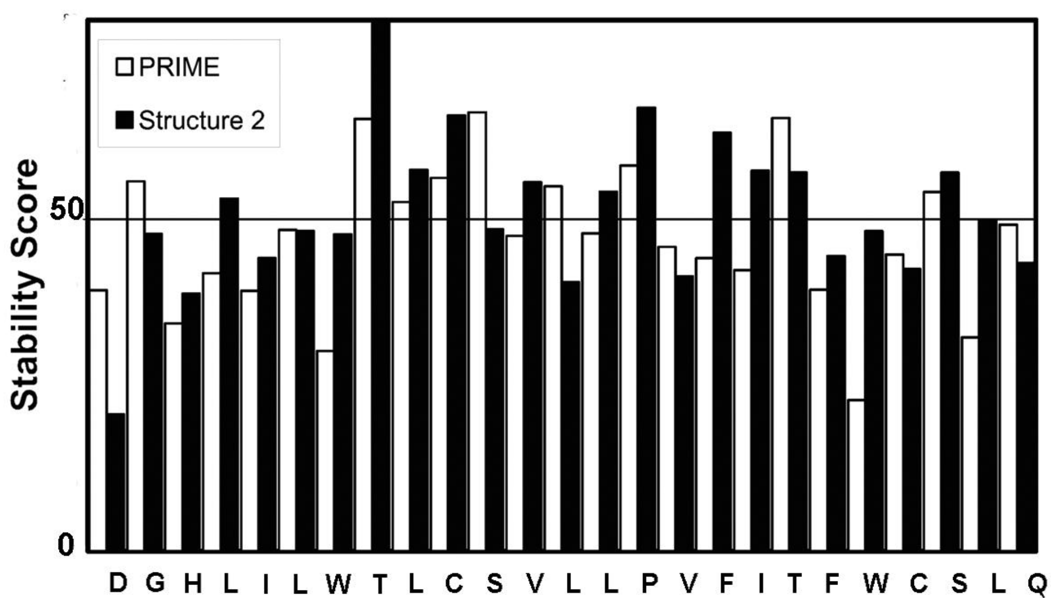

Figure 2.8. Analysis of the native DGKε D18–Q42 model stability. Stability score (in %) of every residue of the two different models of DGKε 18–42.

Analysis of the P32A TM fragment structure and polymorphism

Our calculations show that substitution of Pro32 with Ala greatly favors the straight TM helical conformation of the hydrophobic segment (Fig. 2.9a). All together, the 99 best models for P32A-DGKε 18–42 have a larger helical contribution (mean, 82%) than the native DGKε 18–42 (mean 74%). For the mutant, we also observe two distinct structural populations (Fig. 2.9a and b), but the population with a straight helical conformation now represents up to 89% of the conformations, while the second population contains only 11% of the structures, among which only half adopt the U-bent conformation. In the first subpopulation of P32A-DGKε 18–42, comprising 89%, the models diverge from the Prime with a small variation of secondary structure. This is demonstrated by the fact that the RMSD [9] (Fig. 2.9c) is not higher than 1.6 Å throughout the sequence. The models of the other subpopulations have a low RMSD [9] with respect to the Prime at both ends of the sequence, but diverge in the middle with an RMSD [9] increasing up to 2.6 Å. The standard deviations clearly indicate that models of the Prime's populations are homogenous and that the second population is less homogenous (Fig. 2.9c). The slight kink of the helix that we had noticed for the 50% Prime population of native DGKε 18–42 disappears for the 89% Prime population of P32A-DGKε 18–42, confirming the role of Pro32 in the U-bent formation.

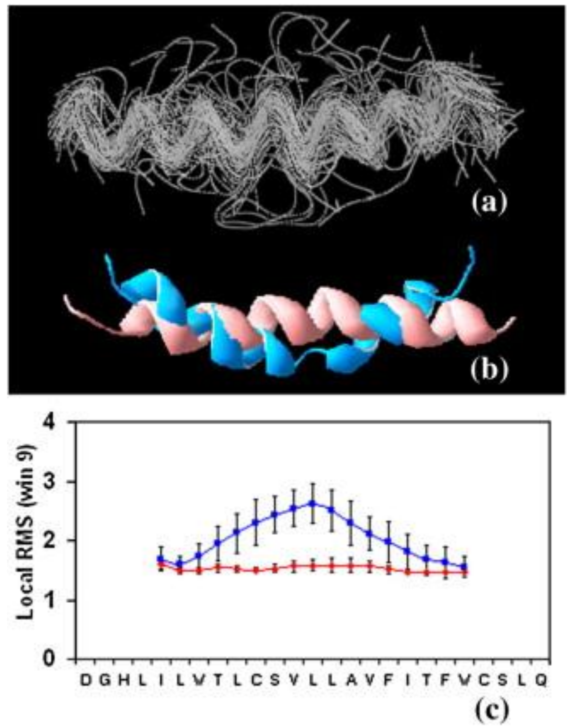

Figure 2.9. D18–Q42 models of the P32A DGKε calculated by PepLook. Calculated conformations of P32A- DGKε 18–42. (a) Snapshot of the 99 best structures provided by PepLook. (b) View of the best model of each population (Prime's structure in pink and representative of the second population in blue). (c) Local RMS (window of nine residues) along the sequence. The reference structure is the Prime. The red plot represents the mean values of all models of the Prime's subpopulation; the blue one represents the mean value for all models of the second subpopulation. The standard deviations clearly indicate that the Prime's populations are homogenous and that the second population is less homogenous.

DISCUSSION

The most hydrophobic segment of DGKε is between residues 20 and 40. Deletion of the 40 N-terminal amino acids from DGKε significantly decreases the membrane affinity of the protein.[14] What is the nature of the membrane insertion of the segment 20 to 40 when DGKε binds to membranes? Membrane proteins have been classified by Blobel on the basis of the number of times their hydrophobic domains span the membrane.[22] Therefore, monotopic proteins are hydrophobically associated with the membrane but do not pass across the bilayer, bitopic proteins cross the membrane only once, and polytopic proteins cross the membrane more than once.[23] Monotopic proteins are less common.[24]

If DGKε was the most common type of bitopic protein, with residues 20–40 forming a TM helix, then either the segment of residues 1–19 with its attached FLAG tag would protrude from the membrane or the topology of the protein would be reversed with the protein being an ectoenzyme having its active site on the extracellular side of the membrane. However, it is unlikely that the protein is an ectoenzyme. This family of enzymes participates in intracellular signal transduction and it is thought to down-regulate the DAG signal produced intracellularly by PtdIns(4,5)P2-specific PLC-catalyzed hydrolysis of PtdIns(4,5)P2. There is an ecto-PLC known[25] that could produce DAG on the outside surface of the cell membrane. However, an additional fact making this orientation unlikely for DGKε is that a green fluorescent protein (GFP)–DGKε construct that does not sequester well to membranes is found in the cytoplasm[26] and is not excreted, as would be the case if it were an ectoenzyme. It is possible, however, that under certain conditions, DGKε can become an ectoenzyme, as has been shown for protein kinase C during apoptosis.[27]

Another possibility is that DGKε is located on an intracellular membrane. However, there is evidence that DGKε is involved in inositol cycling.[8, 11] This cycle can be activated by hormones binding to cell surface receptors resulting in the activation of PtdIns(4,5)P2-specific phospholipase C. The DAG derived from this process will be formed in the PM and is a preferred substrate for DGKε. It is therefore likely that this enzyme is also present in the PM. We have demonstrated directly that there is DGKε in a purified PM fraction (Fig. 2.4). The subcellular localization of a substantial and similar fraction of the wild-type enzyme and the P32A mutant in the PM fraction following density gradient centrifugation confirms this conclusion (Fig. 2.6). Hence, the lack of FLAG-tag staining in the cells expressing wild-type DGKε is not a result of complete sequestration of the enzyme on intracellular membranes. A GFP– DGKε construct has been shown by fluorescent microscopy to colocalize with a marker for the ER.[18] However, these images look very different from the ones shown in this article. Furthermore, with permeabilized cells expressing both intracellular-localizing red fluorescent protein (RFP) and FLAG-DGKε, it is clear that the two proteins are separated. In addition, there is no change in distribution of the P32A-DGKε before and after permeabilization (Fig. 2.3c and d), indicating some PM localization. We do not believe that the FLAG epitope tag alters subcellular distribution. The FLAG tag is small and the FLAG-DGKε maintains enzyme activity and membrane affinity similar to that of the endogenous enzyme.[14] We cannot completely eliminate the possibility that the overexpression of the DGKε in the transfected cells alters its localization, but we do not believe this is likely. Transfecting the cells with different amounts of DNA, resulting in several fold changes in DGKε expression, did not alter the subcellular distribution (not shown). Additionally, even with overexpression, the level of protein is very small and cannot be detected in gels with Coomassie staining. Thus, on the basis of the lack of exposure of the N-terminal FLAG-tag without detergent permeabilization of the membrane, we conclude that DGKε is a monotopic enzyme with both the carboxyl and amino termini of the protein oriented on the cytoplasmic side of the membrane. This topology is altered in the P32A mutant where the hydrophobic segment protrudes through the membrane.

The definition of monotopic proteins does not specify the extent to which the protein inserts into the membrane, only that the protein will not translocate across the membrane. In the case of the wild-type DGKε, the protein inserts deeply into the bilayer so that it has properties partially resembling that of an integral membrane protein. We suggest that this class of monotopic proteins should be distinguished by referring to them as deeply inserted monotopic proteins. The deep insertion of the native DGKε is indicated by the fact that it is poorly extracted from the membrane by both 2 M KCl and 0.2 M Na_2CO_3 at alkaline pH (Fig. 2.1 and Fig. 2.2). However, it is partially extracted by these harsh conditions, indicating that it has properties intermediate between those of an integral membrane protein and those of a peripheral membrane protein; i.e., it is a deeply inserted monotopic protein. In contrast, the P32A mutant is very poorly extracted from the membrane even at high salt concentrations or high pH and therefore it behaves more like an integral membrane protein with a TM helix, as suggested by fluorescence microscopy studies (Fig. 2.3c and d).

The Pro residue is a feature that could disrupt a TM helix. However, in some proteins, such as bacteriorhodopsin, there are several Pro in TM helices that can be mutated without consequence to the topology of the protein in a membrane.[28] There are, however, other examples of motifs in which a Pro-containing hydrophobic segment will insert into a membrane with a conformation different from that of a TM helix. One example is the caveolin-1 protein[29, 30] that presents its hydrophobic domain at the membrane in the form of a hydrophobic loop. Caveolins are a family of proteins that coat the cytoplasmic side of caveolae. The primary sequence of caveolin-1 contains a central hydrophobic domain (104–124) that is believed to anchor the protein to membranes as a deeply inserted monotopic protein. We compared the sequence of this segment with that of the hydrophobic segment of DGKε (Table 2.2). There is little homology and even the Pro residue is in a different location. Nevertheless, the two proteins have in common that they are both monotopic.

Table 2.2. Comparison of the Hydrophobic Segments of DGKε and of Caveolin-1.

DGKε	LILWTLCSVLLPVFITFWCSL
Caveolin-1	ALFGIPMALIWGIYFAILSFL

The modeling studies support our experimental observations and provide a mechanistic rationale. For the native DGKε 18–42 fragment, PepLook detects a tendency to structural polymorphism. The 99 models of lower energy give two equally frequent conformations: a long helix and a U-bent helix. Interestingly, the two representative models (the Prime and the second model) are the two most stable conformations of the 99 models, supporting the conclusion that both conformations might coexist. Since both conformations have low self-stability, their relative ratio might depend upon the medium, and factors such as the protein/lipid ratio, the nature of the lipid and the strength of interactions between the N- and C-termini of the protein may determine which of the two conformations is in greater abundance.

In addition to the intact protein, we have also studied a model peptide corresponding to the fragment of DGKε from residues 22 to 39 and flanked at both carboxyl and amino termini with Lys residues.[13] It would be expected that in the presence of SDS, this peptide would fold into a straight helical conformation, similar to what we have called the Prime structure. From CD studies, we find that the peptide has the greatest helical structure in SDS. However, the peptide has less secondary structure in phospholipid bilayers than in SDS, suggesting that even this short peptide forms a U-bent structure in a membrane.[13]

In summary, although simple predictive algorithms suggest that the hydrophobic segment of DGKε will form a TM helix, calculations using PepLook demonstrate that two different stable conformations are possible for this segment. Experimental studies of the protein expressed in cells indicate that a bent conformation predominates. The conformational state of the protein can be shifted toward the TM arrangement of the helix by a single amino acid mutation, changing the Pro32 residue to Ala.

MATERIALS AND METHODS

DGKε constructs

A FLAG-epitope-tagged DGKε expression vector was prepared as previously described[14] and was transfected into NIH 3T3 or COS-7 cells for subcellular fractionation. In addition, as a marker for transfection efficiency, cells used for fluorescence microscopy were cotransfected with pmRFP-C1 that produces a protein with fluorescence in the visible region that can be monitored.[31] The P32A mutant of the FLAG- DGKε was designed with the use of the QuikChange protocol (Stratagene, La Jolla, CA). A mutated DNA plasmid was amplified from an N-terminal FLAG-tagged DGKε by 12 cycles using *Pfu*Turbo DNA polymerase and the following mutagenic primers: forward, 5′-CGGTCCTGCTGGCGGTGTTCATCAC-3′; reverse, 5′-GTGATGAACACCGCCAGCAGGACCG'3′. After digestion of the nonmutated parental DNA with DpnI restriction enzyme, the resulting PCR mix containing the mutated DNA plasmid was transformed into XL1-Blue supercompetent cells. DNA was purified from the bacterial culture using Wizard Plus Minipreps DNA purification system (Promega). The presence of the desired mutation was verified by sequencing analysis.

Cell culture

COS-7 cells were maintained in Dulbecco's modified Eagle's medium (DMEM, GIBCO/Invitrogen) containing 10% fetal bovine serum (GIBCO/Invitrogen) and 1% penicillin/streptomycin (GIBCO/Invitrogen) at 37 °C in an atmosphere of 5% carbon dioxide. The cells were grown to about 70–80% confluency and harvested after 18–24 h by scraping them off the plate in 1× phosphate-buffered saline (PBS) containing 1:100 protease inhibitor cocktail for use with mammalian cells and tissue (Sigma-Aldrich). The cells were kept at − 70 °C until further use.

Estimation of the amounts of FLAG-tagged recombinant P32A-DGKε protein

Amounts of FLAG-tagged P32A- DGKε protein in the membrane fractions of transfected COS-7 cells were estimated by immunoblotting with a mouse anti-FLAG peptide M2 primary antibody (Sigma-Aldrich). A 3×FLAG-tagged bacterial alkaline phosphatase (Sigma-Aldrich) with a molecular mass of 49.9 kDa was used as a standard in different lanes of the same blots. Details of the procedure are the same as those previously used by us for another FLAG-DGK construct.[14]

Enzyme preparations for kinetic analysis

The transfected cells were harvested after 24–48 h in ice-cold cell lysis buffer (20 mM Tris–HCl, pH 7.5, 150 mM NaCl, 1 mM ethylenediaminetetraacetic acid (EDTA), and 1× protease inhibitor cocktail (Sigma-Aldrich)). The cells were pelleted at low speed (6000*g*) and the pellets were kept at − 70 °C until further use. Prior to assay, cell pellets were resuspended in cell lysis buffer containing 30 mM octylglucoside (OG), allowed to lyse for 10 min on ice and then centrifuged at 100,000*g* for 30 min at 20 °C. The supernatants were used in the assay of DGK activity.

DGK activity assay in OG micelles

The assay was adapted from the method described by Walsh *et al.*[6] as previously employed in our laboratory.[14] Controls were run with the addition of mock-transfected cell lysates or without the addition of lipid substrates. In both cases, the counts remaining in the organic phase were only slightly above background. The DGK activity measured with mock-transfected cells was subtracted from the values obtained using cells overexpressing one of the DGKε constructs. The production of phosphatidic acid was linear with time over 10 min. The assays were done in triplicate and the results presented with errors showing the standard deviation of the mean for one particular experiment. Each experiment was independently repeated at least two times. The day-to-day variations using the same enzyme preparation and the same lipids were not much greater than those for an individual experiment.

Kinetic analysis of the micelle-based assay of DGK activity

A kinetic analysis was performed on the FLAG- DGKε full-length construct and on the P32A-DGKε. The Michaelis–Menten constants V_{max} and K_m were evaluated by a least-squares fit of a two-parameter hyperbolic plot [initial velocity (v_0) *versus* substrate concentration ([S])] as well as by using Hanes plots ([S]/v_0*versus* [S]). The content of FLAG-tagged DGKε protein was determined as described above. Microcal Origin software was used to determine k_{cat} and K_m.

Solubilization of the enzymes from the cell membranes

Two confluent 10-cm dishes of COS-7 cells transfected with 3×FLAG- DGKε or with 3×FLAG-DGKε P32A were scraped into ice-cold cell lysis buffer [20 mM Tris–HCl, pH 7.5, 150 mM NaCl, 1 mM EDTA, and 1× protease inhibitor cocktail (Sigma-Aldrich)] and centrifuged for 5 min at 6000*g*. Cells were adjusted to 1 mL with either extraction buffer (200 mM Na_2CO_3, 10 mM DTT, 2% glycerol, pH 11.5), with physiological buffer (10 mM Tris–HCl, pH 7.5, 10 mM NaCl, 3 mM $MgCl_2 \cdot 6H_2O$, 1 mM DTT) or with high-salt buffer (2 M KCl, 30 mM Tris–HCl, 60 mM NaCl, pH 8). The reaction was incubated on ice for 30 min. Cell pellets extracted with 2 M KCl were centrifuged for 30 min at 73,000 rpm (rotor RP120-AT, Sorvall) at 20 °C, while the samples extracted with carbonate were centrifuged at 80,000 rpm (rotor RP120-AT, Sorvall) for 30 min at 4 °C. The supernatant was removed. A small aliquot of the salt-extracted supernatant was assayed directly for enzymatic activity with the OG assay described above. The carbonate-extracted material was first neutralized with glacial acetic acid and precipitated with 30% trichloroacetic acid. To pellet the precipitated protein, the suspensions were spun at full speed in a tabletop microcentrifuge. The pellet was washed with 50:50 ethanol/ether. This precipitate as well as the original unextracted cell pellet were dissolved in 0.1 M Tris (pH 8.9) and 1% SDS. The presence of 3×FLAG-DGKε and 3×FLAG- DGKε P32A proteins in each fraction was detected by Western blotting using mouse anti-FLAG M2 antibody (Sigma-Aldrich).

Indirect immunofluorescence

NIH 3T3 cells were grown on poly-L-lysine-coated coverslips in a six-well plate. The cells were grown to 50–70% confluency in DMEM with 10% FBS and 1% penicillin/streptomycin. The cells were then transiently transfected with Lipofectamine 2000 reagent from Invitrogen. The medium was replaced after 5 h and the cells were left in the incubator for 16–18 h. The next day, the cells were fixed with 3.7% paraformaldehyde in PBS, pH 7.4, and after several washes, the cells were incubated with 5% bovine serum albumin in PBS for 1.5 h or they were treated with 0.1% Triton X-100 in PBS for 10 min, washed a few times and then incubated with 5% bovine serum albumin in PBS for 1.5 h. The cells were then rinsed with PBS and incubated with the mouse monoclonal anti-FLAG antibody (Sigma-Aldrich) in PBS (1:200) for 1.5 h at 37 °C in 5% CO_2. The cells were rinsed three times with PBS then incubated with Alexa Fluor 488-labeled goat anti-mouse IgG (Molecular Probes/Invitrogen) in PBS (1:500 or

1:1000) for 1 h at 37 °C in 5% carbon dioxide. After washing the glass coverslips five times with PBS, the coverslips were mounted onto the glass slides and left to dry at room temperature in the dark overnight. The coverslips were then sealed onto the slide with nail polish and left to dry. The slides were visualized using a confocal fluorescent microscope. The intensity levels of images from cells before and after permeabilization were kept identical.

Preparation of affinity-purified plasma membrane fraction

The biotinylation protocol was adapted from the work of Zhao *et al.*[17] and from the manufacturer's instructions. NIH 3T3 cells were grown at 37 °C in DMEM with 10% FBS until approaching confluency (80%) and transfected with FLAG-DGKε plasmid DNA. Ten dishes (10 cm) of cells were washed with pre-warmed (37 °C) PBS three times, and then 5 mL of PBS and 167 μL of 10 mM EZ-Link Sulfo-NHS-SS-Biotin (Pierce, Rockford, IL) stock solution in water was added to each dish. The cells were incubated at room temperature for 30 min and the biotinylation reaction was quenched by removal of the biotin solution and addition of 50 mM Tris–HCl (pH 8). The cells were washed twice with ice-cold PBS and scraped into ice-cold PBS containing 1× protease inhibitor cocktail. After centrifugation at 1000*g* for 5 min, 4 °C, the cells were resuspended into 1 mL of ice-cold hypotonic buffer (10 mM Hepes, pH 7.5, 1.5 mM $MgCl_2$, 10 mM KCl, 1× protease inhibitor cocktail, 1 mM NaF and 1 mM Na_3VO_4), incubated on ice for 15 min and broken by Dounce homogenization (50 passes). A post-nuclear supernatant (PNS) was generated by centrifugation at 1000*g* for 10 min at 4 °C. The KCl concentration in this fraction was adjusted to 150 mM, and then the fraction was centrifuged at 12,000*g* for 15 min at 4 °C to obtain the post-mitochondrial fraction (PMF). A 250-μL aliquot of suspended streptavidin magnetic beads (Dynabeads 280, Invitrogen, pre-washed with PBS three times before use) was added to the PMF fraction and the suspension was rotated at 4 °C for 1 h. The beads were collected with the use of a magnetic plate and washed eight times with the hypotonic buffer to obtain the affinity-purified membrane fraction. Proteins were extracted from beads with 2× SDS sample buffer containing 50 mM DTT and precipitated with trichloroacetic acid/acetone. The protein pellet was redissolved in 1% SDS sample buffer prior to SDS-PAGE. The presence of 3×FLAG-DGKε and organelle-specific proteins was detected by Western blotting using mouse anti-FLAG M2 antibody, anti-Na/K ATPase α polyclonal antibody (Santa Cruz Biotechnology) and anti-GRP 94 polyclonal antibody (Santa Cruz Biotechnology).

Subcellular fractionation

Subcellular fractionation was adapted from a previously described procedure.[32] The fractionation was performed using the OptiPrep gradient (Sigma-Aldrich), according to the manufacturer's instructions. Briefly, COS-7 cells were transiently transfected with either FLAG-DGKε or FLAG-DGKε P32A vectors and after 48 h the cells were rinsed twice with PBS, scraped in homogenization buffer [0.25 M sucrose, 10 mM Tris, pH 7.4, 1 mM EDTA, 1 mM KCl, 20 mM NaCl, 1× protease inhibitor cocktail (Sigma-Aldrich)] and centrifuged for 5 min at 1000*g*. Cells were resuspended in 0.5 mL of homogenization buffer plus DNase I, followed by homogenization at 4 °C by 14 passages through a 25-gauge needle syringe. The homogenate was centrifuged at 1000*g* for 10 min to obtain a PNS. The PNS was further centrifuged at 100,000*g* at 4 °C for 1 h and the resulting membrane pellet was resuspended in 1 mL of homogenization buffer containing 25% (w/v) iodixanol. The vesicle suspension was layered underneath an OptiPrep gradient consisting of 3%, 6.5%, 10%, 13.5%, 17% and 20.5% (w/v) iodixanol solutions. Gradients were centrifuged using a SW41Ti rotor in a Beckman Optima L-100 XP ultracentrifuge at 50,000*g* for 18 h, 4 °C. Eighteen fractions were collected, concentrated using Vivaspin-500 columns (30-kDa cut-off, GE Healthcare) and analyzed with SDS-PAGE and Western blotting.

Molecular modeling

The location of the putative TM sequence of DGKε was predicted from the protein sequence by combining the method of Eisenberg *et al.*[33] with a test of the stability of the selected fragment using Impala.[2] The sequence G19–F37 was first identified using the method of Eisenberg *et al*. This TM segment might be too short to completely cross the membrane so we tested the insertion of several longer peptides with Impala. The results support the conclusion that the best putative TM segment is D18–Q42, notably because it allows a matching of the terminal residues (D18 and Q42) with the phospholipids' polar heads (data not shown). We have used this segment for subsequent calculations of the conformational and membrane insertion properties of this region of the protein. Our model protein segment was blocked at the amino and carboxyl termini to remove the charges at the ends of the peptide. The sequence used for modeling was: *N*-acetyl-DGHLILWTLCSVLLPVFITFWCSLQ-amide.

PepLook method (Boltzmann stochastic method)

In order to explore conformational possibilities of the peptide, we used the Boltzmann stochastic *in silico* method, PepLook.[20] This method requires several successive steps of calculation. At each step, a random population of 10,000 conformations of DGKε 18–42 is generated and the energy of all conformations is calculated using the force field described below. The first step uses a set of 64 pairs of Φ/Ψ of angles with equal probability. In the next steps, the probabilities of Φ/Ψ values per residue vary according to whether they had previously contributed in exclusively poor or exclusively good structural solutions for DGKε 18–42, respectively. The calculation is iterated up to when the probability of all Φ/Ψ angles remains constant. Then, the 99 models of lower energy are further minimized using a Simplex method[34, 35] with a precision of 5° and a maximum of 1000 steps.

Force field

The molecule energy was calculated as the sum of four contributions: van der Waals energy, electrostatic energy, internal and external hydrophobicity potential.

Van der Waals contribution is calculated using the 6-12 Lennard–Jones description of interaction energy between unbonded atoms [Eq. (1)]:

(1) $$E_{vdW} = \sum_{ij} \left[A_{ij} \left(\frac{r_i^0 + r_j^0}{d_{ij}} \right)^{12} - B_{ij} \left(\frac{r_i^0 + r_j^0}{d_{ij}} \right)^{6} \right]$$

A_{ij} and B_{ij} are coefficients assigned to atom pairs, $r^0{}_i$ and $r^0{}_j$ are the van der Waals radii of atoms i and j, andd_{ij} is the distance between i and j.

The Coulomb's equation [Eq. (2)] is used for the calculation of electrostatic interaction energy between nonbonded atoms:

(2)
$$E_{elec} = \lambda \sum_{i=1}^{N-1} \sum_{j=i-1}^{N} \frac{q_i q_j}{\varepsilon_{ij}(z)\, d_{ij}}$$

λ is the electronic density unit conversion factor, d_{ij} is the distance between atoms i and j. $\sum_{ij}(z)$ is the medium dielectric constant varying from 1 to 80 with a sigmoid function of d_{ij} (Ref. 36) between 2 and 10 Å. q_i and q_j are the FCPAC charges of atoms i and j.[19]

The intramolecular hydrophobicity contribution is calculated using Eq. (3). In this equation, energy decreases as an exponential function of distance between atoms:

(3)
$$E_{pho\_intra} = \sum_{i=1}^{N-1} \sum_{j=i+1}^{N} \delta_{ij} \left[\left(Etr_i\, f_{ij}\right) + \left(Etr_j\, f_{ji}\right)\right] \exp\left(r_i^0 + r_j^0 - d_{ij}/2\, r_{sol}\right)$$

$\delta_{ij} = -1$ if atoms in the interaction are both hydrophobic or both hydrophilic and $\delta_{ij} = +1$ if atoms i and j are of opposite type. Etr_i and Etr_j are the energy for transferring atoms i and j from a hydrophobic to a hydrophilic phase; f_{ij} and f_{ji} are the ratios of atom I or j surface covered by partner j or i, respectively; $r^0{}_i$and $r^0{}_j$ are the van der Waals radii of atoms i and j, d_{ij} is the distance between i and j and r_{sol} is the radius of a water molecule.

Finally the force field allows calculation of the energy of the structure with respect to the solvent. Solvent contribution is calculated via an implicit external hydrophobicity energy as described in Eq. (4):

(4)
$$E_{pho\_out} = \sum_{i=1}^{N} S_i\, Etr_{Si}$$

where *S* is the solvent-accessible surface of atoms calculated using the method of Shrake and Rupley with a surface precision of 162 points[37] as previously used to compute the hydrophobic and hydrophilic surfaces of residues in soluble proteins.[38] Etr_{Si} is the energy of transfer of atom i expressed in surface area units.[39]

Acknowledgements

The experimental work was supported by a grant to R.M.E. from the Canadian Natural Sciences and Engineering Research Council (NSERC 9848). R.B. is Director of Research at the Belgian Fund for Scientific Research (FNRS). A.T. is Research Director at the French Institute for Medical Research (INSERM). M.D. is supported by Walloon Region (DGTRE, PepSein grant). We are grateful to Mr. Rhandi Singh and Dr. Tony Collins for assistance with the microscopy experiments.

Supplementary Data

Supplementary data associated with this article can be found, in the online version, at doi:10.1016/j.jmb.2008.08.076

REFERENCES

1. Han, G. S., O', H. L., Siniossoglou, S. & Carman, G. M. (2008). Characterization of the yeast DGK1-encoded CTP-dependent diacylglycerol kinase. J. Biol. Chem. 283, 20443–20453.

2. Ducarme, P., Rahman, M. & Brasseur, R. (1998). IMPALA: a simple restraint field to simulate the biological membrane in molecular structure studies. Proteins, 30, 357–371.

3. Deber, C. M., Wang, C., Liu, L. P., Prior, A. S., Agrawal, S., Muskat, B. L. & Cuticchia, A. J. (2001). TM Finder: a prediction program for transmembrane protein segments using a combination of hydrophobicity and nonpolar phase helicity scales. Protein Sci. 10, 212–219.

4. Cserzo, M., Wallin, E., Simon, I., von Heijne, G. & Elofsson, A. (1997). Prediction of transmembrane alphahelices in prokaryotic membrane proteins: the dense

alignment surface method. Protein Eng. 10, 673–676. 808 Membrane Topology of Diacylglycerol Kinase Epsilon5. Tang, W., Bunting, M., Zimmerman, G. A., McIntyre, T. M. & Prescott, S. M. (1996). Molecular cloning of a novel human diacylglycerol kinase highly selective for arachidonate-containing substrates. J. Biol. Chem. 271, 10237–10241.

6. Walsh, J. P., Suen, R., Lemaitre, R. N. & Glomset, J. A. (1994). Arachidonoyl-diacylglycerol kinase from bovine testis. Purification and properties. J. Biol. Chem. 269, 21155–21164.

7. Topham, M. K. & Prescott, S. M. (2002). Diacylglycerol kinases: regulation and signaling roles. Thromb. Haemostasis, 88, 912–918.

8. Milne, S. B., Ivanova, P. T., Armstrong, M. D., Myers, D. S., Lubarda, J., Shulga, Y. V. et al. (2008). Dramatic differences in the roles in lipid metabolism of two isoforms of diacylglycerol kinase. Biochemistry, 47, 9372–9379.

9. Bazan, N. G. (2005). Lipid signaling in neural plasticity, brain repair, and neuroprotection. Mol. Neurobiol. 32, 89–103.

10. Musto, A. & Bazan, N. G. (2006). Diacylglycerol kinase epsilon modulates rapid kindling epileptogenesis. Epilepsia, 47, 267–276.

11. Rodriguez de Turco, E. B., Tang, W., Topham, M. K., Sakane, F., Marcheselli, V. L., Chen et al. (2001). Diacylglycerol kinase epsilon regulates seizure susceptibility and long-term potentiation through arachidonoyl-inositol lipid signaling. Proc. Natl Acad. Sci. USA, 98, 4740–4745.

12. Wattenberg, B. W., Pitson, S. M. & Raben, D. M. (2006). The sphingosine and diacylglycerol kinase superfamily of signaling kinases: localization as a key to signaling function. J. Lipid Res. 47, 1128–1139.

13. Glukhov, E., Shulga, Y. V., Epand, R. F., Dicu, A. O., Topham, M. K., Deber, C. M. & Epand, R. M. (2007). Membrane interactions of the hydrophobic segment of diacylglycerol kinase epsilon. Biochim. Biophys. Acta, 1768, 2549–2558.

14. Dicu, A. O., Topham, M. K., Ottaway, L. & Epand, R. M. (2007). Role of the hydrophobic segment of diacylglycerol kinase epsilon. Biochemistry, 46, 6109–6117.

15. Elofsson, A. & von Heijne, G. (2007). Membrane protein structure: prediction versus reality. Annu. Rev. Biochem. 76, 125–140.

16. Carman, G. M., Deems, R. A. & Dennis, E. A. (1995). Lipid signaling enzymes and surface dilution kinetics. J. Biol. Chem. 270, 18711–18714.

17. Zhao, Y., Zhang, W., Kho, Y. & Zhao, Y. (2004). Proteomic analysis of integral plasma membrane proteins. Anal. Chem. 76, 1817–1823.

18. Kobayashi, N., Hozumi, Y., Ito, T., Hosoya, T., Kondo, H. & Goto, K. (2007). Differential subcellular targeting and activity-dependent subcellular localization of diacylglycerol kinase isozymes in transfected cells. Eur. J. Cell Biol. 86, 433–444.

19. Thomas, A., Milon, A. & Brasseur, R. (2004). Partial atomic charges of amino acids in proteins. Proteins, 56, 102–109.

20. Thomas, A., Deshayes, S., Decaffmeyer, M., Van Eyck, M. H., Charloteaux, B. & Brasseur, R. (2006). Prediction of peptide structure: how far are we? Proteins, 65, 889–897.

21. Lovell, S. C., Davis, I. W., Arendall, W. B., III, de Bakker, P. I., Word, J. M., Prisant, M. G. et al. (2003). Structure validation by Calpha geometry: phi,psi and Cbeta deviation. Proteins, 50, 437–450.

22. Blobel, G. (1980). Intracellular protein topogenesis. Proc. Natl Acad. Sci. USA, 77, 1496–1500.

23. Jennings, M. L. (1989). Topography of membrane proteins. Annu. Rev. Biochem. 58, 999 1027.

24. Fowler, P. W., Balali-Mood, K., Deol, S., Coveney, P. V. & Sansom, M. S. P. (2007). Monotopic enzymes and lipid bilayers: a comparative study. Biochemistry, 46, 3108–3115.

25. Birrell, G. B., Hedberg, K. K., Volwerk, J. J. & Griffith, O. H. (1993). Differential expression of phospholipase C specific for inositol phospholipids at the cell surface of rat glial cells and REF52 rat embryo fibroblasts. J. Neurochem. 60, 620–625.

26. Fukunaga-Takenaka, R., Shirai, Y., Yagi, K., Adachi, N., Sakai, N., Merino, E. et al. (2005). Importance of chroman ring and tyrosine phosphorylation in the subtype-specific translocation and activation of diacylglycerol kinase alpha by D-alpha-tocopherol. Genes Cells, 10, 311–319.

27. Crane, J. K. & Vezina, C. M. (2005). Externalization of host cell protein kinase C during enteropathogenic Escherichia coli infection. Cell Death Differ. 12, 115–127.

28. Yohannan, S., Faham, S., Yang, D., Whitelegge, J. P. & Bowie, J. U. (2004). The evolution of transmembrane helix kinks and the structural diversity of G proteincoupled receptors. Proc. Natl Acad. Sci. USA, 101, 959–963.

29. Spisni, E., Tomasi, V., Cestaro, A. & Tosatto, S. C. (2005). Structural insights into the function of human caveolin 1. Biochem. Biophys. Res. Commun. 338, 1383–1390.

30. Schlegel, A., Schwab, R. B., Scherer, P. E. & Lisanti, M. P. (1999). A role for the caveolin scaffolding domain in mediating the membrane attachment of caveolin-1. The caveolin scaffolding domain is both necessary and sufficient for membrane binding in vitro. J. Biol. Chem. 274, 22660–22667.

31. Campbell, R. E., Tour, O., Palmer, A. E., Steinbach, P. A., Baird, G. S., Zacharias, D. A. & Tsien, R. Y. (2002). A monomeric red fluorescent protein. Proc. Natl Acad. Sci. USA, 99, 7877–7882.

32. Ring, A., Le, L. S., Pohl, J., Verkade, P. & Stremmel, W. (2006). Caveolin-1 is required for fatty acid translocase (FAT/CD36) localization and function at the plasma membrane of mouse embryonic fibroblasts. Biochim. Biophys. Acta, 1761, 416–423.

33. Eisenberg, D., Weiss, R. M. & Terwilliger, T. C. (1982). The helical hydrophobic moment: a measure of the amphiphilicity of a helix. Nature, 299, 371–374.

34. Lagarias, J. C., Reeds, J. A., Wright, M. H. & Wright, P. E. (1998). Convergence properties of the Nelder–Mead simplex method in low dimensions. SIAM J. Optim. 9, 112–147.

35. Nelder, J. A. & Mead, R. (1965). A simplex method for function minimization. Comput. J. 7, 308–313.

36. Smith, P. E. & Pettitt, B. M. (1994). Modeling solvent in biomolecular systems. J. Phys. Chem. 98, 9700–9711.

37. Shrake, A. & Rupley, J. A. (1973). Environment and exposure to solvent of protein atoms. Lysozyme and insulin. J. Mol. Biol. 79, 351–371.

38. Lins, L., Thomas, A. & Brasseur, R. (2003). Analysis of accessible surface of residues in proteins. Protein Sci. 12, 1406–1417.

39. Brasseur, R. (1991). Differentiation of lipid-associating helices by use of three-dimensional molecular hydrophobicity potential calculations. J. Biol. Chem. 266, 16120–16127.

CHAPTER THREE

MOLECULAR SPECIES OF PHOSPHATIDYLINOSITOL-CYCLE INTERMEDIATES IN THE ENDOPLASMIC RETICULUM AND PLASMA MEMBRANE

CHAPTER THREE PREFACE

The work presented in this chapter was published previously in *Biochemistry*, volume 49(2), pages 312-317, in 2010.

Shulga Y.V. conducted sample preparation (cell culture and subcellular fractionation by iodixanol gradient), as well as interpretation of results. Myers D.S., Ivanova P.T., and Milne S.B. conducted mass spectral analysis.

Research objective: to investigate the role of DGKε in the PtdIns cycle occurring between the plasma membrane and endoplasmic reticulum.

Research highlights:

- The acyl chain profile for phosphoinositides is very different from that for phosphatidic acid in mouse embryonic fibroblasts, suggesting that phosphatidic acid is derived from other sources in addition to the action of DGK in the PtdIns cycle;
- In the plasma membrane of DGKε KO cells the levels of phosphoinositides and phosphatidic acid are decreased 3-fold in comparison with those in WT cells;
- The PI cycle is slowed in the DGKε KO cells;
- There is less of an effect of the DGKε depletion in the ER where *de novo* synthesis of phosphatidic acid occurs in comparison with the plasma membrane.

Molecular Species of Phosphatidylinositol-Cycle Intermediates in the Endoplasmic Reticulum and Plasma Membrane

Yulia V. Shulga‡, David S. Myers§, Pavlina T. Ivanova§, Stephen B. Milne§, H. Alex Brown*§, Matthew K. Topham|| and Richard M. Epand*‡

‡ Department of Biochemistry and Biomedical Sciences, McMaster University, Hamilton, Ontario L8N 3Z5, Canada

§ Department of Pharmacology, Vanderbilt University Medical Center, Nashville, Tennessee 37232

|| Huntsman Cancer Institute, University of Utah, Salt Lake City, Utah 84112

*To whom correspondence should be addressed. R.M.E.: Department of Biochemistry and Biomedical Sciences, McMaster University, 1200 Main St. W., Hamilton, Ontario L8N 3Z5, Canada; telephone, (905) 525-9140; fax, (905) 521-1397; e-mail, epand@mcmaster.ca. H.A.B.: Department of Pharmacology, Vanderbilt University School of Medicine, 23rd Ave. S. at Pierce, Nashville, TN 37232-6600; telephone, (615) 936-2189; fax,(615) 936-6833; e-mail, alex.brown@vanderbilt.edu.

Funding Statement

This work was supported in part by a grant from the Natural Sciences and Engineering Research Council of Canada (Grant 9848 to R.M.E.) and by National Institutes of Health Grants R01-CA95463 (to M.K.T.) and U54 GM069338 (to H.A.B.).

Abbreviations

DGK, diacylglycerol kinase; DAG, diacylglycerol; PA, phosphatidic acid; PI, phosphatidylinositol; PIPn, all phosphorylated forms of PI; PLC, phospholipase C; PI(4,5)P2, phosphatidylinositol 4,5-bisphosphate; WT, wild type; KO, DGKε-knockout; ER, endoplasmic reticulum; PM, plasma membrane; SAG, 1-stearoyl-2-

arachidonoylglycerol; SAPA, 1-stearoyl-2-arachidonoylphosphatidic acid; DMEM, Dulbecco's modified Eagle's medium; PNS, postnuclear supernatant; FBS, fetal bovine serum.

ABSTRACT

Phosphatidylinositol (PI) turnover is a process requiring both the plasma and ER membranes. We have determined the distribution of phosphatidic acid (PA) and PI and their acyl chain compositions in these two subcellular membranes using mass spectrometry. We assessed the role of PI cycling in determining the molecular species and quantity of these lipids by comparing the compositions of the two membranes isolated from embryonic fibroblasts obtained from diacylglycerol kinase ε (DGKε) knockout (KO) and wild-type (WT) mice. In the KO cells, the conversion of arachidonoyl-rich DAG to PA is blocked by the absence of DGKε, resulting in a reduction in the rate of PI cycling. The acyl chain composition is very similar for PI and PA in the endoplasmic reticulum (ER) versus plasma membrane (PM) and for WT versus KO. However, the acyl chain profile for PI is very different from that for PA. This indicates that DGKε is not facilitating the direct transfer of a specific species of PA between the PM and the ER. Approximately 20% of the PA in the ER membrane has one short acyl chain of 14 or fewer carbons. These species of PA are not converted into PI but may play a role in stabilizing regions of high positive curvature in the ER. There are also PI species in both the ER and PM for which there is no detectable PA precursor, indicating that these species of PI are unlikely to arise via the PI cycle. We find that in the PM of KO cells the levels of PI and of PA are decreased 3-fold in comparison with those in either the PM of WT cells or the ER of KO cells. The PI cycle is slowed in the KO cells; hence, the lipid

intermediates of the PI cycle can no longer be interconverted and are depleted from the PI cycle by conversion to other species. There is less of an effect of the depletion in the ER where de novo synthesis of PA occurs in comparison with the PM.

INTRODUCTION

A major pathway for hormonal stimulation of cells is through the activation of $PI(4,5)P_2$-specific isoforms of phospholipase C that catalyzes the hydrolysis of $PI(4,5)P_2$[1] to the two signaling molecules, diacylglycerol (DAG) and inositol triphosphate. The efficiency of this system is due in part to the fact that the initial substrate, $PI(4,5)P_2$, is regenerated from DAG through a biochemical cycle termed the PI cycle. The hormone-stimulated initial cleavage of $PI(4,5)P_2$occurs in the PM, but the regeneration of $PI(4,5)P_2$ requires participation of enzymes found only in the ER (Figure 3.1). Thus, the functioning of the PI cycle requires transfer of lipids between these two membranes.

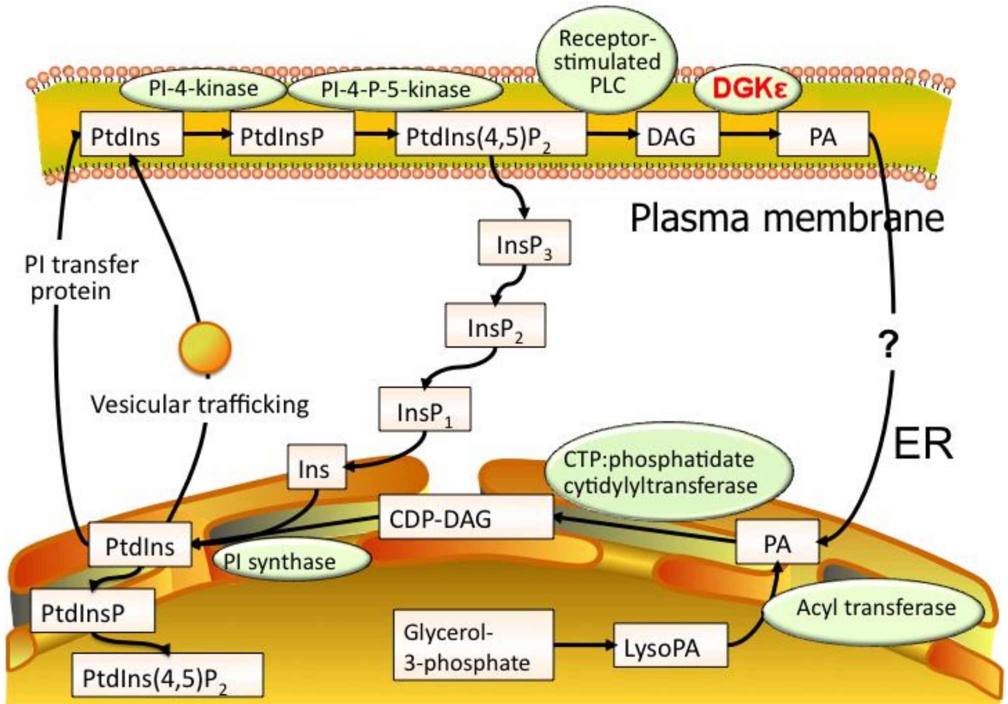

Figure 3.1. PI cycle.

Several of the lipid intermediates of the PI cycle have important signaling properties; however, little is known about how they are distributed between the two membranes involved in the PI cycle, nor is the acyl chain composition for these lipids known in these two membranes. Among the lipid intermediates of the PI cycle with important signaling properties are the various species of phosphorylated PI, PIPn. This lipid class, of PI plus PIPn, comprises only 5−8% of total lipids in mammalian cells (1). However, these lipids regulate fundamental cell processes, including cell growth, cytoskeleton dynamics, membrane trafficking, and nuclear events (2). PI(4,5)P_2 is not the only form of PIPn with important cellular functions; rather, PIPn species undergo rapid interconversion through cycles of phosphorylation and dephosphorylation, tightly regulated by numerous PI and PIPn kinases and phosphatases to form PI and various species of PIPn with varying numbers and positions of phosphorylation in the inositol moiety. All of the different forms of PIPn serve as individual signaling molecules. Another important signaling lipid of the PI cycle is phosphatidic acid (PA). PA is essential in controlling cell processes such as cytoskeletal rearrangement, proliferation, and cell survival (3). PA is required for vesicular trafficking. A decreasing level of PA production results in a reduced level of exocytosis (4). PA regulates fusion through promotion of the negative membrane curvature (3). Another lipid intermediate of the PI cycle, diacylglycerol (DAG), is a lipid second messenger whose importance in cell signaling is well-established (5). DAG's diverse range of effectors allows it to modulate a large variety of cellular events, resulting in its broad effects on the cell (6).

There is interconversion among the three types of lipid signaling molecules, PI/PIPn, PA, and DAG, in the PI cycle. One important step in PI turnover is the conversion of DAG to PA, the first step in the resynthesis of PI, catalyzed by diacylglycerol kinases (DGK), a family of lipid signaling enzymes (7-10). Among all the isoforms of DGK, DGKε appears to be most important for catalyzing this step in the PI cycle (11, 12). DGKε is located in both plasma and ER membranes (13); it has specificity for 1-stearoyl-2-arachidonoylglycerol (14), and through the PI cycle, DGKε contributes to enriching the PI with these acyl chains (14). In this work, we assess the role of the PI cycle in determining the location and acyl chain composition of the lipid intermediates of the cycle by affecting the cycle with the deletion of DGKε. For this purpose, we have compared the PA and PI of the ER and PM isolated from embryonic fibroblasts derived from DGKε KO and WT mice using mass spectrometry. This is a reliable method of detecting PI and PA and also allows determination of the acyl chain composition of these lipids. There have been studies using fluorescent protein-tagged protein domains that specifically recognize PI lipids to determine their cellular localization, but these methods have their own limitations (15). In addition, there is no acceptable fluorescent probe, specific for non-PI lipids, such as PA.

EXPERIMENTAL PROCEDURES

Tissue Culture

Mouse fibroblasts were obtained from embryos of mice that were made deficient in DGKε and are designated as DGKε KO mouse embryonic fibroblasts (MEFs) (11). In each experiment, these cells were compared with wild-type embryonic fibroblasts obtained from siblings of the (−/−) mice. These cells, derived from DGKε (+/+) embryos, are designated as DGKε WT MEFs. All cells were immortalized by transfection with the SV40 large T antigen. Cells were cultured in DMEM supplemented with 10% fetal bovine serum and 25 mM HEPES, at 37 °C in a humidified atmosphere with 5% CO_2.

Subcellular Fractionation

Subcellular fractionation was adapted from a previously described procedure (16). The fractionation was performed using the OptiPrep gradient (Sigma-Aldrich), according to the manufacturer's instructions. The method has been shown to give good separation of the ER and PM despite the fact that these two organelles have very similar densities of 1.16 g/cm^3(17). Briefly, DGKε KO and WT MEF cells were grown at 37 °C in DMEM medium with 10% FBS until they approached confluency (80%). Thirty-two dishes (10 cm) of each cell line were washed two times with ice-cold PBS and scraped into ice-cold PBS containing 1× protease inhibitor cocktail for use with mammalian cell and tissue extracts (Sigma-Aldrich). The cells were collected by centrifugation at 1000*g* for 5 min at 4 °C and resuspended in 850 μL of ice-cold homogenization buffer [0.25 M sucrose, 10 mM HEPES (pH 7.5), 1 mM EDTA, 1 mM KCl, 20 mM NaCl, and 1× protease inhibitor cocktail]. The cells were broken by 20 passages through a 25-gauge needle syringe. Unbroken cells and nuclei were removed from the cell homogenate by centrifugation at 1000*g* for 10 min at 4 °C to generate a postnuclear supernatant (PNS). The crude microsomal sample was diluted with the 50% Optiprep Density Gradient Medium (Iodixanol, from Sigma) to a final concentration of 25% Optiprep. The vesicle suspension was layered underneath an OptiPrep gradient consisting of 3, 6.5, 10, 13.5, 17, and 20.5% (w/v) iodixanol solutions. Gradients were centrifuged using a SW41Ti rotor in a Beckman Optima L-100 XP ultracentrifuge at 50000*g* for 18 h at 4 °C. Eighteen fractions were collected and concentrated using Vivaspin-500 columns (30 kDa cutoff, GE Healthcare). The presence of organelle-specific proteins was detected by SDS−PAGE and Western blotting using rabbit anti-Na/K ATPase α polyclonal antibody (Santa Cruz Biotechnology) and anti-GRP-94 polyclonal antibody (Santa Cruz Biotechnology). Marker enzymes indicate an excellent separation of the PM and ER. It is not likely that there would be much contamination with other organelles that have an even greater difference in density. In addition, we are measuring the total PA and PI species in these membranes, so that a minor contamination with another organelle would not greatly affect the results. This is different, for example, from a common use of subcellular fractionation to determine the location of an enzyme, where a small contamination can falsely identify a fraction as being the one in which the enzyme is located. Nevertheless, we recognize that there is likely some overlap in the distribution of subcellular organelles that is in part unavoidable because several of these membranes undergo exchange of materials and cycling and there are probably membrane particles of intermediate density. The ER contains the largest amount of membrane material in the cell, so any contamination of this fraction would be a small percent of the total. Because of its similar density, the ER would be the most likely contaminant of the PM. However, there is little overlap of the two peaks for the marker enzymes, and the lipid composition is distinctly different between the PM and ER fractions. Furthermore, there is not likely to be a major difference in the contamination of the organelles between the two cell lines since the acyl chain compositions in the PM and ER, although different from each other, are the same for WT and KO cells.

Determination of the Total Protein Concentration

The total protein concentration in the samples was measured using a BCA protein assay kit (Thermo Scientific) according to the product manual.

Glycerophospholipid Analysis

Phospholipids were extracted from the cellular fractions by a modified Bligh and Dyer extraction using acidified methanol. Briefly, an equal volume of ice-cold 0.1 N methanolic HCl and ice-cold $CHCl_3$ was added to each of the fractions. Following a 1 min vortex at 4 °C, layers were separated by centrifugation (18000*g* for 5 min at 4 °C).

After the extraction and addition of standards, solvent was evaporated. The resulting lipid film was dissolved in 100 μL of a 58:40:2 2-propanol/hexane/100 mM $NH_4COOH_{(aq)}$ mixture (mobile phase A).The mass spectrometric analysis and quantitation were performed essentially as described in ref 18. The LC−MS technique was used with the utilization of synthetic odd-carbon phospholipid standards (four per each class). An MDS SCIEX 4000QTRAP hybrid triple-quadrupole/linear ion trap mass spectrometer (Applied Biosystems, Foster City, CA) was used for the analyses. Coupled to it was a Shimadzu HPLC system (Shimadzu Scientific Instruments, Inc., Columbia, MD) consisting of a SCL 10 APV controller, two LC 10 ADVP pumps, and a CTC HTC PAL autosampler (Leap Technologies, Carrboro, NC). Phospholipids were separated on a Phenomenex Luna Silica column (Phenomenex, Torrance, CA) (2 mm × 250 mm, 5 μm particle size) using a 20 μL sample injection. A binary gradient consisting of a 58:40:2 2-propanol/hexane/100 mM $NH_4COOH_{(aq)}$mixture (mobile phase A) and a 50:40:10 2-propanol/hexane/100 mM $NH_4COOH_{(aq)}$ mixture (mobile phase B) was used for the separation. The parameters of the mass spectrometer instrument and solvent gradient were as described in ref 18.

Statistical Analysis

Experiments were performed in five independent repeats of each subcellular fraction and condition (ER/WT, ER/KO, PM/WT, and PM/KO). The concentration of total protein was measured in each sample, and the amount of each lipid was normalized for the amount of the corresponding marker protein, relative to the total protein in the PNS. Results are presented as means ± the standard error of the mean (SEM). Data are analyzed by paired *t* tests across either fractions (ER and PM) or genotypes (WT and KO) from the repeated experiments. Association of enrichment levels of PI in one fraction versus the other (the PM:ER ratio) with acyl chain length and fatty acid unsaturation is assessed by Spearman rank correlation (19).

RESULTS

Subcellular Fractionation of DGKε KO and WT MEF Cells

We tested the role of PI cycling in determining the relative amounts of specific species of PA and PI, as well as their partitioning between the plasma and ER membranes of DGKε KO and WT MEF cells. The membranes of DGKε KO and WT MEF cells were separated using an OptiPrep gradient. We used antibodies to the proteins GRP-94 and Na/K ATPase α as markers for the ER and the PM, respectively. The ER marker was found exclusively in the higher-density fractions, but the PM has a broader distribution, with the major portion being in the lower-density fractions. The distribution of the PM was confirmed previously, using antibodies to caveolin-1, which showed a pattern similar to the distribution of Na/K ATPase α. The density of the bands was quantified by densitometry (Figure 3.2). The standard curve, using different amounts of amino-terminal FLAG-BAP protein (Sigma), was plotted to show that loaded amounts of protein were in the linear range. The fractions containing the maximum amount of the marker proteins were combined and used for mass spectrometry analysis. These were generally fractions 5−9 for the plasma membrane but varied by one or two fractions from one preparation to another and fractions 16−18 for the ER samples.

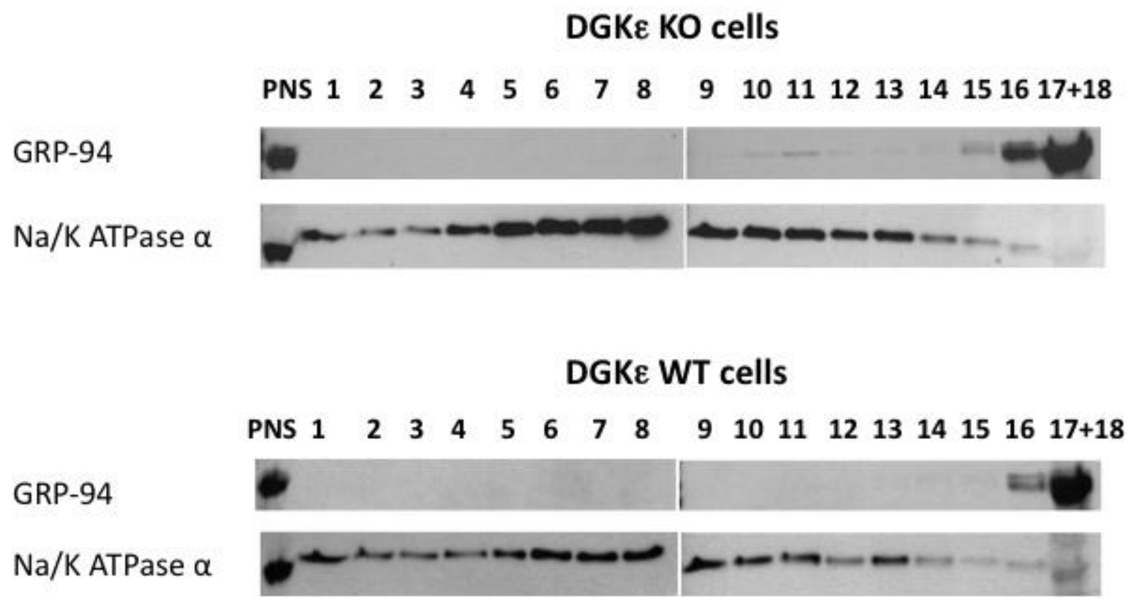

Figure 3.2. Isolation of PM and ER membrane fractions by iodixanol gradient centrifugation. Fractionation was performed using a 3 to 25% OptiPrep gradient, and fractions were analyzed by immunoblotting with antibodies against GRP-94 (ER marker) and Na/K ATPase α (PM marker). PNS is the postnuclear supernatant.

Phospholipid Composition of Plasma and ER Membranes of WT versus DGKε KO Cells

Mass spectrometry analysis of plasma and ER membrane fractions of DGKε KO and WT MEF cells showed a number of significant differences in PA and PI composition. Notably, the PM of KO cells contains only one-third of the PI and PA, as does the ER (Figure 3.3). Although the effect is modest, there is a close relationship between the level of PI enrichment in the PM versus ER to acyl chain length and fatty acid unsaturation in DGKε KO cells, but not in WT cells. In particular, the rank correlation (Spearman's ρ) of the number of carbons to the PM:ER ratio for PI species in the DGKε KO case is −0.74

(p < 0.01) and is even more pronounced for the correlation with the number of double bonds (−0.88, p < 0.01). These correlations are not significant for the WT cells.

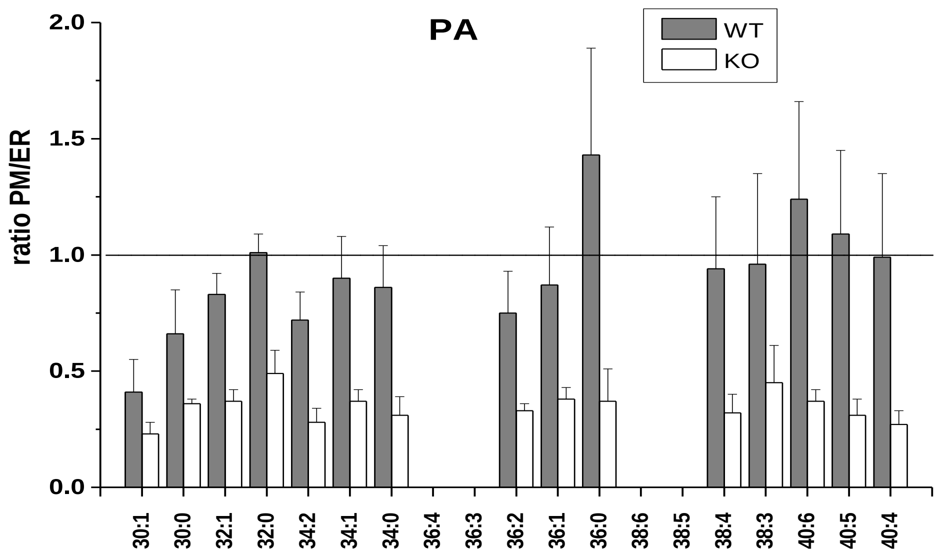

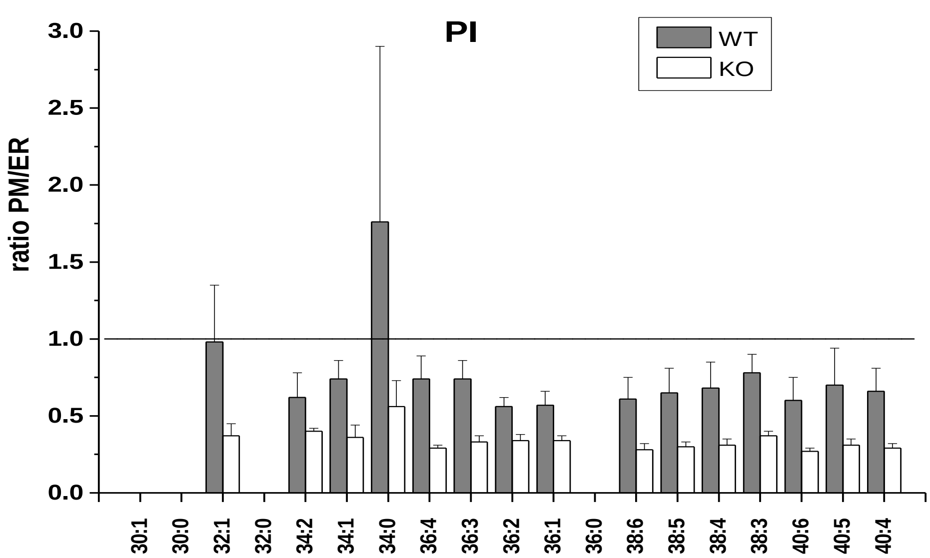

Figure 3.3. Comparison of ratios of PA or PI in the PM to ER for DGKε KO and WT cells. Results are presented as means of the PM:ER ratio ± SEM. In the KO case, all PM:ER ratios shown are significantly less than one with $p < 0.05$ except for 32:0 PA ($p = 0.06$), 36:0 PA ($p = 0.08$), 38:3 PA ($p = 0.08$), and 34:0 PI ($p = 0.19$). The only PM:ER ratios in the WT case that are significantly less than 1 are 36:1 PI ($p = 0.01$) and 36:2 PI ($p = 0.03$).

When taken as a ratio of KO to WT, several PA and PI species, such as 30:1 PA, 38:4 PA, 38:3 PA, 40:4 PA, 36:4 PI, 38:6 PI, and 38:3 PI, show 2-fold decreases in the PM, whereas KO:WT ratios in the ER membrane show almost no significant changes (Figure 3.4).

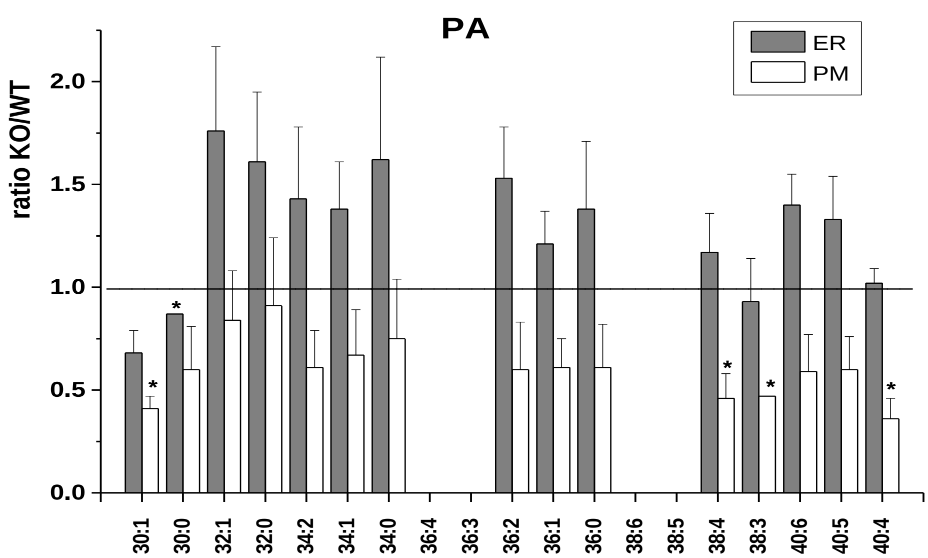

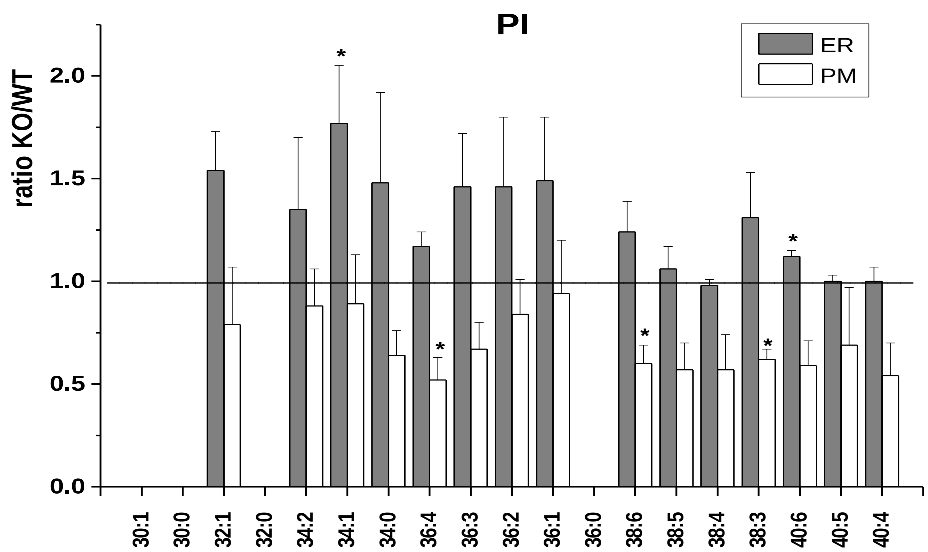

Figure 3.4. Comparison of ratios of PA and PI in DGKε KO to WT cells in plasma and ER membranes. Results are presented as means of the KO:WT ratio ± SEM. Statistically different values ($p < 0.05$) are labeled with asterisks.

Comparison of PM versus the ER Membrane of MEF Cells of Molecular Species of PA and PI

Although the levels of enrichment of PA and PI species in the PM versus the ER in WT cells are similar across the acyl chain distribution (Figure 3.3), the acyl chain profile for PI is very different from that for PA. The PI:PA ratio is >1 for 34:2, 36:1, 38:3, and 38:4, while for most of the other species, it is <1 (Figure 3.5). The overall PI:PA ratios in both the WT ER (1.79 ± 0.21, mean ± SEM) and PM (1.57 ± 0.12) are determined primarily by these major species of PI, which together account for more than half of the PI by mass in each fraction.

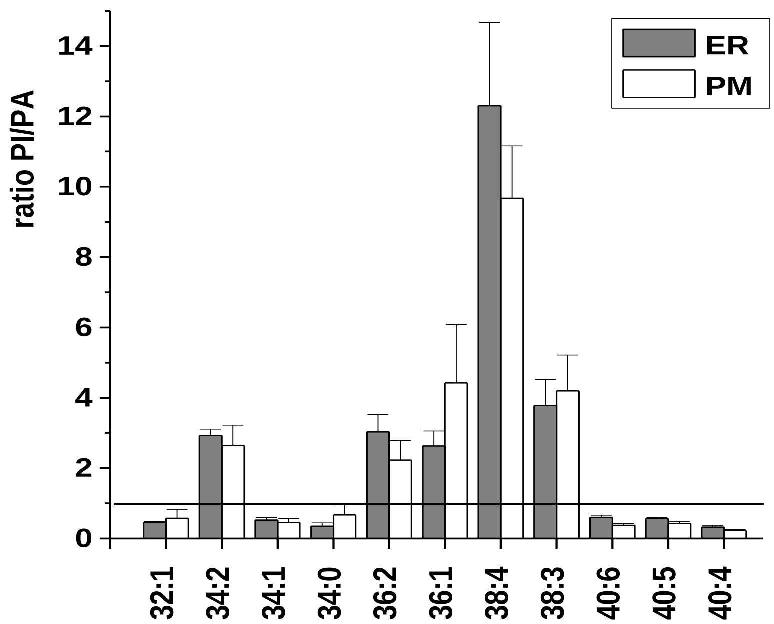

Figure 3.5. Ratios of PI to PA in the plasma and ER membranes of DGKε WT cells. Results are presented as means of the PI:PA ratio ± SEM. All ratios are statistically different from 1.0 ($p < 0.05$) except for 32:1 and 34:0 in the PM.

Also, it is of particular interest that several species are detected either in PI or in PA, but not in both (Table 3.1). With regard to PA, there are two species, 30:1 and 30:0, that make up 21% of the PA in the ER. These species are twice as abundant in the ER compared with the PM. With regard to the unique PI species, they are found equally in the ER and PM, like most other lipid species, but unlike the unique PAs.

Table 3.1. List of PA and PI Species That Do Not Have a Corresponding Pair in the Other Lipid Class[a].

[a]Values given as a percentage of the total lipid of that type.

PA for which there is no corresponding PI			**PI for which there is no corresponding PA**		
species	**ER**	**PM**	**species**	**ER**	**PM**
30:1 PA	9.0	4.4	36:4 PI	5.9	6.4
30:0 PA	12	9.0	36:3 PI	3.3	4.0
32:0 PA	4.9	6.8	38:6 PI	1.8	1.6
36:0 PA	2.6	2.3	38:5 PI	18	16

Comparison of Results to Analysis Using Relative Quantitation of Molecular Species of PA and PI versus Total Phospholipid

To safeguard against variable recovery rates across the subcellular fractions or genotypes, the analyses for Figures 3.3 and 3.4 were repeated on the basis of the percent composition of the PA and PI molecular species, normalized by total phospholipid. These relative quantitation results are presented in Figures S1 and S2 of the Supporting Information, and it is evident that no large differences exist between the respective analyses in Figures 3.3 and 3.4, which use absolute quantitation.

DISCUSSION

For most PA and PI species in WT cells, the ratio of PM to ER is close to 1 (Figure 3.3), despite the fact that there is much more membrane in the ER than in the PM. Thus, the concentration of PI and PA within the ER membrane must be less than in the PM. The equal amount of these lipids in the two compartments may be a consequence of the PI cycle equalizing them. Although one would expect the rate of transfer from the more dilute PA and PI in the ER to be slower than the transfer to the ER from the higher concentration in the PM, this would be compensated by a larger amount of ER membrane, making the net flux of lipids in the two directions similar.

Our results also clearly show that DGKε is an important component of the PI cycle since deletion of this enzyme decreases the amounts of both PI and PA in the PM to approximately one-third of that found in the ER of these cells (Figure 3.3). Since PI is neither a substrate nor a product of the reaction catalyzed by DGKε, its concentration in a particular membrane could most likely change as a consequence of slowing the PI cycle by deletion of DGKε, though we cannot rule out the possibility that the knockout might have more indirect impacts on the PA and PI distributions, as well. The direct effect of slowing the PI cycle would be to specifically reduce the concentrations of arachidonoyl-containing PA and PI. However, we observe that the reduction in relative concentrations of PA and PI in the ER versus the PM extends essentially over all species (Figure 3.3). This is most likely a result of the interconvertion among species of PA and PI with different acyl chain compositions. This can occur by acyl chain remodeling through acylation−deacylation reactions. In addition, DGKε can be bypassed in the PI cycle through PLD-catalyzed formation of PA, including direct conversion of PI(4,5)P_2 to PA. Additionally, other isoforms of DGK, although are not specific for 1-stearoyl-2-arachidonoylglycerol (SAG), can still use it as a substrate to form 1-stearoyl-2-arachidonoyl-PA (SAPA), and the specificity of DGKε for SAG is not absolute; rather, it is the preferred substrate. Hence, the PI cycle will not be completely isolated from other metabolic pathways. Nonetheless, these results show the importance of the association of DGKε with the PI cycle, and this agrees with results reported previously (11, 12) and is consistent with the specificity of this enzyme for 1-stearoyl-2-arachidonoyl lipids (14). In particular, although differences in rates across PI species are relatively small (14), we find that there is a strong relationship (rank correlations with $p < 0.01$) between the level of PI enrichment in the PM versus the ER and acyl chain length and/or fatty acid unsaturation in DGKε KO cells, but not in WT cells (Figure 3.3).

The PM and the ER have different roles in the PI cycle. In the isolated wild-type PM, PI can be converted to PA; however, there are no enzymes in the PM that can synthesize PI from precursors. In addition, in the ER but not in the PM, PA can be synthesized de novo from smaller precursors. However, in the DGKε KO cells, the extent of formation of PA from arachidonoyl-rich DAG is reduced; hence, there is little SAPA produced. PA can also be produced by phospholipase D, including a small amount of SAPA by PI(4,5)P_2-requiring phospholipase D isoenzymes. However, in the PM alone, not all of the components are present to allow the functioning of a PI cycle to regenerate the lipid intermediates of the cycle.

It is known that intermediates in biochemical cycles have the property of being catalysts. They are regenerated each time the cycle repeats. As a consequence of this cyclic nature, the PI cycle lipid intermediates become progressively enriched with 1-stearoyl-2-arachidonoyl acyl chains through multiple iterations of this cycle. The cycle also contributes to the maintenance of the steady state concentration of the intermediates of the cycle. When the cycle is damaged, as in this case of the KO cells, via elimination of DGKε, these lipid intermediates are metabolized to other products. Furthermore, in the PM, several enzymes of the PI cycle are activated by other lipids of the cycle. In particular, PIP-5-kinase, which produces PI(4,5)P_2, is activated by PA (20, 21). Thus, in the absence of DGKε, the functioning of the PI cycle in the PM will also be slowed by the lack of SAPA produced by DGKε. Overall, there will be a lowering of PI and PA levels in the PM, which we observed in DGKε KO cells.

In the case of the ER membrane, the levels of most PI and PA species are slightly higher or remain the same in KO cells in comparison with WT cells. The level of PA in the ER can be maintained in part by an alternative pathway for the de novo synthesis of PA from glycerol 3-phosphate (22) (Figure 3.1). Using acyl-CoAs, PA is first synthesized and undergoes maturation in the remodeling pathway that includes acylation of lyso-PA (Lands cycle) (23). This newly synthesized PA can then enter the PI cycle in the ER through a CDP-dependent reaction catalyzed by CDP-diacylglycerol synthase. CDP-diacylglycerol synthase is not found in the PM, nor can the PM synthesize PA from small molecule precursors. Hence, PA and PI are more rapidly depleted in the PM in DGKε KO cells. Within the ER, PI can be phosphorylated to PI(4)P by PI(4)K, to PI(3,4)P_2, or to PI(4,5)P_2 by PIP(5)K (24).

PI formed in the ER can be transferred to the PM by both vesicular transport and specific lipid transporters. This process will also be slower in KO cells because of the lower level of PA in the PM of these cells. It has been shown that PA is required for vesicular trafficking and that decreasing PA production results in a reduced rate of exocytosis (4). PA regulates fusion through promotion o1f the negative membrane curvature (3). Therefore, in the PM of DGKε KO cells, where the levels of PA are significantly reduced, the fusion process, where the vesicle membrane becomes contiguous with the PM, will be disrupted. Moreover, vesicular transport is also regulated by PI(4,5)P_2 (25). Thus, reduced levels of PI(4,5)P_2 and PA in the PM of KO cells would reduce the level of vesicle fusion with the PM, therefore impairing vesicular trafficking of PI from the ER, further reducing the levels of these phospholipids in the PM. This also can account for the slight accumulations of PI in the ER, which we observed in DGKε KO cells. One interpretation is that the redistribution of PA and PI in the cell due to the knockout could largely be a result of the disruption of vesicular trafficking specifically, thereby altering the turnover of PI.

In further analysis, we also compared the distribution of different PI and PA species in DGKε WT mouse embryonic fibroblasts. The data show that the acyl chain composition of the PI and PA is similar in both plasma and ER membranes of this cell line, and also approximately the same in the WT and KO cells. This suggests that DGKε is not facilitating the transfer of specific species of PA between the PM and ER.

Furthermore, our results show that the acyl chain profile for PI is very different from that for PA. In both cellular fractions, virtually every species is found with a PI:PA ratio significantly greater than or less than 1. The PI:PA ratio is >1 for 34:2, 36:1, 38:3, and 38:4, while for most of the other species, it is <1 (Figure 3.5). These PI species, which together contain more than 50% of the PI mass in both fractions, have PI:PA ratios much higher than those of the other molecular species, and there is certainly no strict stoichiometry between PA and PI species across the acyl distribution. These data suggest that a narrow range of acyl chain lengths is enriched in PI relative to its precursor PA, and that PA is derived from other sources in addition to the action of DGK in the PI cycle. Thus, the species of PA used for the synthesis of PI are either preferred substrates or modulators of the biosynthetic enzymes involved, or these lipids are physically segregated into specific membrane domains.

It is of particular interest that several species with particular acyl chains are detected either as PI or as PA, but not as both (Table 3.1). These lipids are examples of species of PA and PI that do not appear to participate in the PI cycle since they do not have a corresponding partner, and thus, they should be somehow separated from lipids in the PI cycle. With regard to PA, there are two species, 30:1 and 30:0, that constitute 21% of the PA in the ER. These species are twice as abundant in the ER as in the PM. The 30:1 and 30:0 PA have a sum of 30 carbons in the acyl chains, which means that one acyl chain must have 14 or fewer. Only a minor fraction of acyl chains are this short, but these species are highly enriched in PA and in particular in the ER. We suggest that these short chain PA may concentrate on the outer monolayer of the ER. Since short acyl chains will facilitate positive curvature, they would stabilize some of the folds in the ER. This would not be needed in the PM. These species have a decreased level in the KO cells, which may indicate a change in ER morphology in KO compared with WT cells, to a form that is less folded.

With regard to the unique PI species, they are equally distributed in the ER and PM, like most other species of PA and PI, but unlike the unique PA. Our data show that their levels do not differ in KO and WT cells. The results indicate that these lipids are not involved in the PI cycle. In total, these unique PI species comprise 30% of the total PI. They do not have a PA precursor for them to be synthesized from a CDP-dependent reaction catalyzed by CDP-diacylglycerol synthase, an essential step in the PI cycle. Therefore, they could arise from an acyl chain exchange of one of the lipid intermediates of the PI turnover (through Lands cycle), or by a PLD-catalyzed headgroup exchange from another lipid class. Thus, only a specific fraction of PI and PA participates in the PI cycle, and these pools are likely segregated from the other lipids with the same headgroup that are not intermediates in this cycle.

The acyl chain composition is very similar for PI or PA in the ER versus PM and for WT versus KO cells. However, the acyl chain profile for PI is very different from that for PA. Our findings also reveal that DGKε plays an important role in inositol lipid turnover and regulates the lipid composition of the PM in mouse embryonic fibroblasts. The PI cycle is selective for lipids with specific acyl chains in both the PM and ER.

Supporting Information

We present results of an analysis giving the relative quantitation based on the percent composition of the PA and PI molecular species, normalized by total phospholipid. This material is available free of charge via the Internet at http://pubs.acs.org.

REFERENCES

1. Cockcroft, S. and De Matteis, M. A. (**2001**) Inositol lipids as spatial regulators of membrane traffic *J. Membr. Biol.* 180, 187– 194

2. Vicinanza, M., D'Angelo, G., Di Campli, A. and De Matteis, M. A. (**2008**) Function and dysfunction of the PI system in membrane trafficking *EMBO J.* 27, 2457– 2470

3. Cazzolli, R., Shemon, A. N., Fang, M. Q. and Hughes, W. E. (**2006**) Phospholipid signalling through phospholipase D and phosphatidic acid *IUBMB Life* 58, 457– 461

4. Huang, P., Altshuller, Y. M., Hou, J. C., Pessin, J. E. and Frohman, M. A. (**2005**) Insulin-stimulated plasma membrane fusion of Glut4 glucose transporter-containing vesicles is regulated by phospholipase D1 *Mol. Biol. Cell* 16, 2614– 2623

5. Carrasco, S. and Merida, I. (**2007**) Diacylglycerol, when simplicity becomes complex *Trends Biochem. Sci.* 32, 27– 36

6. Yang, C. and Kazanietz, M. G. (**2003**) Divergence and complexities in DAG signaling: Looking beyond PKC *Trends Pharmacol. Sci.* 24, 602– 608

7. Merida, I., Avila-Flores, A. and Merino, E. (**2008**) Diacylglycerol kinases: At the hub of cell signalling *Biochem. J.* 409, 1– 18

8. Topham, M. K. and Epand, R. M. (**2009**) Mammalian diacylglycerol kinases: Molecular interactions and biological functions of selected isoforms *Biochim. Biophys. Acta* 1790,416– 424

9. Cai, J., Abramovici, H., Gee, S. H. and Topham, M. K. (**2009**) Diacylglycerol kinases as sources of phosphatidic acid *Biochim. Biophys. Acta* 1791, 942– 948

10. Sakane, F., Imai, S., Kai, M., Yasuda, S. and Kanoh, H. (**2008**) Diacylglycerol kinases as emerging potential drug targets for a variety of diseases *Curr. Drug Targets* 9, 626–640

11. Rodriguez de Turco, E. B., Tang, W., Topham, M. K., Sakane, F., Marcheselli, V. L., Chen, C., Taketomi, A., Prescott, S. M. and Bazan, N. G. (**2001**) Diacylglycerol kinase epsilon regulates seizure susceptibility and long-term potentiation through arachidonoyl-inositol lipid signaling *Proc. Natl. Acad. Sci. U.S.A.* 98, 4740– 4745

12. Milne, S. B., Ivanova, P. T., Armstrong, M. D., Myers, D. S., Lubarda, J., Shulga, Y. V., Topham, M. K., Brown, H. A. and Epand, R. M. (**2008**) Dramatic Differences in the Roles in Lipid Metabolism of Two Isoforms of Diacylglycerol Kinase *Biochemistry* 47, 9372–9379

13. Decaffmeyer, M., Shulga, Y. V., Dicu, A. O., Thomas, A., Truant, R., Topham, M. K., Brasseur, R. and Epand, R. M. (**2008**) Determination of the Topology of the Hydrophobic Segment of Mammalian Diacylglycerol Kinase ε in a Cell Membrane and Its Relationship to Predictions from Modeling *J. Mol. Biol.* 383, 797– 809

14. Lung, M., Shulga, Y. V., Ivanova, P. T., Myers, D. S., Milne, S. B., Brown, H. A., Topham, M. K. and Epand, R. M. (**2009**) Diacylglycerol kinase ε is selective for both acyl chains of phosphatidic acid or diacylglycerol *J. Biol. Chem.* 284, 31062– 31073

15. Krauss, M. and Haucke, V. (**2007**) Phosphoinositide-metabolizing enzymes at the interface between membrane traffic and cell signalling *EMBO Rep.* 8, 241– 246

16. Ring, A., Le, L. S., Pohl, J., Verkade, P. and Stremmel, W. (**2006**) Caveolin-1 is required for fatty acid translocase (FAT/CD36) localization and function at the plasma membrane of mouse embryonic fibroblasts *Biochim. Biophys. Acta* 1761, 416– 423

17. Garner, J. A. (**2000**) ORGANELLES Centrifugation. In *Encyclopedia of Separation Science*(Ian, D. W., Ed.) pp 3586− 3596, Academic Press, Oxford, U.K.

18. Ivanova, P. T., Milne, S. B., Byrne, M. O., Xiang, Y. and Brown, H. A. (**2007**) Glycerophospholipid identification and quantitation by electrospray ionization mass spectrometry *Methods Enzymol.* 432, 21– 57

19. Spearman, C. (**1904**) The proof and measurement of association between two things *Am. J. Psychol.* 15, 72– 101

20. Jarquin-Pardo, M., Fitzpatrick, A., Galiano, F. J., First, E. A. and Davis, J. N. (**2007**) Phosphatidic acid regulates the affinity of the murine phosphatidylinositol 4-phosphate 5-kinase-Iβ for phosphatidylinositol-4-phosphate *J. Cell. Biochem.* 100, 112– 128

21. Divecha, N., Roefs, M., Halstead, J. R., D'Andrea, S., Fernandez-Borga, M., Oomen, L., Saqib, K. M., Wakelam, M. J. and D'Santos, C. (**2000**) Interaction of the type Iα PIPkinase with phospholipase D: A role for the local generation of phosphatidylinositol 4,5-bisphosphate in the regulation of PLD2 activity *EMBO J.* 19, 5440– 5449

22. Fagone, P. and Jackowski, S. (**2009**) Membrane phospholipid synthesis and endoplasmic reticulum function *J. Lipid Res.* 50 (Suppl.) S311– S316

23. Shindou, H., Hishikawa, D., Harayama, T., Yuki, K. and Shimizu, T. (**2009**) Recent progress on acyl CoA:lysophospholipid acyltransferase research *J. Lipid Res.* 50 (Suppl.) S46–S51

24. De Matteis, M. A. and Godi, A. (**2004**) PI-loting membrane traffic *Nat. Cell Biol.* 6, 487–492

25. Martin, T. F. (**2001**) PI(4,5)P_2 regulation of surface membrane traffic *Curr. Opin. Cell Biol*13, 493– 499

CHAPTER FOUR

STUDY OF ARACHIDONOYL SPECIFICITY IN TWO ENZYMES OF THE PI CYCLE

CHAPTER FOUR PREFACE

The work presented in this chapter was published previously in *Journal of Molecular Biology*, volume 409(2), pages 101-112, in 2011.

Shulga Y.V. conducted all the experiments described in this chapter.

Research objective: to identify a domain responsible for the acyl chain specificity of two enzymes, DGKε and PIP5K.

Research highlights:

- An amino acid pattern similar to that identified for LOX enzymes is present in the two unrelated enzymes DGKε and PIP5K, which have specificity for polyunsaturated acyl chains.
- We show the marked acyl chain substrate specificity of PIP5K and further elucidate the roles of acyl chains in the PA activation of this enzyme.
- These observations contribute to our understanding of the mechanism underlying the enrichment of lipid intermediates of the PI cycle in arachidonic acid.

Study of Arachidonoyl Specificity in Two Enzymes of the PI Cycle

Yulia V. Shulga[1], Matthew K. Topham[2], Richard M. Epand[1]

[1] Department of Biochemistry and Biomedical Sciences, McMaster University, 1200 Main Street West, Hamilton, Ontario L8N 3Z5, Canada

[2] Huntsman Cancer Institute, University of Utah, 2000 Circle of Hope, Salt Lake City, UT 84112, USA

ABSTRACT

We identified a conserved pattern of residues L-$X_{(3\text{-}4)}$-R-$X_{(2)}$-L-$X_{(4)}$-G, in which -$X_{(n)}$- is *n* residues of any amino acid, in two enzymes acting on the polyunsaturated fatty acids, diacylglycerol kinase epsilon (DGKε) and phosphatidylinositol-4-phosphate-5-kinase Iα (PIP5K Iα). DGKε is the only one of the 10 mammalian isoforms of DGK that exhibits arachidonoyl specificity and is the only isoform with the motif mentioned above. Mutations of the essential residues in this motif result in the loss of arachidonoyl specificity. Furthermore, DGKα can be converted to an enzyme having this motif by substituting only one residue. When DGKα was mutated so that it gained the motif, the enzyme also gained some specificity for arachidonoyl-containing diacylglycerol. This motif is present also in an isoform of phosphatidylinositol-4-phosphate-5-kinase that we demonstrated had arachidonoyl specificity for its substrate. Single residue mutations within the identified motif of this isoform result in the loss of activity against an arachidonoyl substrate. The importance of acyl chain specificity for the phosphatidic acid activation of phosphatidylinositol-4-phosphate-5-kinase is also shown. We demonstrate

that the acyl chain dependence of this phosphatidic acid activation is dependent on the substrate. This is the first demonstration of a motif that endows specificity for an acyl chain in enzymes DGKε and PIP5K Iα.

Abbreviations used

AA, arachidonic acid; BEL, PAP inhibitor; DAG, diacylglycerol; DGK, diacylglycerol kinase; LOX, lipoxygenase; PA, phosphatidic acid; PAP, PA phosphatase; PI, phosphatidylinositide; PI(4,5)P_2, phosphatidylinositol-4,5-bisphosphate; PI(4)P, phosphatidylinositol-4-phosphate; PIP5K, phosphatidylinositol 4-phosphate 5-kinase; PKC, protein kinase C; PLD, phospholipases D; di-PUFA-PA, phosphatidic acid with two polyunsaturated acyl chains; PUFA, polyunsaturated fatty acid; WT, wild type

Keywords

diacylglycerol kinase; acyl chain specificity; phosphatidylinositol-4-phosphate-5-kinase; arachidonic acid; PI-cycling

INTRODUCTION

Polyunsaturated fatty acids (PUFAs) are essential nutrients for humans and are major components of cell membrane phospholipids. PUFAs from the diet play an important role in the regulation of prostaglandin and proinflammatory cytokine synthesis.[1]

One of the most abundant PUFAs in mammalian cells is arachidonic acid (AA), and its derivatives are key mediators of a wide variety of physiological and pathophysiological processes, such as atherosclerosis, arthritis, asthma and tumorigenesis.[2-4] AA is the precursor of a large family of bioactive compounds called eicosanoids, produced by cyclooxygenases and lipoxygenases.[5,6] Because of the potent biological actions of eicosanoids and of free AA itself, this fatty acid is maintained at very low levels in the cells, where it is converted into cellular lipids by the enzymes arachidonoyl-CoA synthetase and lysophospholipid acyltransferases.[7] Therefore, under physiological conditions, AA is generally found esterified at the *sn*-2 position of glycerophospholipids, such as choline and ethanolamine glycerophospholipids, phosphatidic acid and phosphatidylinositol.

To utilize the arachidonic acid pathway, the enzymes are required to distinguish the acyl chain length and saturation of the substrate. It is common that only one of the isoforms of a particular enzyme has specificity towards substrates with an arachidonate moiety. Thus, only the epsilon isoform of diacylglycerol kinase (DGKε) shows substrate specificity *in vitro* for diacylglycerols with an arachidonoyl acyl chain at the *sn*-2 position.[8-10] Phosphorylation of 1-stearoyl-2-arachidonoyl-glycerol (SAG) (for lipid abbreviations used in this study, see Table 4.1) is the first step in the resynthesis of phosphatidylinositols (PIs) and, therefore, DGKε contributes to the enrichment of 1-stearoyl-2-arachidonoyl species of PIs.[11,12] It is intriguing that the domain responsible for the substrate recognition and specificity of DGKε and other enzymes with arachidonate specificity has still not been identified. We propose a region located in the accessory domain of DGKε that can recognize an arachidonoyl group. We identified the motif L-$X_{(3-4)}$-R-$X_{(2)}$-L-$X_{(4)}$-G, in which -$X_{(n)}$- is *n* residues of any amino acid in this domain, that is present in DGKε as well as in phosphatidylinositol-4-phosphate-5-kinase type I. This motif is similar to a PUFA-recognizing domain identified recently in lipoxygenases (LOX) on the basis of a 1.85 Å resolution structure of an 8R-lipoxygenase from *Plexaura* *homomalla*, which reveals a U-shaped channel, defined by invariant amino acids that would allow substrate access to the catalytic iron.[13] We show that several residues in this motif are involved in the substrate specificity of two enzymes acting on PUFA-containing substrates, DGKε and PIP5K Iα.

Table 4.1. Lipids used and/or referred to in this study

Abbreviation	Full name	Alternative notation (*sn*-1/*sn*-2)
DAG		
AAG	1-Arachidoyl-2-arachidonoyl-*sn*-glycerol	20:0/20:4 DAG
DOG	1,2-Dioleoyl-*sn*-glycerol	18:1/18:1 DAG
PAG	1-Palmitoyl-2-arachidonoyl-*sn*-glycerol	16:0/20:4 DAG
SAG	1-Stearoyl-2-arachidonoyl-*sn*-glycerol	18:0/20:4 DAG
SLG	1-Stearoyl-2-linoleoyl-*sn*-glycerol	18:0/18:2 DAG
PA		
AAPA	1-Arachidoyl-2-arachidonoyl phosphatidic acid	20:0/20:4 PA
DAPA	1,2-Diarachidonoyl phosphatidic acid	20:4/20:4 PA
PAPA	1-Palmitoyl-2-arachidonoyl phosphatidic acid	16:0/20:4 PA
POPA	1-Palmitoyl-2-oleoyl phosphatidic acid	16:0/18:1 PA
SAPA	1-Stearoyl-2-arachidonoyl phosphatidic acid	18:0/20:4 PA
SLPA	1-Stearoyl-2-linoleoyl phosphatidic acid	18:0/18:2 PA
SOPA	1-Stearoyl-2-oleoyl phosphatidic acid	18:0/18:1 PA
PC		
DOPC	1,2-Dioleoyl-*sn*-glycero-3-phosphocholine	18:1/18:1 PC
PS		
DOPS	1,2-Dioleoyl-*sn*-glycero-3-phospho-L-serine	18:1/18:1 PS
PI4P		
SA-PI4P	1-Stearoyl-2-arachidonoyl phosphatidylinositol-4-phosphate	18:0/20:4 PI4P
DP-PI4P	1,2-Dipalmitoyl phosphatidylinositol-4-phosphate	16:0/16:0 PI4P

RESULTS

Mutations in the LOX-like motif of DGKε greatly affect the activity of the enzyme

We identified the motif L-$X_{(3-4)}$-R-$X_{(2)}$-L-$X_{(4)}$-G in the accessory domain of DGKε (Table 4.2), similar to that in lipoxygenases, but different in having L rather than I as the first residue (Table 4.3). This motif is highly conserved in DGKε among different species. To determine if this motif plays a role in DGKε specificity towards arachidonate-containing substrates, we mutated the residues in this region of the protein and measured the activity of FLAG- DGKε wild type (WT) and mutant proteins using the micelle-based assay with SAG as a substrate. The results showed that the mutations in this LOX-like region of DGKε greatly affect the activity of the enzyme (Fig. 4.1). Notably, this effect is strongly correlated with the size and/or shape of a side chain of the mutated amino acids. From these results for a single concentration of substrate, it is clear that all of the mutations result in a significant loss of enzymatic activity, even substitution of a single amino acid with a similar residue, demonstrating the importance of this region of DGKε for enzymatic activity.

Table 4.2. A partial sequence alignment of vertebrate DGKε. The conserved residues, similar to those in LOX, are colored red. Note the high degree of sequence conservation in this region of the protein from avian to mammalian species.

LOX15 [*Oryctolagus cuniculus*]	389	LIVPHLRYTLEINVRARNGLVSDFGIFDQIM	419
LOX15 [*Homo sapiens*]	388	LIIPHLRYTLEINVRARTGLVSDMGIFDQIM	418
LOX12 [*Homo sapiens*]	388	FLIPHIRYTMEINTRARTQLISDGGIFDKAV	418
LOX12 [*Rattus norvegicus*]	389	LLVPHLLYTMEINVRARSDLISERGFFDKAM	419
LOX5 [*Rattus norvegicus*]	395	LLVAHVRFTIAINTKAREQLNCEYGLFDKAN	425
LOX1 [*Arabidopsis thaliana*]	547	LLEPHFRDTMNINALARQILINGGGIFEITV	577

Table 4.3. A partial sequence alignment of LOX. The conserved residues, located in U-shaped channel, that would allow substrate access to the catalytic iron,[13] are colored in red.

NP_003638 [*Homo sapiens*]	421	KDLNKKVELELDGERVALPSLEGIIVLNIGYWG	453
NP_062378 [*Mus musculus*]	418	KDLNKKIELELDGERVELPNLEGIIVLNIGYWG	450
XP_618342 [*Bos taurus*]	418	KDLNKKVELELDGERVELPNLEGIIVLNIGYWG	450
XP_001503369 [*Equus caballus*]	418	KDLNKKVELELDGERVELPNLEGIIVLNIGYWG	450
XP_548222 [*Canis familiaris*]	418	KDLNKKIELELDGERVELPNLEGIIVLNIGYWG	450
XP_001521727 [*Ornithorhynchus anatinus*]	414	KDLNKKVELELDGERVELPNLEGIIVLNIGYWG	446
XP_523803[*Pan troglodytes*]	421	KDLNKKVELELDGERVALPSLEGIIVLNIGYWG	453
XP_001234226 [*Gallus gallus*]	421	KDLNKKVELELDGERIELPNLEGIIVLNIGYWG	453
XP_002192399[*Taeniopygia guttata*]	407	KDLNKKVELELDGERIELPNLEGIIVLNIGYWG	439

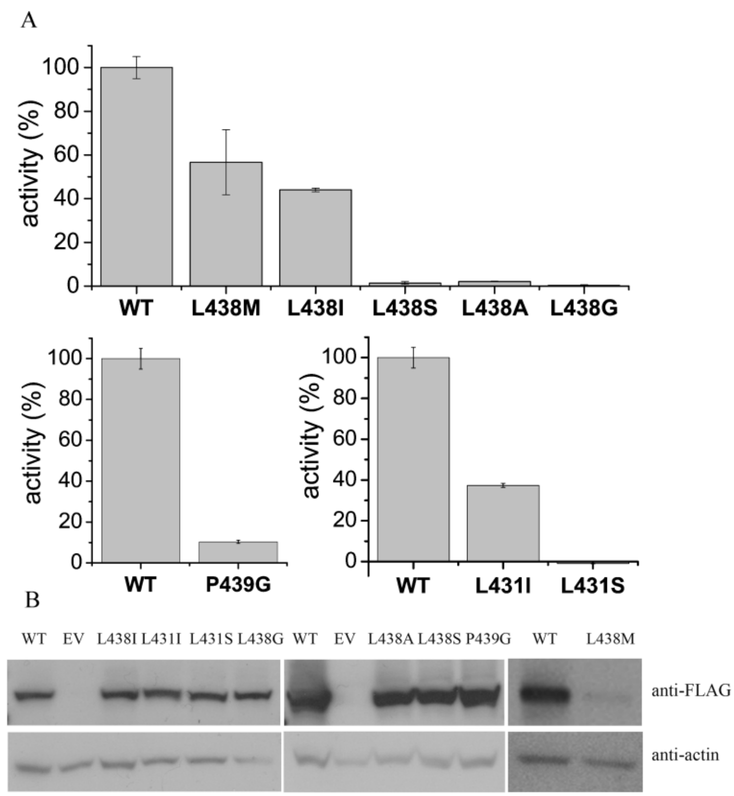

Figure 4.1. (a), Comparison of the enzyme activities for FLAG-DGKε WT and mutants L438M, L438I, L438S, L438A, L438G, L431I, L431S and P439G. Enzyme activity is expressed as a percentage of the activity of FLAG-DGKε WT protein with SAG as a substrate. (b), Western blots showing the expression levels of DGKε WT and mutants (anti-FLAG panel), and the expression levels of actin (anti-actin panel) in the transfected cells. Enzyme activity was normalized for the amount of protein in the lysates. The activity measured with mock-transfected cells was normalized for the amount of

actin and subtracted from the values obtained using cells over-expressing one of the DGKε constructs. The activity measured with mock-transfected cells was, on average, 5–10% of the activity measured with DGKε WT.

Affecting the substrate-binding site would be expected to lower the activity of the enzyme against all substrates. However, if the binding site is specific for arachidonoyl groups, then the loss of activity should be greater for an arachidonoyl-containing substrate. In order to test this more critically, we performed a kinetic analysis and calculated the Michaelis–Menten parameters for FLAG-DGKε WT and its single residue mutants L431I and L438I using SAG and SLG as substrates (Table 4.4). The arachidonoyl-containing substrate SAG, which is the major species of diacylglycerol in the PI-cycle, was compared with a structurally similar diacylglycerol not containing arachidonic acid, SLG, as a critical test of the extent of arachidonoyl specificity. Other more structurally different diacylglycerols, such as dioleoylglycerol or dipalmitoylglycerol, have very low activity with wild type DGKε[12,14] and have very weak activity with mutant forms of this enzyme (data not shown). They therefore do not provide a critical comparison to test relative acyl chain specificity.

Table 4.4. Summary of the kinetic parameters for FLAG-DGKε WT and its L438I and L431I mutants. The results are presented as the mean ± S.D. Kinetics analysis clearly illustrates that both k_{cat}, that represents the catalytic rate constant, as well as k_{cat}/K_m, that represents the pseudo first order rate constant at low substrate concentrations, are affected by the mutations, particularly for the SAG substrate (see Fig. 4.6 for the graphic representation of Table 4.4).

	K_m, mol%	k_{cat}, sec^{-1}	k_{cat}/K_m, $sec^{-1}mol\%^{-1}$
FLAG-DGKε WT			
SAG	2.44 ± 0.14	10.2 ± 0.3	4.16 ± 0.14
SLG	7.0 ± 1.4	4.6 ± 0.6	0.66 ± 0.11
FLAG-DGKε L438I			
SAG	1.88 ± 0.15	2.24 ± 0.07	1.19 ± 0.05
SLG	2.9 ± 0.5	1.56 ± 0.09	0.54 ± 0.04
FLAG-DGKε L431I			
SAG	2.4 ± 0.6	2.1 ± 0.2	0.91 ± 0.14
SLG	5.1 ± 1.2	2.7 ± 0.4	0.53 ± 0.09

Almost all other mutants, L431S, L438S, L438A, L438G and P439G, had very low activity (< 2% of WT), which did not allow us to perform the kinetic analysis. Our results showed that k_{cat}/K_m was reduced for both L431I and L438I mutations of DGKε. However the reduction of k_{cat}/K_m was much greater for SAG as substrate (4-fold decrease) compared with SLG (18% decrease). The number of substrate molecules turned over per enzyme molecule per second (k_{cat}) was also reduced, particularly with the substrate SAG. There was less effect on the affinity of the enzyme for these substrates as measured by K_m.

To test if the L431I and L438I mutations of FLAG-DGKε affect the mode of inhibition by PA, we compared the inhibition of FLAG-DGKε WT and mutant proteins by SOPA and SAPA (Fig. 4.2). Our results showed that L431I and L438I mutations of DGKε do not affect the extent of PA inhibition.

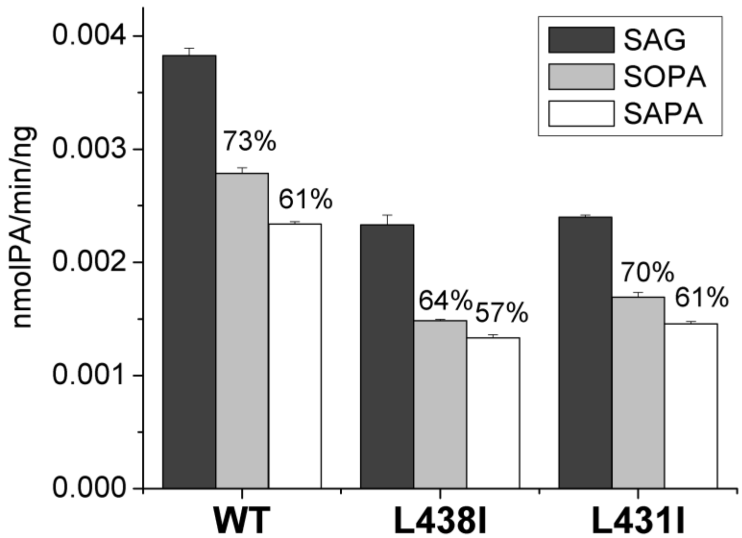

Figure 4.2. Comparison of inhibition of DGKε by PA. DGK enzymatic activity was measured with 15 mM Triton X-100, 0.1 mM [γ-^{32}P]ATP and 2 mol % SAG (shown as dark gray bars) or with the addition of either 2 mol % SOPA (light gray bars) or SAPA (white bars). The numbers above the bars show the enzymatic activity of proteins in the presence of PA as a percentage of the enzymatic activity in the absence of PA.

Arachidonate preference can be introduced into DGKα by mutation V656L

We found that only one other isoform of DGK, DGKα, has a motif with some similarity to the LOX-like motif in DGKε, but with a V656 residue instead of Leu in DGKε (Table 4.5). These motifs are found in the accessory domain of both DGKα and DGKε. We found that DGKα does not have a preference for DAG with an arachidonate moiety.[15] Therefore, to test if the arachidonate specificity could be introduced into DGKα, at least to some extent, we mutated the V656 residue in human DGKα to L to obtain a protein with the same motif as that in DGKε (LxxxRxxLxxxxG) and compared the Michaelis–Menten parameters for 3xHA-DGKα WT and the V656L mutant (Table 4.6). Our results showed that there is no statistically significant difference in K_m or in the overall efficiency, V_{max}/K_m, of DGKα WT and V656L mutant, although it should be noted that there is an intrinsically large error in the determination of K_m. However, there is a difference in the V_{max} for these proteins. There was a significant 22% increase in V_{max} for SAG with the introduction of the mutation in contrast to a 16% decrease for SLG. When taken as a ratio of V_{max} for SAG to V_{max} for SLG, there is a significant difference between DGKα WT and the V656L mutant proteins (Fig. 4.3).

Table 4.5. A partial sequence alignment of mammalian DGKα. The conserved residues, similar to those in DGKε, are colored in red.

NP_963848 [*Homo sapiens*]	639	PDILKTCVPDLSDKRLEVVGLEGAIEMGQIYTK	671
NP_058091 [*Mus musculus*]	634	PDILKTCVPDMSDKRLEVVGIEGAIEMGQIYTR	666
NP_001071328 [*Bos taurus*]	638	PDILKTCVPDLSDKRLEVVGLEGAIEIGQIYTK	670
NP_542965 [*Ruttus Norvegicus*]	631	PDILKTCVPDMSDKRLEVVGIEGVIEMGQIYTR	663
XP_855720 [*Canis familiaris*]	477	PDILKTCVPDLTDKRLEVVGLEGAIEMGQIYTK	509
XP_001112067 [*Macaca mulatta*]	527	PDILKTCVPDLSDKRLEVVGLEGAIEMGQIYTK	559
NP_999197 [*Sus scrofa*]	638	PDILKTCVPDLSDKRLEVVGLEGAIEMGQIYTK	670
XP_001169813 [*Pan troglodytes*]	527	PDILKTCVPDLSDKRLEVVGLEGAIEMGQIYTK	559

Table 4.6. Summary of the kinetic parameters for 3xHA-DGKα WT and the V656L mutant. Kinetic analysis shows that the V656L mutation of DGKα increases V_{max} of the enzyme for SAG and decreases it for SLG, thus introducing the arachidonoyl preference (Fig. 4.3). Values of V_{max} are relative values because the absolute amount of enzyme in the cell preparations is not known. V_{max} of 3xHA-DGKα V656L is normalized to the amount of protein relative to WT. The results are presented as the mean ± S.D.

	K_m, mol%	V_{max}, nmol PA min^{-1}	V_{max}/K_m, $mol\%^{-1}sec^{-1}$
3xHA-DGKα WT			
SAG	2.1 ± 0.4	1.44 ± 0.09	0.70 ± 0.13
SLG	2.8 ± 0.3	1.51 ± 0.08	0.55 ± 0.07
3xHA-DGKα V656L			
SAG	1.8 ± 0.3	1.75 ± 0.11	1.00 ± 0.17
SLG	1.5 ± 0.4	1.26 ± 0.12	0.87 ± 0.25

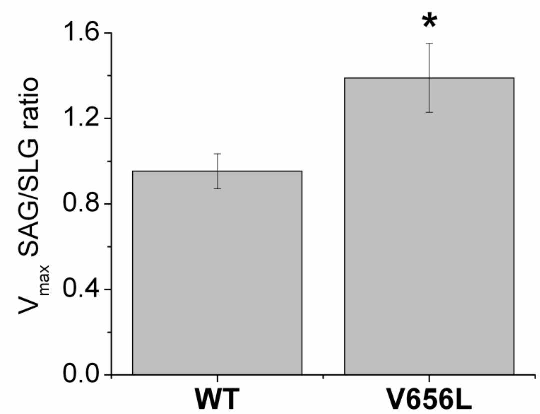

Figure 4.3. Comparison of SAG to SLG ratios for V_{max} parameters for 3xHA-DGKα WT and V656L mutant proteins. The V656L mutation of DGKα increases the arachidonoyl preference of the enzyme. ∗The difference between the V_{max} ratios of SAG to SLG for DGKα WT and V656L mutant is statistically significant ($P < 0.05$).

Phosphatidylinositol 4-phosphate 5-kinase (PIP5K) type I exhibits preference for arachidonoyl-PI(4)P

We found that PIP5K type I, but not type II, has the motif LxxxxRxxLxxxxG. There are three active isoforms of PIP5K type I, α, β and γ, that are encoded by distinct genes. All three isoforms of type I PIP5K have the same L-$X_{(3-4)}$-R-$X_{(2)}$-L-$X_{(4)}$-G motif as DGKε. In this work, we used human PIP5K Iα, which has been suggested to fulfill a "housekeeping" function.[16] To test if PIP5K type I forms have specificity towards an arachidonate-containing substrate, we compared the activity of human PIP5K type Iα with SA-PI(4)P *versus* DP-PI(4)P as substrates. Few molecular forms of the substrate PI(4)P have been synthesized and these two were chosen because of their availability. Our results showed that PIP5K type Iα phosphorylates SA-PI(4)P about eight times faster than DP-PI(4)P (Fig. 4.4). This is the first demonstration that this enzyme exhibits substrate acyl chain preference, although by itself it is not a critical test of arachidonoyl specificity.

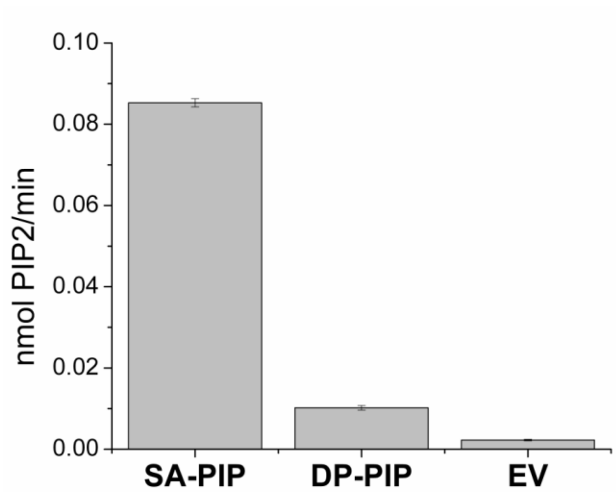

Figure 4.4. Comparison of the enzyme activity of c-myc-PIP5K Iα with SA-PI(4)P and DP-PI(4)P as a substrate. Brain PI(4)P (Avanti Polar Lipids) was used as a source of SA-PI(4)P. Only SA-PI(4)P and DP-PI(4)P were compared, because other PI(4)P material is not commercially available. The negative control (EV) was done with SA-PI(4)P as a substrate with the addition of beads immunoprecipitated from mock-transfected COS-7 cells.

To test the role of the identified motif in the activity of PIP5K type Iα, we made L202I and L210I mutations in this region of the protein and used a kinetic analysis to compare these mutant proteins with the WT PIP5K type Iα. We found that both L202I and L210I mutations decrease the substrate affinity and the enzyme efficiency of PIP5K type Iα for arachidonate-containing PI(4)P (Table 4.7).

Table 4.7. Summary of the kinetic parameters for c-myc-PIP5K Iα WT and mutants L202I and L210I. The results show that mutations L202I and L210I of PIP5K Iα significantly decrease the substrate affinity of the enzyme (12-fold increase in K_m for L202I and twofold for L210I). Consequently, the mutations also affect the enzyme efficiency (~ 6-fold decrease in V_{max}/K_m for L202I and twofold for L210I). Values of V_{max} are relative values because the absolute amount of enzyme in the cell preparations is not known. V_{max} for PIP5K mutants Iα L202I and L210I is normalized for the amount

of protein relatively to WT. Kinetic parameters were calculated using the effective concentration of PI4P at the surface of the micelle. The effective surface concentration of PI(4)P was determined by multiplying the mol fraction of PI(4)P at the surface of the micelle by the total concentration of PI(4)P to be comparable to published work.[45] The results are presented as the mean ± S.D.

K_m, μM	V_{max}, nmol/min	V_{max}/K_m, 1/μM/min
PIP5K Iα WT		
0.3 ± 0.1	0.125 ± 0.008	0.35 ± 0.10
PIP5K Iα L202I		
3.6 ± 0.7	0.200 ± 0.027	0.06 ± 0.01
PIP5K Iα L210I		
0.7 ± 0.2	0.097 ± 0.012	0.14 ± 0.05

We determined the activation of PIP5K Iα with different PAs for both SA-PI(4)P (Fig. 4.5A) and DP-PI(4)P substrates (Fig. 4.5B). Our results using SA-PI(4)P as substrate showed that PIP5K is activated most by polyunsaturated PAs with the same fatty acid at the *sn*-1 and *sn*-2 positions (di-PUFA-PA), such as DAPA, DLPA and DDPA. For the DP-PI(4)P substrate, PIP5K Iα activation was increased 12-fold by DAPA (Fig. 4.5B), showing that PIP5K can exhibit a very specific arachidonate preference for PA activation when DP-PI(4)P is used as substrate.

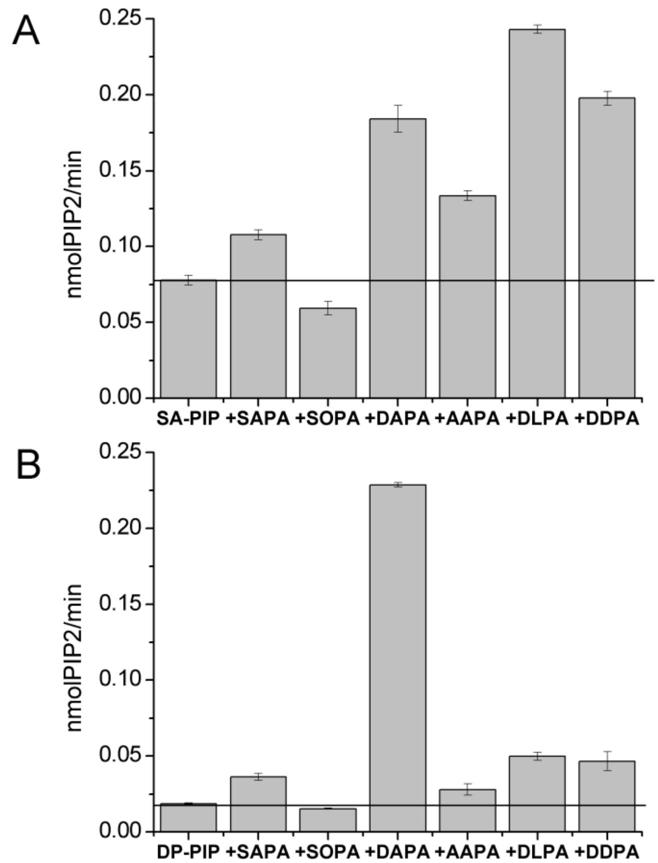

Figure 4.5. Activation of PIP5K by PA with (a) SA-PI(4)P and (b) DP-PI(4)P as substrate. Brain PI(4)P (Avanti Polar Lipids) was used as a source of SA-PI(4)P. PIP5K enzymatic activity was measured with 20 μM PI(4)P and 50 μM PA.

DISCUSSION

Acyl chain specificity of DGKε

Earlier, we showed that the inhibition and substrate specificity of DGKε are both determined by selectivity for a combination of the *sn*-1 and *sn*-2 acyl chains of PA or DAG, respectively, preferring the most prevalent acyl chain composition of lipids involved specifically in the PI cycle, 1-stearoyl-2-arachidonoyl.[12] The inhibition of DGKε by PA is competitive; the active site of DGKε recognizes the lipid headgroup and a combination of the two acyl chains in PA or DAG. Taken together, these findings suggest that the substrate-binding pocket of DGKε should have a specific size and length that are best suited for SAG. This isoform of DGK also contains the motif L-$X_{(3\text{-}4)}$-R-$X_{(2)}$-L-$X_{(4)}$-G and mutations of several residues in this motif result in a marked loss of activity in DGKε (Fig. 4.1). It should be pointed out that this marked sensitivity of the enzymatic activity of DGKε to these single residue substitutions contrasts sharply with the very small changes in the kinetics of this enzyme that were observed when 58 residues were removed from the amino terminus of the enzyme.[12] In general, the less bulky the amino acid side chain in the mutated forms of the LOX-like motif, the lower the enzymatic activity.

The greater loss of activity by introducing mutations with less bulky amino acid side chains can be explained by the location of residues L438 and L431 at the bottom of the substrate-binding pocket, in analogy with the LOX enzyme, although the shape of this binding site might be different in DGKε.[13] In the case of DGKε, the mutation of L438 or L431 to another amino acid with a smaller side chain would increase the volume of the substrate-binding pocket. The less fixed position of the substrate would then decrease the interaction between the hydroxyl group of the substrate and the phosphate group of the ATP that is bound to the ATP-binding site of the catalytic domain, which is outside the acyl chain-binding pocket. This would slow the rate of catalysis and the effect would depend on the size of the side chain of the mutated amino acid.

We compared the mode of inhibition of FLAG- DGKε WT and mutants L438I and L431I by PA (Fig. 4.2). These mutations greatly affect k_{cat}/K_m (~ 4-fold decrease) for

SAG, but not for SLG (Fig. 4.6). In contrast with this large decrease in the rate of phosphorylation of arachidonoyl substrates by mutations of the LOX-like motif, relatively little change in acyl chain specificity of PA inhibition is exhibited in these mutant forms of DGKε compared with the WT protein (Fig. 4.2). This can be explained by the fact that PA competes with the substrate for the substrate-binding site, but the hydroxyl group is already phosphorylated in PA and, therefore, the distance of PA from the ATP-binding site would not affect the extent of inhibition.

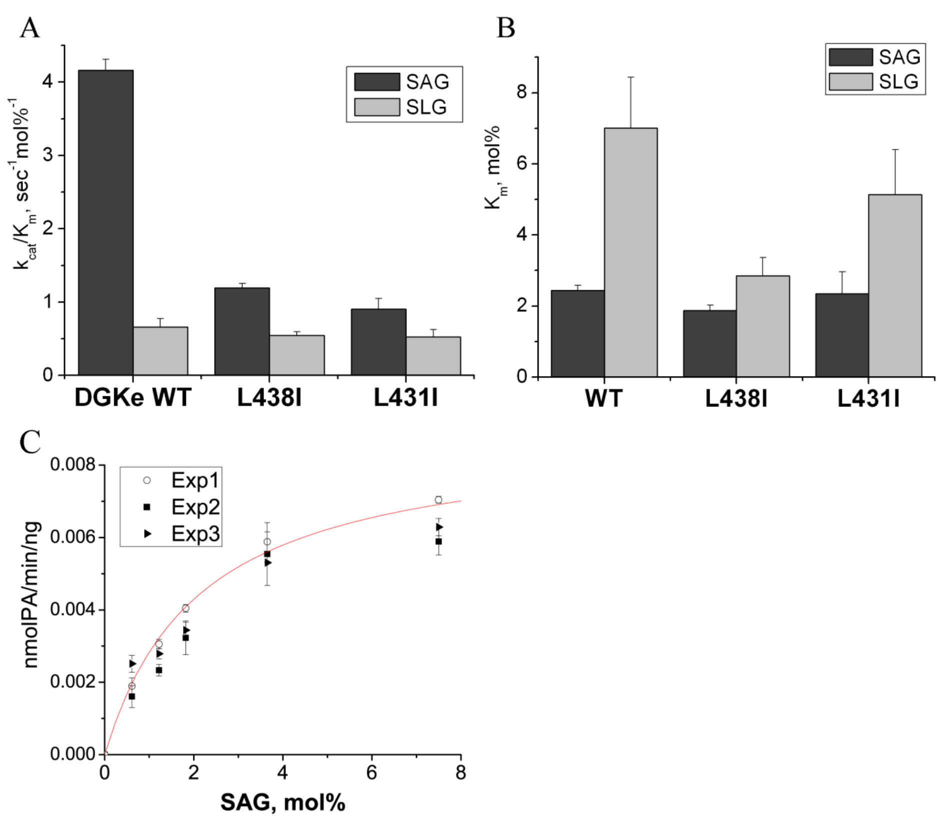

Figure 4.6. Graphic presentation of the kinetic parameters for FLAG- DGKε WT and its L438I and L431I mutants. The results are presented as the mean ± S.D. (a), The results show that k_{cat}/K_m is greatly affected (~ 4-fold decrease) by L438I and L431I mutations of DGKε for SAG, but not SLG substrate. (b), Comparison of K_m parameters

shows that L438I and L431I mutations of DGKε slightly affect the substrate affinity of the enzyme, decreasing the preference for SAG over SLG. (c), An example of kinetic data of three independent experiments (Exp1, Exp2 and Exp3) is shown for FLAG- DGKε WT with SAG as a substrate. Every experiment was done in triplicate. A nonlinear regression curve fitting Exp1 data is shown in red.

Furthermore, DGK shares the catalytic domain with other lipid kinases, such as sphingosine kinase and ceramide kinase, but at the same time it is highly specific for DAG as substrate and does not catalyze the phosphorylation of sphingosine or ceramide.[17,18] This suggests that the accessory domain is responsible for substrate recognition.[19] The LOX-like motif, which we identified in DGKε, is located in the accessory domain of DGKε, further suggesting that it is involved in the substrate recognition and binding.

Acyl chain specificity of DGKα

Notably, DGKε is the only DGK isoform that has an identified LOX-like motif, and it is the only isoform that has specificity for substrates with an arachidonate moiety. One other isoform, DGKα, has a region with some similarity to that in DGKε, but with V656 instead of Leu in DGKε, and with the first Leu (Leu649) not being conserved among mammalian species (Table 4.5).

We found that the V656L mutation of DGKα that introduces a LOX-like motif into this isoform results in SAG having a higher V_{max} than that for SLG (Fig. 4.3). Therefore, this mutation increases the substrate preference of DGKα towards arachidonoyl substrates, making its substrate preference more similar to that of the DGKε isoform. This supports our findings that the essential residues in the LOX-like motif play an important role in arachidonate-containing substrate specificity and recognition. The V656L mutant of DGKα is not as specific as DGKε for arachidonoyl groups but perhaps one should not expect a property newly introduced into a protein by a single residue substitution to result in optimized function.

It is interesting that DGKα also acts preferentially on substrates containing an arachidonoyl group when this group is incorporated in alkylacylglycerols.[15] Although diacylglycerols are better substrates for DGKα than the alkylacylglycerols, no specificity is exhibited for arachidonoyl-containing diacylglycerols. This data might be explained by our observation that DGKα has a region similar to the LOX-like motif in DGKε but, because it is not completely identical, DGKα does not exhibit specificity for arachidonoyl-containing DAG, unless this region is mutated so that the conserved residues are identical with those of DGKε, as shown in this study.

Acyl chain specificity of PIP5K Iα

We identified the motif $L\text{-}X_{(3\text{-}4)}\text{-}R\text{-}X_{(2)}\text{-}L\text{-}X_{(4)}\text{-}G$ in PIP5K type I, which converts PI(4)P to $PI(4,5)P_2$, and we confirmed that this enzyme exhibits preference for arachidonoyl-PI(4)P, and that the mutations in the identified region decrease the catalytic efficiency and substrate affinity for this enzyme (Table 4.7). Moreover, we determined the activation of PIP5K Iα with different PAs for both SA-PI(4)P and DP-PI(4)P substrates (Fig. 4.5). For DP-PI(4)P as substrate, the best activator of PIP5K Iα is DAPA (Fig. 4.5B), showing that PIP5K exhibits arachidonate preference for the substrate and for its activator PA. The relationship between the arachidonoyl requirement for the substrate of PIP5K Iα and the acyl chain requirements for PA as an activator is not known.

However, the role of PA for PIP5K as an activator clearly has to be different from the competitive inhibition that PA exhibits with DGKε.[12] An earlier study identified dilinoleoyl-PA as a potent activator of the phosphorylation of SA-PI(4)P by this enzyme.[20] Our results extend these findings and demonstrate that PIP5K stimulation by PA is sensitive to acyl chain composition and it depends on the substrate as well. We show that the PI cycle intermediate SAPA is not the best activator for the phosphorylation of SA-PI(4)P; instead, it is di-PUFA-PA. The levels of di-PUFA-PA would be low in most tissues, but high in brain, where it would stimulate PI-cycling.

Conclusions

Enzymes and other proteins that interact with lipid exhibit specificity for certain lipid structures. In some cases, this is primarily a consequence of interacting with a lipid headgroup. An example is the PH domain that interacts with phosphatidylinositol phosphates with little specificity for the acyl chain. However, other proteins and enzymes can be specific for the nature of the acyl chain, which can have important physiological consequences, such as the segregation of arachidonoyl groups for signal transduction and perhaps other functions.

There is current interest in the molecular basis of PUFA specificity. A recent proposal, based on the crystallographic structure of a coral lipoxygenase, has identified a pattern of amino acid residues that are important for recognizing arachidonic acid.[13] In this study, we demonstrate that a similar amino acid pattern, L-$X_{(3\text{-}4)}$-R-$X_{(2)}$-L-$X_{(4)}$-G, is found in two other proteins that exhibit relative specificity for PUFA groups. While this motif does not predict a specific conformation of a PUFA-binding site and this motif is found in other proteins that do not interact with PUFA groups, it has allowed us to identify the region in DGKε that is involved in its unique arachidonoyl specificity among the 10 isoforms of mammalian DGK. We present further evidence supporting this hypothesis by demonstrating that the arachidonoyl specificity of DGKα can be increased by a site-specific mutation that results in the introduction of this proposed motif. In addition, we show that the enzyme PIP5K Iα that also contains this motif exhibits specificity for PUFA moieties in both the substrate and in PA activators. Among the enzymes lipoxygenases, DGK and PIP5K there are gross differences in the structure of the substrate and in the nature of the reaction that is catalyzed. One would therefore not expect *a priori* the amino acid pattern or the extent of acyl chain specificity to be identical in all three cases. One of the differences is that in lipoxygenases the first residue of this motif is I rather than L. Nevertheless, we demonstrate that there is a strong relationship between the amino acid pattern that we have identified and the property of PUFA specificity in two enzymes, DGKε and PIP5K Iα. It is possible that a similar amino acid pattern can play a role in the substrate specificity and recognition of other enzymes with specificity towards PUFA-containing substrates, but further studies are needed to address this issue.

Amino acid patterns forming structures that recognize particular features of substrates or ligands have been discovered in a number of proteins. There is also the so-called CRAC motif that has been proposed to be responsible for cholesterol recognition.[21,22] This amino acid pattern is also quite flexible in definition, it does not define a specific structure and the molecular basis of its relationship to cholesterol binding is not known. Nevertheless, there are an increasing number of examples of this motif being responsible for cholesterol interactions in proteins.[23-27] Other examples include a phosphorylation site for Aurora B kinase, the mitosis-specific serine/threonine protein kinase, (R/K)1-3-X-(S/T) or (R/K)-(R/K)-X0-2-(S/T) where X is any amino acid;[28.29] the Phox homology domain for binding PI, (R/K)(R/K)(Y/F)xxFxxLxxxL or R(R/K)xxLxx(Y/F);[30] the lysosomal targeting sequences, Tyr-X-X-Hyd and LL (where Hyd is any hydrophobic amino acid).[31] In all of these cases, as in the motif described in this work, the motif is part of a structurally specific interaction site. However, the structure of this site is not determined solely by the motif with its large degree of variation and limited number of constraints. Nevertheless, identification of such motifs has been found to be a valuable tool in cell biology. Thus, this work extends this concept to PUFA recognition in two studied enzymes. This is of particular importance because of the roles of arachidonic acid in prostanoid metabolism and as an *sn*-2 acyl chain of lipids in the PI-cycle.

MATERIALS AND METHODS

DGKε constructs

The FLAG epitope-tagged DGKε, 3xHA-DGKα and c-Myc-PIP5K type Iα expression vectors all correspond to human forms of the respective enzymes and were prepared as described.[32-34] The mutants of FLAG- DGKε, 3xHA-DGKα and c-Myc-PIP5K type Iα were designed using the QuikChange Lightning Kit (Stratagene, La Jolla, CA) according to the manufacturer's instructions. The presence of the desired mutations was verified by sequencing analysis.

Cell culture

COS-7 cells were maintained at 37 °C in an atmosphere of 5% CO_2 in Dulbecco's modified Eagle's medium (DMEM, GIBCO/Invitrogen) containing 10% (v/v) fetal bovine serum (GIBCO/Invitrogen). The cells were grown to about 70%–80% confluency and transiently transfected with the expression vectors using Lipofectamine 2000 (Invitrogen) according to the manufacturer's instructions. The cells were harvested at 48 h after transfection by scraping them into PBS containing 1:100 (v/v) Protease Inhibitor Cocktail for use with mammalian cells and tissues (Sigma-Aldrich). The cells were pelleted at 5000***g*** at 4 °C and stored at – 90 °C.

Immunoblot analysis

Amounts of protein in the lysates of transfected COS-7 cells were quantified by immunoblotting. Protein samples for immunoblot analysis were prepared by incubation with 2% (w/v) SDS buffer at 95 °C for 5 min. The resultant proteins were separated by Tris–glycine SDS-PAGE (7.5% (w/v) polyacrylamide gel) and electroblotted onto an Immobilon-P polyvinylidenedifluoride membrane (Millipore), which was then incubated with a 1:2000 (v/v) dilution of mouse anti-FLAGM2 (Sigma), 0.5 μg/ml mouse THE™ anti-HA tag IgG1 (GenScript, A01244), 1:800 (v/v) dilution of mouse anti-c-Myc (Santa Cruz, sc-40), or 1:800 (v/v) dilution of goat anti-actin (Santa Cruz, sc-1616) as the primary antibody and a 1:2000 (v/v) dilution of horseradish peroxidase-conjugated goat anti-mouse (Santa Cruz, sc-2005) or donkey anti-goat antibody (Santa Cruz, sc-2020) as the secondary antibody. The antibody complexes were visualized using Western Lightning Chemiluminescence Reagent Plus (PerkinElmer Life Sciences) and X-Omat LS film (Eastman Kodak Co.) according to the manufacturer's instructions. A 3xFLAG®-tagged bacterial alkaline phosphatase (3xFLAG-BAP) (Sigma-Aldrich) with a molecular mass of 49.9 kDa was used for DGKε and its mutants as a standard in different lanes of the same blots.

Enzyme preparations for enzymatic activity assay

Before the assay, pellets of COS-7 cells over-expressing human 3xFLAG- DGKε WT, 3xHA-DGKα WT or mutants were suspended in ice-cold cell lysis buffer (1% (v/v) (octylphenoxy)polyethoxyethanol (Nonidet P-40), 20 mM Tris–HCl (pH 7.5), 150 mM NaCl, 1 mM EDTA, 2.5 mM sodium pyrophosphate, 1 mM β-glycerophosphate, 1 mM activated sodium orthovanadate and 1:100 (v/v) diluted Protease Inhibitor Cocktail for use with mammalian cells and tissue (Sigma-Aldrich)), left to lyze for 10 min on ice, sonicated for 5 min and then centrifuged at 100,000***g*** for 30 min at 4 °C. The supernatants were used in the assay of DGK activity. For the PIP5K enzyme, cell pellets of COS-7 cells over-expressing human c-Myc-PIP5K type Iα were suspended in ice-cold cell lysis buffer (2% (v/v) (octylphenoxy)polyethoxyethanol (Nonidet P-40), 20 mM Tris–HCl pH 7.5, 150 mM NaCl, 5 mM EDTA, 1 mM Na_3VO_4, 10 μg/ml aprotinin, 10 μg/ml leupeptin, 1 mM PMSF, 5 mM NaF, 100 μg/ml soybean trypsin inhibitor and 1:100 (v/v) diluted Protease Inhibitor Cocktail for use with mammalian cells and tissue (Sigma-Aldrich)), left to lyze for 10 min on ice, sonicated for 10 min and then incubated with agarose beads conjugated with anti-c-Myc antibodies (Santa Cruz, sc-40 AC) at 4 °C overnight. The beads were then centrifuged and washed sequentially with: IP kinase buffer (25 mM Tris, pH 7.5, 100 mM NaCl, 0.1% (v/v) Triton X-100); PBS pH 6.0, 0.5%

Triton X-100; 25 mM Tris, pH 8, 100 mM NaCl, 0.1% Triton X-100; 25 mM Tris, pH 7.5, 500 mM NaCl, 0.1% Triton X-100; and, finally, IP kinase buffer.[20] After the final wash the beads were centrifuged briefly and then suspended in assay buffer (200 mM Tris–HCl (pH 7.5), 400 mM NaCl, 20 mM $MgCl_2$, 4 mM EGTA, 1 mM dithiothreitol).

Quantification of phosphatidic acid and PI(4)P

The concentration of all PA and PI(4)P stocks used in this study was determined with an assay for inorganic phosphate as described.[35] Briefly, 30 µl of 10% (w/v) $Mg(NO_3)_2$ in 95% (v/v) ethanol was added to PA (up to 80 nmol) in an acid-washed Pyrex tube, which was flamed until the organic phosphate was completely ashed. After that, 350 µl of 0.5 M HCl was added, the mixture was heated at 100 °C for 15 min, 750 µl of a 1:6 (v/v) mixture of 10% (w/v) L-ascorbic acid and 0.42% (w/v) ammonium molybdate tetrahydrate in 0.5 M H_2SO_4 was added, the mixture was incubated at 60 °C for 10 min then allowed to cool to room temperature when the absorbance at 820 nm was measured.

Detergent-phospholipid-mixed micelle-based DGK enzymatic activity assay

DGK was assayed for enzymatic activity using a detergent-phospholipid-mixed micelle-based protocol described by Walsh *et al*.[9] that was used earlier in our laboratory.[32] Lipid films composed of the substrate (DAG) along with any phospholipid component required in the assay (PA and/or 1,2-dioleoyl-*sn*-glycero-3-phosphocholine (DOPC) (for DGKε) and/or 1,2-dioleoyl-*sn*-glycero-3-[phospho-L-serine] (DOPS) (for DGKα)) were made at a constant total lipid concentration of 5.75 mM. Mixed micelles were formed by hydrating these lipid films with 50 µl of 4× assay buffer containing

60 mM Triton X-100 and subsequently vortex mixing the hydrated lipid film for 2 min. Lysates from COS-7 cells expressing DGK were added to the mixed micelles along with double-distilled water to a final volume of 180 μl. The reaction was initiated by adding 20 μl of 1 mM [γ-^{32}P]ATP (50 μCi/ml) (PerkinElmer Life Sciences), incubated for 10 min at 25 °C, and terminated by addition of 2 ml of stop solution (1:1 (v/v) $CHCl_3/CH_3OH$, 0.25 mg/ml dihexadecyl phosphate). The organic layer was washed three times, each with 2 ml of wash solution (7:1 (v/v) H_2O/CH_3OH, 1% (v/v) $HClO_4$, 0.1% (v/v) H_3PO_4). A sample of the organic layer was used to quantify the incorporation of ^{32}P into PA using Cerenkov counting. All enzymatic activity data presented in this study were obtained from initial rate experiments, because the formation of the product PA was linear over the 10 min reaction period. Negative controls were run with the addition of lysates from mock-transfected COS-7 cells and were confirmed to have activity levels significantly below that of lysates from cells over-expressing DGK. The activity of DGK enzymes could be detected only if exogenous lipid substrate was added, further indicating that endogenous lipids do not provide a sufficient concentration of substrate for the phosphorylation to be detected. In addition, the DGK activity of cells transfected with DGKε is specific for SAG, whereas cells expressing DGKα can phosphorylate SAG and SLG equally well. This finding is in accord with the known substrate specificities of these isoforms and is additional evidence that we are measuring the properties of the over-expressed enzyme. The activity measured with mock-transfected cells was subtracted from the values obtained using cells over-expressing one of the DGKε or DGKα constructs. The assays were performed in triplicate and are presented as the mean ± S.D.

Each experiment was independently repeated at least twice. The day-to-day variations using the same enzyme preparation and the same lipids were not much greater than those for an individual experiment. The concentrations of the individual lipid components of the mixed micelles are listed as their mol percentage of the detergent–phospholipid mixed micelle, because DGKs are interfacial enzymes and, therefore, the concentrations of the individual lipid components at the surface of the mixed micelle are important in affecting DGK enzymatic activity rather than the bulk concentrations of the lipid components.

We confirmed that the measured activity of DGK was not affected substantially by product degradation as a result of the hydrolysis of PA by endogenous PA phosphatases (PAP), or as a result of the upregulation by endogenous protein kinase C (PKC) and phospholipases D (PLD). Our results showed that the DGKε activity measured in the absence and in the presence of either propranolol (PAP[36] and PKC[37] inhibitor; Sigma- Aldrich), bromoenol lactone (BEL, PAP inhibitor;[38] Sigma-Aldrich) (Fig. 4.7a), or PLD inhibitors (Fig. 4.7b; equimolar mix of VU0359595,[39] VU0155056[40] and VU0285655-1[41] inhibitors; Avanti Polar Lipids) are not significantly different.

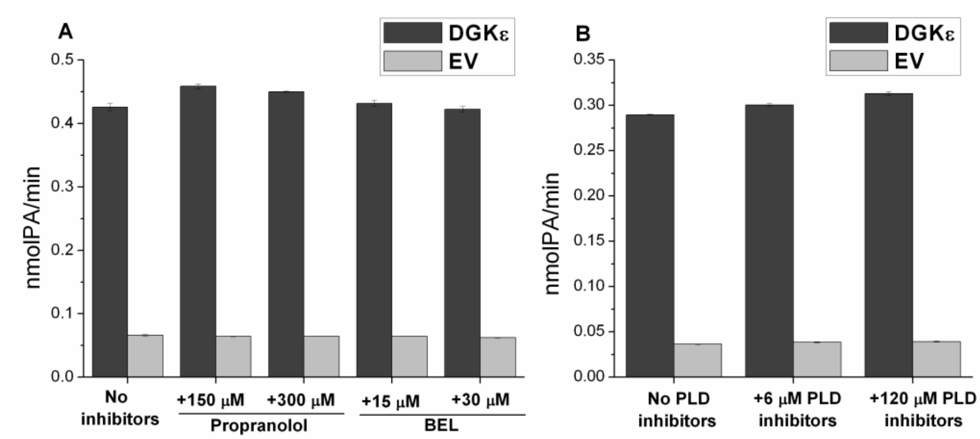

Figure 4.7. Comparison of the FLAG-DGKε enzyme activity in the absence and in the presence of PA phosphatase (PAP) inhibitors, protein kinase C (PKC) and phospholipase D (PLD) inhibitors. a, Propranolol (PAP and PKC inhibitor) and bromoenol lactone (BEL, PAP inhibitor) do not affect the measured DGKε activity. b, PLD inhibitors (Avanti Polar Lipids, equimolar mix of VU0359595, VU0155056 and VU0285655-1 inhibitors) at concentrations of 6 μM or 120 μM do not significantly affect the measured DGKε activity. The negative control (EV) was done with the lysates from COS-7 cells transfected with empty vector (p3XFLAG-CMV-7.1, Sigma-Aldrich).

Detergent–phospholipid mixed micelle-based PIP5K enzymatic activity assay

PIP5 kinase activity assay was done essentially as described but with the following modifications.[42] Reactions were performed in a 100 μl reaction volume in a standard buffer; 50 mM Tris–HCl (pH 7.5), 10 mM $MgCl_2$, 100 mM NaCl, 1 mM EGTA, 0.1% Triton X-100, 50 μM [γ-^{32}P]ATP (2 μCi/reaction). The reaction was stopped after 10 min by the simultaneous addition of 500 μl of 1 M HCl and 2 ml of 1:1 (v/v) chloroform/methanol. The assay was washed twice with 1 ml of methanol, 1 M HCl. A sample of the organic layer was used to quantify the incorporation of ^{32}P into PI(4,5)P_2 using Cerenkov counting. Negative controls were run with the addition of beads immunoprecipitated from mock-transfected COS-7 cells and were confirmed to have activity levels significantly below that of immunoprecipitates from cells over-expressing PIP5K. Kinetic parameters were calculated using the effective concentration of PI4P at the surface of the micelle. To be consistent with previously data on this enzyme presented earlier,[42] the effective surface concentration of PI(4)P was calculated by multiplying the mol fraction of PI(4)P at the surface of the micelle by the total concentration of PI(4)P.

Kinetic analysis of the micelle-based assay of DGK and PIP5K activity

The Michaelis–Menten constants V_{max} and K_m were evaluated by a nonlinear regression analysis (initial velocity (v_0) *versus* substrate concentration ([S])), as well as by Hanes plots ([S]/v_0 *versus* [S]). The content of DGK and PIP5K was determined using immunoblot analysis as described above. Microcal Origin software was used to determine k_{cat}, V_{max} and K_m.

Acknowledgements

We are grateful to Ms Jessica Ngui-Yen for assistance in preparing one of the mutant proteins. This work was supported, in part, by a grant from the Natural Sciences and Engineering Research Council of Canada (9848 to R.M.E.) and, in part, by a grant from the National Institutes of Health (R01CA095463 to M.K.T.).

REFERENCES

1. Laye, S. (2010). Polyunsaturated fatty acids, neuroinflammation and wellbeing. Prostaglandins Leukot. Essent. Fatty Acids, 82, 295–303.

2. Back, M. (2009). Leukotriene signaling in atherosclerosis and ischemia. Cardiovasc. Drugs Ther. 23, 41–48.

3. Chen, X., Wang, S., Wu, N. & Yang, C. S. (2004). Leukotriene A4 hydrolase as a target for cancer prevention and therapy. Curr. Cancer Drug Targets, 4, 267–283.

4. Rådmark, O. & Samuelsson, B. (2009). 5-Lipoxygenase: mechanisms of regulation. J. Lipid Res. 50, S40–S45.

5. Funk, C. D. (2001). Prostaglandins and leukotrienes: advances in eicosanoid biology. Science, 294, 1871–1875.

6. Buczynski, M. W., Dumlao, D. S. & Dennis, E. A. (2009). An integrated omics analysis of eicosanoid biology. J. Lipid Res. 50, 1015–1038.

7. Pérez-Chacón, G., Astudillo, A. M., Balgoma, D., Balboa, M. A. & Balsinde, J. (2009). Control of free arachidonic acid levels by phospholipases A2 and lysophospholipid acyltransferases. Biochim. Biophys. Acta, 1791, 1103–1113.

8. Rodriguez de Turco, E. B., Tang, W., Topham, M. K., Sakane, F., Marcheselli, V. L., Chen, C. et al. (2001). Diacylglycerol kinase epsilon regulates seizure susceptibility and long-term potentiation through arachidonoylinositol lipid signaling. Proc. Natl Acad. Sci. USA, 98, 4740–4745.

9. Walsh, J. P., Suen, R., Lemaitre, R. N. & Glomset, J. A. (1994). Arachidonoyl-diacylglycerol kinase from bovine testis. Purification and properties. J. Biol. Chem. 269, 21155–21164.

10. Thirugnanam, S., Topham, M. & Epand, R. (2001). Physiological implications of the contrasting modulation of the activities of the epsilon- and zetaisoforms of diacylglycerol kinase. Biochemistry, 40, 10607–10613.

11. Milne, S. B., Ivanova, P. T., Armstrong, M. D., Myers, D. S., Lubarda, J., Shulga, Y. V. et al. (2008). Dramatic differences in the roles in lipid metabolism of two isoforms of diacylglycerol kinase. Biochemistry, 47, 9372–9379.

12. Lung, M., Shulga, Y. V., Ivanova, P. T., Myers, D. S., Milne, S. B., Brown, H. A. et al. (2009). Diacylglycerol kinase epsilon is selective for both acyl chains of phosphatidic acid or diacylglycerol. J. Biol. Chem. 284, 31062–31073.

13. Neau, D. B., Gilbert, N. C., Bartlett, S. G., Boeglin, W., Brash, A. R. & Newcomer, M. E (2009). The 1.85 Å structure of an 8R-lipoxygenase suggests a general model for lipoxygenase product specificity. Biochemistry, 48, 7906–7915.

14. Tang, W., Bunting, M., Zimmerman, G. A., McIntyre, T. M. & Prescott, S. M. (1996). Molecular cloning of a novel human diacylglycerol kinase highly selective for arachidonate-containing substrates. J. Biol. Chem. 271, 10237–10241.

15. Epand, R. M., Kam, A., Bridgelal, N., Saiga, A. & Topham, M. K. (2004). The alpha isoform of diacylglycerol kinase exhibits arachidonoyl specificity with alkylacylglycerol. Biochemistry, 43, 14778–14783.

16. Volpicelli-Daley, L. A., Lucast, L., Gong, L. W., Liu, L., Sasaki, J., Sasaki, T. et al. (2010). Phosphatidylinositol-4-phosphate 5-kinases and phosphatidylinositol 4,5-bisphosphate synthesis in the brain. J. Biol. Chem. 285, 28708–28714.

17. Kohama, T., Olivera, A., Edsall, L., Nagiec, M. M., Dickson, R. & Spiegel, S. (1998). Molecular cloning and functional characterization of murine sphingosine kinase. J. Biol. Chem. 273, 23722–23728.

18. Sugiura, M., Kono, K., Liu, H., Shimizugawa, T., Minekura, H., Spiegel, S. & Kohama, T. (2002). Ceramide kinase, a novel lipid kinase. Molecular cloning and functional characterization. J. Biol. Chem. 277, 23294–23300.

19. Mérida, I., Avila-Flores, A. & Merino, E. (2008). Diacylglycerol kinases: at the hub of cell signalling. Biochem. J. 409, 1–18.

20. Jarquin-Pardo, M., Fitzpatrick, A., Galiano, F. J., First, E. A. & Davis, J. N. (2007). Phosphatidic acid regulates the affinity of the murine phosphatidylinositol 4-phosphate 5-kinase-Iβ for phosphatidylinositol-4-phosphate. J. Cell. Biochem. 100, 112–128.

21. Epand, R. M. (2006). Cholesterol and the interaction of proteins with membrane domains. Prog. Lipid Res. 45, 279–294.

22. Li, H. & Papadopoulos, V. (1998). Peripheral-type benzodiazepine receptor function in cholesterol transport. Identification of a putative cholesterol recognition/interaction amino acid sequence and consensus pattern. Endocrinology, 139, 4991–4997.

23. Boesze-Battaglia, K., Brown, A., Walker, L., Besack, D., Zekavat, A., Wrenn, S. et al. (2009). Cytolethal distending toxin-induced cell cycle arrest of lymphocytes is dependent upon recognition and binding to cholesterol. J. Biol. Chem. 284, 10650–10658.

24. Saher, G., Quintes, S., Mobius, W., Wehr, M. C., KramerAlbers, E. M., Brugger, B. & Nave, K. A. (2009). Cholesterol regulates the endoplasmic reticulum exit of the major membrane protein P0 required for peripheral myelin compaction. J. Neurosci. 29, 6094–6104.

25. Schroeder, C. (2010). Cholesterol-binding viral proteins in virus entry and morphogenesis. Subcell. Biochem. 51, 77–108.

26. Scolari, S., Müller, K., Bittman, R., Herrmann, A. & Müller, P. (2010). Interaction of mammalian seminal plasma protein PDC-109 with cholesterol: implications for a putative CRAC domain. Biochemistry, 49, 9027–9031.

27. Jafurulla, M., Tiwari, S. & Chattopadhyay, A. (2011). Identification of cholesterol recognition amino acid consensus (CRAC) motif in G-protein coupled receptors. Biochem. Biophys. Res. Commun. 404, 569–573.

28. Kim, H. J., Kwon, H. R., Bae, C. D., Park, J. & Hong, K. U. (2010). Specific primary sequence requirements for Aurora B kinase-mediated phosphorylation and subcellular localization of TMAP during mitosis. Cell Cycle, 9, 2027–2036.

29. Guse, A., Mishima, M. & Glotzer, M. (2005). Phosphorylation of ZEN-4/MKLP1 by aurora B regulates completion of cytokinesis. Curr. Biol. 15, 778–786.

30. Sato, T. K., Overduin, M. & Emr, S. D. (2001). Location, location, location: membrane targeting directed by PX domains. Science, 294, 1881–1885.

31. Worby, C. A. & Dixon, J. E. (2002). Sorting out the cellular functions of sorting nexins. Nat. Rev. Mol. Cell. Biol. 3, 919–931.

32. Dicu, A. O., Topham, M. K., Ottaway, L. & Epand, R. M. (2007). Role of the hydrophobic segment of diacylglycerol kinase epsilon. Biochemistry, 46, 6109–6117.

33. Topham, M. K. & Prescott, S. M. (2001). Diacylglycerol kinase zeta regulates Ras activation by a novel mechanism. J. Cell Biol. 152, 191135–191143.

34. Luo, B., Regier, D. S., Prescott, S. M. & Topham, M. K. (2004). Diacylglycerol kinases. Cell Signal. 16, 983–989.

35. Ames, B. N. (1966). Assay of inorganic phosphate, total phosphate and phosphatases. Methods Enzymol. 8, 115–118.

36. Pappu, A. S. & Hauser, G. (1983). Propranolol-induced inhibition of rat brain cytoplasmic phosphatidate phosphohydrolase. Neurochem. Res. 8, 1565–1575.

37. Sozzani, S., Agwu, D. E., McCall, C. E., O'Flaherty, J. T., Schmitt, J. D., Kent, J. D. & McPhail, L. C. (1992). Propranolol, a phosphatidate phosphohydrolase inhibitor, also inhibits protein kinase C. J. Biol. Chem. 267, 20481–20488.

38. Balsinde, J. & Dennis, E. A. (1996). Bromoenol lactone inhibits magnesium-dependent phosphatidate phosphohydrolase and blocks triacylglycerol biosynthesis in mouse P388D1 macrophages. J. Biol. Chem. 271, 31937–31941.

39. Lewis, J. A., Scott, S. A., Lavieri, R., Buck, J. R., Selvy, P. E., Stoops, S. L. et al. (2009). Design and synthesis of isoform-selective phospholipase D (PLD) inhibitors. Part I. Impact of alternative halogenated privileged structures for PLD1 specificity. Bioorg. Med. Chem. Lett. 19, 1916–1920.

40. Scott, S. A., Selvy, P. E., Buck, J. R., Cho, H. P., Criswell, T. L., Thomas, A. L. et al. (2009). Design of isoform-selective phospholipase D inhibitors that modulate cancer cell invasiveness. Nature Chem. Biol. 5, 108–117.

41. Lavieri, R., Scott, S. A., Lewis, J. A., Selvy, P. E., Armstrong, M. D., Brown, H. A. & Lindsley, C. W. (2009). Design and synthesis of isoform-selective phospholipase D (PLD) inhibitors. Part II. Identification of the 1,3,8-triazaspiro[4,5]decan-4-one privileged structure that engenders PLD2 selectivity. Bioorg. Med. Chem. Lett. 19, 2240–2243.

42. Parker, G. J., Loijens, J. C. & Anderson, R. A. (1998). Detection of phosphatidylinositol-4-phosphate 5-kinase activity using thin-layer chromatography. Methods Mol. Biol. 105, 127–139.

CHAPTER FIVE

SUBSTRATE SPECIFICITY OF DIACYLGLYCEROL KINASE-EPSILON AND THE PHOSPHATIDYLINOSITOL CYCLE

CHAPTER FIVE PREFACE

The work presented in this chapter was published previously in *FEBS Letters*, volume 585(24), pages 4025-4028, in 2011.

Reprinted with permission from "Shulga Y.V., Topham M.K., Epand R.M. (2011) Substrate specificity of diacylglycerol kinase-epsilon and the phosphatidylinositol cycle. *FEBS Lett.* 585(24):4025-8." Copyright (2011) Elsevier.

Shulga Y.V. conducted all the experiments described in this chapter.

Research objective: to study in more details the specificity of DGKε for *sn*-1 and *sn*-2 acyl chains of diacylglycerol.

Research highlights:

- Several different acyl chains can occupy the *sn*-1 position of good DAG substrates.
- 18:2 and 20:4 are only chains possible at *sn*-2 of good DAG substrates.
- The best substrate is the PI-cycle intermediate 18:0/20:4-DAG.
- 20:4/20:4-DAG surprisingly has equivalent activity to 18:0/20:4-DAG.

Substrate Specificity of Diacylglycerol kinase-epsilon and the Phosphatidylinositol Cycle

Yulia V. Shulga[1], Matthew K. Topham[2], and Richard M. Epand[1]

[1]Department of Biochemistry and Biomedical Sciences, McMaster University, 1280 Main Street West, Hamilton, Ontario L8S 4K1, CANADA

[2]Huntsman Cancer Institute, University of Utah, 2000 Circle of Hope, Salt Lake City, Utah 84112, U.S.A.

Address correspondence to: Richard M. Epand, Department of Biochemistry and Biomedical Sciences, McMaster University, 1280 Main Street West, Hamilton, Ontario L8S 4K1, CANADA; Tel. 905 525-9140; Fax 905 521-1397; E-mail: epand@mcmaster.ca

Abbreviations

DGK, diacylglycerol kinase; DAG, diacylglycerol; PA, phosphatidic acid; PI, phosphatidylinositol; DAG, diacylglycerol; 18:0/20:4-DAG, 1-stearoyl-2-arachidonoyl-DAG; 20:4/20:4-DAG, 1,2-diarachidonoyl-DAG; DHA, docosahexaenoic acid.

ABSTRACT

We show that diacylglycerol kinase-ε (DGKε) has less preference for the acyl chain at the *sn*-1 position of diacylglycerol (DAG) than the one at the *sn*-2 position. Although DGKε discriminates between 1-stearoyl-2-arachidonoyl-DAG and 1-palmitoyl-2-arachidonoyl-DAG, it has similar substrate preference for 1-stearoyl-2-arachidonoyl-DAG and 1,2-diarachidonoyl-DAG. We suggest that in addition to binding to the enzyme,

the acyl chain at the *sn*-1 position may contribute to the depth of insertion of the DAG into the membrane. Thus, the DAG intermediate of the PI-cycle, 1-stearoyl-2-arachidonoyl-DAG, is not unique in being a good substrate for DGKε, the DGK isoform involved in PI-cycling.

Keywords:

Diacylglycerol kinase, diacylglycerol, polyunsaturated acyl chain, phosphatidylinositol cycling, acyl chain specificity

INTRODUCTION

Diacylglycerol kinases (DGKs) phosphorylate diacylglycerol (DAG), a second messenger involved in cell signalling, to produce phosphatidic acid (PA), which has signalling roles as well [1]. It is now widely accepted that conversion of DAG to PA by DGKs is the major pathway to remove the potent signaling molecule DAG.

It appears that the physiologically relevant DAGs are those containing a polyunsaturated acyl chain in the *sn*-2 position. DGKε is the only DGK isoform that shows substrate specificity *in vitro* for DAG with an arachidonoyl acyl chain at the *sn*-2 position [2,3]. Phosphorylation of 1-stearoyl-2-arachidonoyl-DAG (18:0/20:4-DAG), catalyzed by DGK, is the first step in the resynthesis of phosphatidylinositol (PI). It was shown that among all the isoforms of DGK, DGKε appears to be the most important for catalyzing this step in the PI cycle, since deletion of this enzyme significantly decreases the amounts of both PI and PA in the plasma membrane of the cells [4]. 1-stearoyl-2-arachidonoyl-DAG is formed as a result of phosphatidylinositol-4,5-bisphosphate-specific phospholipase C catalyzed hydrolysis of phosphatidylinositol-4,5-bisphosphate that itself is highly enriched in arachidonic acid at the same position. Thus, DGKε may be responsible for down-regulating the DAG signalling resulting from phosphatidylinositol cycling.

The product of the reaction catalyzed by DGK, PA, is also involved in the regulation of a wide variety of cellular events, including cell survival, cytoskeletal rearrangement and proliferation [5]. It is believed that each PA species can differentially activate proteins depending on the saturation and length of the acyl chains [6]. It was shown that the PA produced by different DGKs can fulfill different roles in the cell. Thus, PA produced by DGKε is enriched in polyunsaturated fatty acids, particularly arachidonate, and it is involved in the PI cycle. PA produced by DGKα is necessary to progress to S phase of the cell cycle in stimulated T lymphocytes [7] and PA produced by DGKζ is involved in the initialization of the cascade to cause actin rearrangements [8]. Therefore, DGK substrate specificity is crucial for the regulation of many cellular processes. In the present work we studied the substrate specificity of DGKε and for the first time showed that the DAG intermediate of the PI cycle, 1-stearoyl-2-arachidonoyl-DAG (18:0/20:4-DAG), is not the only preferred substrate for DGKε, but that this enzyme exhibits similar preference towards 1,2-diarachidonoyl-DAG (20:4/20:4-DAG).

MATERIALS AND METHODS

Preparation of Sf21 cells overexpressing DGKε and DGKζ

Baculovirus-infected Sf21 cells overexpressing either human DGKε with a C-terminal hexahistidine (DGKε-His6) or DGKζ with a C-terminal FLAG epitope (DGKζ-FLAG) were prepared as previously described [9].

Enzyme Preparations for Enzymatic Activity Assay

Prior to assay, baculovirus-infected Sf21 cells overexpressing either human DGKε-His6 or DGKζ-FLAG were resuspended in ice-cold cell lysis buffer (1% (v/v) (octylphenoxy)polyethoxyethanol (Nonidet P-40), 20 mM Tris-HCl (pH 7.5), 150 mM NaCl, 1 mM EDTA, 2.5 mM sodium pyrophosphate, 1 mM β-glycerophosphate, 1 mM activated sodium orthovanadate, and 1:100 protease inhibitor cocktail for use with mammalian cells and tissue (Sigma-Aldrich)), allowed to lyse for 10 minutes on ice, sonicated for 5 minutes and then centrifuged at 100,000 g, 30 min at 4 °C. The supernatants were used in the assay of DGK activity.

Quantification of Phosphatidic Acid

The concentration of all PA stocks used in this study was determined experimentally based on their phosphate content, as described previously [10].

Detergent-Phospholipid-Mixed Micelle-based DGK Enzymatic Activity Assay

DGK was assayed for enzymatic activity using a detergent-phospholipid-mixed micelle-based protocol described by Walsh et al. [2] as previously employed in our laboratory [11]. Lipid films composed of the substrate (DAG) and 1,2-dioleoyl-*sn*-glycero-3-phosphocholine (DOPC, for DGKε) or 1,2-dioleoyl-*sn*-glycero-3-[phospho-L-serine] (DOPS, for DGKζ)) were prepared. Enzymatic activity was measured with 15 mM Triton X-100, 0.1 mM [γ-^{32}P]-ATP, 1.52 mol % DAG and 22.5 mol % DOPC or 22.5

mol% DOPS. The assays were performed in triplicate and the results are presented as the mean ± S.D.

Kinetic Analysis of the Micelle-Based Assay of DGK Activity

The Michaelis-Menten constants, V_{max} and K_m, were evaluated by a nonlinear regression analysis (initial velocity (v_0) *versus* substrate concentration ([S])), as well as by using Hanes plots ([S]/v_0 *versus* [S]). Origin (version 7.5) software was used to determine V_{max} and K_m parameters. Inhibition by PA was observed to be competitive, in agreement with previous observations [12]. K_i constants were evaluated by a nonlinear regression analysis for a competitive type of enzyme inhibition, using the GraphPad Prism software program (version 5.00).

RESULTS AND DISCUSSION

It has been recognized earlier that DGKε exhibits specificity for arachidonoyl-containing forms of DAG [13]. It has more recently been established that this isoform of DGK has a particularly important role in catalyzing one of the steps of the PI-cycle [3,14]. This finding correlated well with the known arachidonoyl specificity, since the predominant acyl chain in the *sn*-2 position of lipid intermediates of the PI-cycle is arachidonic acid. It is also established that these PI-cycle lipid intermediates contain predominantly stearoyl chains at the *sn*-1 position. We have shown that among saturated acyl chains, the stearoyl (18:0) chain is the most favoured for substrates of DGKε [12]. Furthermore, there is a decrease in 18:0 chains in PIs species in mouse embryo fibroblasts that have been knocked out for DGKε [12]. Thus the best substrate that we found for

DGKε was 18:0/20:4-DAG, the form of DAG that is a precursor for the synthesis of PIs. The result of the present study, that 20:4/20:4-DAG has a similar activity to 18:0/20:4-DAG (Fig. 5.1, Table 5.1) was surprising. We therefore studied in more detail the acyl chain requirements for the substrates of DGKε.

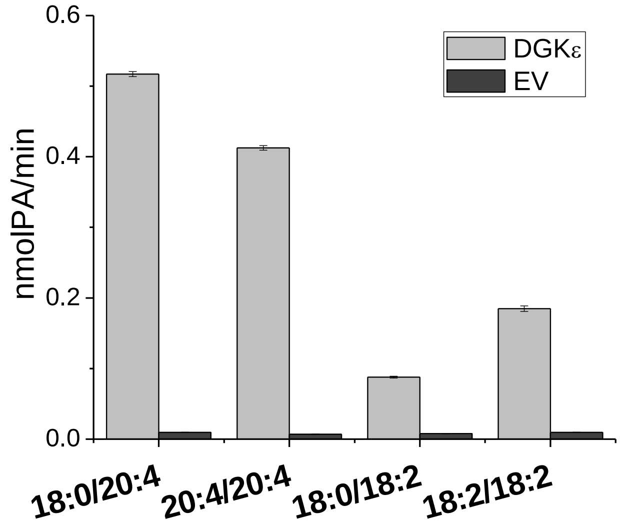

Figure 5.1. Comparison of the enzyme activities for DGKε with 18:0/20:4-DAG, 20:4/20:4-DAG, 18:0/18:2-DAG and 18:2/18:2-DAG as substrates. Negative control (EV) is performed with the lysates from mock baculovirus-infected Sf21 cells.

Table 5.1. Summary of the kinetic parameters for DGKε with 18:0/20:4-DAG, 20:4/20:4-DAG and 18:2/18:2-DAG as substrates. Results are presented as the mean ± S.D. Values of V_{max} are relative values since the absolute amount of enzyme in the cell preparations is not known.

Substrate	**K_m (mol%)**	**V_{max} (nmol PA min^{-1})**	**V_{max}/K_m ($mol\%^{-1}sec^{-1}$)**
18:0/20:4 DAG	2.0 ± 0.7	1.7 ± 0.3	0.8 ± 0.3
20:4/20:4 DAG	2.0 ± 0.7	1.6 ± 0.2	0.8 ± 0.3
18:2/18:2 DAG	3.5 ± 0.4	0.89 ± 0.06	0.26 ± 0.03

Maintaining 18:0 as the *sn*-1 acyl chain, we confirmed that a linoleoyl chain (18:2) at the *sn*-2 position is also a substrate for DGKε, but one that is poorer than 18:0/20:4-DAG (Fig. 5.1). Although 18:0 at *sn*-1 of DAG makes a better DGKε substrate than 16:0, the difference is not very great [12]. However, 16:0/16:0-DAG is a poor substrate for DGK [15,16]. We showed that 16:0/18:1-DAG and 18:1/18:1-DAG are also poor substrates (Fig. 5.2). DGKε is very abundant in the brain and retina, suggesting an important physiological role of this enzyme in CNS and visual function. At the same time, docosahexaenoic acid (DHA, 22:6-fatty acid) is the most abundant omega-3 fatty acid in the brain and retina, comprising 40% of the polyunsaturated fatty acids in the brain and 60% in the retina. Despite these facts, 18:0/22:6-DAG is not a substrate for DGKε (Fig. 5.3A). This is in contrast with the behaviour of another DGK isoform, DGKζ, that does not discriminate among DAGs with different acyl chains (Fig. 5.3B). Thus, for DGKε there is a very high specificity for the acyl chain at the *sn*-2 position with only two acyl groups, arachidonoyl or linoleoyl, showing any substantial activity. Interestingly, these two acyl chains are also the only two that are recognized by lipoxygenases. Generally mammalian lipoxygenases are more specific for arachidonic acid, while the homologous enzymes from plants have greater specificity for linoleic acid. Recognition of polyunsaturated acyl chains by both DGKε and by lipoxygenases is due in part to a common amino acid motif in a segment of both proteins [17].

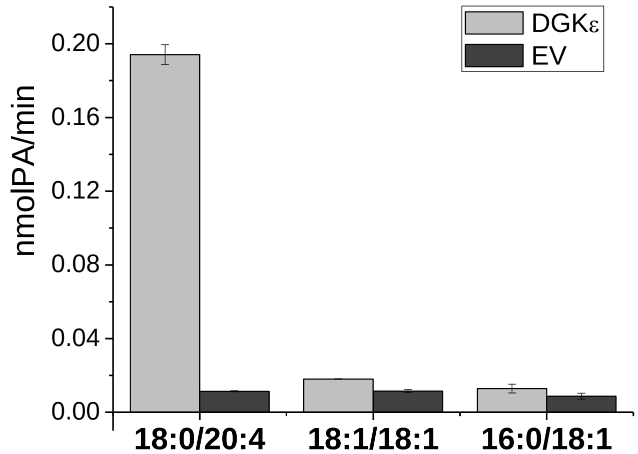

Figure 5.2. A. Comparison of the enzyme activities for DGKε with 18:0/20:4-DAG, 18:1/18:1-DAG and 16:0/18:1-DAG as substrates. Negative control (EV) is performed with the lysates from mock baculovirus-infected Sf21 cells.

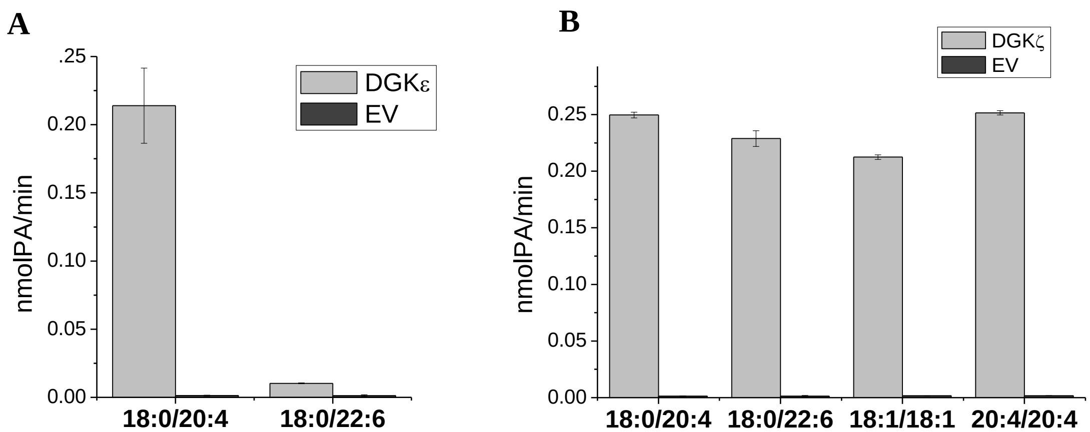

Figure 5.3. A. Comparison of the enzyme activities for DGKε with 18:0/20:4-DAG and 18:0/22:6-DAG as substrates. Negative control (EV) is performed with the lysates from mock baculovirus-infected Sf21 cells. B. Comparison of the enzyme activities for DGKζ with 18:0/20:4-DAG, 18:1/18:1-DAG, 18:0/22:6-DAG and 20:4/20:4-DAG as substrates. Negative control (EV) is performed with the lysates from mock baculovirus-infected Sf21 cells.

The requirements for the acyl chain of DAG at the *sn*-1 position are much more flexible as shown by the finding that 20:4/20:4-DAG has similar activity to 18:0/20:4-

DAG (Fig. 5.1, Table 5.1). Although, with 20:4 in the *sn*-2 position, 18:0 was the best acyl chain for *sn*-1 among saturated acyl chains and had a higher affinity with DGKε than either 16:0/20:4-DAG or 20:0/20:4-DAG [12], the 18:0 acyl chain at *sn*-1 can be replaced by 20:4 with almost complete retention of activity. Furthermore, 18:2/18:2-DAG has a higher activity than even 18:0/18:2-DAG (Fig. 5.1). 18:2/18:2-DAG is also the precursor for PA with this acyl chain composition. 18:2/18:2-PA is a potent inhibitor of insulin receptor signalling [18].

Studies of the crystal structure of different fatty acids bound to autotaxin has shown that acyl chains containing unsaturation turn sharply at the unsaturated bonds, allowing longer lipid tails to be accommodated in a hydrophobic pocket [19]. A similar phenomenon can explain the finding that longer acyl chains can be incorporated into the *sn*-1 position of DAG and still be a good substrate for DGKε, provided that the longer chains have unsaturation.

Another factor that may affect the efficiency of phosphorylation of different species of DAG is the extent to which the substrate penetrates into the membrane. It is suggestive that this may be a factor, although at the present time the evidence is incomplete and indirect. There is however evidence from neutron diffraction studies showing that the position of tocopherol in a lipid environment is very similar for tocopherol embedded into 20:4/20:4-PC as it is when embedded in 16:0/20:4-PC and different from results with other forms of PC not containing polyunsaturated acyl chains [20]. Thus, replacement of 16:0 in the *sn*-1 position with a 20:4 chain does not alter the depth of burial of tocopherol and thus this change of acyl group would also not likely effect the depth of burial of DAG, despite the large difference in structure and properties of these acyl groups. The similar location of 18:0/20:4-DAG and 20:4/20:4-DAG in the membrane can contribute to their similar location with respect to the enzyme active site, resulting in similar activities.

Previously we showed that 18:0/20:4-PA is the best inhibitor of DGKε [12]. We tested if DGKε inhibition by this PA depends on the acyl chains of the substrate. Our results showed that 18:0/20:4-PA is still the most potent inhibitor of DGKε with three different substrates 18:0/20:4-DAG, 20:4/20:4-DAG and 18:1/18:1-DAG (Fig. 5.4). Further, we determined the inhibition constants K_i for 20:4/20:4-PA as an inhibitor of DGKε activity with 18:0/20:4-DAG and 20:4/20:4-DAG as substrates (Table 5.2). Comparison of K_i suggests that 20:4/20:4-PA binds and inhibits DGKε activity somewhat to a greater extend with 20:4/20:4-DAG as a substrate than 18:0/20:4-DAG. PA is a competitive inhibitor of DAG phosphorylation [12]. Thus, the potency of inhibition of different species of PA depends on how well that PA binds to the active site of DGKε. In contrast, to be a good substrate, the DAG must not only bind to the active site, but must also be at an optimal location with regard to the catalytic groups of the enzyme to undergo efficient catalysis. We suggest that 20:4/20:4-DAG is at the optimal location for catalysis because its depth of insertion into the membrane is optimal and therefore it is a good substrate, even though it does not bind optimally to the enzyme. Furthermore, with 20:4/20:4-PA, inhibition is slightly stronger because of lower binding of the substrate to the enzyme.

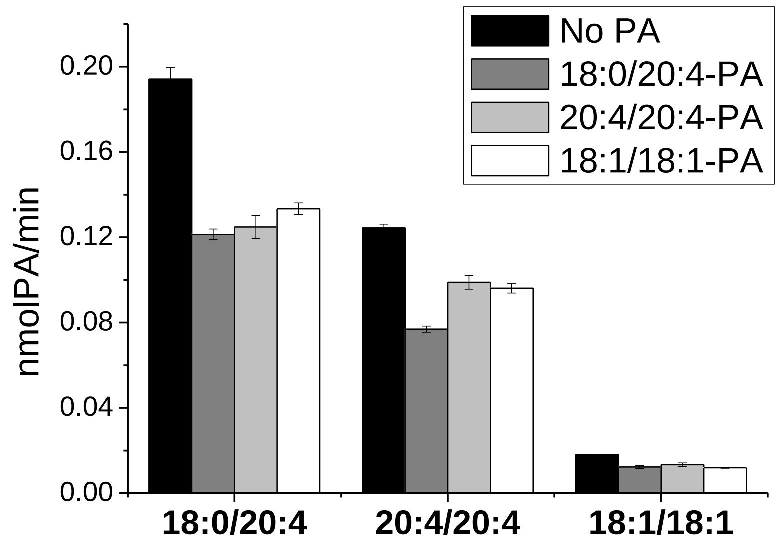

Figure 5.4. Comparison of inhibition of DGKε by PAs in presence of different substrates. DGKε enzymatic activity was measured with 15 mM Triton X-100, 0.1 mM [γ-^{32}P]-ATP, 30 mol % DOPC, and 1.34 mol % either 18:0/20:4-DAG, 20:4/20:4-DAG and 18:1/18:1-DAG (shown as black bars) or with the addition of either 0.67 mol % 18:0/20:4-PA (grey bars), 20:4/20:4-PA (light grey bars) or 18:1/18:1-PA (white bars).

Table 5.2. Summary of the inhibition constants K_i for DGKε with 18:0/20:4-DAG and 20:4/20:4-DAG as substrates and 20:4/20:4-PA as inhibitor. Results are presented as the mean ± S.D.

Substrate	**K_i, mol%**
18:0/20:4-DAG	4.4 ± 1.0
20:4/20:4-DAG	2.6 ± 0.3

In summary, our results demonstrate that 18:0/20:4-DAG is not unique in being a good substrate for DGKε and that there is a qualitative difference between the nature and extent of acyl chain specificity of DGKε for the *sn*-1 and *sn*-2 positions of the substrate.

Acknowledgements

This work was supported in part by a grant from the Natural Sciences and Engineering Research Council of Canada, grant 9848 (to R.M.E.) and from the National Institutes of Health Grant R01CA095463 (to M.K.T.). We wish to thank Dr. Stephen Wassall for providing us with the neutron diffraction results prior to publication.

REFERENCES

[1] Topham, M.K. and Prescott, S.M. (1999). Mammalian diacylglycerol kinases, a family of lipid kinases with signaling functions. *J. Biol. Chem.* 274, 11447-50.

[2] Walsh, J.P., Suen, R., Lemaitre, R.N., and Glomset, J.A. (1994). Arachidonoyl-diacylglycerol kinase from bovine testis. Purification and properties. *J. Biol. Chem.* 269, 21155-64.

[3] Rodriguez de Turco, E. B., Tang, W., Topham, M.K., Sakane, F., Marcheselli, V.L., Chen, C., Taketomi, A., Prescott, S.M., and Bazan, N.G. (2001). Diacylglycerol kinase epsilon regulates seizure susceptibility and long-term potentiation through arachidonoylinositol lipid signaling. *Proc. Natl. Acad. Sci. U. S. A.* 98, 4740-5.

[4] Shulga, Y.V., Myers, D.S., Ivanova, P.T., Milne, S.B., Brown, H.A., Topham, M.K., and Epand, R.M. (2010). Molecular species of phosphatidylinositol-cycle intermediates in the endoplasmic reticulum and plasma membrane. *Biochemistry* 49(2), 312-7.

[5] Cazzolli, R., Shemon, A.N., Fang, M.Q., and Hughes, W.E. (2006). Phospholipid signalling through phospholipase D and phosphatidic acid. *IUBMB Life* 58(8), 457-61.

[6] Shulga, Y.V., Topham, M.K., and Epand, R.M. (2011). Regulation and Functions of Diacylglycerol Kinases. *Chem. Rev.* 111(10), 6186-208.

[7] Flores, I., Casaseca, T., Martinez-A, C., Kanoh, H., and Merida, I. (1996). Phosphatidic acid generation through interleukin 2 (IL-2)-induced alpha-diacylglycerol kinase activation is an essential step in IL-2-mediated lymphocyte proliferation. *J. Biol. Chem.* 271(17), 10334-40.

[8] Abramovici, H., Mojtabaie, P., Parks, R.J., Zhong, X.P., Koretzky, G.A., Topham, M.K., and Gee, S.H. (2009). Diacylglycerol kinase zeta regulates actin cytoskeleton reorganization through dissociation of Rac1 from RhoGDI. *Mol. Biol. Cell.* 20(7), 2049-59.

[9] Epand, R.M., Shulga, Y.V., Timmons, H.C., Perri, A.L., Belani, J.D., Perinpanathan, K., Johnson-McIntire, L.B., Bajjalieh, S., Dicu, A.O., Elias, C., Rychnovsky, S.D., and Topham, M.K. (2007). Substrate chirality and specificity of diacylglycerol kinases and the multisubstrate lipid kinase. *Biochemistry* 46(49), 14225-31.

[10] Ames, B.N. (1966). Assay of inorganic phosphate, total phosphate and phosphatases. *Methods Enzymol.* 8, 115-8.

[11] Dicu, A.O., Topham, M.K., Ottaway, L., and Epand, R.M. (2007). Role of the hydrophobic segment of diacylglycerol kinase epsilon. *Biochemistry* 46, 6109-17.

[12] Lung, M., Shulga, Y.V., Ivanova, P.T., Myers, D.S., Milne, S.B., Brown, H.A., Topham, M.K., and Epand, R.M. (2009). Diacylglycerol kinase epsilon is selective for both acyl chains of phosphatidic acid or diacylglycerol. *J. Biol. Chem.* 284, 31062-73.

[13] Tang W., Bunting M., Zimmerman G. A., McIntyre T. M., and Prescott S. M. (1996). Molecular cloning of a novel human diacylglycerol kinase highly selective for arachidonate-containing substrates. *J. Biol. Chem.* 271, 10237-41.

[14] Milne, S.B., Ivanova, P.T., Armstrong, M.D., Myers, D.S., Lubarda, J., Shulga, Y.V., Topham, M.K., Brown, H.A., and Epand, R.M. (2008). Dramatic Differences in the Roles in Lipid Metabolism of Two Isoforms of Diacylglycerol Kinase. *Biochemistry* 47, 9372-9.

[15] Zulian, S., Ilincheta de Boschero, M., and Giusto, N. (2009). Insulin Action on Polyunsaturated Phosphatidic Acid Formation in Rat Brain: An In Vitro Model with Synaptic Endings from Cerebral Cortex and Hippocampus. *Neurochem. Res.* 34, 1236-48.

[16] Ide, H. and Weinhold, P.A. (1982). Properties of diacylglycerol kinase in adult and fetal rat lung. *Biochim. Biophys. Acta.* 713 (3), 547-54.

[17] Shulga, Y.V., Topham, M.K., and Epand, R.M. (2011). Study of Arachidonoyl Specificity in Two Enzymes of the PI Cycle. *J. Mol. Biol.* 409, 101-12.

[18] Cazzolli, R., Mitchell, T.W., Burchfield, J.G., Pedersen, D.J., Turner, N., Biden, T.J., and Schmitz-Peiffer, C. (2007). Dilinoleoyl-phosphatidic acid mediates reduced IRS-1 tyrosine phosphorylation in rat skeletal muscle cells and mouse muscle. *Diabetologia* 50, 1732-42.

[19] Nishimasu, H., Okudaira, S., Hama, K., Mihara, E., Dohmae, N., Inoue, A., Ishitani, R., Takagi, J., Aoki, J., and Nureki, O. (2011). Crystal structure of autotaxin and insight into GPCR activation by lipid mediators. *Nat. Struct. Mol. Biol.* 18(2), 205-12.

[20] Williams, J.A., Marquardt, D., Stillwell, W., Atkinson, J., Harroun, T.A., and Wassall, S.R. (2011). Vitamin E Responds to its Lipid Environment. *Biophys. J.* 100(3), 493a.

CHAPTER SIX

PHOSPHATIDYLINOSITOL-4-PHOSPHATE 5-KINASE ISOFORMS EXHIBIT ACYL CHAIN SELECTIVITY FOR BOTH SUBSTRATE AND PHOSPHATIDIC ACID

CHAPTER SIX PREFACE

Chapter 6 encompasses the manuscript prepared for a submission.

Shulga Y.V. conducted all the experiments described in this chapter.

Research objective: to study the specificity of phosphatidylinositol-4-phosphate 5-kinase isoforms for the acyl chains of the substrates and activator phosphatidic acid.

Research highlights:

- Background: Do isoforms of phosphatidylinositol-4-phosphate 5-kinase select specific lipid substrates and activators?
- Results: There are different extents of acyl chain selectivity of these enzymes, but their preference for the acyl chains of the substrate does not correspond with that of phosphatidic acid.
- Conclusion: The gamma isoform is the most selective for interacting with lipids with different acyl chains.
- Significance: Selectivity of phosphatidylinositol-4-phosphate 5-kinases type I for the acyl chains of the substrate and activator could be part of a tightly regulated mechanism producing physiologically active unsaturated PtdIns(4,5)P_2 species in the cell.

Phosphatidylinositol-4-phosphate 5-kinase Isoforms Exhibit Acyl Chain Selectivity for Both Substrate and Phosphatidic Acid

Yulia V. Shulga[1], Richard A. Anderson[2], Matthew K. Topham[3], and Richard M. Epand[1]

[1]Department of Biochemistry and Biomedical Sciences, McMaster University, 1280 Main Street West, Hamilton, Ontario L8S 4K1, CANADA

[2]Department of Pharmacology, University of Wisconsin Medical School, Madison, Wisconsin 53706, U.S.A.

[3]Huntsman Cancer Institute, University of Utah, 2000 Circle of Hope, Salt Lake City, Utah 84112, U.S.A.

*Running title: Acyl chain specificity of PIP5K

To whom correspondence should be addressed: Richard M. Epand, Department of Biochemistry and Biomedical Sciences, McMaster University, 1280 Main Street West, Hamilton, Ontario L8S 4K1, CANADA; Tel. 905 525-9140; Fax 905 521-1397; E-mail: epand@mcmaster.ca

Keywords:

Phosphatidylinositol-4-phosphate 5-kinase; phosphatidic acid activation; acyl chain specificity

Abbreviations used:

DGK, diacylglycerol kinase; PtdIns, phosphatidylinositol; PtdIns4*P*, phosphatidylinositol-4-phosphate; PIP5K, PtdIns4*P* 5-kinase; PtdIns(4,5)P_2, phosphatidylinositol-(4,5)-bisphosphate; PLD, phospholipase D. For the abbreviation of the variety of lipids with specific acyl chains used in this work, see Table 1.

SUMMARY

Phosphatidylinositol 4,5-bisphosphate (PtdIns(4,5)P_2), mostly produced in the cell by phosphatidylinositol-4-phosphate 5-kinases (PIP5K), plays a crucial role in numerous signaling events. Here we demonstrate that *in vitro* all three isoforms of PIP5K, α, β and γ, discriminate among substrates with different acyl chains for both the substrates phosphatidylinositol-4-phosphate (PtdIns4*P*) and phosphatidylinositol (PtdIns), although to a different extent, with isoform γ being the most sensitive. Fully saturated dipalmitoyl-PtdIns4*P* was a poor substrate for all three isoforms but both the 1-stearoyl-2-arachidonoyl and the 1-stearoyl-2-oleoyl forms of PtdIns4*P* were good substrates. V_{max} was greater for the 1-stearoyl-2-arachidonoyl form compared with the 1-stearoyl-2-oleoyl form, although for PIP5Kβ the difference was small. For the α and γ isoforms, K_m was much lower for 1-stearoyl-2-oleoyl PtdIns4*P*, making this lipid the better substrate of the two under most conditions. Activation of PIP5K by PA is also acyl chain dependent. Species of PA with two unsaturated acyl chains are much better activators of PIP5K than those containing one saturated and one unsaturated acyl chain. PtdIns is a poor substrate for PIP5K but it also shows acyl chain selectivity. Curiously, there is no acyl chain discrimination among species of phosphatidic acid in the activation of the phosphorylation of PtdIns. Together, our findings indicate that PIP5K isoforms α, β and γ

act selectively on substrates and activators with different acyl chains. This could be a tightly regulated mechanism of producing physiologically active unsaturated PtdIns(4,5)P_2 species in the cell.

INTRODUCTION

The phosphatidylinositol phosphate kinases have a multitude of important roles in cell signaling (1-3). This family of enzymes is responsible for the regulation of cytoskeleton dynamics, vesicular trafficking, cell migration, as well as transcription control at the nucleus. The headgroup specificity of these enzymes has been extensively investigated with regard to number and position of phosphate groups required on the substrate as well as the position on the inositol that is phosphorylated by each of these enzymes. However, there has been very little investigation regarding the role of the acyl chains in the substrate specificity of these enzymes. In some studies natural forms of the substrates were used, while in other studies dipalmitoylated lipids were used because of their greater stability and commercial availability. However, we recently showed that the dipalmitoylated form of phosphatidylinositol-4-phosphate (PtdIns4*P*) was a much poorer substrate for phosphatidylinositol-4-phosphate 5-kinase (PIP5K) than natural form of PtdIns4*P* (4).

In the current study we focused on type I isoforms of PIP5K (PIP5K) that catalyze the phosphorylation of PtdIns4*P* to form the important secondary messenger, phosphatidylinositol-(4,5)-bisphosphate (PtdIns(4,5)P_2) (5). There are three isoforms of PIP5K given the designations α, β and γ. Each PIP5K isoform produces multiple splicing variants (6-9). Although all three isoforms have a high degree of homology and all catalyze the same reaction, each appears to have some unique properties. PIP5Kα promotes the depolymerization of neuronal microtubules (10). The α isoform suppresses phagocytosis and accumulates transiently on forming phagosomes (11). This isoform also appears in PDGF-induced membrane ruffles in platelets (12). PIP5Kα also interacts directly with diacylglycerol kinase ζ that promotes the formation of PtdIns(4,5)P_2, likely through the activation of PIP5K by phosphatidic acid (PA), the product of the reaction catalyzed by diacylglycerol kinase (DGKζ) (13, 14). The β isoform of PIP5K is activated by both Ser/Thr and by Tyr phosphorylation that is promoted by oxidative stress (15). This isoform controls neutrophil polarity and directional movement (16, 17). The γ isoform of PIP5K affects cell to cell contacts and its activity correlates with a poor prognosis for breast cancer (18). This isoform also regulates distinct stages of Ca^{2+} signaling in mast cells (19). PIP5Kγ is also the most important isoform for producing PtdIns(4,5)P_2 in the brain (20, 21).

Enzymatic activity of all three PIP5Ks was shown to be activated by phosphatidic acid (PA) (22), produced either through phospholipase D (PLD) or several isoforms of diacylglycerol kinase (DGK) (8, 23). There has been only limited assessment of the role of the acyl chains of PA in this activation. Activation by PA of the enzyme that synthesizes PtdIns(4,5)P_2 as part of the PtdIns cycle, PIP5K, is particularly interesting since both PA and PtdIns(4,5)P_2 are lipid intermediates in the PtdIns-cycle and as intermediates in this cycle they are highly enriched in stearoyl and arachidonoyl acyl chains. There is thus potential for a forward feedback activation of the PtdIns-cycle by PA activating PIP5K.

EXPERIMENTAL PROCEDURES

Materials – SO-PtdIns4*P* and SA-, SO-, SL- and DL-PtdIns were custom synthesized by Avanti Polar Lipids. As source of SA-PtdIns4*P*, brain PtdIns4*P* (Avanti Polar Lipids) was used. DP-PtdIns4*P* was purchased from Echelon Biosciences Inc. All PAs were purchased from Avanti Polar Lipids. The abbreviations, full names and alternative notations of all lipids used in this study are listed in Table 6.1.

Table 6.1. Lipids used and/or referred to in this study

Abbreviation	Full name	Alternative notation (*sn*-1/*sn*-2)
PA		
AAPA	1-Arachidoyl-2-arachidonoyl phosphatidic acid	20:0/20:4 PA
DAPA	1,2-Diarachidonoyl phosphatidic acid	20:4/20:4 PA
DLPA	1,2-Dilinoleoyl phosphatidic acid	18:2/18:2 PA
DOPA	1,2-Dioleoyl phosphatidic acid	18:1/18:1 PA
SAPA	1-Stearoyl-2-arachidonoyl phosphatidic acid	18:0/20:4 PA
SOPA	1-Stearoyl-2-oleoyl phosphatidic acid	18:0/18:1 PA
PtdIns		
DL- PtdIns	1,2-Dilinoleoyl phosphatidylinositol	18:2/18:2 PtdIns
SA- PtdIns	1-Stearoyl-2-arachidonoyl phosphatidylinositol	18:0/20:4 PtdIns
SL- PtdIns	1-Stearoyl-2- linoleoyl phosphatidylinositol	18:0/18:2 PtdIns
SO- PtdIns	1-Stearoyl-2-oleoyl phosphatidylinositol	18:0/18:1 PtdIns
PtdIns4*P*		
DP- PtdIns4*P*	1,2-Dipalmitoyl phosphatidylinositol-4-phosphate	16:0/16:0 PtdIns4*P*
SA- PtdIns4*P*	1-Stearoyl-2-arachidonoyl phosphatidylinositol-4-phosphate	18:0/20:4 PtdIns4*P*
SO- PtdIns4*P*	1-Stearoyl-2-oleoyl phosphatidylinositol-4-phosphate	18:0/18:1 PtdIns4*P*

PIP5K constructs – HA-PIP5K isoforms α and γ expression vectors were prepared as previously described. HA-PIP5K isoform β expression vector was a kind gift of Drs. Santos Mañes and Rosa Ana Lacalle of the Centro Nacional de Biotecnologia, Madrid, Spain. c-Myc-PIP5Kα expression vector was prepared as previously described (13). HA-PIP5Kα and c-Myc-PIP5Kα correspond to the human form of the respective enzyme, splicing variant 2; HA-PIP5Kβ – to the mouse form (96% protein homology with human PIP5Kβ); HA-PIP5Kγ – to the human form, splicing variant 1 (640aa). The mutants of c-Myc-PIP5Kα were designed using the QuikChange Lightning Kit (Stratagene, La Jolla, CA) according to the instructions of the manufacturer. The presence of the desired mutations was verified by sequencing analysis.

Cell culture – COS-7 cells were maintained in Dulbecco's modified Eagle's medium (DMEM, GIBCO/Invitrogen) containing 10% fetal bovine serum (GIBCO/Invitrogen) at 37 °C in an atmosphere of 5% CO_2. The cells were grown to about 80% confluency and transiently transfected with the expression vectors using Lipofectamine 2000 (Invitrogen) according to the manufacturer's instructions. The cells were harvested 48 hours after transfection by scraping them into 1X PBS containing 1:100 protease inhibitor cocktail for use with mammalian cells and tissue (Sigma-Aldrich). The cells were pelleted at 5000*g* at 4 °C and kept at -90 °C until further use.

Enzyme Preparations for Enzymatic Activity Assay – Cell pellets of COS-7 cells overexpressing one of the PIP5K proteins were resuspended in ice-cold cell lysis buffer (2% (v/v) (octylphenoxy)polyethoxyethanol (Nonidet P-40), 20 mM Tris/HCl pH 7.5, 150 mM NaCl, 5 mM EDTA, 1 mM Na_3VO_4, 10 μg/mL aprotinin and leupeptin, 1 mM PMSF, 5 mM NaF, 100 μg/mL soybean trypsin inhibitor, and 1:100 protease inhibitor cocktail for use with mammalian cells and tissue (Sigma-Aldrich)), allowed to lyse for 10 minutes on ice, sonicated for 10 minutes and then incubated with agarose beads conjugated with anti-HA (Santa Cruz, sc-7392 AC) or anti-c-Myc antibodies (Santa Cruz, sc-40 AC) at 4 ˚C overnight. After that the beads were centrifuged and washed 1 time with IP kinase buffer (25 mM Tris, pH 7.5, 100 mM NaCl, 0.1% Triton X-100); 1 time with PBS pH 6.0, 0.5% Triton X-100; 1 time with 25 mM Tris, pH 8, 100 mM NaCl, 0.1% Triton X-100; 1 time with 25 mM Tris, pH 7.5, 500 mM NaCl, 0.1% Triton X-100; and 1 time with IP kinase buffer (24). After the final wash the beads were briefly centrifuged and resuspended in 1× assay buffer. Purity of the PIP5K immunoprecipitate was confirmed by Coomassie Blue staining of the gel.

Immunoblot Analysis – Amounts of protein in the immunoprecipitates from transfected COS-7 cells were determined by immunoblotting as described previously (4). The membranes were incubated with either a 0.5 μg/ml concentration of mouse THE^{TM} anti-HA tag IgG1 (GenScript, A01244) or 1:800 dilution of mouse anti-c-Myc (Santa Cruz, sc-40) as the primary antibody and a 1:2000 dilution of horseradish peroxidase-conjugated goat anti-mouse (Santa Cruz, sc-2005) as the secondary antibody.

Quantification of phospholipids PA, PtdIns4P and PtdIns – The concentrations of all PA, PtdIns4*P* and PtdIns stocks used in this study were determined experimentally based on an assay for inorganic phosphate as described previously (4, 25).

Detergent-Phospholipid-Mixed Micelle-based PIP5K Enzymatic Activity Assay –

PIP5 kinase activity assay was performed as described by Parker et al. (26) with the following modifications. Mixed micelles were formed by hydrating the lipid films, composed of the substrate (PtdIns4*P* or PtdIns) with or without addition of PA (see Table 1 for the list of lipids used and their abbreviations), with 2× assay buffer and subsequently vortexing the hydrated lipid film for 2 min. Reactions were performed in a 100 μL reaction volume in an assay buffer containing 50 mM Tris-HCl (pH 7.5), 10 mM $MgCl_2$, 100 mM NaCl, 1 mM EGTA, 0.1% Triton X-100 and 50 μM [γ-^{32}P]ATP (2μCi/reaction). The reaction was stopped after 10 min by the addition of 500 μL of 1 N HCl and 2 mL of chloroform:methanol (1:1) simultaneously. The assay was washed twice with 1 mL of methanol:1N HCl (1:1). An aliquot of the organic layer was used to quantify the incorporation of ^{32}P into the lipid product using Cerenkov counting. Negative controls were run with the addition of beads immunoprecipitated from mock-transfected COS-7 cells and were confirmed to have activity levels significantly below immunoprecipitates from cells overexpressing PIP5K. Results are presented as the mean ± S.D. It was implicated previously that substrate binding by PIP5Ks follows the surface dilution kinetic model described by Hendrickson and Dennis (24). Therefore, in this study the substrate and PA concentrations are presented as the effective concentration of the substrate or PA at the surface of the micelle. The effective surface concentration of the substrate (C_{eff}) was calculated by multiplying the mole fraction of the substrate at the surface of the micelle by the total concentration of the substrate (24).

Kinetic Analysis of the Micelle-Based Assay of PIP5K Activity – Kinetic parameters were calculated using the effective concentration of the substrate at the surface of the micelle following the formula from Jarquin-Pardo et al. (24). Using this treatment the data fit Michaelis-Menten kinetics. The Michaelis-Menten constants, V_{max} and K_m, were evaluated by a nonlinear regression analysis (initial velocity (v_0) *versus* substrate concentration ([S])) using GraphPad Prism software program (version 5.00).

RESULTS

PIP5Ks are sensitive for the acyl chain composition of substrate PtdIns4P – To determine if PIP5K isoforms discriminate between PtdIns4*P* with different acyl chain compositions, we compared the activity of PIP5K isoforms α, β and γ with three different substrates – SA-PtdIns4*P*, SO-PtdIns4*P* and DP-PtdIns4*P* (see Table 6.1 for lipid abbreviations). Our results showed that all isoforms exhibit a significant preference for the two substrates containing an unsaturated acyl chain (SA- and SO-PtdIns4*P*) compared to the substrate with only saturated acyl chains (DP-PtdIns4*P*) (Fig. 6.1A-C). At low substrate concentrations (C_{eff} = 0.23 μM) PIP5Ks have preference for SO-PtdIns4*P* over SA-PtdIns4*P*, with PIP5Kγ isoform showing the largest difference between these two substrates (Fig. 6.1A-C). Nevertheless, at higher substrate concentrations (C_{eff} > 2 μM for PIP5Kα and β, C_{eff} > 4 μM for PIP5Kγ) the enzyme activity is higher for SA-PtdIns4*P* than for SO-PtdIns4*P* (Fig. 6.1D-F).

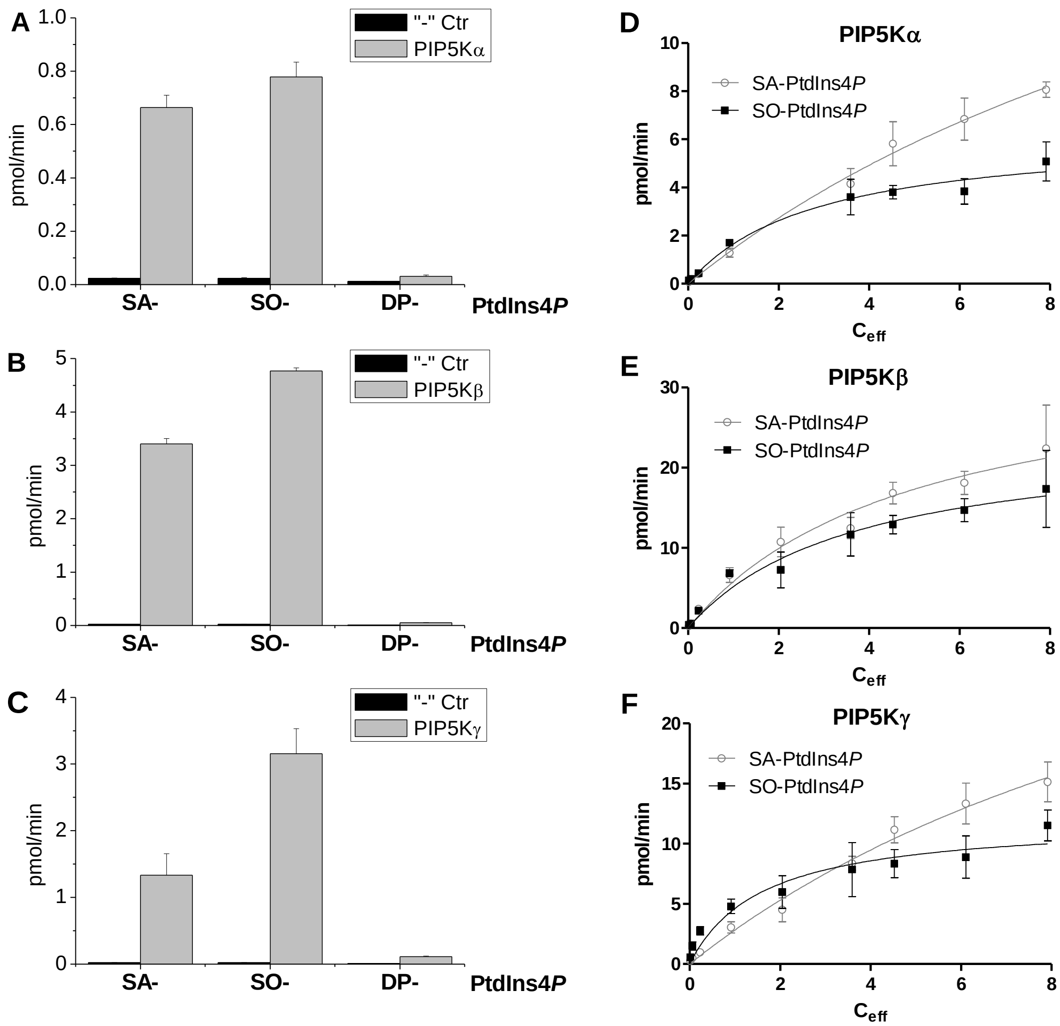

Figure 6.1. HA-PIP5K isoforms α, β and γ show sensitivity for the acyl chain composition of PtdIns4*P* substrate. A-C. Comparison of PIP5K activities with SA-, SO- and DP-PtdIns4*P* at low substrate concentrations (total substrate concentration = 20 μM, equal to C_{eff} = 0.23 μM). The effective surface concentration (C_{eff}) of the substrate was calculated by multiplying the mole fraction of the substrate at the surface of the micelle by the total concentration of the substrate (24). D-E. Comparison of PIP5K activities with SA-, SO- and DP-PtdIns4*P* over the wide range of substrate concentrations (C_{eff} from 0.015 to 7.91 μM).

If certain isoforms of PIP5K preferentially phosphorylated SA-PtdIns4*P*, it would indicate that this isoform is involved in the PtdIns cycle, contributing to the enrichment of phosphatidylinositols with the 1-stearoyl-2-arachidonoyl species. Kinetic analysis determined that PIP5K isoforms α and γ have a significantly lower K_m for SO-PtdIns4*P*, than for SA-PtdIns4*P*, whereas PIP5Kβ has similar K_m for both substrates (Table 6.2). The V_{max} parameter is higher for SA-PtdIns4*P* for all isoforms of PIP5K, although PIP5Kβ shows only a marginal difference (Table 6.2). As a result, the V_{max} /K_m value is the same, within error, for the three isoforms. V_{max} /K_m parameter also corresponds to the rate constant at low substrate concentration.

Table 6.2. Summary of the kinetic parameters for HA-PIP5K isoforms α, β and γ. Kinetic parameters are calculated using the effective concentration of PtdIns4*P* at the surface of the micelle. The effective surface concentration of PtdIns4*P* was determined by multiplying the mole fraction of PtdIns4*P* at the surface of the micelle by the total concentration of PtdIns4*P*. Values of V_{max} are relative values since the absolute amount of enzyme in the cell preparations is not known. Results are presented as the mean ± S.D.

Isoform	**Substrate**	**K_m, μM**	**V_{max}, pmol min^{-1}**	**V_{max}/K_m, μM^{-1}min^{-1}**
HA-PIP5K α	SA-PtdIns4*P*	16 ± 5	25 ± 5	1.5 ± 0.6
	SO-PtdIns4*P*	2.8 ± 0.9	6.3 ± 0.7	2.2 ± 0.7
HA-PIP5K β	SA-PtdIns4*P*	4.9 ± 1.4	34 ± 5	6.9 ± 2.2
	SO-PtdIns4*P*	3.7 ± 1.1	24 ± 3	6.6 ± 2.2
HA-PIP5K γ	SA-PtdIns4*P*	15 ± 4	44 ± 10	3.0 ± 1.2
	SO-PtdIns4*P*	1.6 ± 0.6	12 ± 1	7.5 ± 3.1

Together these findings indicate that all isoforms of PIP5Ks (with isoform β to a smaller extent) distinguish among different acyl chains of PtdIns4*P*. The acyl chain selectivity of the PIP5Ks is large when there is a large difference in acyl chain structure, such as DP- vs. SA- or SO-PtdIns4*P* species.

PIP5K activation by PA depends on the acyl chain composition of both substrate and activator – Previously we showed that PIP5K isoform α is sensitive to the acyl chain composition of phosphatidic acid, and that the extent of PA activation is different for SA-PtdIns4*P* and DP-PtdIns4*P* (4). To determine if all isoforms of PIP5K exhibit similar acyl chain preference for PA, we compared the activation of PIP5K isoforms α, β and γ by different species of PA (Fig. 6.2). Because acyl chain length and saturation of SA-PtdIns4*P* and DP-PtdIns4*P* differs significantly, we also tested SO-PtdIns4*P* as a substrate, as it has the same *sn*-1 acyl chain as SA-PtdIns4*P* (18:0), but a different *sn*-2 acyl chain.

Our results showed that all three isoforms of PIP5K have similar profiles of PA activation, but differ in the extent of activation, with isoform α being activated the most and isoform β activated the least with all three tested substrates (Fig. 6.2). When DP-PtdIns4*P* is used as a substrate, DAPA is undoubtedly the best activator of all PIP5Ks (Fig. 6.2G-I). Further, the extent of DAPA activation is much higher than when other substrates are used (28-, 12- and 24-fold for PIP5K isoforms α, β and γ respectively when DP-PtdIns4*P* is used as a substrate). When SA-PtdIns4*P* is used as a substrate, DLPA has a tendency to be a better activator, especially for PIP5Kα (Fig. 6.2A-C). For SO-PtdIns4*P*, the profile of PA activation is somewhat similar to that of SA-PtdIns4*P*, but there is no significant preference for DLPA over other PAs with two unsaturated acyl chains (Fig. 6.2D-F). Surprisingly, the only tested species of PA that does not activate all PIP5Ks is SOPA, and in most cases SAPA is the next least potent activator (Fig. 6.2).

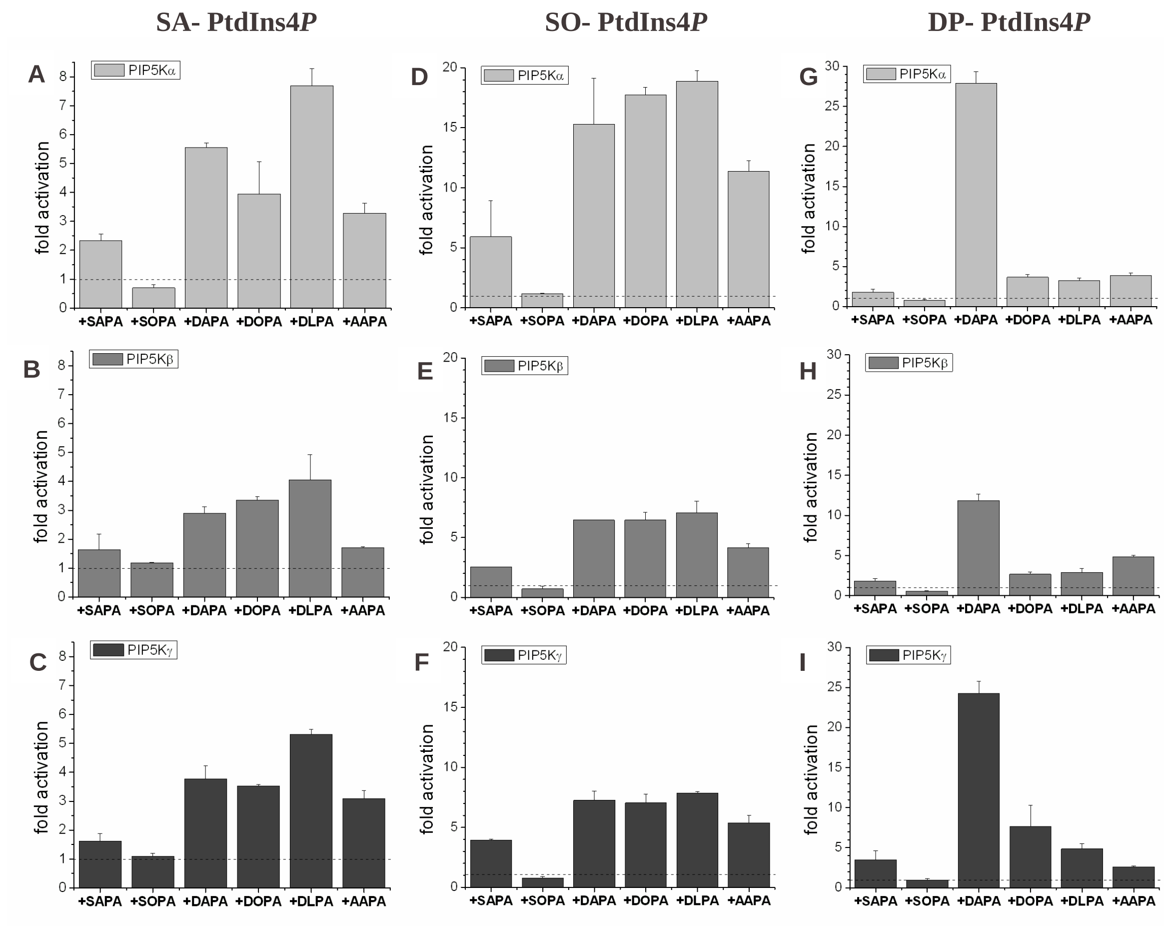

Figure 6.2. Activation of HA-PIP5K isoforms α, β and γ by different PAs with A-C) SA-PtdIns4*P*, D-F) SO-PtdIns4*P* and G-I) DP-PtdIns4*P* as substrates. PIP5K enzymatic activity was measured with 10 μM (equal to C_{eff} = 0.06 μM) PtdIns4*P* and 50 μM (equal to C_{eff} = 1.42 μM) PA.

Thus, PIP5K isoforms α, β and γ differ in the degree of PA activation, but all of them clearly discriminate between the acyl chains of both the substrate and the activator. The presence of a saturated acyl chain at the *sn*-1 position of PA considerably lowers the extent of activation. PIP5Ks have been implicated in a variety of distinct cellular processes, suggesting that different PIP5K isoform may regulate endocytosis of different types of cargo (27). Therefore, variations in the acyl chain sensitivity and degree of PA activation could be a way of commitment of different isoforms to the distinct cellular pathways.

PIP5Ks are sensitive for the acyl chain composition of substrate PtdIns – We next examined whether PIP5Ks are sensitive for the acyl chain composition of other substrates, such as phosphatidylinositol (PtdIns). First, we compared the activity of PIP5K with PtdIns4*P* and PtdIns as substrates. Our data confirm that *in vitro* PIP5Ks phosphorylate PtdIns4*P* at much higher rate than PtdIns (Fig. 6.3) (28). For PIP5Kα with SA-PtdIns as a substrate we determined the K_m parameter to be significantly higher (5-times) than for SA-PtdIns4*P* (K_m (SA-PtdIns) = 127 ± 36 μM), and respectively V_{max} to be much lower (V_{max} (SA-PtdIns) = 0.14 ± 0.01 pmol/min *versus* V_{max} (SA-PtdIns4*P*) = 25 ± 5 pmol/min).

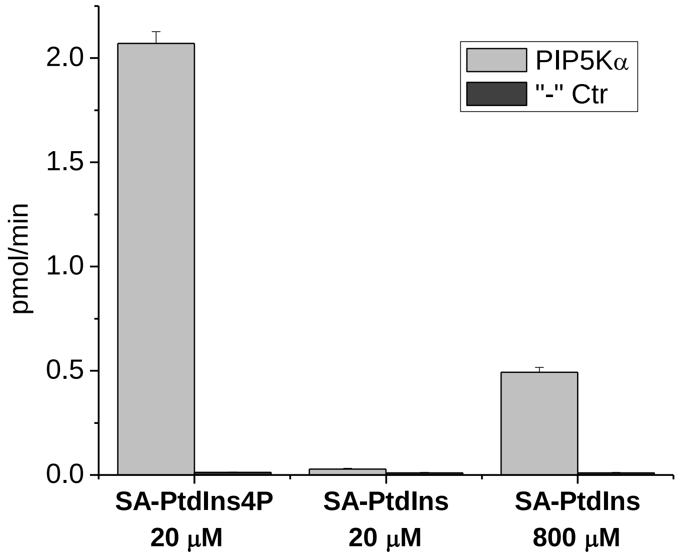

Figure 6.3. PIP5Kα has a strong preference for PtdIns4*P* as a substrate over PtdIns. PIP5K enzymatic activity was measured with either 20 μM SA- PtdIns4*P*, 20 μM SA-PtdIns (equal to C_{eff} = 0.23 μM) or 800 μM (equal to C_{eff} = 256 μM) SA-PtdIns.

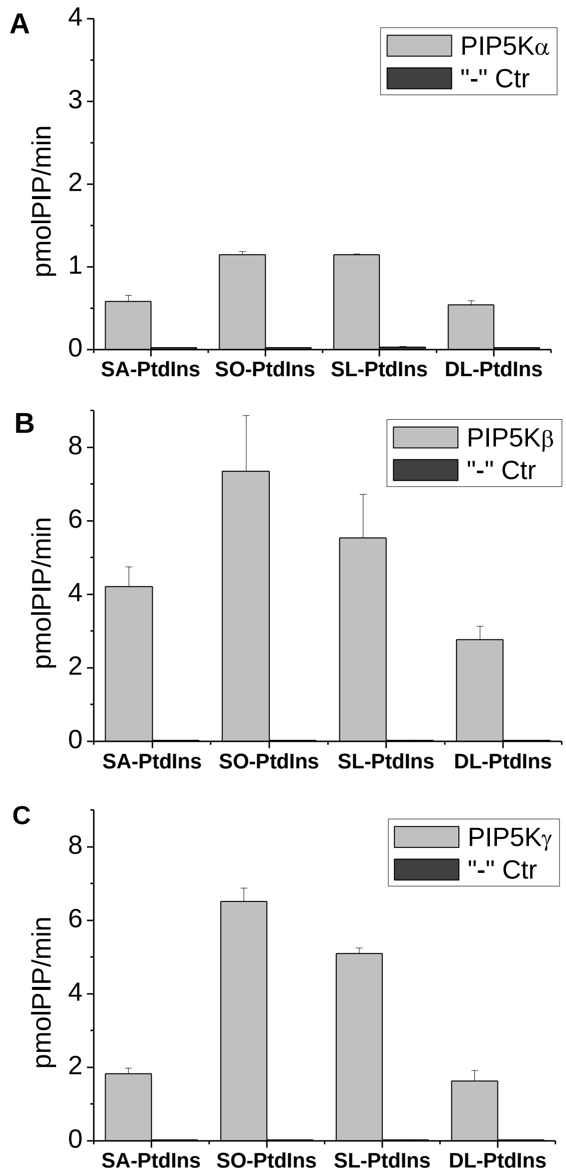

Figure 6.4. HA-PIP5K isoforms α, β and γ show sensitivity for the acyl chain composition of PtdIns substrate. PIP5K enzymatic activity was measured with 700 μM (equal to C_{eff} = 204 μM) PtdIns.

To test acyl chain preference of PIP5Ks for PtdIns, we compared their enzyme activities with four different PtdIns species – SA-, SO-, SL- and DL-PtdIns (see Table 6.1 for lipid abbreviations). The results show that all isoforms of PIP5Ks exhibit preference for SO- and SL-PtdIns, with isoform γ showing the strongest discrimination toward SO-PtdIns (Fig. 6.4). These data are in a good agreement with the acyl chain preference of PIP5K isoforms for PtdIns4*P*s at low substrate concentrations (Fig. 6.1A-C), where PIP5K isoform γ also shows the strongest preference for SO- over SA-PtdIns4*P*.

Next we examined whether PIP5Ks exhibit acyl chain preference for activator PA when different species of PtdIns are used as substrates. We used PIP5K isoform γ for these experiments, as it has the greatest acyl chain sensitivity for the tested substrates. Interestingly, our data show that there is no significant difference between the degrees of activation by four tested PA species with PtdIns as a substrate (Fig. 6.5). Further, PIP5Kγ is less activated by PAs when the more preferred substrate (SO-PtdIns) is used. It is also surprising that SOPA activates this enzyme when PtdIns is used as a substrate, in contrast to PtdIns4*P* (Fig. 6.2).

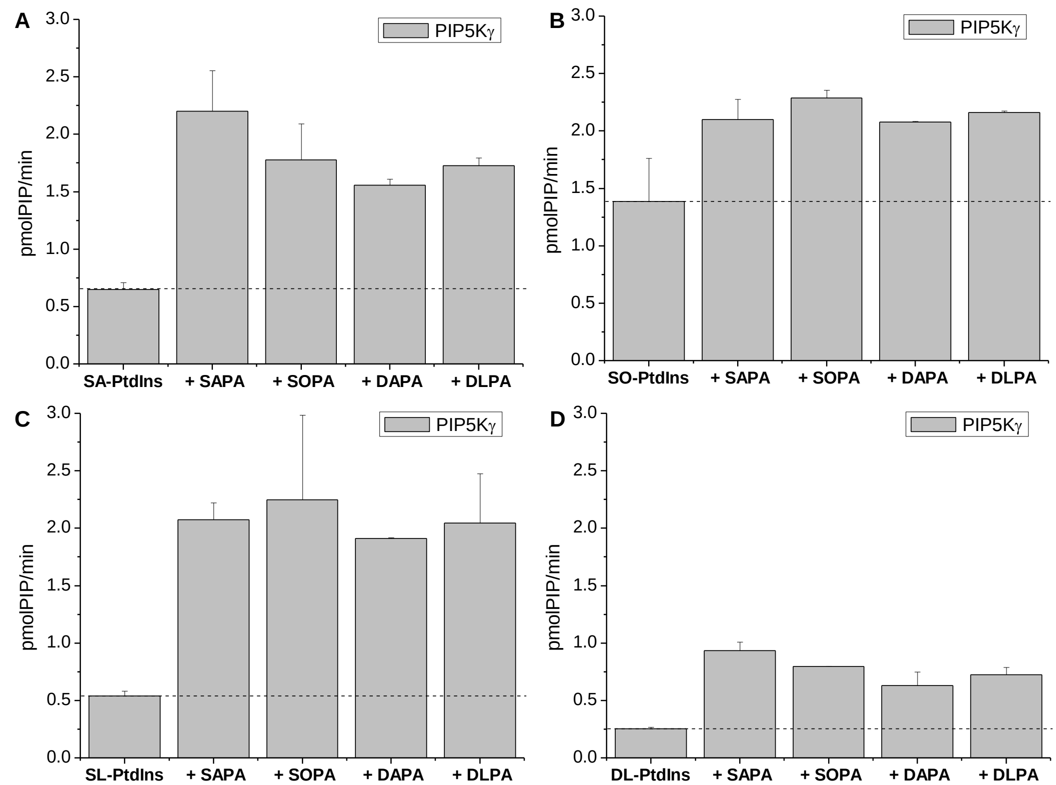

Figure 6.5. HA-PIP5Kγ does not discriminate between different acyl chains of PA when either A) SA- PtdIns, B) SO- PtdIns, C) SL- PtdIns, or D) DL- PtdIns used as a substrate. PIP5K enzymatic activity was measured with 600 μM (equal to C_{eff} = 150 μM) PtdIns and 100 μM (equal to C_{eff} = 4.1 μM) PA.

Thus, PIP5Ks display similar preference for the acyl chain composition of a substrate when either PtdIns or PtdIns4*P* is used. Nevertheless, there is a remarkable difference in that PIP5K does not show any acyl chain preference for its activator PA when PtdIns used as a substrate.

Mutants L202I and L210I of PIP5Kα increase the extent of enzyme activation by PA – Previously we demonstrated that both L202I and L210I mutations of PIP5Kα decrease the substrate affinity and the enzyme efficiency for SA-PtdIns4*P* (4). Based on the structure of PIP4KIIβ and protein homology of PIP4K and PIP5K (29, 30), residues L202 and L210 of PIP5K are located within the conserved kinase catalytic core and in the putative ATP binding site. To test if the mutations of these residues also affect PA activation of PIP5K, we compared the activation by PA of PIP5Kα WT, L202I and L210I with three substrates, SA-PtdIns4*P*, SO-PtdIns4*P* and DP-PtdIns4*P*. Both studied mutations of PIP5Kα significantly increase the extent of enzyme activation by DAPA with all three tested substrates (Fig. 6.6). However, these mutations do not change the effect of SOPA which does not activate PIP5Ks with PtdIns4*P* as a substrate. SAPA, one of the weakest PA activators with PtdIns4*P* as a substrate, shows only statistically insignificant tendency toward increased activation for the L202I and L210I mutants of PIP5Kα (Fig. 6.6). Therefore, these findings indicate that residues L202 and L210 of PIP5Kα are important for the activation of this enzyme by PA.

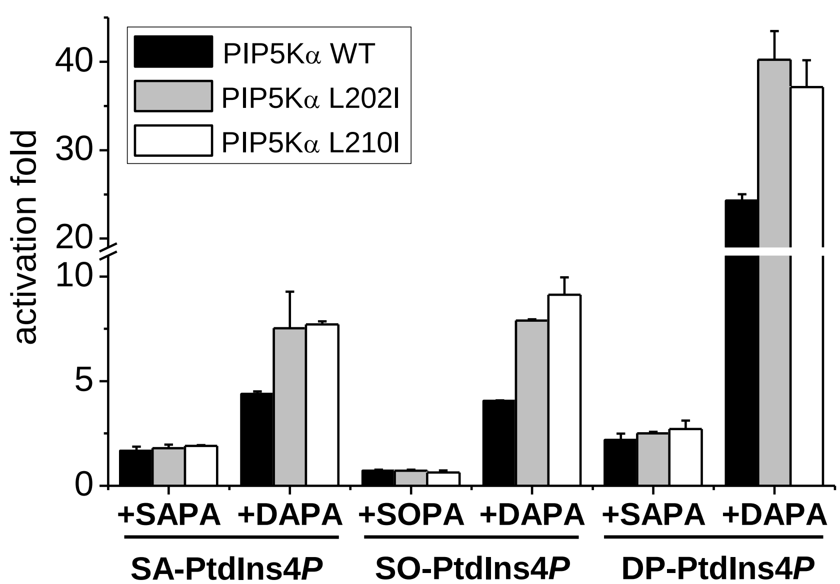

Figure 6.6. Mutations L202I and L210I of c-Myc-PIP5Kα increase enzyme activation by DAPA. PIP5K enzymatic activity was measured with 10 μM (equal to C_{eff} = 0.06 μM) PtdIns4*P* and 50 μM (equal to C_{eff} = 1.42 μM) PA.

DISCUSSION

PIP5K sensitivity for the acyl chains of substrate – The acyl chain composition of various lipid classes differs widely (31). Phosphoinositol lipids are mainly polyunsaturated, with 30–80% (depending on the cell type) of total phosphoinositides being the 1-stearoyl-2-arachidonyl species (32-35). 1-stearoyl-2-oleoyl phosphoinositols were shown to be common species as well, comprising about 11% of total phosphoinositide species in fibroblasts (32). Several lipids serve as secondary messengers, and the proteins that they interact with are greatly affected by their acyl chain composition. For example, PtdIns(4,5)P_2 plays a critical role in endocytosis in synapses, by recruiting several essential proteins to the synaptic membranes, including dynamin and the clathrin adaptor proteins (36). At later stages of endocytosis, to decrease the affinity of the clathrin adaptor proteins for the membrane of a synaptic vesicle, PtdIns(4,5)P_2 is dephosphorylated by synaptojanin-1 (37). A previous *in vitro* study showed that the catalytic domain of synaptojanin has a substrate preference for a natural PtdIns(4,5)P_2 compared with DP- PtdIns(4,5)P_2 (38). Therefore, it seems possible that the acyl chain preference of PIP5Ks may facilitate the production of PtdIns(4,5)P_2 species, required for proper downstream cascade in endocytosis.

PA activation of PIP5Ks – Activation of PIP5K by PA has been shown to be an important factor in the enzyme regulation (24, 39). Several studies demonstrated that PA generated by phospholipase D (PLD), as well as DGKα (40) and DGKζ (13) activate

PIP5K *in vivo*, in contrast to PA produced by DGKε (40). Therefore, it has been proposed that PA containing monounsaturated and di-unsaturated fatty acids activate PIP5K, as these PA species are predominantly generated by PLD (41). DGKα and ζ isoforms do not exhibit pronounced acyl chain specificity *in vitro*, phosphorylating different diacylglycerols to a similar extent (42, 43). Our findings indicate that not all monounsaturated and di-unsaturated PAs act equally on PIP5Ks. In general, for both SA- and SO-PtdIns4*P* substrates, there is a noticeable tendency for PAs with both acyl chains being unsaturated to be better activators (DAPA, DOPA, DLPA). This seems to be an important aspect of PIP5K acyl chain preference for PA, as DOPA (18:1/18:1) is a good activator of PIP5K, while SOPA (18:0/18:1), having the same lengths of both acyl chains and differing only by one double bond, does not activate the enzyme. Another example is DAPA (20:4/20:4), which is a better activator than AAPA (20:0/20:4) and SAPA (18:0/20:4).

For the physiologically more abundant substrate SA-PtdIns4*P*, DLPA (18:2/18:2) shows the strongest activation among tested PA species (Fig. 6.2A-C). Surprisingly, when DP-PtdIns4*P* is used as a substrate, DAPA becomes a very potent activator of all PIP5Ks. Taken together, these findings provide evidence that allosteric activation of the catalytic site of PIP5K by PA is acyl chain dependant.

PA is also a lipid intermediate of the PtdIns cycle. It is thus possible that different species of PA can result in the feedback activation of the PtdIns cycle. Nevertheless, none of the PIP5K isoforms result in very large feedback activation of the major species of PA in the PtdIns cycle, i.e. SAPA. However, DAPA is a good activator with all three of the substrates used and for all three of the isoforms of PIP5K (Fig. 6.2). In addition to SAPA, DAPA can also be produced efficiently by DGKε (43), the isoform of DGK that is closely associated with the PtdIns cycle (44). Thus, there can be a positive feedback activation of the PtdIns cycle by DAPA. However, it should be also noted that PA produced by DGKε *in vivo*, SAPA, does not activate PIP5K (40). SAPA will normally be the major product of DGKε catalysis. If it did activate PIP5K it would result in progressively more rapid PtdIns-cycling that could be detrimental to the cell. However, it is possible that in particular organs and/or membrane domains or under particular nutritional or pathological states, DAPA may become the major product of DGKε catalysis, leading to this feedback activation of the PtdIns-cycle.

Interestingly, PIP5K does not exhibit sensitivity for the acyl chains of PA when PtdIns is used as a substrate (Fig. 6.5). This may also have physiological relevance, as the product of PtdIns conversion by PIP5K is PtdIns5*P* and not PtdIns(4,5)P_2, which activates PLD. PLD generates PA species that are shown to activate PIP5K, therefore forming a positive feedback loop between these enzymes. In the case when PtdIns is used as a substrate, the PtdIns cycle is not completed and PLD is not activated. This result also implicates the interplay between the substrate and the activation of PIP5K.

Based on the acyl chain discrimination of PIP5Ks between four tested species of PtdIns and three PtdIns4*P* substrates, the enzyme preference for the acyl chains of the substrate does not correspond with that of PA. Thus, PIP5Ks have the lowest K_m value for SO-PtdIns4*P* (Table 6.2), and exhibit preference for SO-PtdIns among other PtdIns (Fig. 6.3), while SOPA does not activate the enzyme (Fig. 6.2). On the other hand, DLPA is one of the best activators when SA- or SO-PtdIns4*P* used as substrates, while DL-PtdIns is not among the preferred substrates (Fig. 6.5). These findings indicate that PIP5K binding sites for the substrate and PA have different conformations/ tertiary structures, allowing interaction of lipids with different acyl chains.

A previous study (24) proposed that there are two binding sites for PtdIns4*P* in murine PIP5Kβ (corresponding to human PIP5Kα), one of which inhibits the catalytic activity of the other, although it is not clear if these binding sites are located within the same enzyme or on two different subunits of a dimer. Furthermore, multiple PA binding domains were identified in the C-terminal region of PIP5K (24). Therefore when substrates with different acyl chains are compared, it is difficult to determine if differences in the degree of activation by PAs with different acyl chains is caused by the positive allosteric conformational changes in the catalytic site or negative regulation of the second inhibitory substrate binding site, or possibly both.

Role of L202 and L210 residues in PIP5K activation by PA – Previously we showed that L202I and L210I mutants of PIP5Kα affect the kinetic parameters of this enzyme for SA-PtdIns4*P* (4). Here we demonstrate that these mutations also significantly elevate PIP5Kα activation by DAPA, but not SOPA or SAPA (Fig. 6.6). PA binding sites were shown to reside within C-terminal region of PIP5Kα (residues 239–546 for murine form of enzyme). Moreover, this region also mediates interactions with the substrate through the activation and catalytic loops (29, 45). Residues L202 and L210 are located outside these domains, but within the conserved kinase catalytic core and proposed ATP binding site. In addition, these residues form part of a segment that resembles the pattern of residues (4, 46) found essential for binding arachidonic acid to lipoxygenase (47). Therefore, our results indicate that residues L202 and L210 of PIP5Kα are important for augmenting the activation of this enzyme by DAPA. This observation is consistent with this segment of the protein being involved with the phosphorylation of polyunsaturated substrates (not necessarily binding, most effect is on Vmax) (4).

PtdIns(4,5)P_2, produced by PIP5Ks, has an essential role in numerous signaling pathways, including actin cytoskeleton remodeling and endocytosis (48). PtdIns(4,5)P_2 is the precursor for the second messengers diacylglycerol and inositol triphosphate, and also acts directly to modify multiple effectors. The acyl chain composition of PtdIns(4,5)P_2 will be determined in part by the specificity for substrate and activator of PIP5K. This may be an important factor, determining the involvement of different PtdIns(4,5)P_2 species in cellular events.

Acknowledgements: We are grateful to Drs. Santos Mañes and Rosa Ana Lacalle of the Centro Nacional de Biotecnologia, Madrid, Spain, for kindly providing us with a construct to express HA-PIP5Kβ. We also acknowledge useful discussions with Dr. L.J. Marnett. This study was supported by the Natural Sciences and Engineering Research Council of Canada, grant 9848 (to R.M.E.) and from the National Institutes of Health Grant CA095463 (to M.K.T.), and NCI R01CA104708 (to R.A.A.).

REFERENCES

1. van, d. B., and Divecha, N. (2009) *J. Cell. Sci.* **122,** 3837-3850

2. Heck, J. N., Mellman, D. L., Ling, K., Sun, Y., Wagoner, M. P., Schill, N. J., and Anderson, R. A. (2007) *Crit. Rev. Biochem. Mol. Biol.* **42,** 15-39

3. Schill, N. J., and Anderson, R. A. (2009) *Biochem. J.* **422,** 473-482

4. Shulga, Y. V., Topham, M. K., and Epand, R. M. (2011) *J. Mol. Biol.* **409,** 101-112

5. Toker, A. (1998) *Curr. Opin. Cell Biol.* **10,** 254-261

6. Itoh, T., Ijuin, T., and Takenawa, T. (1998) *J. Biol. Chem.* **273,** 20292-20299

7. Ishihara, H., Shibasaki, Y., Kizuki, N., Katagiri, H., Yazaki, Y., Asano, T., and Oka, Y. (1996) *J. Biol. Chem.* **271,** 23611-23614

8. Ishihara, H., Shibasaki, Y., Kizuki, N., Wada, T., Yazaki, Y., Asano, T., and Oka, Y. (1998) *J. Biol. Chem.* **273,** 8741-8748

9. Loijens, J. C., and Anderson, R. A. (1996) *J. Biol. Chem.* **271,** 32937-32943

10. Noda, Y., Niwa, S., Homma, N., Fukuda, H., Imajo-Ohmi, S., and Hirokawa, N. (2012) *Proc. Natl. Acad. Sci. U. S. A.* **109,** 1725-1730

11. Coppolino, M. G., Dierckman, R., Loijens, J., Collins, R. F., Pouladi, M., Jongstra-Bilen, J., Schreiber, A. D., Trimble, W. S., Anderson, R., and Grinstein, S. (2002) *J. Biol. Chem.* **277,** 43849-43857

12. Doughman, R. L., Firestone, A. J., Wojtasiak, M. L., Bunce, M. W., and Anderson, R. A. (2003) *J. Biol. Chem.* **278,** 23036-23045

13. Luo, B., Prescott, S. M., and Topham, M. K. (2004) *Cell Signal.* **16(8),** 891-897

14. Rincón, E., Gharbi, S. I., Santos-Mendoza, T., and Mérida, I. (2012) *Prog. Lipid Res.* **51,** 1-10

15. Chen, M. Z., Zhu, X., Sun, H. Q., Mao, Y. S., Wei, Y., Yamamoto, M., and Yin, H. L. (2009) *J. Biol. Chem.* **284,** 23743-23753

16. Lacalle, R. A., Peregil, R. M., Albar, J. P., Merino, E., Martinez, A., Merida, I., and Manes, S. (2007) *J. Cell Biol.* **179,** 1539-1553

17. Manes, S., Fuentes, G., Peregil, R. M., Rojas, A. M., and Lacalle, R. A. (2010) *FASEB J.* **24,** 3381-3392

18. Sun, Y., Turbin, D. A., Ling, K., Thapa, N., Leung, S., Huntsman, D. G., and Anderson, R. A. (2010) *Breast Cancer Res.* **12,** R6

19. Vasudevan, L., Jeromin, A., Volpicelli-Daley, L., De Camilli, P., Holowka, D., and Baird, B. (2009) *J. Cell. Sci.* **122,** 2567-2574

20. Wieffer, M., Haucke, V., and Krauss, M. (2012) *Methods Cell Biol.* **108C,** 209-225

21. Yu, Y. L., Chou, R. H., Chen, L. T., Shyu, W. C., Hsieh, S. C., Wu, C. S., Zeng, H. J., Yeh, S. P., Yang, D. M., Hung, S. C., and Hung, M. C. (2011) *J. Biol. Chem.* **286,** 9657-9667

22. Moritz, A., De Graan, P. N., Gispen, W. H., and Wirtz, K. W. (1992) *J. Biol. Chem.* **267,** 7207-7210

23. Pettitt, T. R., Martin, A., Horton, T., Liossis, C., Lord, J. M., and Wakelam, M. J. (1997) *J. Biol. Chem.* **272,** 17354-17359

24. Jarquin-Pardo, M., Fitzpatrick, A., Galiano, F. J., First, E. A., and Davis, J. N. (2007) *J Cell Biochem.* **100(1),** 112-128

25. Ames, B. N. (1966) *Methods Enzymol* **8,** 115-118

26. Parker, G. J., Loijens, J. C., and Anderson, R. A. (1998) *Methods Mol Biol.* **105,** 127-139

27. Roth, M. G. (2004) *Physiol. Rev.* **84,** 699-730

28. Tolias, K. F., Rameh, L. E., Ishihara, H., Shibasaki, Y., Chen, J., Prestwich, G. D., Cantley, L. C., and Carpenter, C. L. (1998) *J. Biol. Chem.* **273,** 18040-18046

29. Rao, V. D., Misra, S., Boronenkov, I. V., Anderson, R. A., and Hurley, J. H. (1998) *Cell* **94,** 829-839

30. Fairn, G. D., Ogata, K., Botelho, R. J., Stahl, P. D., Anderson, R. A., De Camilli, P., Meyer, T., Wodak, S., and Grinstein, S. (2009) *J. Cell Biol.* **187,** 701-714

31. Hicks, A. M., DeLong, C. J., Thomas, M. J., Samuel, M., and Cui, Z. (2006) *Biochim. Biophys. Acta.* **1761,** 1022-1029

32. Pessin, M. S., and Raben, D. M. (1989) *J Biol Chem* **264,** 8729-8738

33. Pettitt, T. R., and Wakelam, M. J. (1993) *Biochem. J.* **289 (2),** 487-495

34. Holbrook, P. G., Pannell, L. K., Murata, Y., and Daly, J. W. (1992) *J. Biol. Chem.* **267,** 16834-16840

35. Lee, C., Fisher, S. K., Agranoff, B. W., and Hajra, A. K. (1991) *J. Biol. Chem.* **266,** 22837-22846

36. Haucke, V. (2005) *Biochem. Soc. Trans.* **33(Pt 6),** 1285-1289

37. Wenk, M. R., and De Camilli, P. (2004) *Proc.Natl.Acad.Sci (USA)* **101,** 8262-8269

38. Schmid, A. C., Wise, H. M., Mitchell, C. A., Nussbaum, R., and Woscholski, R. (2004) *FEBS Lett.* **576,** 9-13

39. Jenkins, G. H., Fisette, P. L., and Anderson, R. A. (1994) *J. Biol. Chem.* **269,** 11547-11554

40. Jones, D. R., Sanjuan, M. A., and Merida, I. (2000) *FEBS Lett.* **476,** 160-165

41. Pettitt, T. R., McDermott, M., Saqib, K. M., Shimwell, N., and Wakelam, M. J. (2001) *Biochem. J.* **360,** 707-715

42. Epand, R. M., Kam, A., Bridgelal, N., Saiga, A., and Topham, M. K. (2004) *Biochemistry* **43,** 14778-14783

43. Shulga, Y. V., Topham, M. K., and Epand, R. M. (2011) *FEBS Lett.* **585,** 4025-4028

44. Shulga, Y. V., Topham, M. K., and Epand, R. M. (2011) *Chem. Rev.* **111(10),** 6186-6208

45. Kunz, J., Fuelling, A., Kolbe, L., and Anderson, R. A. (2002) *J. Biol. Chem.* **277,** 5611-5619

46. Richard M., E. (2012) *Biochim. Biophys. Acta.* **1818,** 957-962

47. Neau, D. B., Gilbert, N. C., Bartlett, S. G., Boeglin, W., Brash, A. R., and Newcomer, M. E. (2009) *Biochemistry* **48(33),** 7906-7915

48. Czech, M. P., (2000) *Cell* **100,** 603-606

CHAPTER SEVEN

DIACYLGLYCEROL KINASE EXPRESSION IN ADIPOCYTES

Abbreviations: AGPAT2, *sn*-1-acylglycerol-3-phosphate acyltransferase 2; BAT, brown adipose tissue; DAG, diacylglycerol; DGK, diacylglycerol kinase; GPAT3, glycerol-3-phosphate acyltransferase 3; IRS-1, insulin receptor substrate 1; LPtdOH, lysophosphatidic acid; PKC, protein kinase C; PPARγ2, peroxisome proliferator-activated receptor γ2; Pref-1, pre-adipocyte factor-1; PtdOH, phosphatidic acid; Rps29, 40S ribosomal protein S29; TBP, TATA-box binding protein; WAT, white adipose tissue.

ABSTRACT

Type 2 diabetes mellitus is a progressive metabolic disorder with the increase rates characterized as an epidemic, and it is expected to afflict around 439 million people worldwide by 2030. Type 2 diabetes is characterised by hyperglycaemia, altered lipid metabolism and impaired insulin action in peripheral tissues. We identified a difference in the mRNA expression levels of several diacylglycerol kinase (DGK) isoforms in adipocytes isolated from KK/A^y diabetic mice in comparison with control mice. We also showed that seven isoforms of DGKs are expressed in 3T3-L1 cells, and that DGK expression levels change significantly during differentiation of 3T3-L1 preadipocytes into adipocytes. Particularly the delta and epsilon isoforms of DGK showed 8- and 4-fold increase respectively. Therefore, we reveal previously unrecognized changes of DGKs in adipocyte differentiation, as well as a possible contribution to type 2 diabetes.

INTRODUCTION

Diacylglycerol kinases (DGK) catalyze the phosphorylation of diacylglycerol (DAG) to phosphatidic acid (PtdOH), thus terminating the DAG signal and producing the PtdOH signal in the cell. Up to date, ten mammalian DGK isoforms have been identified and shown to fulfill distinct roles in the cellular processes.[1] DAG plays multiple roles as a second messenger in cellular signaling, and also in lipid metabolism as a precursor of phospholipids and triglycerides. An increase in intracellular DAG content is associated with insulin resistance induced by glucose infusion in muscle and liver of rats.[2] These elevated levels of intracellular DAG activate protein kinase C (PKC), which phosphorylates the insulin receptor and insulin receptor substrate 1 (IRS-1), leading to subsequent downregulation of glucose transport.[3] These events in turn cause insulin resistance, abnormal lipid accumulation and altered cellular signal transduction.[4, 5]

DGK isoform δ was identified to contribute to hyperglycemia-induced peripheral insulin resistance, thus aggravating the severity of type 2 diabetes.[6] Here we demonstrated that the mRNA expression of several other isoforms of DGK is altered in adipocytes isolated from diabetic mice. Therefore, it is possible that not only DGKδ, but other DGK isoforms could be contributing to the insulin resistance in adipocytes.

Adipocytes are specialized in storing energy in the form of triacylglycerides during periods of energy excess, and releasing this energy during periods of energy deprivation. The key intermediates for triglyceride and phospholipid synthesis are the enzymes glycerol-3-phosphate acyltransferase 3 (GPAT3), *sn*-1-acylglycerol-3-phosphate acyltransferase 2 (AGPAT2) and lipin 1, catalysing the conversion of glycerol 3-

phosphate into lysophosphatidic acid (LPtdOH), LPtdOH into PtdOH, and PtdOH into DAG, respectively. In the developing adipocyte, lipogenesis and adipogenic transcription are tightly regulated. Thus, a loss of GPAT3 or AGPAT2 expression inhibits adipogenic gene expression at an early stage.[7, 8] Lipin 1 can also activate PPARγ during adipogenesis[9] and regulate adipogenic transcription.[10]

DGKs are also involved in phospholipid synthesis by converting DAG to PtdOH. According to expressed sequence tags (ESTs) database from the National Center for Biotechnology Information, which approximates the levels of DGK mRNA in a given tissue, DGKε is the only isoform identified in adipose tissue. Here we tested the mRNA expression of DGK isoforms in adipocytes isolated from mouse white adipose tissue, as well as in differentiating 3T3-L1 cells, and we showed that at least seven DGK isoforms are expressed in adipocytes. Moreover, the expression profile of several DGK isoforms changes significantly during adipocyte differentiation, indicating their possible involvement in adipogenesis.

EXPERIMENTAL PROCEDURES

Differentiation of 3T3-L1 cells. 3T3-L1 pre-adipocytes were cultured in DMEM, 10% calf serum and 1% penicillin/streptomycin. For adipogenesis, 2 days after cells reached 100% confluency (day 0) they were treated with 3T3-L1 Differentiation Medium (Zen-bio). The medium was replaced with Adipocyte Maintaining Medium (Zen-bio) at day 3 post differentiation. 3T3-L1 pre-adipocytes were only differentiated and used prior to passage 10; greater than 90% of cells displayed the fully differentiated phenotype, characterized by lipid accumulation, by day 12 post differentiation. Lipid accumulation in adipocytes was visualized by staining with Oil Red-O.[11]

Animals. KK-A^y mice (heterozygous for A^y, background strain KK/Upj) and normal wild-type non-agouti (a/a homozygous) mice were obtained from The Jackson Laboratory (Bar Harbor, ME) at 8 weeks old. All mice used in the study were males, housed in pathogen–free micro-isolators and maintained on a 12-hour light/12-hour dark cycle with lights on at 7:00 A.M. Mice were given standard rodent chow and *water ad libitum*. Experimental procedures on mice used in this study were approved by the McMaster University Animal Ethics Committees. At 14 weeks old mice were fasted overnight, and blood glucose concentration was assessed with a glucometer on whole blood sampled from the tail vein. Mice were anesthetized by intraperitoneal injection with ketamine (150 mg/kg) and xylazine (10 mg/kg), and tissues were rapidly collected and stored in RNA*later*® solution (Life Technologies) at -20°C until RNA isolation.

Adipocyte isolation from epididymal white adipose tissue depot. Epididymal fat pads were minced and digested for 35 minutes at 37°C with type I collagenase (1 mg/ml; Worthington) in Adipocyte Wash buffer (120 mM NaCl, 4 mM KH_2PO_4, 1 mM $MgSO_4$, 1 mM $CaCl_2$, 10 mM $NaHCO_3$, 500 nM adenosine, 30 mM HEPES, 1.5% BSA, pH 7.4). The cell suspension was filtered through 250 μm nylon mesh and centrifuged at 190 x *g* for 10 minutes to separate floating adipocytes from the stromal-vascular fraction (SVF). The top layer of adipocytes was collected and washed 5 times with Adipocyte Wash buffer. After final wash, adipocytes were transferred to a T25 flask filled completely with DMEM/F12. The flask was placed bottom side down and incubated 2 hours at 37°C, 5%

CO_2, to allow the non-adipocyte cells to sediment and attach to the bottom. After incubation, all medium containing adipocytes was transferred to a new 50 ml tube and centrifuged at 190 x g for 5 min. The supernatant beneath the adipocyte layer was removed, and 0.75 mL of TRIzol LS Reagent (Invitrogen) was added per 0.25 mL of adipocytes for the following RNA isolation. The SVF pellet was incubated with Erythrocyte Lysis Buffer (154 mM NH_4Cl, 10 mM $KHCO_3$, 0.1 mM EDTA) for 5 min and filtered through a 20 μm mesh to remove endothelial cell clumps. The solution was centrifuged at 500 x g for 5 min, and the resultant SVF pellet was resuspended in TRIzol LS Reagent (Invitrogen) for the following RNA isolation. Adipogenesis markers and markers for pre-adipocytes and macrophages were used to confirm the purity of isolated adipocytes (Fig. 7.1).

Total RNA isolation. Total RNA was isolated from 3T3-L1 cells at day 0, 7 and 12 post differentiation using TRIzol reagent with the PureLink™ RNA Mini Kit (Invitrogen) according to the manufacturer's manual. For RNA preparation from isolated adipocytes and SVF, TRIzol LS Reagent (Invitrogen) was used. For RNA isolation from murine tissues, the tissues were homogenized with 1 mm zirconia/silica beads in 1 ml of TRIzol reagent using the Mini-Beadbeater-1 (Bio Spec Products). On–column PureLink™ DNase treatment (Invitrogen) was performed during RNA purification of all samples to obtain DNA–free total RNA.

Real-time RT-PCR. Total RNA was reverse-transcribed using AccuScript PfuUltra II RT-PCR Kit (Agilent Technologies) and analyzed via real time PCR on the Rotorgene 6000 (Corbett Research) using TaqMan Assay-on-Demand gene expression kits (Applied

Biosystems) following the manufacturer's recommendations. qPCR was performed in a 20 μl reaction volume containing 0.5 U of AmpliTaq Gold DNA polymerase (Applied Biosystems, Foster City, CA, USA), 1×PCR Gold buffer, 2.5 mM $MgCl_2$, 0.2 mM dNTP mix, 10 μl of diluted cDNA, 450 nM of primers and 125 nM of TaqMan MGB probes (Applied Biosystems, Foster City, CA, USA). After an initial step for enzyme activation at 95°C for 10 min, 50 cycles were performed consisting of 95°C for 10 sec and 58°C for 45 sec. Relative expression was calculated using the comparative critical threshold (C_t) method[12, 13] and was normalized to TATA-box binding protein.

In order to use the $\Delta\Delta C_t$ method for comparison of mRNA expression levels of different targets, the efficiency of the amplification of these targets must be approximately equal.[13, 14] Therefore, we chose to use TaqMan Gene Expression Assays, because the amplification efficiencies of all TaqMan Gene Expression Assays are indicated to be equivalent to any other target assay.[15] According to the manufacturer, the design parameters have been tested extensively and the resulting assays have 100% efficiency (+/-10%) when measured over a 6-log dilution range, in samples that are free of PCR inhibitors.[15] Therefore, it has been suggested that it is not necessary to measure efficiency when using TaqMan Gene Expression Assays. Nevertheless, we tested the amplification efficiencies of five used TaqMan Gene Expression Assays, and showed that those assays have the efficiencies ranging from 0.91 to 1.12 (Fig. S7.1).

RESULTS AND DISCUSSION

DGK mRNA expression profile during adipocyte differentiation of 3T3-L1 cells. To determine if DGK mRNA expression changes during adipocyte differentiation, we performed real-time RT-PCR on RNA samples isolated from 3T3-L1 cells at day 0, 7 and 12 post differentiation. The 3T3-L1 cell line is one of the most reliable and well-characterized models for studying the adipocyte differentiation.[16] In culture, differentiated 3T3-L1 cells exhibit most of the ultrastructural characteristics of adipocytes from animal tissue,[17] and when injected into mice, 3T3-L1 cells differentiate and form subcutaneous fat pads that are indistinguishable from normal adipose tissue.[18]

Differentiation of 3T3-L1 cells into adipocytes was confirmed by Oil Red O staining of accumulated lipid droplets (Fig. 7.2, right panel), as well as by measuring the expression levels of the adipogenesis markers, such as adiponectin and peroxisome proliferator-activated receptor γ2 (PPARγ2) (Fig. 7.1, right panel).

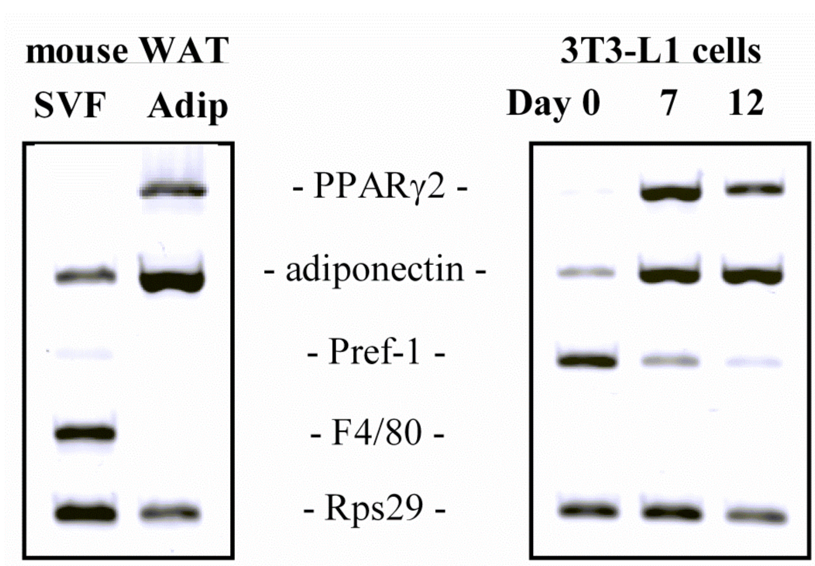

Figure 7.1. Expression of markers in 3T3-L1 cells during adipocyte differentiation (right panel) and in isolated adipocytes (Adip) and stromal-vascular

fraction (SVF) from mouse epididymal white adipose tissue (WAT) depot (left panel). Peroxisome proliferator-activated receptor γ2 (PPARγ2) and adiponectin are used as markers of adipogenesis. Pre-adipocyte factor-1 (pref-1) is used as a pre-adipocyte marker, as it exerts negative control of adipogenesis.[19] The mouse macrophage F4/80 receptor (F4/80) is used as a specific cell-surface marker for murine macrophages.[20] 40S ribosomal protein S29 (Rps29), a house-keeping gene, is used as a reference gene.

Our results showed that seven DGK isoforms are expressed in 3T3-L1 cells – all except DGKβ, γ, and κ, whose mRNA expression was below detectable levels (Fig. 7.2).

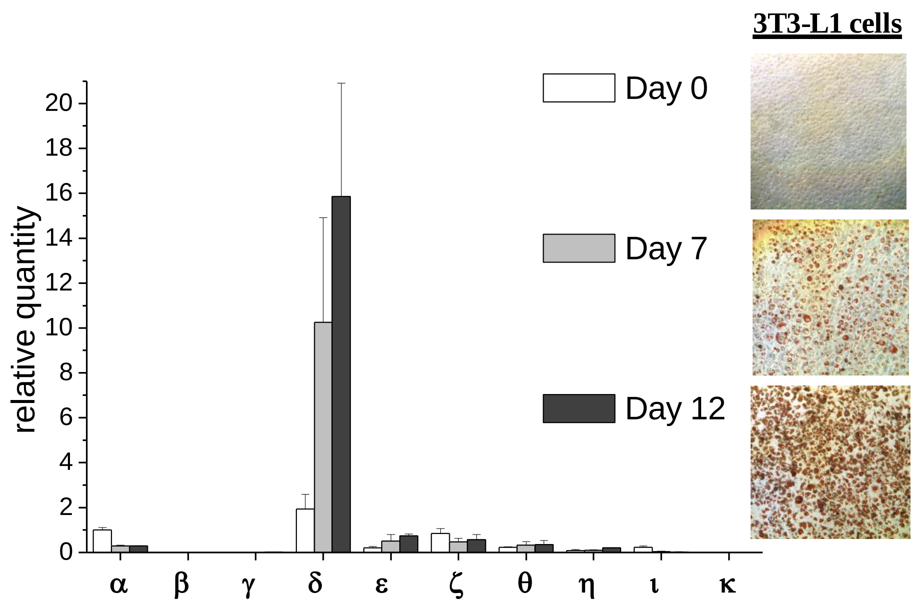

Figure 7.2. mRNA expression of DGK isoforms in 3T3-L1 cells during differentiation into adipocytes. White bars represent expression levels at day 0 post differentiation, light grey bars – at day 7, and black bars – at day 12 post differentiation. DGK expression is normalized for TBP and presented as the quantity relative to the expression of DGK isoform α at day 0 post differentiation. Normalization for another house-keeping gene Rps29 showed similar results. Results are presented as the mean ± S.D. Panel on the right shows the staining of 3T3-L1 cells with Oil Red O at days 0, 7 and 12 post differentiation.

DGKδ exhibits the highest mRNA expression among other DGK isoforms in 3T3-L1 pre-adipocytes, and its expression level increases dramatically during adipocyte differentiation (8-fold increase at day 12 compared to day 0 post differentiation) (Fig. 7.2 and 7.3). Expression of two other DGK isoforms, DGKε and DGKη, also increases during differentiation of 3T3-L1 cells, while the expression levels of DGKα and DGKι decrease significantly (Fig. 7.3). DGKζ and DGKθ do not change during adipocyte differentiation.

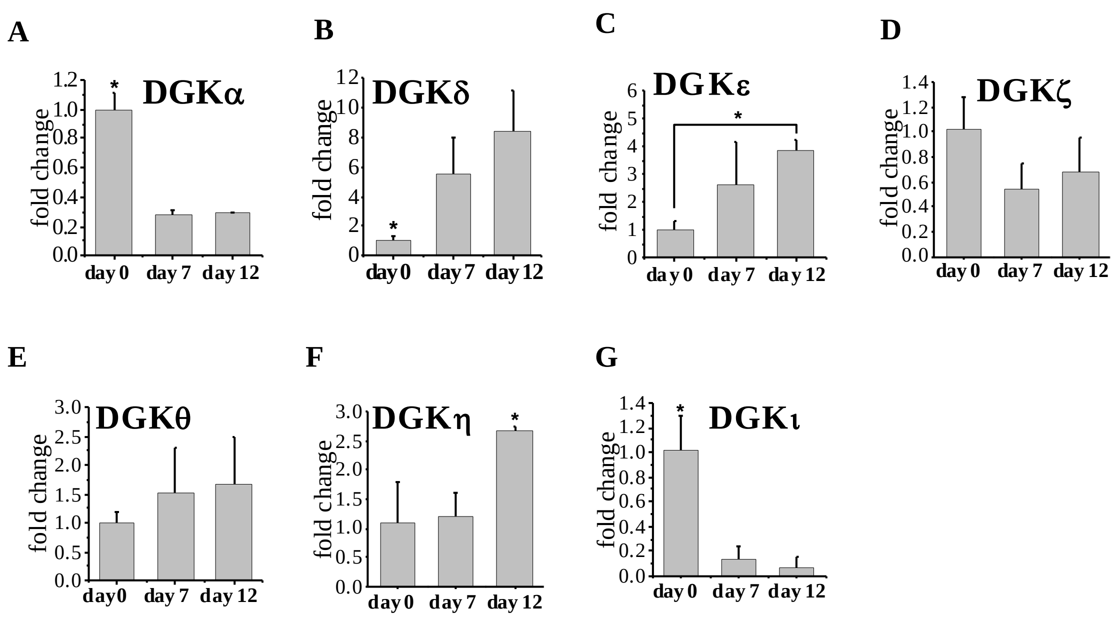

Figure 7.3. mRNA expression of DGK isoforms A) α, B) δ, C) ε, D) ζ, E) θ, F) η, G) ι in 3T3-L1 cells during adipocyte differentiation. Data are presented as a fold change relative to the expression level of each DGK at day 0 post differentiation. Results are presented as the mean ± S.D. * - values are statistically different with $p < 0.05$.

Lipid amount and composition in 3T3-L1 cells changes dramatically with accumulation of lipid droplets within the cells and their transformation into adipocytes. Therefore, it would be expected that the expression levels of many lipid metabolizing enzymes, including DGKs, increase during adipocyte differentiation. Nevertheless, our results show that it is not the case for all isoforms of DGK, and that each DGK isoform exhibits a unique behavior during differentiation of 3T3-L1 cells (Fig. 7.3). These data support the idea that each DGK has isoform-specific functions and plays an individual role in adipocyte differentiation. The DGK substrate, diacylglycerol, is a precursor for triglycerides, and it also stimulates the formation of lipid droplets. Thus, in the absence of activated DGK, more diacylglycerol can be converted to triglycerides and form lipid droplets. Further study is required to investigate specific involvement of DGK isoforms in this process. Adipocyte dysfunction contributes substantially to human metabolic diseases, such as obesity; therefore it is of major importance to understand the mechanism of adipogenesis.[21]

DGK mRNA expression in type 2 diabetes. To determine if DGK mRNA expression is affected in type 2 diabetes, we compared DGK mRNA expression in adipocytes isolated from epididymal WAT of KK/A^y mice in comparison with control mice. KK/A^y mice (strain KK/Upj-A^y/J, available from Jackson Laboratory, USA) serve as a good model for type 2 diabetes and obesity and are used widely for screening different classes of antidiabetic agents.[22-25] KK/A^y mice develop severe obesity, hyperglycaemia, hyperinsulinaemia, and glucose intolerance.[26, 27] Insulin sensitivity becomes impaired at 10 weeks and by 16 weeks of age these mice are completely insulin resistant.[28]

At 14 weeks old KK/A^y mice showed increased body weight by 18% (Fig. 7.4A), increased epididymal WAT depot weight by 100% and liver weight by 60% (Fig. 7.4C) in comparison with control mice. Fasting glucose levels were elevated by 76% (Fig. 7.4B).

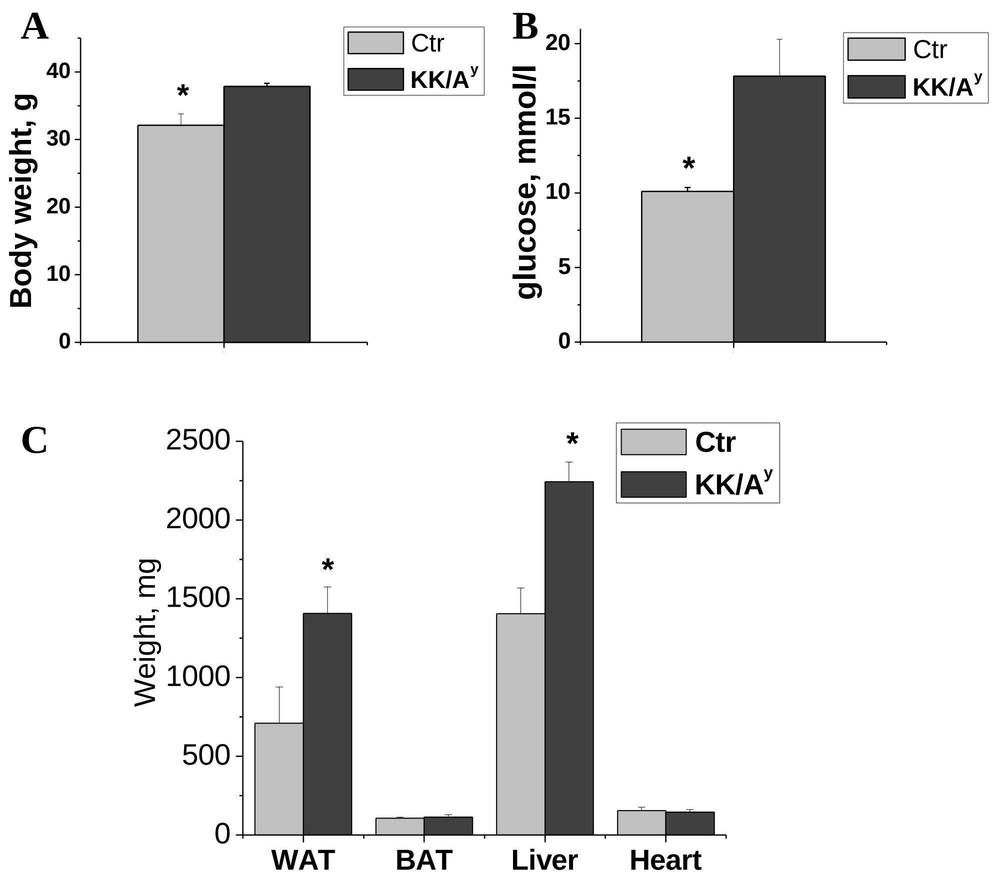

Figure 7.4. Characterization of KK/A^y mice in comparison with normal wild-type non-agouti mice from the colony (Ctr). Comparison of A) mouse body weight, B) fasting glucose levels, C) organ and tissue depot weights. Results are presented as the mean ± S.D. * - values are statistically different with $p < 0.05$.

Adipocytes isolated from epididymal WAT of diabetic KK/A^y mice at age of 14 weeks showed a significantly altered profile of DGK mRNA expression in comparison with control mice (Fig. 7.5). Murine isolated adipocytes exhibit a profile of DGK mRNA expression similar to differentiated 3T3-L1 cells, with DGKδ being the most abundant isoform. Nevertheless, in adipocytes from diabetic mice, DGKδ mRNA expression is considerably decreased (about 2-fold) (Fig. 7.5).

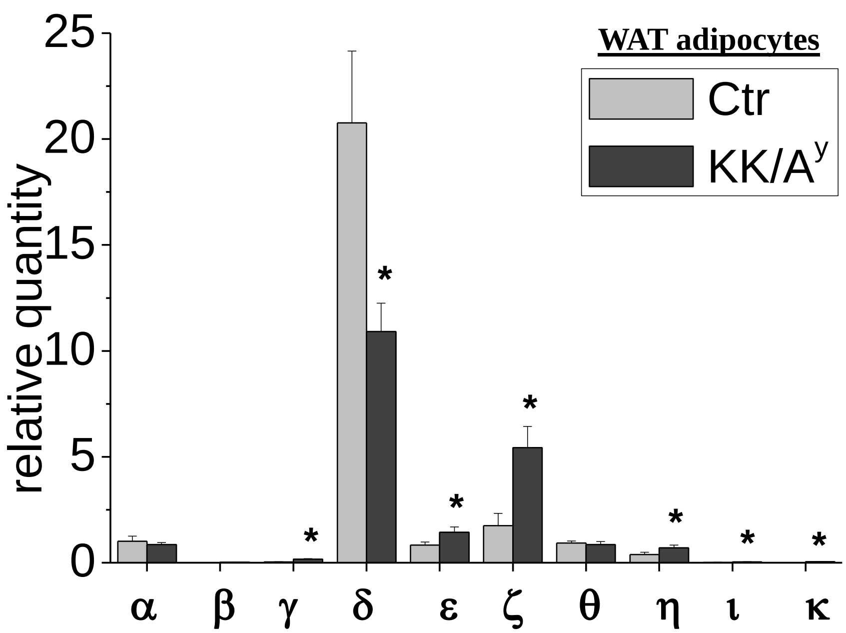

Figure 7.5. mRNA expression of DGK isoforms in adipocytes isolated from epididymal WAT of diabetic KK/A^y mice (N=4) in comparison with control mice (N=3). DGK expression is normalized for TBP and presented as the quantity relative to the expression of DGK isoform α in control mice. Normalization for other house-keeping genes (β-actin and Rps29) showed similar results. Results are presented as the mean ± S.D. * - values are statistically different with $p < 0.05$.

In contrast, several other isoforms, DGK γ, ε, ζ and η, showed elevated mRNA expression in adipocytes from diabetic mice in comparison with control mice. DGK isoforms ι and κ were below detectable level in adipocytes from control mice, but could be detected in adipocytes from diabetic mice.

DGK mRNA expression in stromal-vascular fraction isolated from epididymal WAT does not show any statistically significant difference between diabetic KK/A^y mice and control mice (data are not shown).

To assess if DGK mRNA expression is altered in other adipocyte depots in diabetic mice, we compared DGK mRNA expression profiles in brown adipose tissue (BAT) from KK/A^y and control mice (Fig. 7.6).

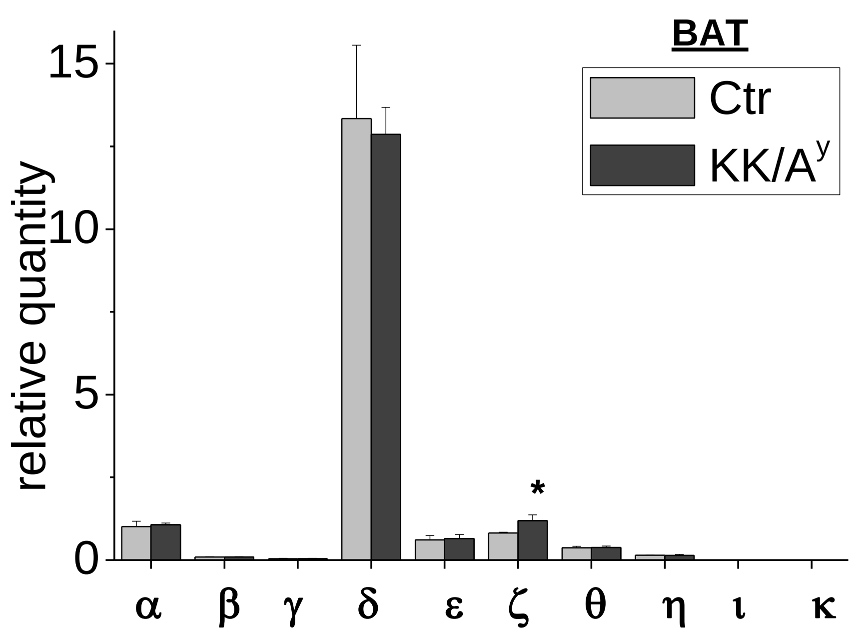

Figure 7.6. mRNA expression of DGK isoforms in brown adipose tissue (BAT) of diabetic KK/A^y mice (N=4) in comparison with control mice (N=3). DGK expression is normalized for TBP and presented as the quantity relative to the expression of DGK isoform α in control mice. Results are presented as the mean ± S.D. * - values are statistically different with $p < 0.05$.

Our results showed that DGKζ expression level is slightly increased in BAT from diabetic animals, while expression of all other DGK isoforms is not changed.

DGK mRNA expression profiles in murine tissues and organs. Further we tested the mRNA expression of DGKs in several other tissues, including liver, heart and gastrocnemius muscle. Our data showed no statistically significant differences between diabetic KK/A^y mice and control mice in these tissues (data are not shown). Nevertheless, these data demonstrated that DGK isoforms have different profiles in different tissues, such as liver, heart, white adipose tissue (WAT), brown adipose tissue (BAT), and gastrocnemius muscle (Fig. 7.7). Our results revealed that DGKδ is the most abundant isoform in murine WAT, BAT and heart tissues, while in muscle DGKδ and ζ have comparable levels, and in liver tissue DGKζ and θ are more prevalent.

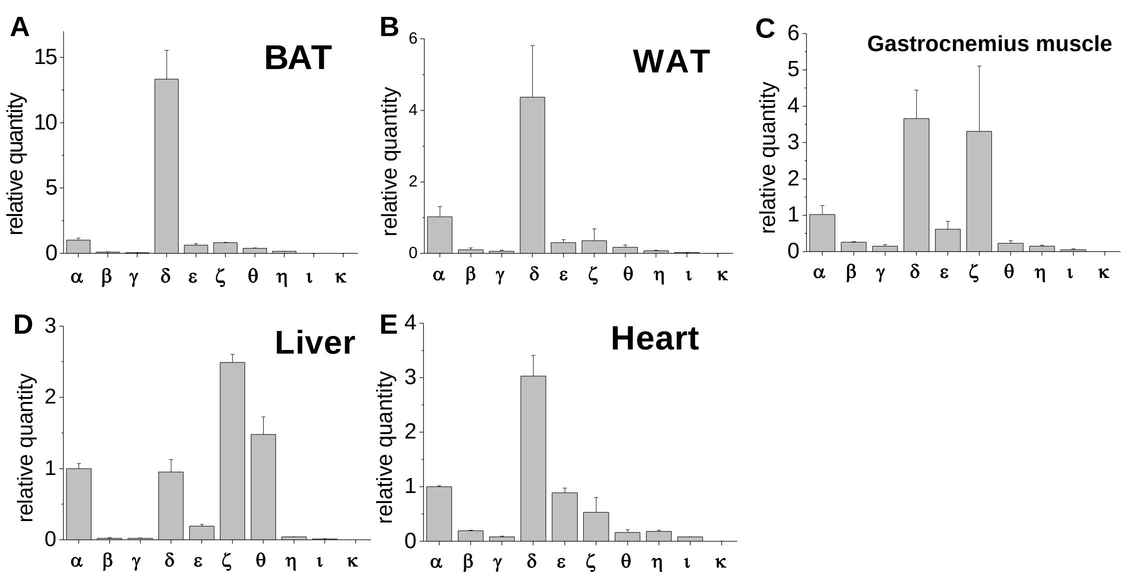

Figure 7.7. mRNA expression of DGK isoforms in A) brown adipose tissue (BAT), B) white adipose tissue (WAT), C) gastrocnemius muscle, D) liver, and E) heart of normal wild-type non-agouti mice. DGK expression is normalized for TBP and presented as the quantity relative to the expression of DGK isoform α in control mice. Results are presented as the mean ± S.D.

These findings demonstrate the diversity of DGK family and further suggest the individual tissue- and isoform-specific functions for each DGK.

The involvement of DGK isoform δ in type 2 diabetes was demonstrated previously by Chibalin et al.[6] It was found that reduced DGKδ protein expression in haploinsufficient DGKδ (DGKδ+/-) mice contributes to the development of obesity and peripheral insulin resistance. Further, in type 2 diabetic patients and diabetic rats, DGKδ protein expression in skeletal muscle and total DGK activity was reduced and normalized upon correction of hyperglycemia. Therefore, it was suggested that DGKδ undergoes downregulation caused by the altered metabolic environment. The decrease in whole-body insulin-mediated glucose uptake in DGKδ+/- mice may be caused by accumulation of DAG, which in turn elevates PKC activity and serine phosphorylation of IRS-1, leading to peripheral insulin resistance.[6]

We found that the adipocytes of diabetic mice not only demonstrate decreased mRNA expression of DGKδ, but also the elevated expression levels of several other DGK isoforms, particularly ζ, ε and η (Fig. 7.5). The increased expression of these DGKs do not compensate for the loss of DGKδ function, since KK/A^y mice show hyperglycemia, mild obesity and other signs of diabetes. Therefore, the altered mRNA expression of these DGK isoforms is likely due to the impaired regulation of metabolism in diabetic animals.

DGK isoforms regulate the balance between their substrate DAG and product PtdOH by terminating DAG signals and producing PtdOH signals.[1, 29] DAG was implicated in the development of insulin resistance, since DAG levels were shown to be elevated in skeletal muscle from insulin-resistant rodents and humans.[2, 4] Therefore, through regulation of DAG signal, DGK isoforms may play an important role in insulin signaling.

Taken together, our findings indicate the importance of DGK function in adipocyte differentiation and proper insulin signaling in these cells.

Acknowledgments. I would like to thank Morgan Fullerton for the help with euthanizing mice and excising murine tissues.

SUPPLEMENTARY INFORMATION

A

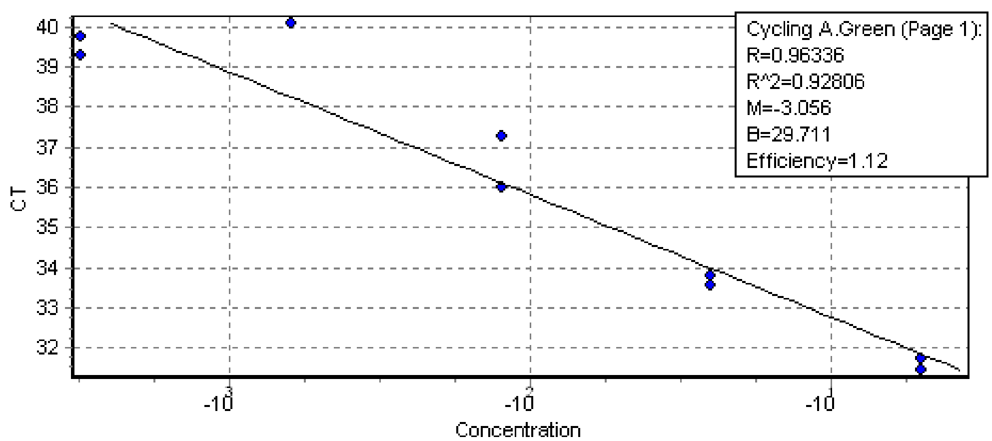

B

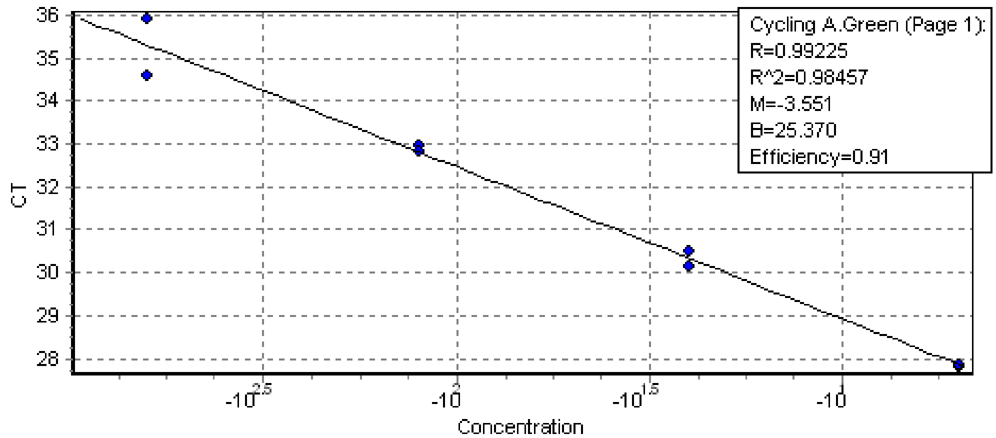
Cycling A.Green (Page 1):
R=0.99225
R^2=0.98457
M=-3.551
B=25.370
Efficiency=0.91
CT
Concentration

C

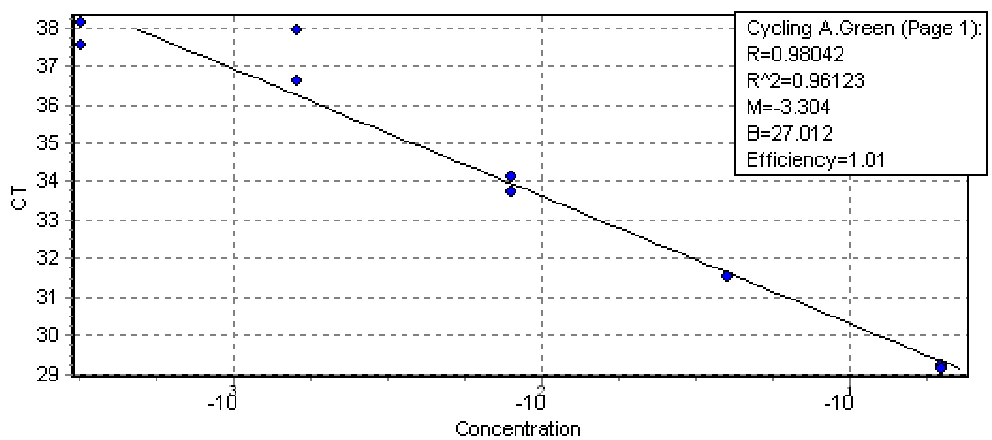
Cycling A.Green (Page 1):
R=0.98042
R^2=0.96123
M=-3.304
B=27.012
Efficiency=1.01
CT
Concentration

D

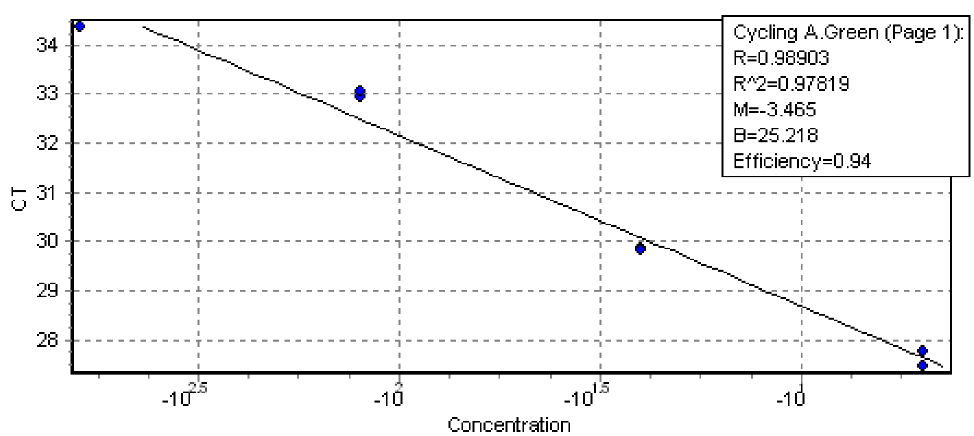
Cycling A.Green (Page 1):
R=0.98903
R^2=0.97819
M=-3.465
B=25.218
Efficiency=0.94
CT
Concentration

E

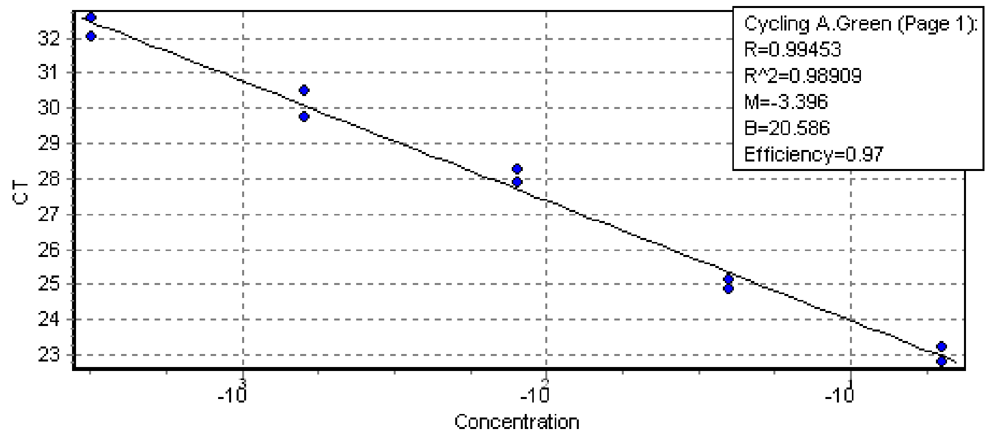

Figure S7.1. Measured amplification efficiencies of TaqMan Gene Expression Assays for the following targets: A) DGKα, B) DGKγ, C) DGKδ, D) DGKε and E) DGKζ. cDNA was reverse-transcribed from mouse whole brain total RNA and used as a template in all reactions, since brain tissue are known to express all isoforms of DGK. Reactions were run in duplicates. 5 series of dilutions were used ranging from 1/5 to 1/3125 of the original cDNA sample.

REFERENCES

1. Shulga, Y. V., Topham, M. K. & Epand, R. M. Regulation and Functions of Diacylglycerol Kinases. *Chem. Rev.* **111(10)**, 6186-6208 (2011).

2. Kraegen, E. W. *et al*. Increased malonyl-CoA and diacylglycerol content and reduced AMPK activity accompany insulin resistance induced by glucose infusion in muscle and liver of rats. *Am. J. Physiol. Endocrinol. Metab.* **290**, E471-9 (2006).

3. Yu, C. *et al*. Mechanism by Which Fatty Acids Inhibit Insulin Activation of Insulin Receptor Substrate-1 (IRS-1)-associated Phosphatidylinositol 3-Kinase Activity in Muscle. *J. Biol. Chem.* **277**, 50230-50236 (2002).

4. Itani, S. I., Ruderman, N. B., Schmieder, F. & Boden, G. Lipid-induced insulin resistance in human muscle is associated with changes in diacylglycerol, protein kinase C, and IkappaB-α. *Diabetes* **51**, 2005-2011 (2002).

5. Montell, E. *et al*. DAG accumulation from saturated fatty acids desensitizes insulin stimulation of glucose uptake in muscle cells. *American Journal of Physiology - Endocrinology And Metabolism* **280**, E229-E237 (2001).

6. Chibalin, A. V. *et al*. Downregulation of Diacylglycerol Kinase Delta Contributes to Hyperglycemia-Induced Insulin Resistance. *Cell* **132**, 375-386 (2008).

7. Gale, S. E. *et al*. A Regulatory Role for 1-Acylglycerol-3-phosphate-O-acyltransferase 2 in Adipocyte Differentiation. *J. Biol. Chem.* **281**, 11082-11089 (2006).

8. Shan, D. *et al*. GPAT3 and GPAT4 are regulated by insulin-stimulated phosphorylation and play distinct roles in adipogenesis. *J. Lipid Res.* **51**, 1971-1981 (2010).

9. Koh, Y. *et al*. Lipin1 Is a Key Factor for the Maturation and Maintenance of Adipocytes in the Regulatory Network with CCAAT/Enhancer-binding Protein alpha and Peroxisome Proliferator-activated Receptor gamma2. *J. Biol. Chem.* **283**, 34896-34906 (2008).

10. Takeuchi, K. & Reue, K. Biochemistry, physiology, and genetics of GPAT, AGPAT, and lipin enzymes in triglyceride synthesis. *American Journal of Physiology - Endocrinology And Metabolism* **296**, E1195-E1209 (2009).

11. Erickson, R. L., Hemati, N., Ross, S. E. & MacDougald, O. A. p300 Coactivates the Adipogenic Transcription Factor CCAAT/Enhancer-binding Protein alpha. *J. Biol. Chem.* **276**, 16348-16355 (2001).

12. Aarskog, N. & Vedeler, C. Real-time quantitative polymerase chain reaction. *Hum. Genet.* **107**, 494-498 (2000).

13. Guide to Performing Relative Quantitation of Gene Expression Using Real-Time Quantitative PCR, Applied Biosystems Application Note (Part # 4371095, Rev B).

14. Applied Biosystems User Bulletin #2 (part number 4303859).

15. Amplification Efficiency of TaqMan® Gene Expression Assays, Applied Biosystems Application Note (Stock # 127AP05-03).

16. Ntambi, J. M. & Young-Cheul, K. Adipocyte Differentiation and Gene Expression. *J. Nutr.* **130**, 3122S-3126S (2000).

17. Novikoff, A. B., Novikoff, P. M., Rosen, O. M. & Rubin, C. S. Organelle relationships in cultured 3T3-L1 preadipocytes. *J. Cell Biol.* **87**, 180-196 (1980).

18. Green, H. & Kehinde, O. Formation of normally differentiated subcutaneous fat pads by an established preadipose cell line. *J. Cell Physiol.* **101(1)**, 169-171 (1979).

19. Boney, C. M., Fiedorek, F. T., Paul, S. R. & Gruppuso, P. A. Regulation of preadipocyte factor-1 gene expression during 3T3-L1 cell differentiation. *Endocrinology* **137**, 2923-2928 (1996).

20. Austyn, J. M. & Gordon, S. F4/80, a monoclonal antibody directed specifically against the mouse macrophage. *Eur. J. Immunol.* **11**, 805-815 (1981).

21. Unger, R. H., Clark, G. O., Scherer, P. E. & Orci, L. Lipid homeostasis, lipotoxicity and the metabolic syndrome. *Biochim. Biophys. Acta* **1801**, 209-214 (2010).

22. Kato, H. *et al*. Mechanism of Amelioration of Insulin Resistance by Î²3-Adrenoceptor Agonist AJ-9677 in the KK-Ay/Ta Diabetic Obese Mouse Model. *Diabetes* **50**, 113-122 (2001).

23. Sakata, A. *et al*. Improvement of cognitive impairment in female type 2 diabetes mellitus mice by spironolactone. *Journal of Renin-Angiotensin-Aldosterone System* **13**, 84-90 (2012).

24. Ramarao, P. & Kaul, C. L. Insulin resistance: Current therapeutic approaches. *Drugs Today* **35(12)**, 895-911 (1999).

25. Saha, T. K., Yoshikawa, Y. & Sakurai, H. Improvement of hyperglycaemia and metabolic syndromes in type 2 diabetic KKAy mice by oral treatment with [meso-

tetrakis(4-sulfonatophenyl) porphyrinato]oxovanadium(IV)(4-) complex. *J. Pharm. Pharmacol.* **59**, 437-444 (2007).

26. Srinivasan, K. & Ramarao, P. Animal models in type 2 diabetes research: an overview. *Indian J. Med. Res.* **125(3)**, 451-472 (2007).

27. Okazaki, M. *et al*. Diabetic nephropathy in KK and KK-Ay mice. *Exp. Anim.* **51(2)**, 191-196 (2002).

28. Iwatsuka, H., Shino, A. & Suzuoki, Z. General survey of diabetic features of yellow KK mice. *Endocrinol. Jpn.* **17(1)**, 23-35 (1970).

29. Topham, M. K. Signaling roles of diacylglycerol kinases. *J. Cell. Biochem.* **97(3)**, 474-484 (2006).

CHAPTER EIGHT

CONCLUSIONS

Conversion of diacylglycerol (DAG) to phosphatidic acid (PtdOH) catalyzed by diacylglycerol kinases (DGKs) is a central point for several lipid biosynthetic pathways and signaling pathways. The reaction catalyzed by DGK is the first step in the re-synthesis of phosphatidylinositol (PtdIns), thus DGK contributes to the phospholipid synthesis, as well as to the signaling pathway through polyphosphoinositides, phosphorylated forms of PtdIns, such as PtdIns(4,5)P_2 and PtdIns(3,4,5)P_3. Phosphatidylinositol 4-phosphate 5-kinase (PIP5K) catalyzes the phosphorylation of PtdIns4*P* to form PtdIns(4,5)$P_{2,}$ is another crucial player in the PtdIns-cycle.[1]

During my graduate studies, my primary focus was on the epsilon isoform of DGK. I investigated several structural and functional aspects of this enzyme. Thus, we have been able to elucidate the topology of the hydrophobic segment of FLAG-DGKε *in vivo*, demonstrating that the N-terminal FLAG-tagged form of this enzyme is a deeply-inserted monotopic protein (Chapter 2). Moreover, a single mutation P32A in the middle of the hydrophobic segment causes the protein to acquire a transmembrane topology. Our findings were later confirmed by a study performed using *in vitro* translation in the presence of dog pancreas rough microsomes.[2] The results of these experiments confirm that the FLAG-tagged DGKε N-terminal segment adopts a monotopic topology, while the P32A mutant version spans the membrane. Interestingly, DGKε with a native-like N-terminus was shown to attain a bitopic topology *in vitro* under the experimental conditions used. Thus, it is possible that a highly charged epitope like the FLAG tag can affect the topology of a protein.

Unfortunately, at present the sequence determinants for the monotopic and bitopic topologies are not studied well, and current bioinformatics tools distinguish poorly between these two protein topologies. The influence of an epitope tag on protein topology is also not addressed in many studies. Our findings serve as an example of such a study, showing that an epitope tag can impact the protein topology. Further experiments *in vivo* comparing different epitope tags would be beneficial for clarifying the topology of DGKε.

The epsilon isoform of DGK is unique among other isoforms in having acyl chain specificity for diacylglycerols with an arachidonate moiety. We studied several aspects of DGKε substrate specificity, including its preference for acyl chains at the *sn*-1 position of DAG (Chapter 5). Surprisingly, we found that *in vitro* DGKε can metabolize with a high rate DAGs with *sn*-1 acyl chains other than 18:0, which was considered the preferred acyl chain at the *sn*-1 position of DAG. Thus, 20:4/20:4-DAG is phosphorylated with a similar rate and efficiency to 18:0/20:4-DAG. Nevertheless, *in vivo* the intermediates of PtdIns-cycle are highly enriched in 18:0/20:4 species,[3-6] and studies with cells from DGKε KO mice showed significant reductions in 18:0/20:4-containing lipids for several phospholipid classes involved in PtdIns cycling.[7] The overall abundance of the 18:0/20:4 species can be possibly contributing to the DGKε substrate preference *in vivo* by means of local substrate availability and prevalence. However, it is possible that in particular tissues and/or membrane domains or under particular nutritional or pathological states, 20:4/20:4-DAG may become the major substrate of DGKε catalysis, leading to different downstream regulatory events.

We also made significant progress in identifying the region of DGKε responsible for its substrate specificity (Chapter 4). DGKε is the smallest mammalian DGK and lacks any structural domains except the catalytic domain. Previously we made a deletion of first 58 residues from the N-terminus of DGKε and showed that it doesn't affect the substrate specificity of this enzyme.[8] We identified a motif located in the accessory domain of DGKε, similar to the motif in lipoxygenases (LOX), and demonstrated its involvement in DGKε substrate specificity.[9] These findings lead us to the discovery that this motif is common for several other enzymes, exhibiting specificity for the substrates containing polyunsaturated fatty acids (PUFA), such as PIP5K and membrane-bound O-acyltransferase 7. We confirmed that the mutations in the LOX-like motif of PIP5Kα affect its kinetic parameters for the 18:0/20:4-substrate. While this motif does not predict a specific conformation of a substrate-binding site, and it is found in other proteins that do not interact with PUFA groups, the presence of this motif can be an important indication for identifying the isoforms of the enzyme with specificity for the PUFA-containing substrates. Identification of such motifs has been demonstrated to be a valuable tool in biochemistry.

It has been suggested that cell localization is a major factor determining the specific roles of the various DGK isoforms. Therefore, a substantial part of my graduate studies was devoted to a determination of the cellular and organ distribution of DGKs, particularly the epsilon isoform. Thus, we demonstrated that DGKε is present in both the endoplasmic reticulum and plasma membrane (Chapter 2). In the plasma membrane, DGKε does not co-localize with the lipid rafts (unpublished observations), indicating that

DGKε-coupled signaling pathway should occur through other plasma membrane compartments, probably through PtdIns(4,5)P_2 cluster domains. We demonstrated that DGKε is important for proper functioning of PtdIns-cycle in the plasma membrane (Chapter 3).

There are no published systematic studies assaying the relative expression levels of the DGK family in different tissues. At present, one available way to compare the levels of DGKs in organs is to use expressed sequence tags database from the National Center for Biotechnology Information. Unfortunately, these data only approximate the levels of DGK mRNA and are not meant to be definitive. We measured DGK expression levels in several murine tissues (Chapter 7), providing a valuable set of data, which can be used for studying the tissue-specific functions of DGK isoforms.

We also expanded our knowledge of DGK expression in diabetic animals, showing that the expression profiles of several DGK isoforms are altered in adipocytes isolated from diabetic mice (Chapter 7). DGKδ has been already shown to play an important role in hyperglycemia-induced insulin resistance.[10] Further studies using KO animals are necessary to elucidate the role of other DGK isoforms in type 2 diabetes.

We showed that DGK expression profiles change dramatically during adipocyte differentiation (Chapter 7). Currently, the experiments with mouse embryonic fibroblasts from DGKα, δ and ε KO and WT mice are being carried out in our laboratory to determine if the deletion of one of these isoforms can affect adipocyte differentiation. These data would significantly advance our knowledge of DGK involvement in adipocyte differentiation.

DGKs comprise a very diverse family of enzymes. Different isoforms of DGK affect various metabolic and signaling pathways to different extents. These differences rise due to isoform-specific subcellular localization and expression of DGKs in different organs, thus determining the interaction with different lipid and protein partners that may be part of other signaling or metabolic pathways. Structurally distinct regulatory domains of DGK isoforms also contribute to different modes of enzyme activation. Interestingly, in some cases, DGK isoforms exhibit opposite effects to each other.[11] The heterogeneity of the DGK family is well illustrated by the differences in the phenotype of KO animals for different DGK isoforms.

DGK isoforms have been proposed to be used as drug targets for a number of diseases.[12-15] For example, thiazolidinedione compounds have been suggested as possible new therapeutic agents for diabetic nephropathy that prevent glomerular dysfunction through DGK activation and following inhibition of the DAG-PKC-extracellular signal-regulated kinase pathway.[16] In addition, α-tocopherol and ω-3 fatty acids were shown to enhance DGK activity, preventing glomerular dysfunction in diabetic rats and improving insulin sensitivity in skeletal muscle.[17, 18]

Additionally, DGK inhibitors have been implicated for a potential therapeutic use in cancer chemotherapy.[19] Unfortunately, no specific inhibitors for individual isoforms have been designed so far, due to the large number of DGK isoforms and overlapping of isoform functions.[20] Nevertheless, several DGK inhibitors have been tested as anti-cancer agents. Thus, the type II DGK inhibitor, R59022, suppresses tumor cell polarity and inhibits cell locomotion in Walker carcinosarcoma cells by increasing intracellular DAG levels.[21] Type I DGKs have been suggested as a suitable target for the development of therapies of estrogen receptor negative breast cancer.[22] It was shown that stimulation by hepatocyte growth factor induces the DGK activation in a human breast cancer cell line, causing the migration and invasion of tumor cells. The inhibition of DGK activity with the type I DGK inhibitor R59949 abolished the effects induced by hepatocyte growth factor.

DGKε isoform has been demonstrated to play an important role in synaptic function, and DGKε-PtdIns signaling was shown to modulate rapid kindling epileptogenesis, suggesting this isoform as a novel therapeutic target for epilepsy.[23] DGKε also may be a novel drug target for prevention of cardiac hypertrophy and progression to heart failure.[24] It was shown that this enzyme restores heart function and improves survival under chronic pressure overload by controlling DAG concentration and expression of transient receptor potential channel 6.

Phosphatidylinositol 4-phosphate 5-kinases (PIP5K) play crucial roles in a wide variety of cellular functions by producing PtdIns(4,5)P_2. Numerous studies demonstrated that each PIP5K isoform is involved in distinct and specific cellular functions. Inhibiting PIP5K activity has been suggested as a strategy for tumor therapy, since PtdIns(4,5)P_2–PI3K and -PLC signaling pathways are upregulated in tumors, leading to increased cell survival and stimulated cell migration.[25] PIP5K activity is also required for Rho-mediated neuronal retraction, which contributes to axonal growth inhibition.[26] Therefore, it has been proposed that pharmacological inhibition of PIP5K might have a therapeutic potential against injuries to the human central nervous system, such as spinal cord injuries. Another interesting example demonstrates that PIP5Kα deficiency improves glucohomeostasis and decreases obesity in mice by altering insulin secretion,[27] thus indicating a possible role for PIP5Kα inhibition in the treatment of obesity and type 2 diabetes.

Thus, it is clear that both PIP5K and DGK enzymes have a strong potential for use as drug targets, although their medical importance has not been completely assessed. During my graduate studies I investigated several fundamental aspects of DGK and PIP5K properties, such as protein topology, subcellular and organ distribution, substrate specificity and involvement in PtdIns cycling. These findings can help further understanding of the regulation of these two enzymes, as well as help to identify their interacting partners. This knowledge in turn is likely to yield new targets for therapy in a variety of clinical areas.

REFERENCES

1. Toker, A. The synthesis and cellular roles of phosphatidylinositol 4,5-bisphosphate. *Curr. Opin. Cell Biol.* **10**, 254-261 (1998).

2. Norholm, M. H. H., Shulga, Y. V., Aoki, S., Epand, R. M. & von Heijne, G. Flanking Residues Help Determine Whether a Hydrophobic Segment Adopts a Monotopic or Bitopic Topology in the Endoplasmic Reticulum Membrane. *J. Biol. Chem.* **286**, 25284-25290 (2011).

3. Pessin, M. S. & Raben, D. M. Molecular species analysis of 1,2-diglycerides stimulated by alpha-thrombin in cultured fibroblasts. *J. Biol. Chem.* **264**, 8729-8738 (1989).

4. Pettitt, T. R. & Wakelam, M. J. Bombesin stimulates distinct time-dependent changes in the sn-1,2-diradylglycerol molecular species profile from Swiss 3T3 fibroblasts as analysed by 3,5-dinitrobenzoyl derivatization and h.p.l.c. separation. *Biochem. J.* **289 (2)**, 487-495 (1993).

5. Holbrook, P. G., Pannell, L. K., Murata, Y. & Daly, J. W. Molecular species analysis of a product of phospholipase D activation. Phosphatidylethanol is formed from

phosphatidylcholine in phorbol ester- and bradykinin-stimulated PC12 cells. *J. Biol. Chem.* **267**, 16834-16840 (1992).

6. Lee, C., Fisher, S. K., Agranoff, B. W. & Hajra, A. K. Quantitative analysis of molecular species of diacylglycerol and phosphatidate formed upon muscarinic receptor activation of human SK-N-SH neuroblastoma cells. *J. Biol. Chem.* **266**, 22837-22846 (1991).

7. Milne, S. B. *et al*. Dramatic differences in the roles in lipid metabolism of two isoforms of diacylglycerol kinase. *Biochemistry* **47(36)**, 9372-9379 (2008).

8. Lung, M. *et al*. Diacylglycerol Kinase ϵ Is Selective for Both Acyl Chains of Phosphatidic Acid or Diacylglycerol. *J. Biol. Chem.* **284**, 31062-31073 (2009).

9. Shulga, Y. V., Topham, M. K. & Epand, R. M. Study of Arachidonoyl Specificity in Two Enzymes of the PI Cycle. *J. Mol. Biol.* **409**, 101-112 (2011).

10. Chibalin, A. V. *et al*. Downregulation of Diacylglycerol Kinase Delta Contributes to Hyperglycemia-Induced Insulin Resistance. *Cell* **132**, 375-386 (2008).

11. Sakane, F., Imai, S., Kai, M., Yasuda, S. & Kanoh, H. Diacylglycerol kinases: Why so many of them? *Biochim. Biophys. Acta* **1771**, 793-806 (2007).

12. Mérida, I., Avila-Flores, A. & Merino, E. Diacylglycerol kinases: at the hub of cell signalling. *Biochem. J.* **409(1)**, 1-18 (2008).

13. Goto, K., Hozumi, Y., Nakano, T., Saino-Saito, S. & Martelli, A. M. Lipid Messenger, Diacylglycerol, and its Regulator, Diacylglycerol Kinase, in Cells, Organs, and Animals: History and Perspective. *The Tohoku Journal of Experimental Medicine* **214**, 199-212 (2008).

14. Raben, D. M. & Wattenberg, B. W. Signaling at the membrane interface by the DGK/SK enzyme family. *J. Lipid Res.* **50 Suppl**, S35-S39 (2009).

15. Sakane, F., Imai, S., Kai, M., Yasuda, S. & Kanoh, H. Diacylglycerol kinases as emerging potential drug targets for a variety of diseases. *Curr. Drug Targets.* **9(8)**, 626-640 (2008).

16. Isshiki, K. *et al*. Thiazolidinedione compounds ameliorate glomerular dysfunction independent of their insulin-sensitizing action in diabetic rats. *Diabetes* **49(6)**, 1022-1032 (2000).

17. Koya, D., Haneda, M., Kikkawa, R. & King, G. L. d-alpha-tocopherol treatment prevents glomerular dysfunctions in diabetic rats through inhibition of protein kinase C-diacylglycerol pathway. *Biofactors* **7(1-2)**, 69-76 (1998).

18. McCarty, M. F. Complementary measures for promoting insulin sensitivity in skeletal muscle. *Med. Hypotheses* **51(6)**, 451-464 (1998).

19. Riese, M. J. *et al*. Decreased Diacylglycerol Metabolism Enhances ERK Activation and Augments CD8+ T Cell Functional Responses. *J. Biol. Chem.* **286(7)**, 5254-5265 (2011).

20. Shulga, Y. V., Topham, M. K. & Epand, R. M. Regulation and Functions of Diacylglycerol Kinases. *Chem. Rev.* **111(10)**, 6186-6208 (2011).

21. Zimmermann, A. & Keller, H. Shape changes and chemokinesis of Walker carcinosarcoma cells: effects of protein kinase inhibitors (HA-1004, polymyxin B, sangivamycin and tamoxifen) and an inhibitor of diacylglycerol kinase (R 59022). *Anticancer Res.* **13(2)**, 347-354 (1993).

22. Filigheddu, N. *et al*. Diacylglycerol kinase is required for HGF-induced invasiveness and anchorage-independent growth of MDA-MB-231 breast cancer cells. *Anticancer Res.* **27**, 1489-1492 (2007).

23. Cole-Edwards, K. K. & Bazan, N. G. Lipid signaling in experimental epilepsy. *Neurochem. Res.* **30(6-7)**, 847-853 (2005).

24. Niizeki, T. *et al*. Diacylglycerol kinase-epsilon restores cardiac dysfunction under chronic pressure overload: a new specific regulator of Galpha(q) signaling cascade. *Am. J. Physiol. Heart Circ. Physiol.* **295**, H245-H255 (2008).

25. van, d. B. & Divecha, N. PIP5K-driven PtdIns(4,5)P2 synthesis: Regulation and cellular functions. *J. Cell. Sci.* **122**, 3837-3850 (2009).

26. Kubo, T., Hata, K., Yamaguchi, A. & Yamashita, T. Rho-ROCK inhibitors as emerging strategies to promote nerve regeneration. *Curr. Pharm. Des.* **13(24)**, 2493-2499 (2007).

27. Huang, P. *et al*. Phosphatidylinositol-4-Phosphate-5-Kinase alpha Deficiency Alters Dynamics of Glucose-Stimulated Insulin Release to Improve Glucohomeostasis and Decrease Obesity in Mice. *Diabetes* **60**, 454-463 (2011).